SYNTHESIS, BIOPHYSICAL ANALYSIS AND BIOLOGICAL EVALUATION OF TRICYCLIC PYRONES AND PYRIDINONES AS ANTI-ALZHEIMER AGENTS

by

SANDEEP RANA

B.Sc. (H), Maharishi Dayanand University, 2003
M.Sc., University of Delhi, 2003

AN ABSTRACT OF A DISSERTATION

submitted in partial fulfillment of the requirements for the degree

DOCTOR OF PHILOSOPHY

Department of Chemistry
College of Arts And Sciences

KANSAS STATE UNIVERSITY
Manhattan, Kansas

2009

Abstract

The objectives of this research project were to (i) synthesize different bicyclic and tricyclic pyrone and pyridinone compounds; (ii) study the mechanism of action of these compounds in solution as anti-Aβ (amyloid β) agents using different biophysical techniques; and (iii) study the biological activity of pyrone compounds for the counteraction of Aβ toxicity using MC65 cells, a human neuroblastoma cell line and 5X- familial Alzheimer's disease (5X FAD, a transgenic mice with five different mutations) mice.

A series of tricyclic pyrone and pyridinone compounds were investigated. The tricyclic pyrones and pyridinones were synthesized utilizing a condensation reaction between cyclohexenecarboxaldehye (**25**) and 4-hydroxy-6-methyl-2-pyone (**24**) or 4-hydroxy-6-methyl-2-pyridinone (**51**), respectively. A tricylic pyrone molecule **CP2** (**2**, code name) was synthesized and has an adenine base unit attached to the pyrone core. For structure activity relationship (SAR) studies, the adenine group of CP2 was replaced with other DNA base units (thymine, cytosine and guanine) and various heterocyclic moieties. Since nitrogen containing compounds often exhibit increased bioactivity and brain-penetrating abilities, oxygen atom (O5') was displaced with a nitrogen atom in the middle ring of the tricyclic pyrone. A condensation reaction of pyrone **51** and **25** was carried out to give the linear pyranoquinoline **(52)** and the L-shaped pyranoisoquinoline (**53)**.

The neurotoxicity of amyloid-β protein (Aβ) is widely regarded as one of the fundamental causes of neurodegeneration in Alzheimer's disease (AD). Recent studies suggest that soluble Aβ oligomers rather then protofibrils and fibrils may be the primary toxic species. Different biophysical techniques including atomic force microscopy (AFM), circular dichroism (CD), surface plasmon resonance (SPR) spectroscopy, and protein quantification assays were used to study the mechanism of aggregation of Alzheimer Aβ peptide in solution.

In search of potentially bioactive compounds for AD therapies, MC65 cell line was used as a screening model. Different tricyclic pyrone and pyridinone compounds protect MC65 cells from death. We studied the efficacy of CP2 *in vivo* by treatment of 5X FAD mice, a robust Aβ42-producing animal model of AD, with a 2-week course of CP2, which resulted in 40% and 50% decreases in non-fibrillar and fibrillar Aβ species respectively.

SYNTHESIS, BIOPHYSICAL ANALYSIS AND BIOLOGICAL EVALUATION OF TRICYCLIC PYRONES AND PYRIDINONES AS ANTI-ALZHEIMER AGENTS

by

SANDEEP RANA

B.Sc. (H), Maharishi Dayanand University, 2003
M.Sc., University of Delhi, 2003

A DISSERTATION

submitted in partial fulfillment of the requirements for the degree

DOCTOR OF PHILOSOPHY

Department of Chemistry
College of Arts and Sciences

KANSAS STATE UNIVERSITY
Manhattan, Kansas

2009

Approved by:

Major Professor
Duy H Hua

Abstract

The objectives of this research project were to (i) synthesize different bicyclic and tricyclic pyrone and pyridinone compounds; (ii) study the mechanism of action of these compounds in solution as anti-Aβ (amyloid β) agents using different biophysical techniques; and (iii) study the biological activity of pyrone compounds for the counteraction of Aβ toxicity using MC65 cells, a human neuroblastoma cell line and 5X- familial Alzheimer's disease (5X FAD, a transgenic mice with five different mutations) mice.

A series of tricyclic pyrone and pyridinone compounds were investigated. The tricyclic pyrones and pyridinones were synthesized utilizing a condensation reaction between cyclohexenecarboxaldehye (**25**) and 4-hydroxy-6-methyl-2-pyone (**24**) or 4-hydroxy-6-methyl-2-pyridinone (**51**), respectively. A tricylic pyrone molecule **CP2** (**2**, code name) was synthesized and has an adenine base unit attached to the pyrone core. For structure activity relationship (SAR) studies, the adenine group of CP2 was replaced with other DNA base units (thymine, cytosine and guanine) and various heterocyclic moieties. Since nitrogen containing compounds often exhibit increased bioactivity and brain-penetrating abilities, oxygen atom (O5') was displaced with a nitrogen atom in the middle ring of the tricyclic pyrone. A condensation reaction of pyrone **51** and **25** was carried out to give the linear pyranoquinoline **(52)** and the L-shaped pyranoisoquinoline (**53)**.

The neurotoxicity of amyloid-β protein (Aβ) is widely regarded as one of the fundamental causes of neurodegeneration in Alzheimer's disease (AD). Recent studies suggest that soluble Aβ oligomers rather then protofibrils and fibrils may be the primary toxic species. Different biophysical techniques including atomic force microscopy (AFM), circular dichroism (CD), surface plasmon resonance (SPR) spectroscopy, and protein quantification assays were used to study the mechanism of aggregation of Alzheimer Aβ peptide in solution.

In search of potentially bioactive compounds for AD therapies, MC65 cell line was used as a screening model. Different tricyclic pyrone and pyridinone compounds protect MC65 cells from death. We studied the efficacy of CP2 *in vivo* by treatment of 5X FAD mice, a robust Aβ42-producing animal model of AD, with a 2-week course of CP2, which resulted in 40% and 50% decreases in non-fibrillar and fibrillar Aβ species respectively.

Table of Contents

List of Figures viii
List of Tables xii
Structure – Number Correlation List xiii
List of Schemes xx
List of Graphs xxi
List of Abbreviations xxii
List of Publications xxiii
Acknowledgements xxv
CHAPTER 1 - Synthesis of tricyclic pyrone and pyridinone compounds 1
1.1 Introduction 1
1.2 Background 1
1.2.1 Reported small compounds with potential Anti-Aβ activity 8
1.2.2 Natural bioactive compounds with lactone core 10
1.2.3 Previous studies in our laboratory 12
1.3 Results and Discussion 14
1.3.1 Modification at C-11 position of CP2 15
1.3.2 Synthesis of CP2 analog with a double bond at C12 16
1.3.3. Synthesis of heterocyclic pyrone analogs 17
1.3.4 Synthesis of pyrone compounds having nitrogen in middle ring: pyranoquinolinone and pyranoisoquinonlinone compounds 22
1.3.5 Synthesis of novel pyranopyridinone analogs (N2'-analogs) 24
1.3.6. Synthesis of bicyclic pyrone and pyridinones analogs 27
1.4 Conclusion and future work 28
1.5 Experimental Section 29
1.6 References 61
CHAPTER 2 - Insight into the inhibition of aggregation of Alzheimer's Aβ peptides and disaggregation of Aβ oligomers using various biophysical techniques 70
2.1 Introduction 70
2.2 Background 70

2.3 Biophysical experiments conducted to study the inhibition of aggregation of amyloid Aβ peptides and disaggregation of Aβ oligomers and protofibrils..... 72
2.3.1 Use of atomic force microscopy to study the inhibition of aggregation and disaggregation of Aβ peptide..... 72
2.3.1.1 Introduction and background..... 72
2.3.1.2 Preparation of Aβ40 stock solution..... 74
2.3.1.3 Preparation of Aβ42 stock solution..... 74
2.3.1.4 AFM instrumentation and sample preparation..... 74
2.3.1.5 Inhibition of aggregation of Aβ40 with several compounds..... 75
2.3.1.6 Inhibition of aggregation of Aβ42 with several compounds..... 78
2.3.1.7 Disaggregation of Aβ42 oligomers with several compounds..... 81
2.3.1.8 Disaggregation of Aβ42 protofibrils with CP2..... 83
2.3.1.9 Disaggregation of Aβ42 oligomers with CP2 over the period of five days..... 84
2.3.1.10 Result and discussion..... 85
2.3.2 Use of surface plasmon resonance spectroscopy to study the interaction of tricyclic pyrone and Aβ peptide..... 92
2.3.2.1 Introduction and background..... 92
2.3.2.2 Binding of CP2 and TP17 to Aβ40 and Aβ42 monomers..... 93
2.3.2.3 Binding of CP2 to Aβ42 oligomers using anti-oligomer antibody (AB9234)..... 96
2.6.2.4 Result and discussion..... 97
2.3.3 Use of protein quantification assay to study the inhibition of aggregation of Aβ with and without tricyclic pyrone molecule CP2..... 99
2.3.3.1 Introduction and background..... 99
2.3.3.2 Inhibition of aggregation of Aβ40 and Aβ42 with CP2..... 99
2.6.3.3 Result and discussion..... 101
2.3.4 Use of circular dichroism (CD) spectroscopy to study the inhibition of aggregation of Aβ with and without tricyclic pyrone molecule CP2..... 102
2.3.4.1 Introduction and background..... 102
2.3.4.2 Study of inhibition of aggregation of Aβ42 with CP2 (1.25 equivalents)..... 104
2.3.4.3 Results and discussion..... 106

2.4 Conclusion 107
2.5 References 108
CHAPTER 3 - Biological evaluation of tricyclic pyrone and pyridinone compounds: *in vitro* and *in vivo* studies 113
3.1 Introduction 113
3.2 Background 113
3.3 MC65 cell death is related to the intracellular generation and aggregation of Aβ 115
3.4 Tricyclic pyrone and pyridinone molecules inhibit the formation of Aβ oligomers and protect MC65 cell death 118
3.5 Tricyclic pyrone molecule CP2 penetrates MC65 cell 122
3.6 *In vivo* studies of CP2 on 5X FAD mice 123
3.6.1 Introduction and background 123
3.6.2 Experimental for in vivo studies 124
3.6.3 Aβ42 ELISA 124
3.6.4 Results and discussion 125
3.7 Conclusion 126
3.8 References 127
Appendix: ^{1}H-NMR spectra, ^{13}C-NMR spectra, MS spectra, 2D-NOESY, 2D-COSY, 2D-HMBC, 2DHSQC 130

List of Figures

Figure 1.1. Proposed pathway of generation of Aβ peptide. (modified from reference 18 without the Author's permission)..... 4
Figure 1.2. Proposed mechanism of Aβ aggregation from monomers to fibrils. (Modified from reference 18 without the author's permission)..... 5
Figure 1.3. The hydrophobicity indexes of amyloid (1-42) sequence. (Modified from reference 22 without the author's permission) 5
Figure 1.4. Contributing factors promoting Aβ aggregation and neuronal damage. 6
Figure 1.5. Structure of pyripyropene A and CP2. 8
Figure 1.6. Reported organic compounds with anti-AD activity. 9
Figure 1.7. Bioactive microbial metabolites possessing pyran functionality. 10
Figure 1.8. Structures of engineered type II polyketides.[70] 11
Figure 1.9. Aldehyde used (17 - 19) and the pyranopyrones prepared (20 – 23) in this study.[70]. 12
Figure 2.1 Structural model for Aβ42 fibrils, (Taken from protein data bank, provided by Luhrs *et al.*).[6] 71
Figure 2.2. Structure of CP2, TP4, TP17, thioflavin T, Congo red and curcumin. 76
Figure 2.3. AFM images of inhibition of aggregation of Aβ40 monomers (Scale bar 1 μm). 78
Figure 2.4. AFM images of inhibition of aggregation of Aβ42 monomers. 80
Figure 2.5. AFM images of disaggregation of Aβ42 oligomers. 83
Figure 2.6. AFM images of disaggregation of Aβ42 protofibrils; (a) Aβ42 protofibrils formed form the incubation of Aβ42 monomer (37 μM) at 4ºC for 4 days. (b) Incubation of Aβ42 protofibrils with CP2 (two equivalents) for 24 h at room temperature. 84
Figure 2.7. Disaggregation of Aβ42 oligomers with different equivalents of CP2 over the period of five days. Quantitative analysis of particle density in 25 μm^2. Aβ oligomeric density from three independent AFM scans was calculated using Image J program. 85
Figure 2.8. Inhibition of aggregation of Aβ40 with two equivalents of CP2, TP17, thioflavin T, curcumin and congo red separately over 24 h and 48 h. Quantitative analysis of particle

density in 25 μm^2 AFM scans. Aβ oligomeric density from three independent AFM scans was calculated using Image J program. Error bars represent standard deviation. 87
Figure 2.9. Inhibition of aggregation of Aβ42 with two equivalents of CP2, TP17, thioflavin T, curcumin and congo red separately over 24 h and 48 h. Quantitative analysis of particle density 88
Figure 2.10. Disaggregation of Aβ42 oligomers with two equivalents of CP2, TP17, thioflavin T, curcumin and congo red separately over 24 h and 48 h. Quantitative analysis of particle density in 25 μm^2 AFM scans. Aβ oligomeric density from three independent AFM scans was calculated using Image J program. Error bars represent standard deviation. n =3, *p, **p, ***p, ****p, *****p < 0.01 compared with their respective controls. 90
Figure 2.11. Schematic representation of SPR principle.[28] (This picture is modified from the manufacturer's handbook) 93
Figure 2.12. Immobilization of Aβ on to CM5 gold chip. (1) Activation and immobilization of Aβ on gold CM5 sensor chip. (2) The surface activated by EDC/NHS was exposed to a fresh Aβ40/ Aβ42 solution to form a peptide bond between the amine group on the peptide and the carboxylic group on the CM5 surface. (3) The deactivation of unreacted sites was achieved by blocking NHS-activations with ethanolamine.[31] 94
Figure 2.13. Real-time detection of the binding of tricyclic pyrone to Aβ40 (A and B) and Aβ42 (C and D) by SPR. The results from a typical experiment are shown. Color code: Blue is cell surface without immobilized Aβ and Red is cell surface with immobilized Aβ. 95
Figure 2.14. SPR sensogram of the in real-time binding of CP2 to Aβ42 oligomers-AB9234 antibody complex. The first two injections showed the immobilization of anti-amyloid oligomer antibody, the following five injections were Aβ42 oligomers, and the last injection was CP2. Lower concentrations of Aβ42 were used in the first four injections and higher concentration of Aβ was used in the fifth injection to ensure that the immobilized antibody was bound with the oligomer. 97
Figure 2.15. Quantification of soluble Aβ40 and Aβ42 peptide separately in PBS buffer (pH 7.4) at 25°C over 7 days using a micro BCA™ protein assay reagent kit in the absence (marked in square for Aβ40 and circle for Aβ42) and presence (marked in diamond for Aβ40 and triangle for Aβ42) of 2 equivalents of CP2..... 101

Figure 2.16. CD spectrum of different conformations of Aβ peptide.[37] 103
Figure 2.17. CD spectrum showing the effect of TFE on Aβ42 peptide. 104
Figure 2.18. CD spectra of Aβ42 (40 μM) in phosphate buffer (7.7 mM) containing NaCl (8.9 mM), Na2CO3 (15.5 μM), NaOH (0.91 mM), and 5.1% acetonitrile solution with and without CP2 over 48 h. The control solutions that contained the above incubation buffer with and without CP2 were prepared and their contribution was subtracted in the CD spectra. Left panel: Aβ42 alone; 0 h: black; 9 h: light blue; 19 h: green; 21 h: dark blue; 45 h: brown; and 48 h: red. Right panel: Aβ42 + CP2 (1.25 equivalents); 0 h: black; 9.5 h: light blue; 15.5 h: green; 20 h: dark blue; 23 h: brown; and 48 h: red. 105
Figure 2.19. Trend of β-sheet content over time: circle is Aβ42 alone and square is Aβ42 + CP2. 106
Figure 3.1. Schematic representation of C99 expression. 115
Figure 3.2. MC65 cell death is dependent upon Aβ generation and closely related to Aβ aggregation into Aβ-Oligomeric complexes. 116
Figure 3.3. Treatment of MC65 cells with TP compounds and a γ-secretase inhibitor, L-685 458 (A) MC65 cells: –TC, without TC to induce C99 expression; +TC, with TC to suppress C99 expression. n = 3, **p < 0.001 compared with the –TC group. (B) L-685 458 of indicated concentrations was added at the same time as TC removal. Cellular proteins from 24 h cultures were analyzed by western blot using 6E10. 117
Figure 3.4. Dose dependent study of CP2. CP2 inhibits the formation of Aβ-OCs. (A) MC65 cells were treated with the indicated compounds for 24 h (2 μM N9'- analog and TP17 were used). Western blot of cellular proteins was analyzed with 6E10 (B) MC65 cells were treated with TC or without TC, but with the indicated concentrations of CP2 for 24 h. Cellular proteins were analyzed by western blots using 6E10. 118
Figure 3.5. Structures of various tricyclic pyrone molecules. 119
Figure 3.6. Synthesized tricylic pyrone and pyridinone compounds. 120
Figure 3.7. MC65 protection assay for different TP compounds. L-685 458 of indicated concentrations was added at the same time as TC removal. At 72 h, viability was assessed by MTT assay. Data are expressed as mean percentage viability (n = 7) with parallel +TC cultures set at 100% viability. Error bars represent standard error. ***p < 0.001, **p < 0.01, compared with untreated –TC controls. 121

Figure 3.8. CP2 rapidly accumulates inside cells. MC65 cells were incubated with [^{14}C]CP2 for the indicated periods of time, washed, and the cell-associated counts that were trypsinizable from cell pellets (cell surface CP2, empty circles) and those remaining in cells after trypsinization (intracellular CP2, filled circles) were quantified. Expressed values are quantities of CP2 calculated from the radioactivity of 10^5 cells. 123

Figure 3.9. CP2 treatment reduces the level of cerebral Aβ. Brains from mice treated with CP2 or mock solution were sequentially extracted with RIPA and FA. Aβ42 levels in the RIPA and FA extracts (RIPA soluble and FA soluble, respectively) were measured by ELISA. Aβ levels were expressed in nanograms per milligram of brain protein. CP2 reduced the levels of both RIPA and FA soluble Aβ42. Error bars represent standard error. $n = 6$. The p values were obtained by comparing the two groups using t-test. 126

List of Tables

Table 1.1. Neurodegenerative diseases: protein and pathology.[7] 3
Table 2.1. Amount of Aβ40 peptide (μM) over 7 days at 25ºC in PBS buffer (pH 7.4) at 25ºC with and without CP2 (two equivalents) determined by micro BCA™ protein assays..... 102
Table 2.2. Amount of Aβ40 peptide (μM) over 7 days at 25ºC in PBS buffer (pH 7.4) at 25ºC with and without CP2 (two equivalents) determined by micro BCA™ protein assays..... 102
Table 3.1. TP compounds and their IC50 inhibitory activities. 122

Structure – Number Correlation List

1

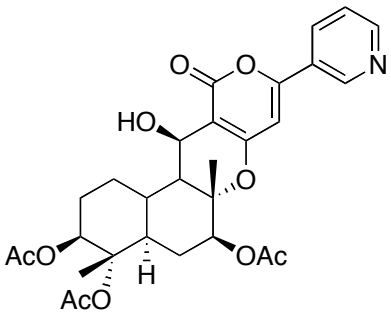

2

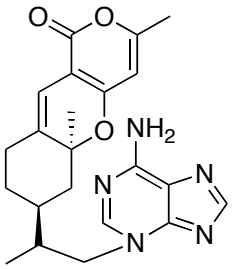

3

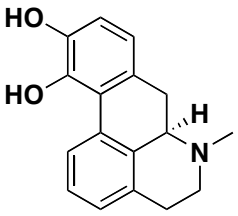

4

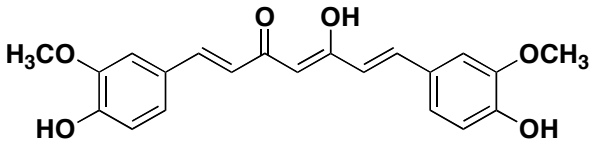

5

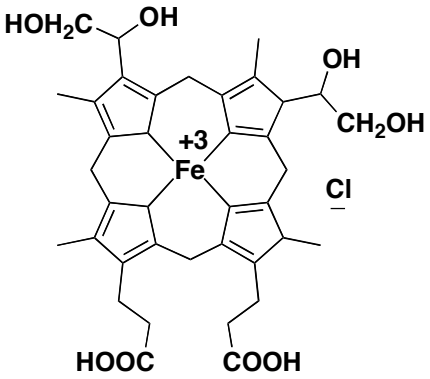

6

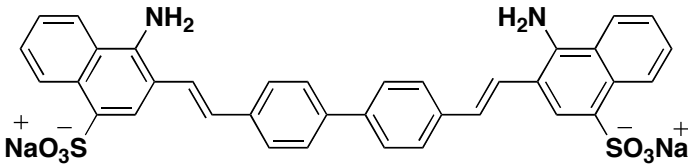

7

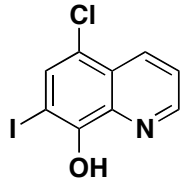

8

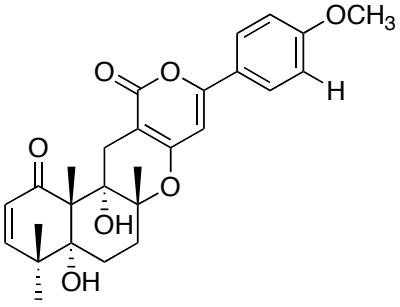

9

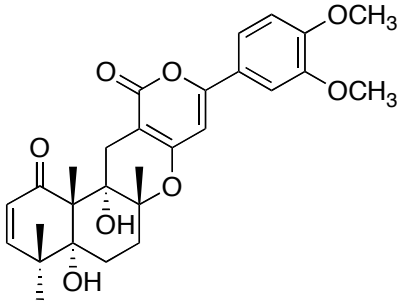

10

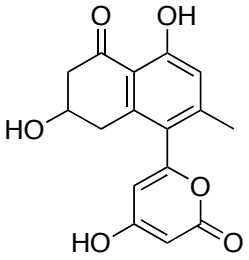

11

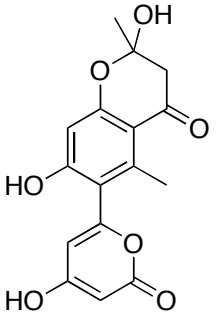

12

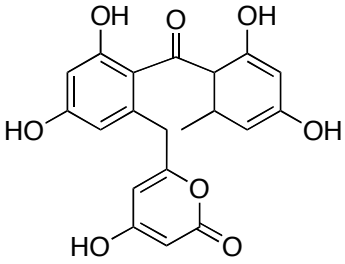

13

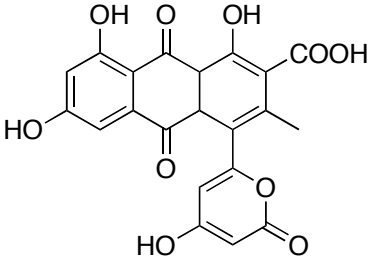

14

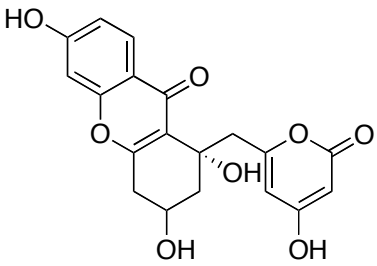

15

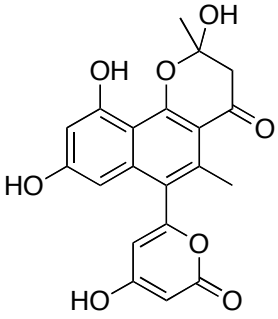

16

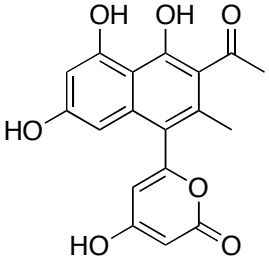

17

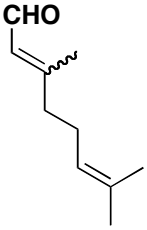

18

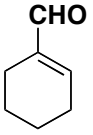

19

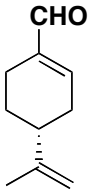

20

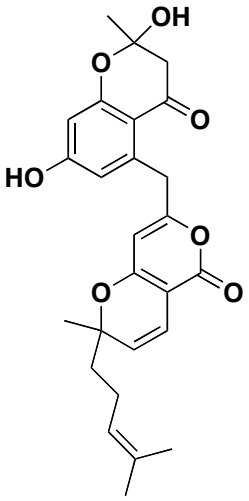

21

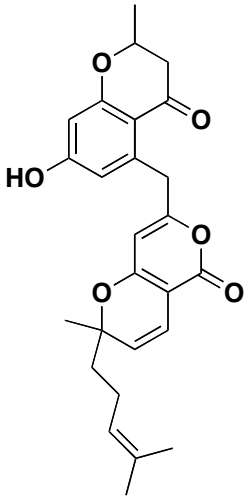

22

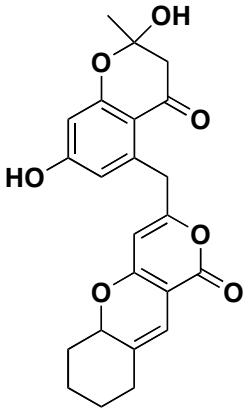

23

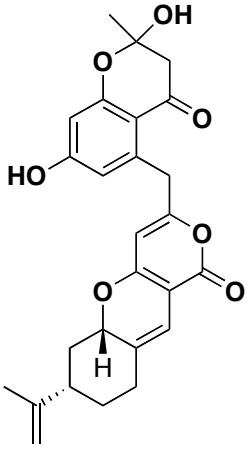

24

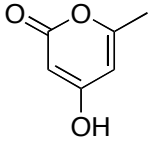

25

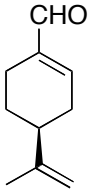

26

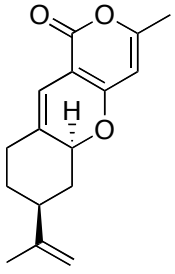

27

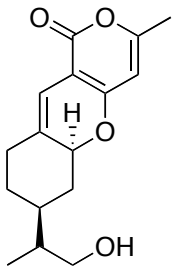

28

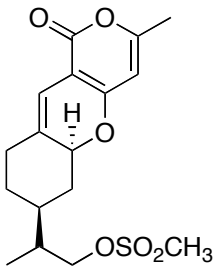

29

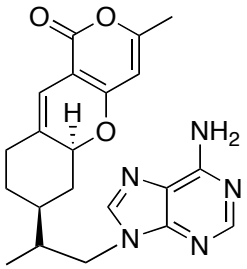

30

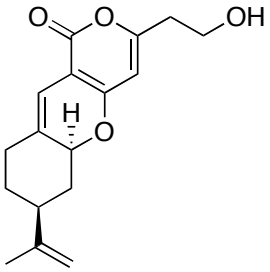

31

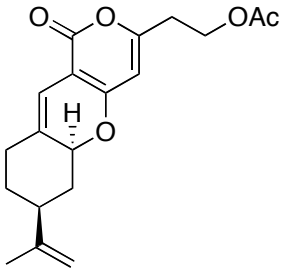

32

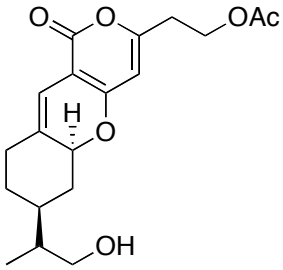

33

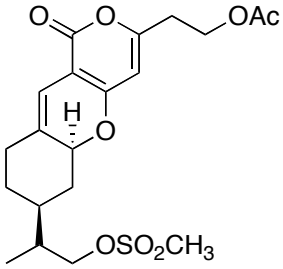

34

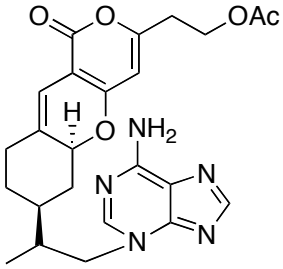

35

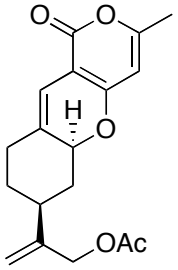

36

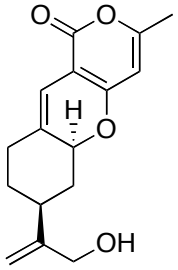

37

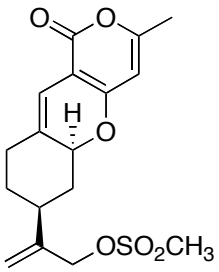

38

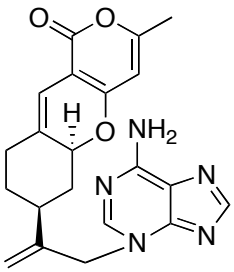

39

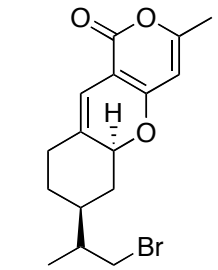

40

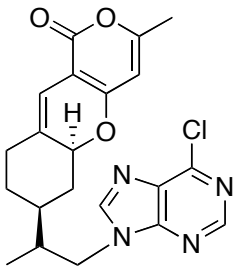

41

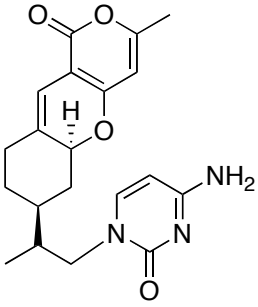

42

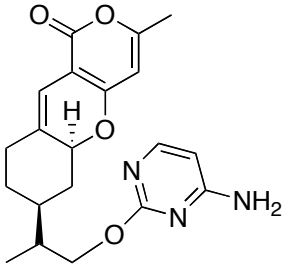

43

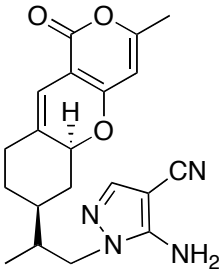

44

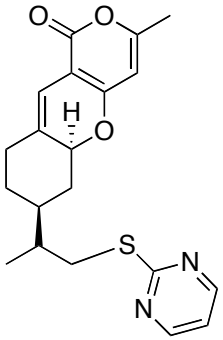

45

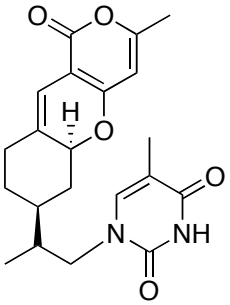

46

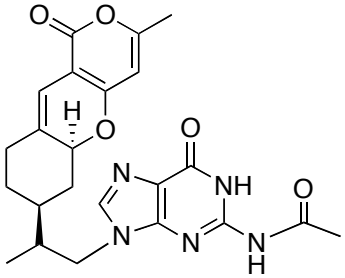

47

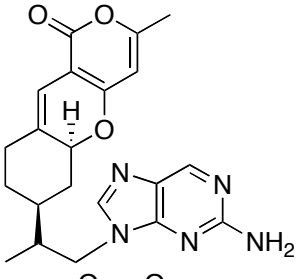

48

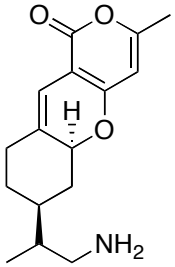

49

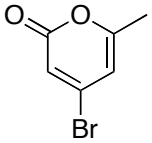

50

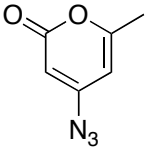

51

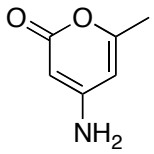

52

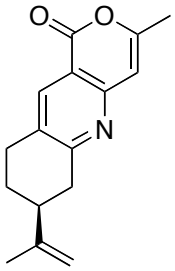

53

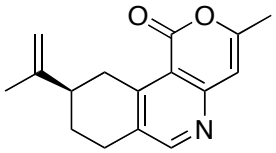

54

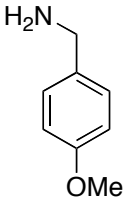

55

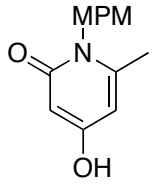

56

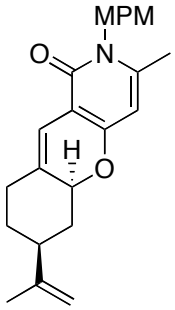

57

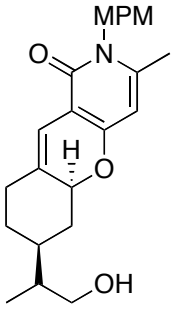

58

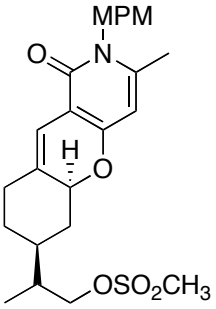

59

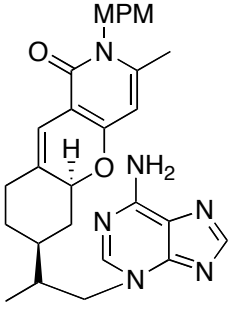

60

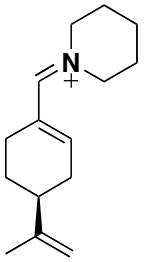

61

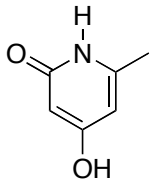

62

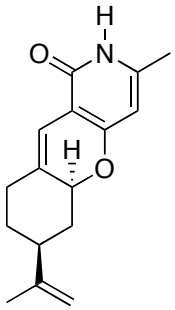

63

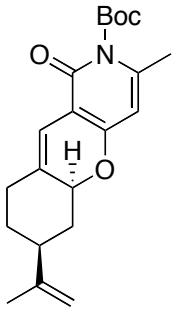

64

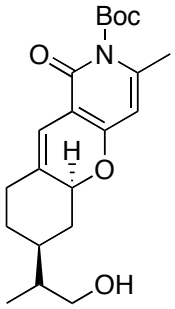

65

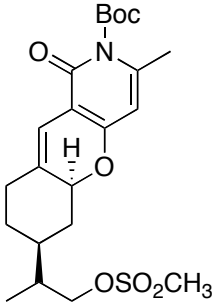

66

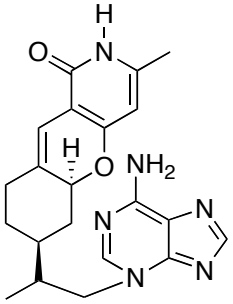

67

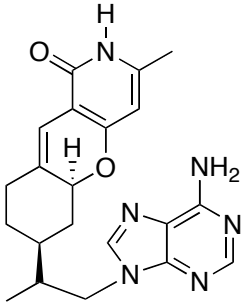

68

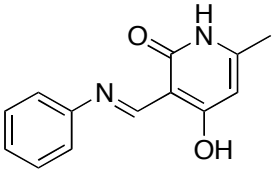

69

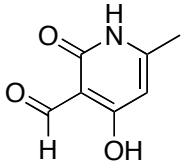

70

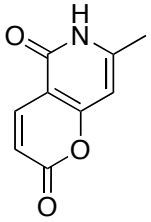

List of Schemes

Scheme 1.1 Syntheses of CP2 (code name; 2) and TP3 (code name; 29). 13
Scheme 1.2. Proposed mechanism for the synthesis of tricyclic pyrone molecule 33. 14
Scheme 1.3. Modification at C-11 methyl of CP2. 16
Scheme 1.4. Synthesis of CP2 analog, compound 38. 17
Scheme 1.5. Synthesis of TP analog 40. 18
Scheme 1.6. Syntheses of TP analogs 41 and 42 18
Scheme 1.7. Syntheses of TP analogs 43, 44, 45 and 46. 20
Scheme 1.8. Synthesis of TP analogs 47. 21
Scheme 1.9.Synthesis of TP analog 48. 22
Scheme 1.10. Synthesis of pyranoquinolinone 52 and pyranoisoquinonlinone 53. 23
Scheme 1.11. Proposed mechanism for synthesis of 53. 24
Scheme 1.12. Synthesis of a novel protected N2' pyridinone compound. 25
Scheme 1.13. Proposed mechanism for the synthesis of tricyclic pyrone molecule 56. 26
Scheme 1.14. Synthesis of novel pyridinone compounds. 27
Scheme 1.15. Synthesis of novel bicyclic pyridinone compounds using a Wittig reagent. 28

List of Graphs

Graph 2.1. Correlations of concentrations of monomeric Aβ40 and Aβ42 separately versus UV absorbance with and without CP2 using Micro BCA™ protein assay reagent kit. Left panel: Aβ40, diamond is Aβ40 with CP2 and square is Aβ40 without CP2; Right panel: Aβ42, triangle is Aβ42 with CP2 and circle is Aβ42 without CP2. 100

List of Abbreviations

Ac_2O	Acetic anhydride
BCA	Bicinchoninic acid
BnBr	Benzyl bromide
$BnNH_2$	Benzyl amine
CSA	Camphorsulfonic acid
DCC	Dicyclohexylcarbodiimide
DHP	Dihydropyrane
DIBALH	Diisobutyl aluminium hydride
DMAP	4-Dimethylaminopyridine
DMSO	Dimethyl sulfoxide
DMF	Dimethylformamide
FA	Formic acid
HFIP	Hexafluoroisopropanol
HMPA	Hexamethylphosphoramide
LDA	Lithium diisopropylamine
MCPBA	*meta*-Chloroperbenzoic acid
MsCl	Methanesulfonyl chloride
PBS	Phosphate-buffered saline
PTSA	*p*-Toluenesulfonic acid
RIPA	Radioimmune precipitation assay
TBDMSCl	*t*-Butyldimethylchlorosilane
TFA	Trifluoroacetic acid

List of Publications

1. Anil Kumar, Nidhi Jain, **Sandeep Rana** and SMS Chauhan. Ytterbium(III)Triflate Catalyzed Conversion of Carbonyl Compounds into 1,3-Oxathiolanes in Ionic Liquids. *Synlett*., **2004**, *15*, 2785-2787.

2. Izumi Maezawa, Hyun-Seok Hong, Hui-Chuan Wu, Srinivas K. Battina, **Sandeep Rana**, Takeo Iwamato, Gary A. Radke, Erik Petterson, George M. Martin, Duy H. Hua, and Lee-Way Jin. A Novel Tricyclic Pyrone Compound Ameliorates Cell Death Associated with Intracellular Amyloid-β Oligomeric Complexes. *J. Neurochem.*, **2006**, *98,* 57-67.

3. Hyun-Seok Hong, Izumi Maezawa, Nianhuan Yao, Bailing Xu, Ruben Diaz-Avalos, **Sandeep Rana**, Duy H. Hua, R. Holland Cheng, Kit S. Lam, and Lee-Way Jin. Combining the Rapid MTT Formazan Exocytosis Assay and the MC65 Protection Assay led to the Discovery of Carbazole Analogs as Small Molecule Inhibitors of Aβ Oligomer-induced Cytotoxicity. *Brain Research*, **2007**, *1130*, 223-234.

4. Charan Ganta, Aibin Shi, Srinivas K. Battina, Marla Pyle, **Sandeep Rana**, Duy H. Hua, Masaaki Tamura, Deryl Troyer. Combination of Nanogel Polyethylene Glycol-Polyethylenimine and 6(hydroxymethyl)-1,4-anthracenedione as an Anticancer Nanomedicine. *J. of Nanoscience and Nanotechnology*, **2008**, *8*, 2334-2340

5. Aibin Shi, Thu A. Nguyen, Srinivas K. Battina, **Sandeep Rana**, Dolores J. Takemoto, Peter K. Chiang, and Duy H. Hua. Synthesis and Anti-breast Activities of Substituted Quinolines. *Bioorg. Med. Chem. Lett.*, **2008**, 18, 3364-*3368*.

6. Hyun-Seok Hong, Izumi Maezawa, Madhu Budmagunta, **Sandeep Rana**, Aibin Shi, Chun-Yi Wu, Duy H. Hua, Robert Vasser, Mei-Ping Kung, Ruiwu Liu, Kit S. Lam, R. Holland Cheng, John C. Voss, and Lee-Way Jin. Candidate Anti-Aβ Fluorine

Compounds Selected from Analogs of Amyloid Imaging Agents. *Neurobiology of Aging*, **2008**, *doi:10:1016/j.neurobiolaging.2008.09.019*.

7. Hyun-Seok Hong, **Sandeep Rana**, Lydia Barrigan, Aibin Shi, Yi Zhang, Feimeng Zhou, Lee-Way Jin, and Duy H. Hua. Inhibition of Alzheimer's Amyloid Aβ42 Toxicity with a Tricyclic Pyrone Molecule *in vitro* and *in vivo*. *J. Neurochem.*, **2009**, *108*, 1097-1108.

8. **Sandeep Rana**, Hyun-Seok Hong, Lydia Barrigan, Lee-Way Jin and Duy H. Hua. Syntheses of Tricyclic Pyrones and Pyridinones and Protection of Aβ-Peptide Induced MC65 Neuronal Cell Death. *Bioorg. Med. Chem. Lett.*, **2009,** *19,* 670-674.

9. Eugenia Trushina, **Sandeep Rana**, Cynthia T. McMurray, and Duy H. Hua. Tricyclic Pyrone Compounds Reverse Cellular Phenotype Caused By Expression of Mutant Huntington Protein In Striatal Neurons. *BMC Neuroscience*, **2009**, *10*, E-ISSN: 1471-2202.

10. Yuan-Ping Pang, Fredrik Ekström, Gregory A. Polsinelli, Yang Gao, **Sandeep Rana**, Duy H. Hua, Björn Andersson, Per Ola Andersson, Lei Peng, Sanjay K. Singh, Rajesh K. Mishra,, Kun Yan Zhu, Ann M. Fallon, David W. Ragsdale, Stephen Brimijoin. Selective and Irreversible Inhibitors of Mosquito Acetylcholinesterases for Controlling Malaria and Other Mosquito-Borne Diseases. *PLoS One*, **2009**, *4*, 8, e6851

Acknowledgements

I would like to give my most sincere gratitude to my research advisor, Dr. Duy H. Hua, for his insightful guidance, constant encouragement, and full support during my Ph.D. period. I have learned a lot from him both in experimental skills and moral character, especially in his dedication and persistent effort towards a scientific goal. I would also like to thank Dr. Stefan Bossmann, Dr. Kenneth Klabunde and Dr. Om Prakash and Dr. Kyeong-ok Chang for their time and instructions in serving on my advisory committee. I am also grateful to all other faculty and staff members in the Department of Chemistry for their help and support.

I sincerely thank all former and current members in Dr. Hua's group for their help in research and daily life. Special thanks go to Dr. Srinivas Battina and Dr. Yi Chen for their previous work in the synthesis of tricyclic pyrone compounds for the Alzheimer's project and Arleen Wu for her help during the biophysical studies of pyrone compounds. I also thank Lydia Roberts and Liang Zhang for providing me the starting material for my project. I am also grateful to Srinivas Battina, Kaiyan Lou, Huiping Zhao, Angelo Aguilar, Bernard Wiredu, Ana Jimenez, Aibin Shi, Mahendra Thapa, Keshar Prasain, Laxman Pokhrel, Thi Nyugen, Weier Bao, Allan Prior, and Angela for their help and friendship.

Special thanks are due to Dr. John Tomich and Sushanth Gudlur at Department of Biochemistry for their constant help and resources for the biophysical studies and to Dr. Om Prakash for his help in NMR studies of Alzheimer peptide.

Finally, I would like to thank my parents for their love and support through this period of my life and to my loving wife Rashmi Dhankhar for her immense support.

CHAPTER 1 - Synthesis of tricyclic pyrone and pyridinone compounds

1.1 Introduction

Neurodegenerative diseases[1] including Alzheimer's disease (AD),[2] Huntington's disease (HD),[3] Parkinson's disease,[4] amyotrophic lateral sclerosis (ALS or Lou Gehrig's disease)[5] and prion diseases[6] involve protein misfolding which produce aggregates in different regions of the brain. It has been observed that different neurodegenerative diseases have different protein aggregates and pathologies as described in **Table 1.1**.[7] Alzheimer's disease (AD) is a neurological protein misfolding disease and is the fourth leading cause of death. It is characterized by progressive dementia that leads to incapacitation and death. It includes synaptic loss and neuronal death, which over course of time is responsible for the loss of memory, personality and eventual death.[8] AD affects 15 million people worldwide, and its incidence increases from 3.5% per year at age 65 to 19% at age 85 and to 47% over 85 years old.[8] To date, there is no successful treatment for AD patients. In this chapter I will discuss the synthesis of different tricyclic pyrone and pyridinone compounds and evaluate their bioactivities for counteracting AD protein misfolding.

1.2 Background

Alzheimer's disease involves protein misfolding and is a progressive and irreversible brain disorder with no cure. There are two characteristic neuropathological lesions that define AD namely, (i) extracellular plaques, also called amyloid plaques which are mainly composed of amyloid beta (Aβ) peptides consisting of 39-43 amino acids, proteolytic cleavage products from amyloid precursor protein (APP)[9]; and (ii) intracellular tangles, also called neurofibrillary tangles (NFT), which are aggregates of Aβ and microtubule associated tau protein.[10]

The Aβ peptide segment is generated by the endoproteolysis of APP transmembrane protein by beta (β) and gamma (γ) secretase enzymes.[11] APPs are synthesized as N- and O-glycosylated integral transmembrane protein. They have a large amino (NH_2) terminal extracellular domain and a short 47 amino acids long cytoplasmic domain.[12] The biological function of APP is unknown and it hinders the understanding of pathophysiology of AD. Suspected functions of APP include inhibition of extracellular serine proteases,[13] involvement in cell adhesion[14], and synaptic plasticity.[15] APP may function as a cell receptor.[16]

Firstly, APP is first cleaved by α- or β- secretase. α- Secretase cuts close to transmembrane domain, in the middle of the Aβ region of APP (**Figure 1.1**) and a a-APP ectodomain and a 83-residue carboxy terminal (C83) fragment is formed. On the other hand, β-secretase enzyme cleaves the APP forming β-APP ectodomain and a 99-residue carboxy terminal (C99) fragment. Proteolysis of C99 peptide residue fragment by gamma- (γ) secretase enzyme produces the heterogeneous Aβ (39-43 amino acids) peptide as shown in **Figure 1.1**.[17]

Disease	Etiology	Regions affected	Characteristic pathology	Disease protein deposited
Alzheimer's disease	1.Amyloid precursor protein 2. PS1 and PS2 3.Sporadic (ApoE risk factor)	Cortex, hippocampus, basal forebrain, brain stem	Neuritic plaque and neurofibrillary tangles.	Aβ peptide and hyperphosphorolated tau protein.
Huntington's disease	Huntingtin (dominant) Protein	Striatum, other basal ganglia	Intracellular inclusions	Huntingtin with polyglutamine expansion
Parkinson's disease	Sporadic α-Synuclein	Cortex, substantia nigra, locus ceruleus	Lewy bodies and lewy neurites	α-Synuclein
Amyotropic lateral sclerosis (ALS)	Sporadic Superoxide dismutase-1	Same as sporadic	Bomina bodies and axonal spheroids	Unknown
Prion disease	Sporadic, genetic and infectious	Cortex, thalamus, brain stem, cerebellum, other areas	Spongiform degeneration amyloid, other aggregates	Prion protein

Table 1.1. Neurodegenerative diseases: protein and pathology.[7]

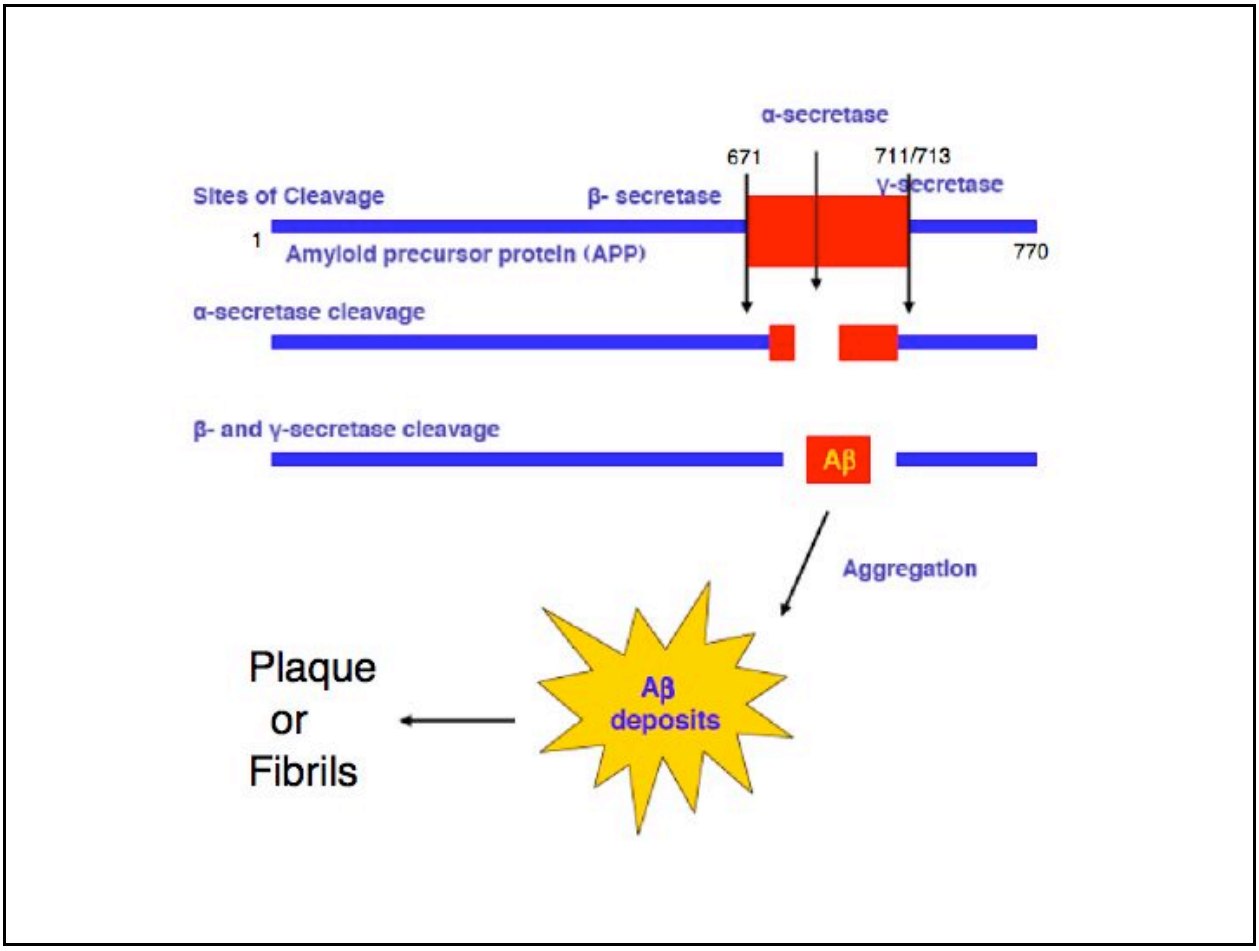

Figure 1.1. Proposed pathway of generation of Aβ peptide. (modified from reference **18** without the Author's permission)

Although the detailed mechanism of aggregation and its causes in brain remain unknown, extensive research has been conducted and it is widely accepted that Aβ monomer is non-toxic, soluble and possess random coil/ alpha helix secondary structure. These Aβ monomeric species can undergo physiological changes/ conformation changes and aggregation to form soluble oligomers (5-10 nm diameter and 6 nm height) and protofibrils (~180 nm length). The soluble oligomers undergo nucleation polymerization to form protofibrils and insoluble fibrils (**Figure 1.2**).[18] Recent studies have shown that soluble Aβ oligomers, rather than insoluble Aβ fibrils are the primary toxic species in AD.[19] Hence, the conversion of Aβ from a soluble, monomeric form to a soluble, aggregated forms appears to be the initial process of amyloid neurotoxicity. It is also

hypothesized that the intraneuronal accumulation of Aβ is the first step of the amyloid cascade.[20] Also it has been proved that intracellular Aβ induces a higher toxicity, being at least 10,000 times more toxic than extracellular Aβ.[21]

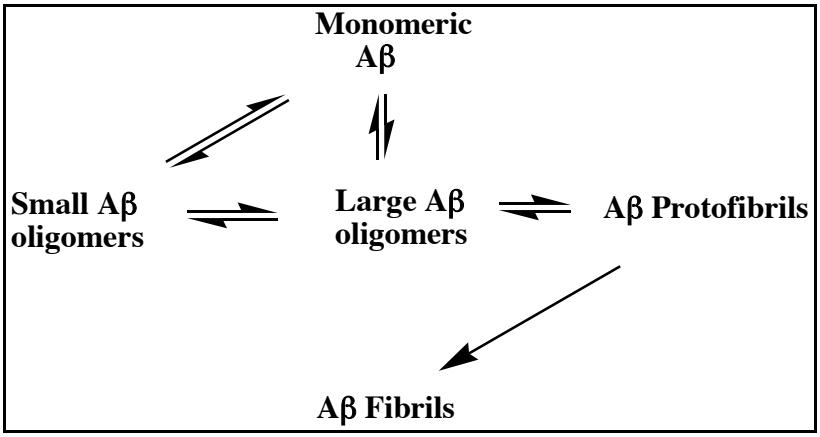

Figure 1.2. Proposed mechanism of Aβ aggregation from monomers to fibrils. (Modified from reference **18** without the author's permission)

Aβ oligomers and protofibrils are highly neurotoxic, even in nanomolar concentrations, *in vitro*.[21] Aβ42 is more toxic and tends to aggregate faster than Aβ40 due to its hydrophobicity. The following diagram shows the hydrophobicity indexes of the Aβ(1-42) peptide segment. The more positive units refer to the more hydrophobic β-sheet forming fragments. The more negative units refers to the more hydrophilic fragments (**Figure 1.3**).[22]

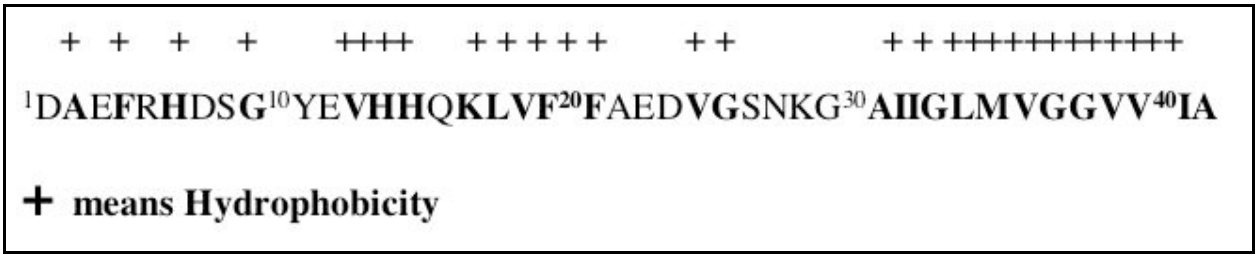

Figure 1.3. The hydrophobicity indexes of amyloid (1-42) sequence. (Modified from reference **22** without the author's permission)

Although the elucidation of the genetic, biochemical and biophysical origin of AD is very complex, a number of factors have been determined to be involved in neuronal damage.

Alzheimer's disease occur in two forms: (1) the rare, early onset familial AD (FAD), an autosomal disorder caused by mutations in APP, presenilin1 (PS1) and presenilin 2 (PS2) membrane proteins. (2) A common sporadic non-familial AD, which results in the generation of Aβ42.[23] Presenilins (PS1 and PS2) are integral membrane proteins with six to eight transmembrane domains. PS are mainly localized in the Endoplasmic reticulum (ER) and Golgi system.[24] Presenilin 1 (PS1) is believed to be an important component of the γ-secretase complex. Mutations in PS1 result in over production of the Aβ42.[25] The toxicity of Aβ peptide also includes individual or combinations of apoptosis[26] and the disruption of calcium ion homeostatis,[27] toxic radicals,[28] metal ions,[29] pH[30] etc as depicted in **Figure 1.4**.

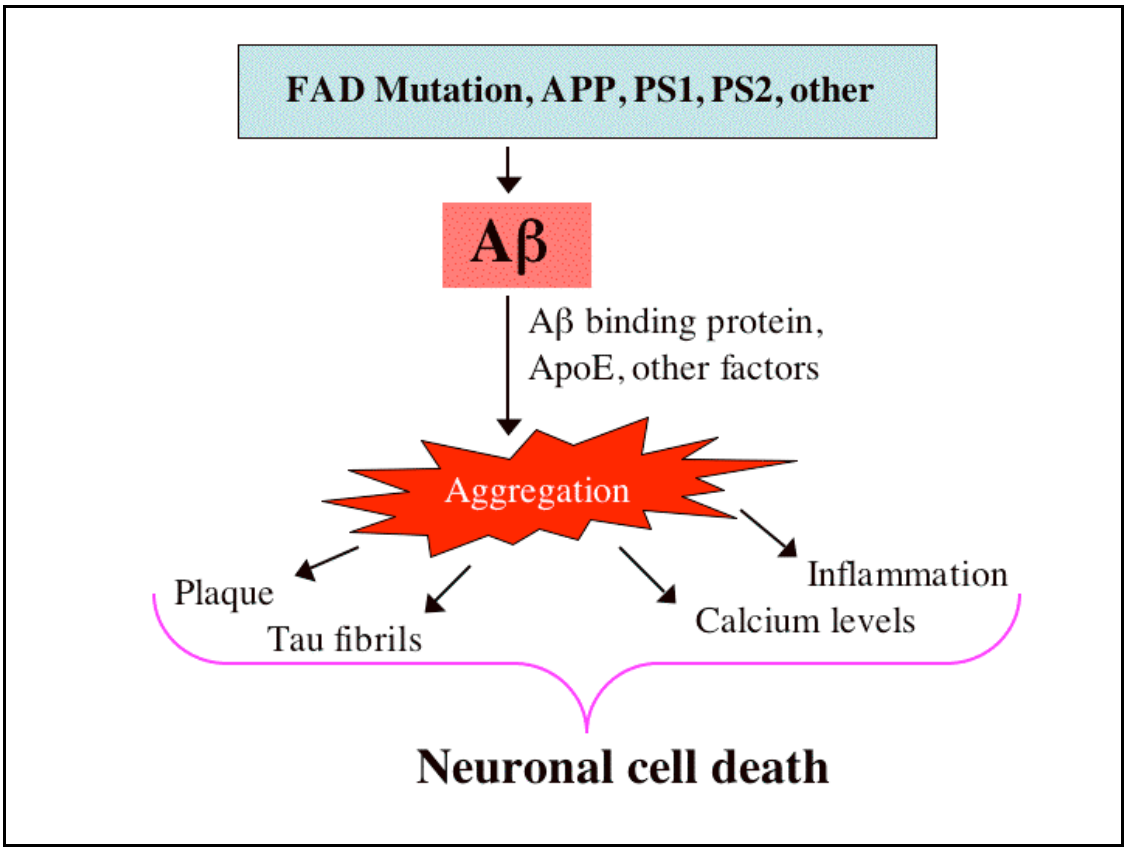

Figure 1.4. Contributing factors promoting Aβ aggregation and neuronal damage.

Recent studies have linked the Aβ aggregation with apolipoprotein E (ApoE).[31-32] ApoE is a 34 KDa (~299 amino acids) lipid transport protein, which is synthesized in liver and brain. It

exists in three isoforms in the human population, ApoE2, ApoE3 and ApoE4. In central nervous system ApoE is a common apolipoprotein in cerebrospinal fluid (CSF) and is secreted by glia cells in a high-density lipoprotein (HDL) like particle.[33] Strittmatter *et al.* showed that E4 allele of ApoE is a genetic risk factor of late onset Alzheimer's disease (LOAD).[34] The interaction of ApoE and Aβ was suggested when ApoE immunoreactivity was detected in extracellular amyloid deposits in AD brain. Recently, binding of the C-terminus residue of ApoE was observed with Aβ plaques and ApoE help to aid in the progression of small deposits to large deposits.[35] *In vitro* and *in vivo* data suggest that ApoE interaction with Aβ can affect mechanisms of both clearance and deposition of Aβ.[36-38]

It has been shown that several tricyclic pyrone (TP) compounds protect MC65 cells from cell death.[39] The structures of TP compounds are similar to that of pyripyropene A (**1**),[40] an acyl-coenzyme A cholesterol O-acyl-transferase (ACAT) inhibitor (**Figure 1.5**). Pyripyropenes were isolated from *Aspergillus fumigatus* FO-12189 as microbial metabolites that strongly inhibit ACAT. ACAT is an enzyme that catalyzes intracellular esterification of cholesterol. ACAT plays a critical role in the events that are contributing to atherosclerosis. Inhibitors of ACAT hold a promise as antiatherosclerotic agents. Recently, there is a growing body of evidence that links cholesterol to the development of Alzheimer's disease.[41,42] It has been showed that animals fed with cholesterol rich diets exhibit increased levels of Aβ over the normal or low cholesterol diet.[43] *In vivo* studies also support the above theory as increased cellular cholesterol levels result in the increase of Aβ production in rabbits and mouse models.[44] It was found that hypercholesterolemia induced by high cholesterol diet accelerated the Aβ deposition in APP-transgenic mice model of AD.[44] Refolo. et.al. reported that a cholesterol lowering drugs that inhibits 7-dehydrocholesterol-reductase enzyme (this enzyme increases the cholesterol biosynthesis), reduces the Aβ deposition in APP transgenic mice model.[44] Studies have been carried out on the interaction of Aβ with the plasma membranes, lipids including cholesterol and fatty acids.[45,46] Binding of Aβ to the lipids is dependent on the aggregation state of Aβ i.e. monomeric Aβ does not bind to the lipids, and aggregated form of Aβ was found to bind to lipids.[46] On the other hand, different groups have investigated the modulation effect of cholesterol on the interaction of Aβ and neuronal cell surface.[47-49] Probst *et al.* suggested that the initial deposition of Aβ occurs on the neuronal plasma membrane.[50] Later, Mori *et al.* found the

abnormal accumulation of cholesterol in Aβ plaques and suggested that cholesterol plays an important role in the formation of senile plaques.[51] Based on these findings, we synthesized and screened a number of tricyclic pyrone analogs, and discovered that a small molecule named CP2 (**2**) can protects MC65 cells from cell death. Synthesis of these tricyclic pyrone derivatives originated from our initial plan of synthesis of pyripyropenes. CP2 was found to be lipophilic and cell permeable with the ability to block Aβ aggregation and disaggregates toxic Aβ oligomers and protofibrils to non-toxic monomers in solution.[39, 52-54]

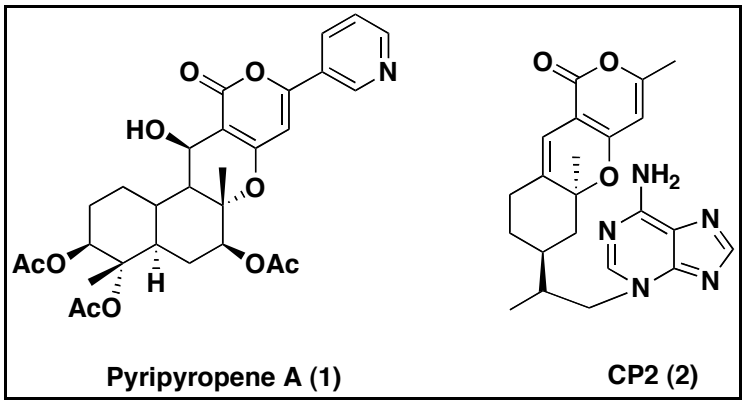

Figure 1.5. Structure of pyripyropene A and CP2.

1.2.1 Reported small compounds with potential Anti-Aβ activity

In the past decade, different organic compounds have been studied for the inhibition of aggregation of amyloid Aβ peptide as a therapeutic strategy for the treatment of AD. It includes apomorphine (**3**),[55] curcumin (**4**),[56] porphyrins (**5**),[57] congo red (**6**)[58], and Cu/Zn chelators such as Clioquinol, a 5-chloro-7-iodo-8-hydroxyquinoline (**7**)[59]. Congo red was the first reported small molecule to bind to the amyloid plaque. These compounds and their various analogs have shown to inhibit Aβ aggregation. Although the mechanism of inhibition of aggregation is still unknown, many reported small molecules inhibitors share a structural similarity i.e. planarity and aromaticity that allows the alignment with the β-sheet structure (**Figure 1.6**). Current research is also looking at metal mediated oxidative stress.[60,61] Abnormal levels of Cu, Zn and Fe have been reported in different parts of brain in neutrophil and plaque of a brain with AD. Concentration of

metal is 3-5 folds in AD patients when compared to a normal brain.[62] Iron, copper and zinc have shown to enhance toxicity in *in vitro* Aβ cultures.[63,64] It has been observed that Aβ peptides exert toxicity due to generation of cellular hydrogen peroxide, which facilitates apoptosis in neuron cell cultures.[65] Toxicity due to generation of H_2O_2 was confirmed by addition of catalase enzyme, which converts H_2O_2 to water.[66] It has been found that addition of Cu/Zn or Fe in 0.1-5mM initiate seeding of Aβ which induces aggregation. Resolubilzation of Aβ plaque from the postmortem AD brain has also been reported using metal chelators.[67] Since metals interact with Aβ peptide and induce aggregation, ligands with intermediate affinity can be utilized to bind to the metal atom and thus disrupt the metal protein interactions responsible for Aβ aggregation. Clioquinol, a 5-chloro-7-iodo-8-hydroxyquinoline (CQ) has shown to have strong complexation with Cu and Zn thus has shown promising results (Phase II clinical trails) towards AD therapy.[59]

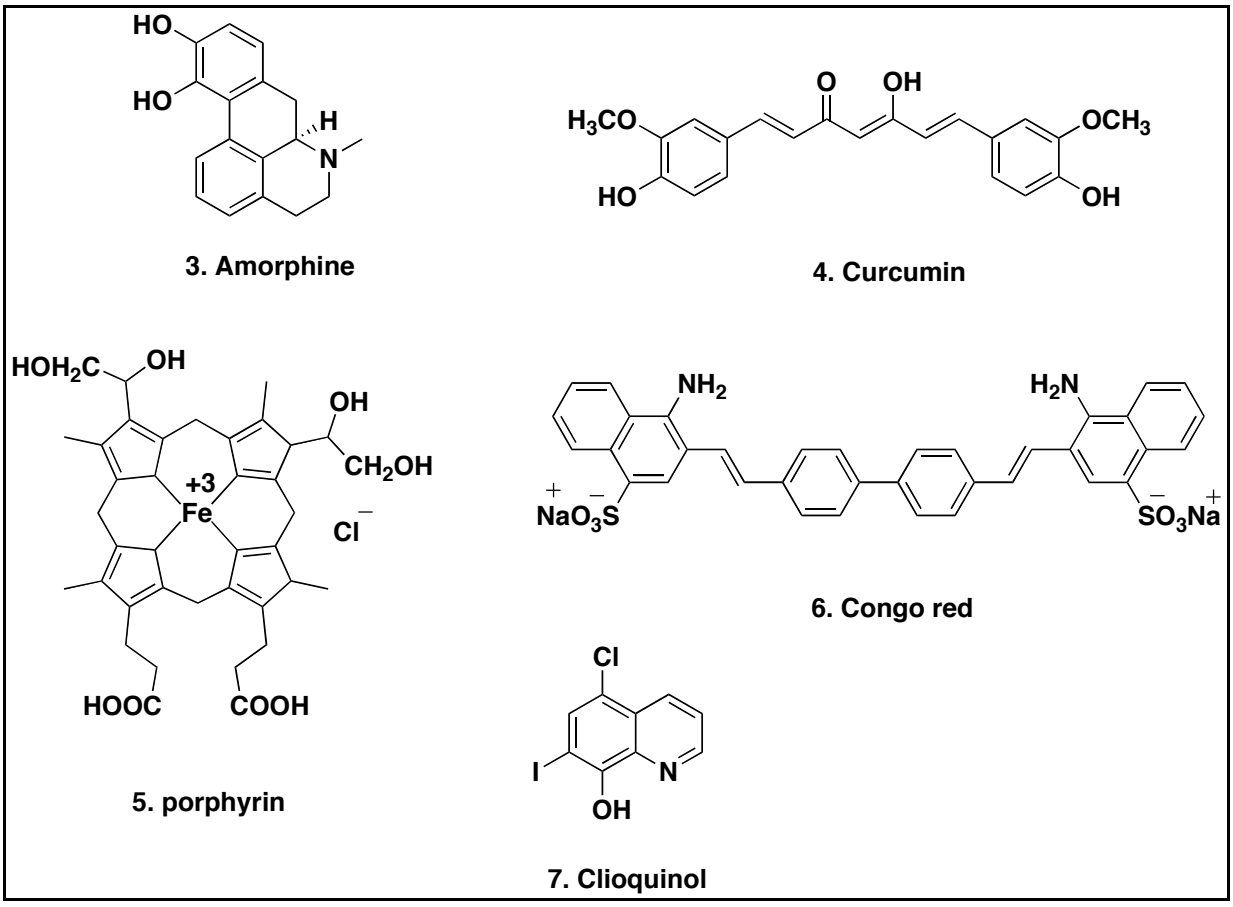

Figure 1.6. Reported organic compounds with anti-AD activity.

1.2.2 Natural bioactive compounds with lactone core

Tricyclic pyrone molecule CP2 has pyran functionality, and it exists in a range of biologically active compounds. Arisugacins A (**8**) and B (**9**) metabolites, structurally similar to pyripyropenes, are extracted from the culture broth of *Penicillium sp*. and possess potent and selective acethlcholinesterage (ACHE) inhibitory activities. The IC_{50} of arisugacins A and arisugacins B is 1 nM and 26 nM respectively.[68-69]

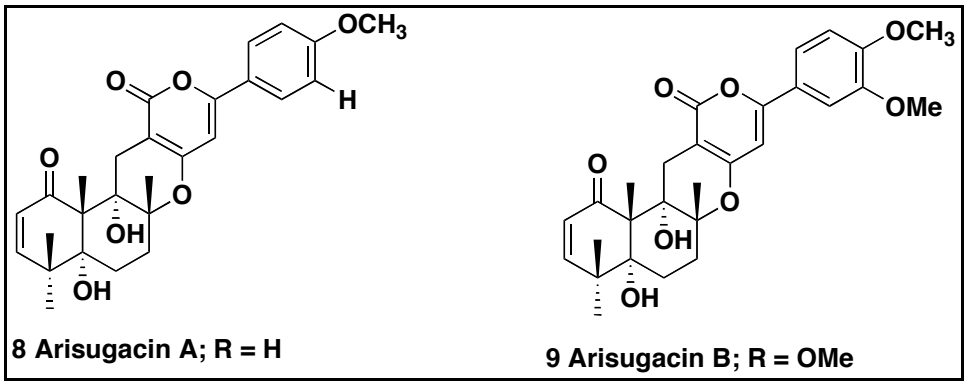

Figure 1.7. Bioactive microbial metabolites possessing pyran functionality.

Over the past 15 years, a number of engineered aromatic polyketides (**figure 1.8**) have been synthesized by using enzyme subunits (polyketides synthase enzymes; PKSs). These natural polyketide compounds have different structural backbones, but all contain 4-hydroxy-6-methyl-2-pyrone functionality.[70] These engineered polyketides can be viewed as a library of aromatic pyrones, which can be used for the synthesis of different bioactive compounds of medicinal interest.[70] Ridley *et al.* synthesized a series of polyketides from the compounds shown in **Figure 1.9** by exploiting their pyrone core moiety, which was condensed with different α,β-unsaturated aldehyde (**17**, **18** and **19**). Rearrangement proceeds via a Knoevenegal 6π-electrocyclic ring closing reaction mechanism, whereby the amine-activated aldehyde undergoes a nucleophilic attack by the pyrone. Novel engineered pyranopyrones (**Figure 1.9**) were evaluated as tumor inhibitors in three different cell lines.[70] Hua *et al*. also reported the synthesis of a library of tricyclic pyranopyrones and found that only tricyclic pyrone with pyridine ring at position C11 are toxic to cells (structurally similar to arisugasin) and thus studied for

acetylcholinesterase (AChE) inhibitory activity whereas methyl group at C11 position are completely non-toxic to cells.[71]

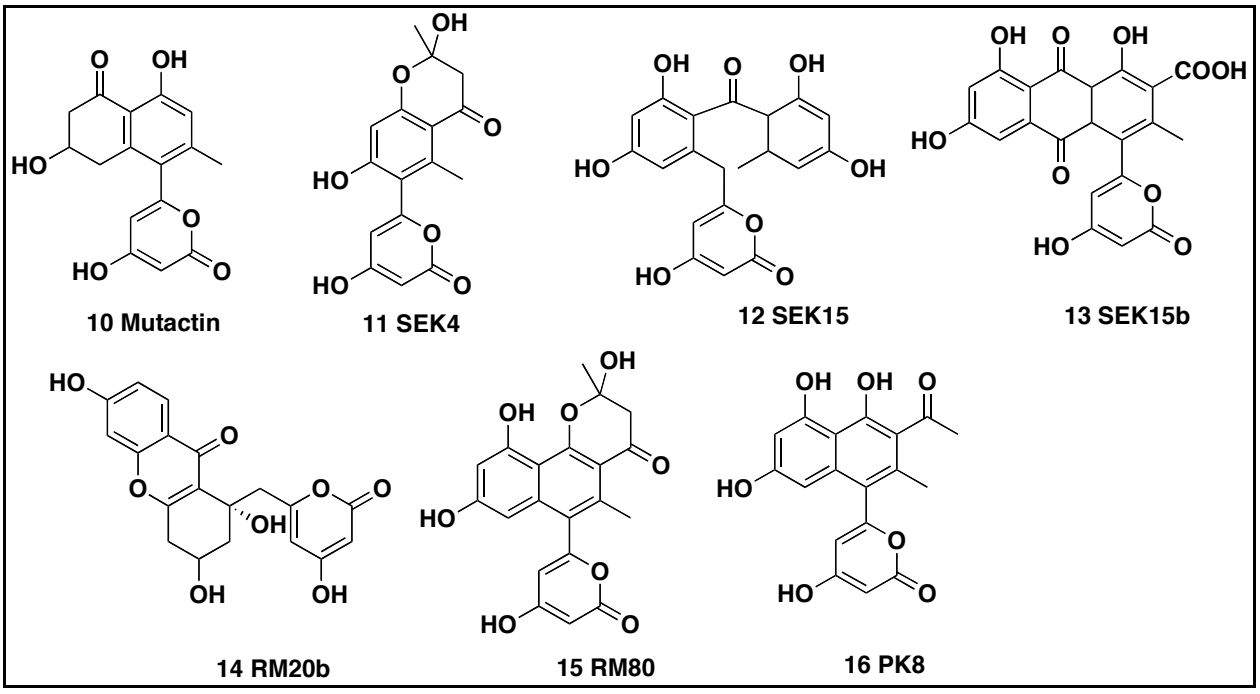

Figure 1.8. Structures of engineered type II polyketides.[70]

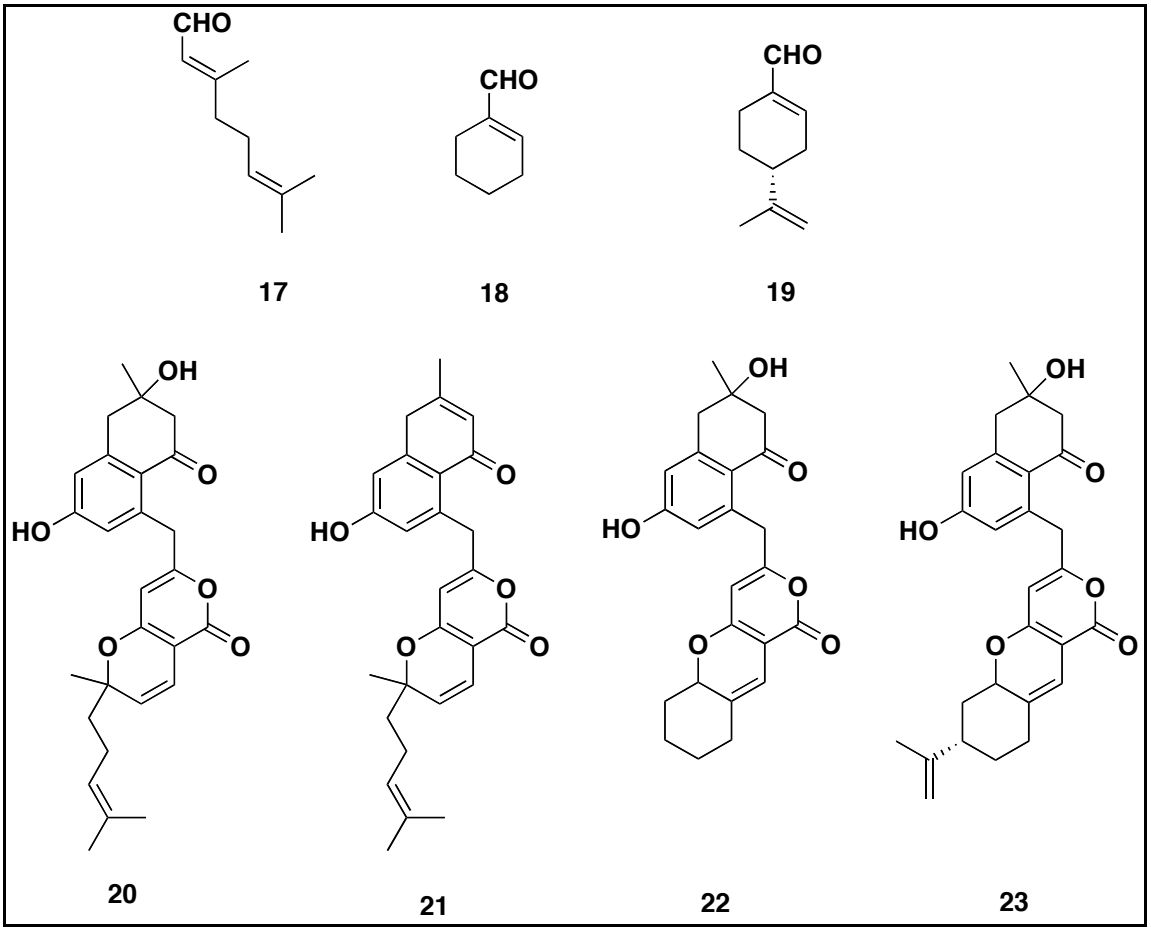

Figure 1.9. Aldehyde used (**17 - 19**) and the pyranopyrones prepared (**20 – 23**) in this study.[70]

1.2.3 Previous studies in our laboratory

Previous studies in our laboratory have found that a tricyclic pyrone compound namely CP2 showed protection against MC65 cells, a human neuroblastoma cell line with IC_{50} = 0.18mM.[52] In our laboratory, Dr. Yi Chen[72] synthesized CP2 in four steps (**Scheme 1.1**). 4-hydroxy-6-methyl-2-pyrone (**24**) and perillaldehyde were condensed in the presence of L-proline and ethyl acetate to afford a tricyclic pyrone. In order to induce chirality, (*S*)-(-)- perillaldehyde (**25**) was employed, and when refluxed with pyrone molecule (**24**) and L-proline, a single diastereoisomer (**26**) of tricyclic pyrone was obtained in a 78% yield.[71] The compound obtained was purified by crystallization from hot ethyl acetate to afford yellow needle shape crystals and the structure and stereochemistry at C-5 was unambiguously determine through X-ray

crystallography analysis.[71] The mechanism for this condensation reaction has been proposed to take place via a 1,2 addition followed by dehydration and subsequent 6π- electrocyclic ring closing reaction (**Scheme 1.2**).[71] The reason for the asymmetric induction might be from the isopropylene group since it needs to adopt the equatorial conformation to keep low transition energy, thus inducing an axial stereochemistry at C5 carbon. Selective hydroxylation of the terminal double bond in **26** was carried out by hydroboration followed by oxidation to yield two diastereomers (1:1) of alcohol (**27**) in a 69% yield. Mesylation of the alcohol (**27**) was achieved by treating alcohol with triethylamine and methanesulfonyl chloride to afford **28** in 94% yield. The mesylate **28** and adenine were taken together and heated in freshly distilled dimethylacetamide (DMA dried by CaH_2) at 150°C for 8 h. Column chromatographic separation provided two diastereomeric products (**2,** more polar, N-3) and (**29,** less polar, N-9 analog) in 10:1 ratio respectively.[52]

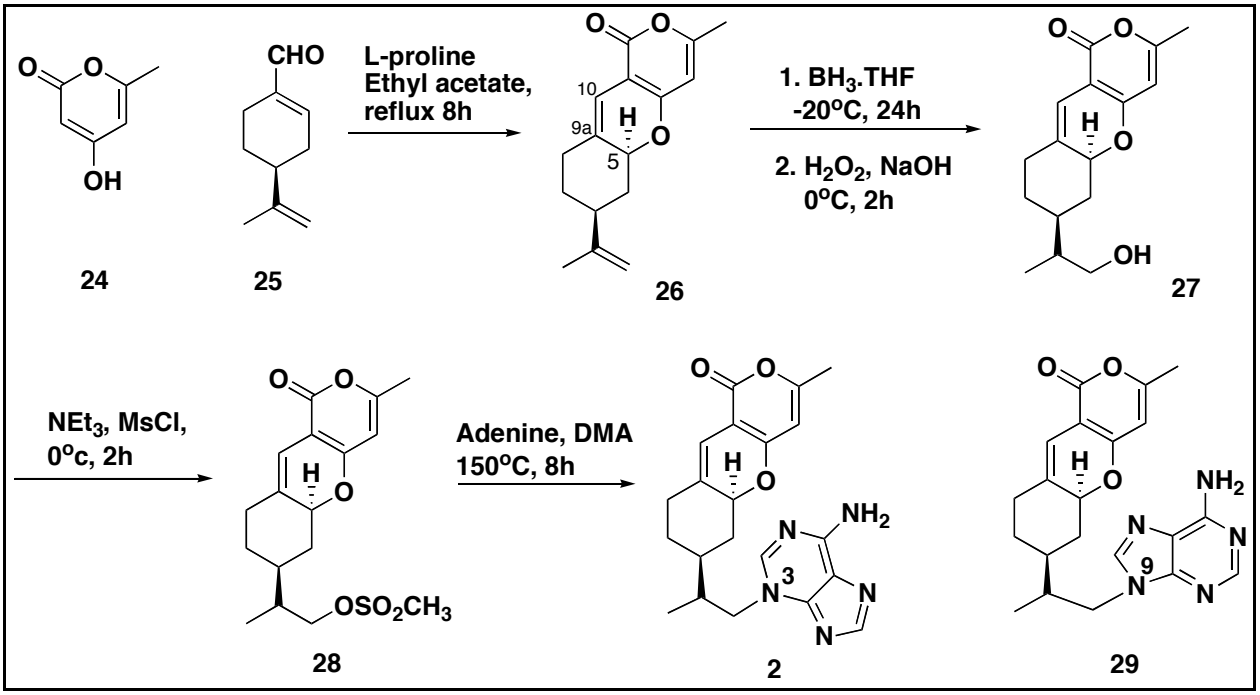

Scheme 1.1 Syntheses of CP2 (code name; **2**) and TP3 (code name; **29**).

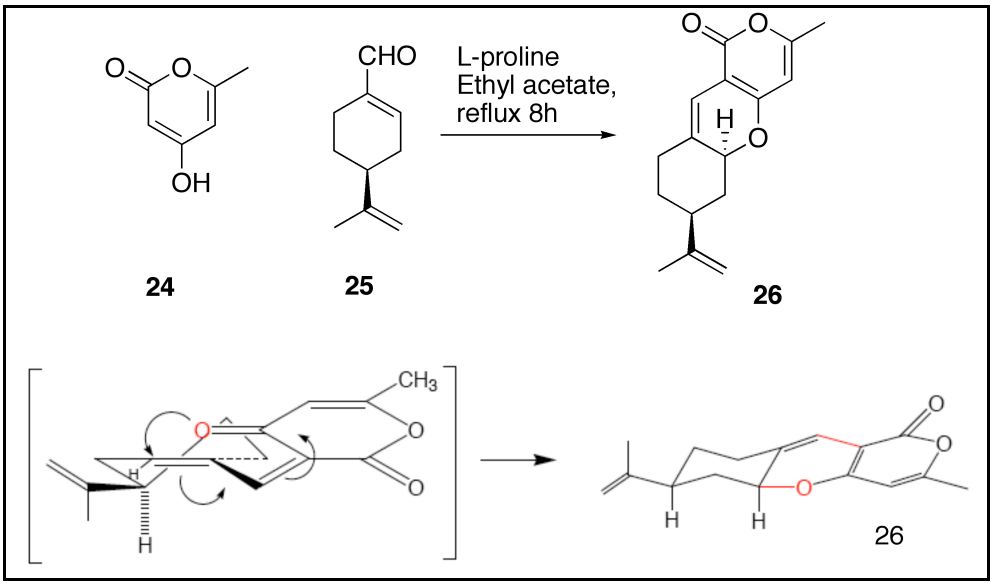

Scheme 1.2. Proposed mechanism for the synthesis of tricyclic pyrone molecule **33**.

A successful condensation reaction between a 4-hydroxy pyrone cyclohexen-1-carbonaldehyde was accomplished in good yield and has substantial applicability in forming fused ring structures. Although there were multiple double bonds in TP structure, but selective hydroxylation was achieved by using 0.33 equivalents of borane and the reaction was carried out at low temperature. If the hydroboration was performed at room temperature both the isopropylene double bond and internal C9a and C10 would have been hydroxylated. Regiochemistry at N3 and N9 in compound **2** and **29** was unequivocally assigned with the help of ^{2}D-HMBC spectroscopy, where the correlation between carbon of CH_2N and adenine proton was observed.

1.3 Results and Discussion

My research project involved the synthesis and modification of tricyclic pyrones and pyridinones and the study of their anti-alzheimer activities. First project involved the modification of CP2 molecule. Our purpose is to make these tricyclic compounds more water-soluble and to improve their biological activity. Introducing a polar group such as alcohol at C-11 position, might improve the hydrophilicity and thus form better hydrogen bonding with the

Aβ peptide. Since CP2 has a stereocenter at position C-12, another modification of CP2 is to have a double bond at C-12 and avoid diastereomeric mixture and study its biological activity. Since nitrogen containing compounds often increase bioactivities and brain–penetrating ability, a prudent modification is the displacement of oxygen atom at position 2 and position 5 with a nitrogen atom. CP2 molecule has adenine unit attached to it, we want to examine the effect of other purine- and pyrimidine- units to the TP and their M65 cell protective activities.

1.3.1 Modification at C-11 position of CP2

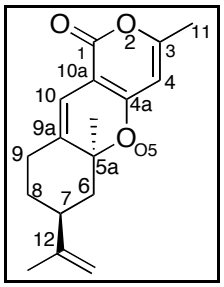

The first modification involved the addition of a hydroxyl group on the C-11 methyl group. Dr. Chen first introduced an acid group at C-11 position by treating pyrone (**26**) with 1.5 equivalent of freshly prepared LDA at –78°C for 3 h. Anion formation was visible by the appearance of a blue color in the reaction mixture. Anion formed was stabilized by the addition of HMPA. The reaction mixture was stirred for 3h and the reaction was quenched by carbon dioxide. The product was obtained in excellent yield. Similarly, when anon was quenched by the addition of excess para-formaldehyde, compound (**30**) was obtained in 28% yield. Several attempts have been made to improve the yield but went in vain. The compound **30** was not stable at room temperature and was used quickly in the next reaction. Alcohol **30** was treated with acetic anhydride in pyridine at 0°C overnight to afford **31** in a 62% yield. Selective hydroxylation of **31** was obtained by hydroboration followed by oxidation. This afforded two diastereomers at C-12 of alcohol **32** in 1:1 ratio with a 56% yield. Alcohol **32** was mesylated using methanesulfonyl chloride and triethylamine at 0°C in 90% yield. Mesylate **33** was displaced with adenine by heating the reaction mixture in dry DMA in 150°C to afford **34** in 8% yield after purification by column chromatography (**Scheme 1.3)**. Low yields were due to the

decomposition of reaction at high temperature, and no reaction was observed at a low temperature.[72] The final step involved the removal of acetate group, but compound **34** was decomposed in basic conditions.

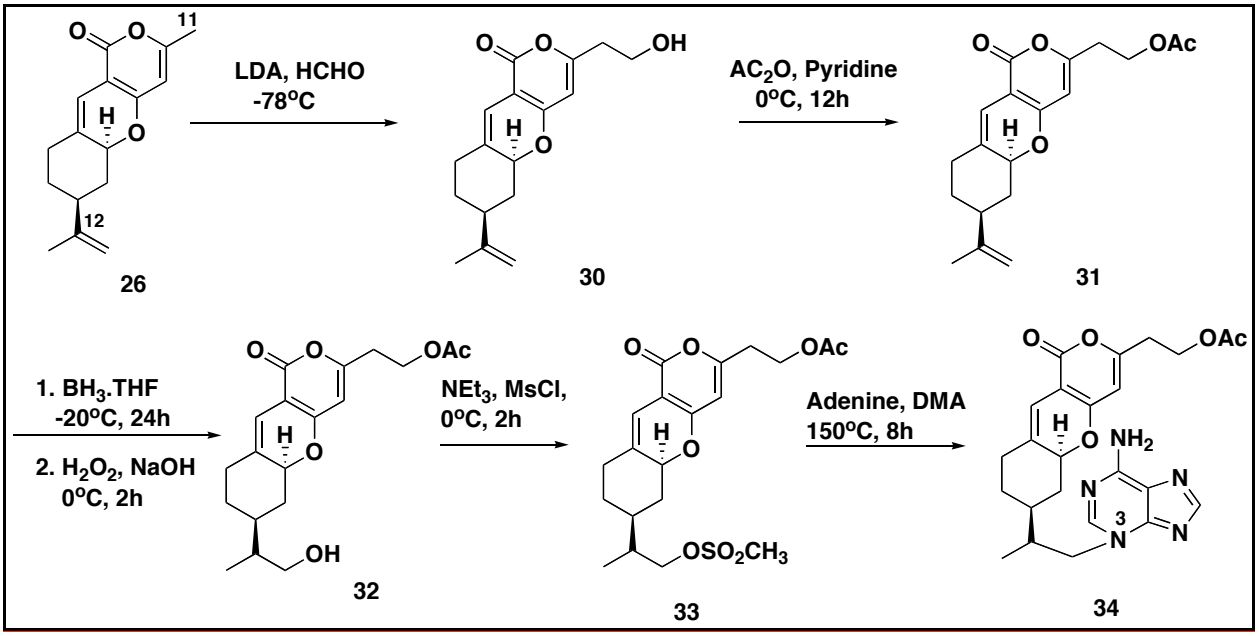

Scheme 1.3. Modification at C-11 methyl of CP2.

1.3.2 Synthesis of CP2 analog with a double bond at C12

Since CP2 compound contains two diastereomers, they were difficult to separate. We want to remove the stereocenter at C12 by introducing a double bond. Pyrone **26** was treated with SeO_2 and t-butylhydrogen peroxide in methylene chloride solvent, which produced **36** with a 22% yield. An alternative method was employed. This method involved the treatment of pyrone **26** with 0.1 equivalents of palladium (II) acetate, 3 equivalents of hydroquinone, and 0.2 equivalents of diethyl malonate, together in acetic acid solvent, which afforded compound **35** in a 60% yield after purification by column chromatography.[74] Hydrolysis of the acetate function of **35** was carried out using potassium carbonate in methanol at 0°C for 1h, which furnished **36** in a 82% yield. Alcohol **36** was treated with triethylamine followed by the addition of methanesulfonyl chloride to obtain compound **37** in 41% yield. Displacement of the mesylate

moiety with adenine was obtained by heating the reaction mixture in DMA at 150°C for 8 h to give compound **38** in a 26% yield.[75] The regiochemistry at N3 position of **38** was unequivocally assigned by 2D-HMBC NMR spectroscopy where a cross peak between CH_2N and C2'H (δ 8.02) was observed **(Scheme 1.4)**.

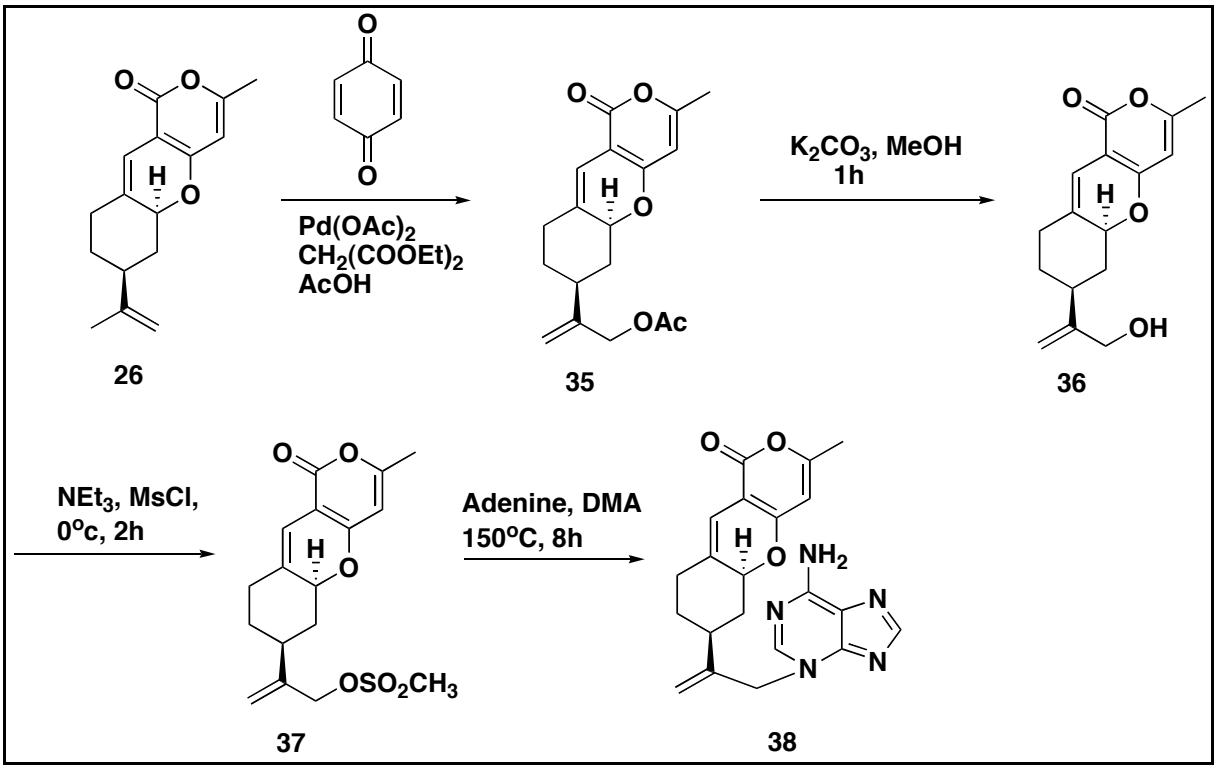

Scheme 1.4. Synthesis of CP2 analog, compound **38**.

1.3.3. Synthesis of heterocyclic pyrone analogs

The CP2 molecule has adenine unit attached to it. We want to examine the effect of other purine, pyrimidine, units and heterocyclic compounds to the TP and their M65 cell protective activities. Similar to CP2 synthesis, other heterocyclic TP analogs can be synthesized by treating mesylate (**28**) with other heterocyclic compounds. Yields obtained using same condition were moderate and required high temperatures. An alternate route was designed where alcohol **27** was converted to bromide (**39**) using PPh_3 and CBr_4 in 91% yield (**Scheme 1.5**). Adenine has a C6

amino electron donating effect, which leads to the nucleophilic attack at the N-3 position. 6-chloropurine has no such electron donating effect thus no nucleophilic displacement reaction with bromide was observed. On the other hand, use of NaH with bromide and 6-chloropurine at 80°C for 12 h yielded N9 analog **40** in 82% yield (**Scheme 1.5**).[75]

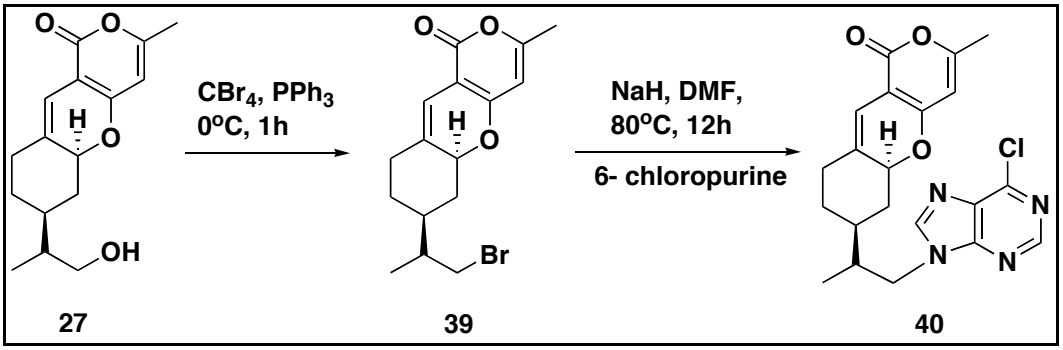

Scheme 1.5. Synthesis of TP analog **40.**

Treatment of bromide and cytosine was studied and two compounds, **41** and **42,** were obtained. Compound **41** was the obtained in 28% yield, and the regiochemistry at N1 was unequivocally assigned by 2D-NOESY NMR spectroscopy where NOE correlation between CH_2N (δ 3.93 and 3.37 ppm) and C6-H of cytosine (δ 7.21 ppm) was observed. Also, the C13 carbon peak of CH_2N in **41** is 53.9 ppm whereas the C13 carbon peak of CH_2O in **42** is 69.7 ppm (**Scheme 1.6**).[76,77] Other bases such as Cs_2CO_3 and K_2CO_3 were also used but no improvement in the yield was observed.

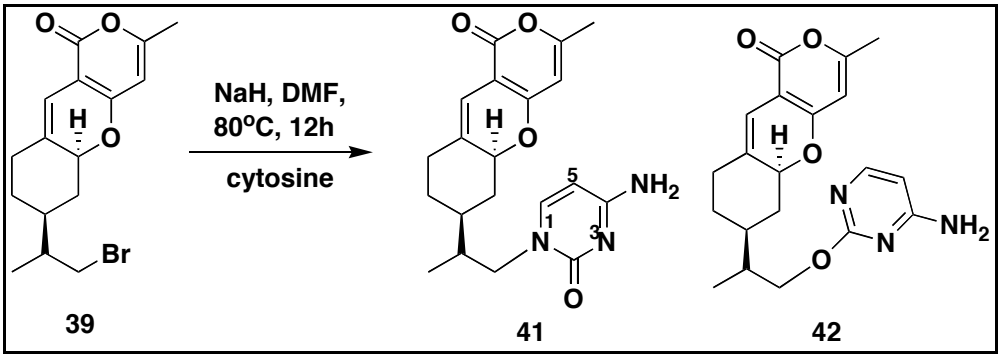

Scheme 1.6. Syntheses of TP analogs **41** and **42**

Using similar conditions, other heterocyclic analogs were synthesized from 3-amino-pyrazole-4-carbonitrile, 2-mercaptopyrimidine, thymine, and guanine respectively. The separate displacement reaction of bromide **39** with 3-amino-pyrazole-4-carbonitrile, 2-mercaptopyrimidine, thymine and acetylated guanine with sodium hydride afforded displacement products **43**, **44, 45** and **46** respectively. The N1 regiochemistry of **43** was unequivocally assigned by NOE spectroscopy.[78] Treatment of bromide and 2-mercaptopyrimidine with NaH was carried out and compound **44** was obtained, which is consistent to the reported literature.[79] (**Scheme 1.7**)

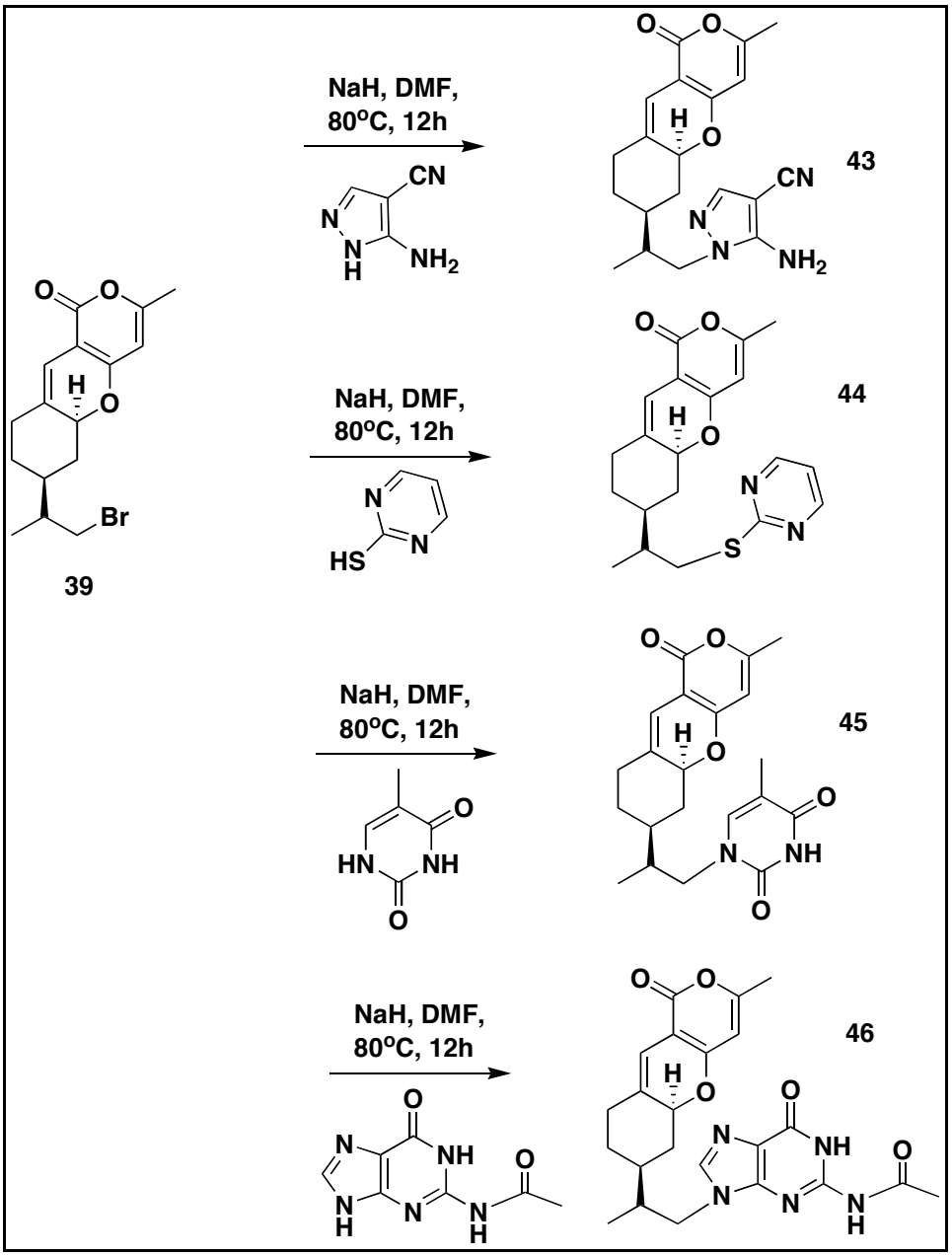

Scheme 1.7. Syntheses of TP analogs **43, 44, 45** and **46.**

Similarly, the N1 regiochemistry of **45** was unequivocally assigned by NOE spectroscopy. NOE correlation was observed between the CH_2N (δ 3.82 and 3.40 ppm) and the C6-H of thymine (δ 6.94 ppm).[80] Treatment of bromide (**39**) and guanine with 1 equivalent was studied, and to our surprise, no product was obtained. When heated at high temperature, the starting material was decomposed and bases other than NaH were used but no product was isolated. The literature has shown some evidence that in order to obtain N9 alkylation, we have

to protect the C2 amino group of guanine.[81-82] N9-alkylated product **46** was isolated with a 15% yield when N2-acetylated guanine and NaH when treated with bromide. NOE correlation was observed between the CH_2N (δ 4.46 and 4.03 ppm) and C8-H (δ 7.73 ppm) proton (**Scheme 1.7**).

Compound **47** has a structure similar to CP2 but is fluorescent in nature thus can be used for staining of plaques with fluorescence microscopy. No displacement reaction of 2-aminopurine and bromide was observed, when no base was used. Different bases were used and Cs_2CO_3 yielded the compound **47** in 48% yield. The N9 regiochemistry was assigned by NOE correlation between the CH_2N ((δ 4.10 and 3.89 ppm) and the C8-H proton ((δ 7.71 ppm) and no correlation was observed between CH_2N and C6-H proton (**Scheme 1.8**).[83]

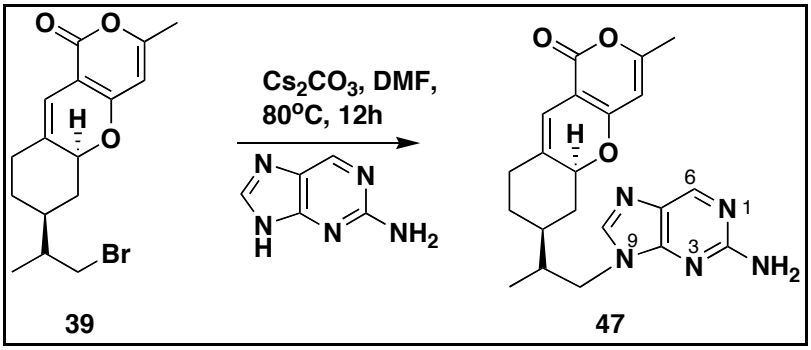

Scheme 1.8. Synthesis of TP analogs **47**.

The amine group is a polar group and is known to be important in lots of compounds. Therefore, efforts were made to attach an amino group directly to the tricyclic pyrone core. Dr. Yi Chen did it by selective hydroxylation of tricyclic pyrone **26** followed by oxidation to produce **27**. Mesylation, nucleophilic substitution and reduction of azide were carried out and the desired amine **48** was obtained. We are interested in this amine moiety because various polar heterocyclic aldehydes can be coupled to the tricyclic pyrone core. An alternative route to the amine synthesis was followed. The desired amine was obtained, which is being used to synthesize different analogs, by treating the tricyclic pyrone with BH_3•THF and in situ refluxing with hydroxylamine-*O*-sulfonic acid (**Scheme 1.9**).

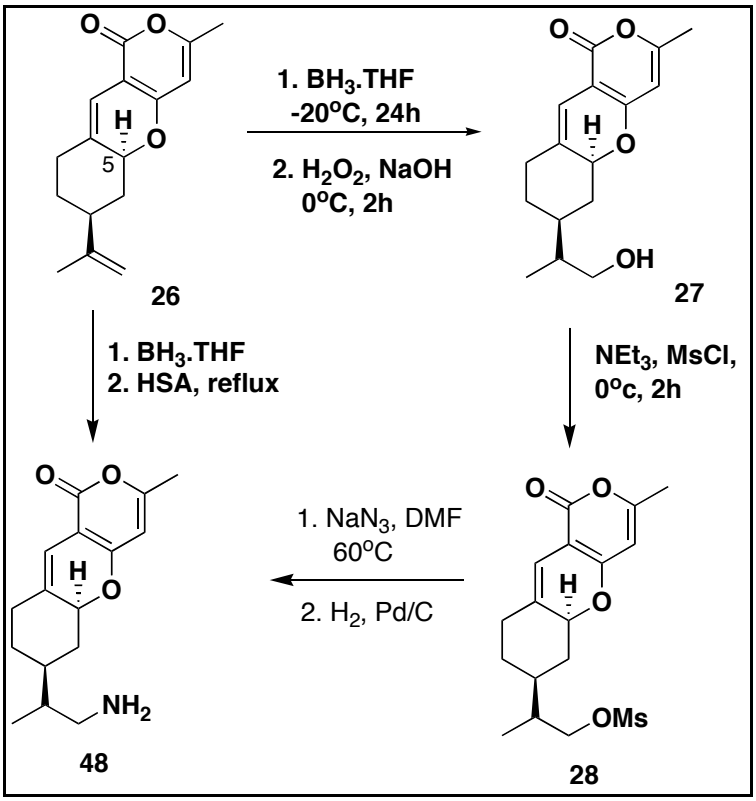

Scheme 1.9. Synthesis of TP analog **48**.

1.3.4 Synthesis of pyrone compounds having nitrogen in middle ring: pyranoquinolinone and pyranoisoquinonlinone compounds

Since nitrogen containing compounds often exhibit increased bioactivity and brain-penetrating abilities, only O5'-analogs have been synthesized in our laboratory. Another prudent modification with a potentially interesting anti-Alzheimer activity would involve the displacement of the oxygen atom (O5') with a nitrogen atom in the middle ring of tricyclic pyrone. Dr. Chen synthesized 4-amino-6-methyl-2-pyrone (**51**) from 4-hydroxy-6-methyl-2-pyrone (**24**) in three steps (**Scheme 1.10**).[84] He was interested in expanding the application of new condensation reaction (**Scheme 1.2**) towards the synthesis of biologically potent compounds. Compound **24** was stirred in DMF. Then PBr_3 in diethyl ether was added dropwise with constant stirring at 0°C followed by heating the reaction mixture at 60°C overnight. This

yielded compound **49**, which was purified by column chromatography (81% yield).[84] The bromide was converted to azide by its treatment with sodium azide in DMF at 0°C followed by column chromatography which afforded compound **50** in a 80% yield. Reduction of azide **50** to amine **51** was achieved by treating the azide with Pd/C in ethanol at room temperature to form the product in a quantitative yield.[84] To their surprise, when amine **51** and cyclohexene-2-carbonaldehyde was refluxed in ethyl acetate, no reaction was observed. Several other attempts have been made but in vain. Eventually, a successful condensation reaction between amine (**51**) and aldehyde was observed in 0.1 equivalents of (S)-(+)-10-camphorsulfonic acid to give a mixture of linear tricyclic pyranoquinoline (19%) and L-shaped pyranoisoquinoline (48%). We extended the application of the reaction by using amine **51** and (*S*)-(-)-perillaldehyde (**25**) and (*d*)-camphor sulfonic acid, using toluene as a solvent and heated to 85°C for 3 days. This resulted in the formation of two compounds (**52** and **53)** in 1:1 ratio, which were separated by column chromatography in 36% yield (**Scheme 1.10**).[75]

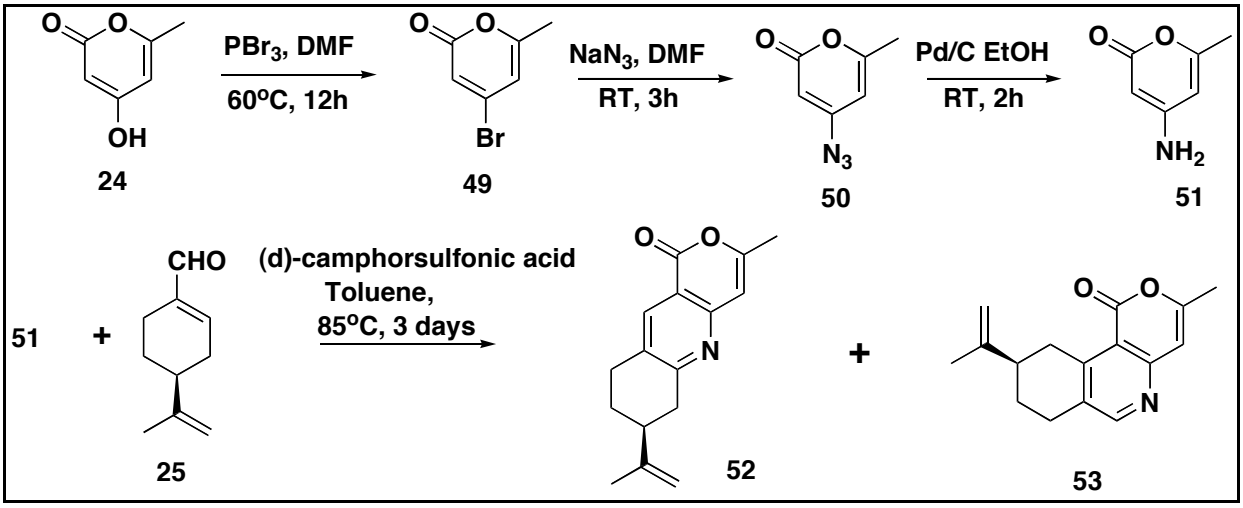

Scheme 1.10. Synthesis of pyranoquinolinone **52** and pyranoisoquinonlinone **53**.

The reaction proceeds in two different pathways for the formation of **52** and **53**. The proposed mechanism for the formation of **52** is same as that of tricyclic pyrone. The condensation reaction has been proposed to take place via a 1,2 addition followed by dehydration and subsequent 6π- electrocyclic ring closing reaction. Compound **53** involved the imine formation followed by 6π- electrocyclic ring closing reaction (**Scheme 1.11**).

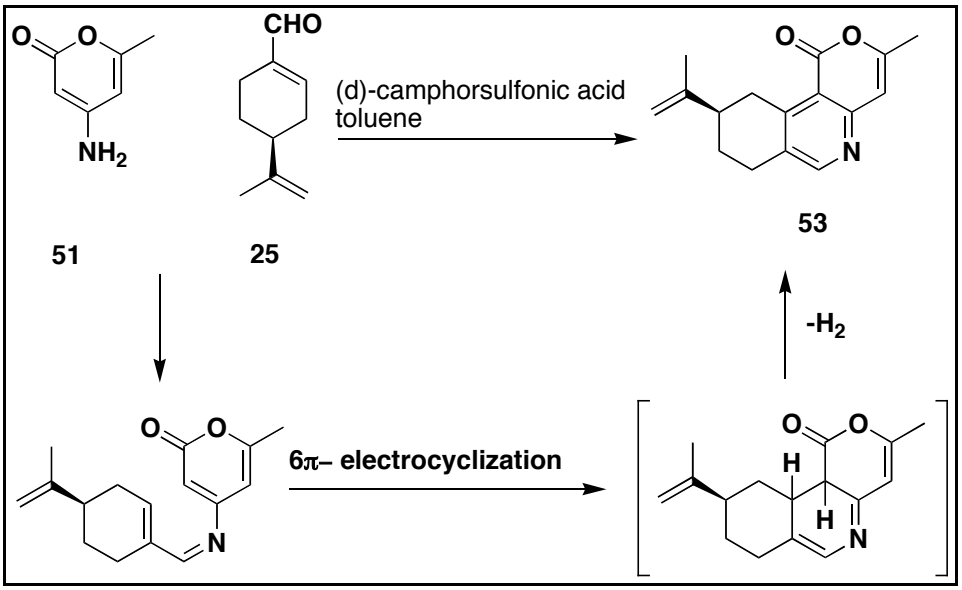

Scheme 1.11. Proposed mechanism for synthesis of **53.**

1.3.5 Synthesis of novel pyranopyridinone analogs (N2'-analogs)

Water solubility is an important factor for any compound to be used in a biological system. With this aim in mind, an attempt has been made to increase the solubility of these tricyclic compounds. It can be achieved by replacing the oxygen atom at position 2 of pyrone with a nitrogen atom. This was achieved by heating 4-hydroxy-6-methyl-2-pyrone (**24**) and *p*-methoxy benzyl amine MPM (**54**) in water for 24h followed by filtration of desired compound **55** in 60% yield.[80] We suspect the attack of amine group to MPM to the pyrone and leads to ring opening followed by dehydration to form a MPM-protected pyridinone. Compound **55** was treated with perialdehyde (**25**) in the presence of piperidine and glacial acetic acid and refluxed overnight in chloroform to give **56** in a 90% yield as a single diastereomer.[85] The proposed mechanism is shown in **Scheme 1.12**. Selective hydroxylation of **56** was achieved by hydroboration followed by oxidation to furnish compound **57** in a 69% yield. The mesylated product **58** was obtained by treating the alcohol with triethylamine and methanesulfonyl chloride. Displacement of methanesulfonyl functional group with adenine was achieved by

heating the reaction mixture in DMA at 150°C. Compound **59** was purified by column chromatography. The N3'-regiochemistry is similar to that of CP2 (**2**) and is unequivocally assigned by 2D NOESY NMR spectroscopy (**Scheme 1.12**). The final step involved the removal of the MPM group but was unsuccessful with DDQ, CAN, and TFA as either no reaction or decomposition of the starting material was observed. An alternate approach was therefore employed (**Scheme 1.12**).[75]

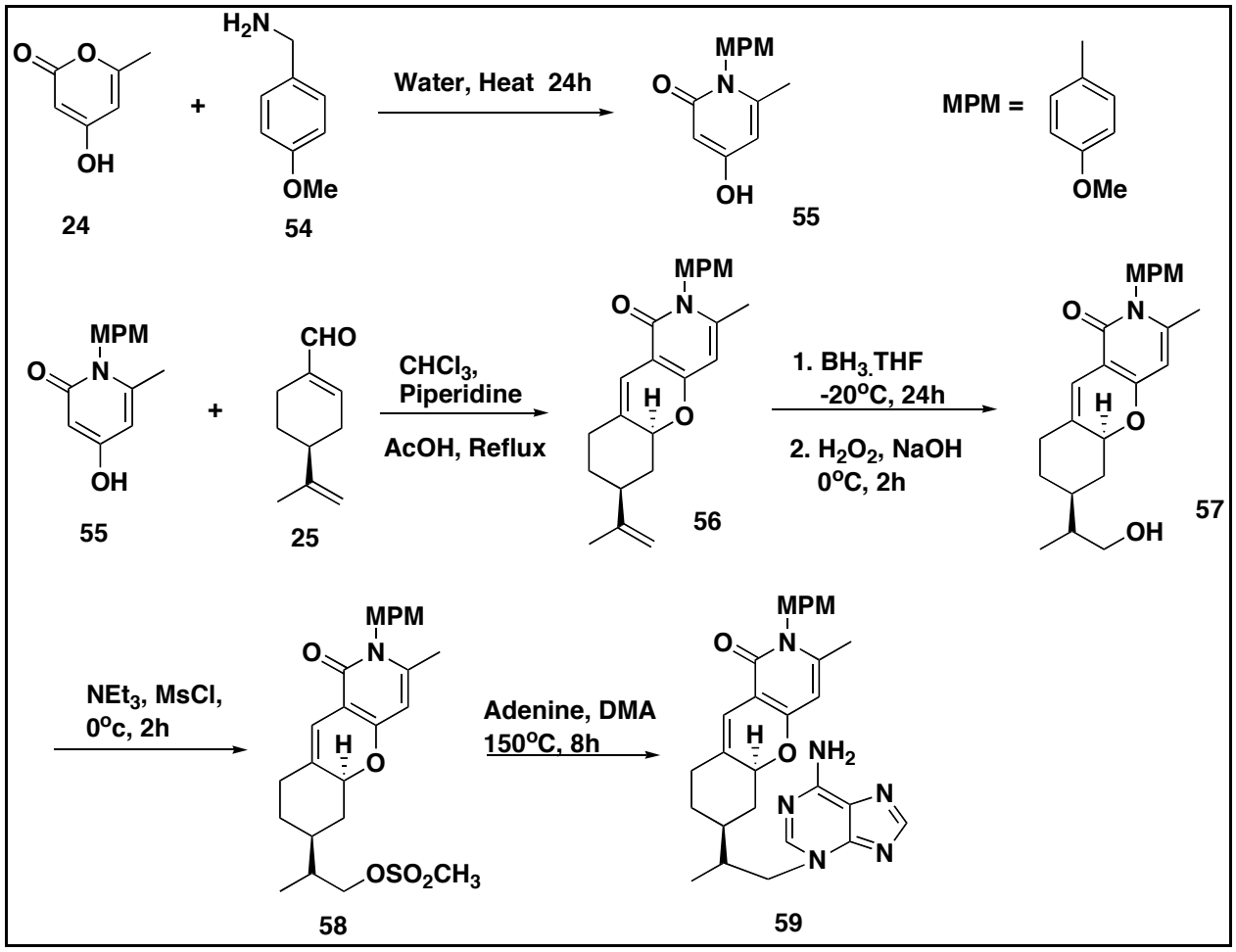

Scheme 1.12. Synthesis of a novel protected N2' pyridinone compound.

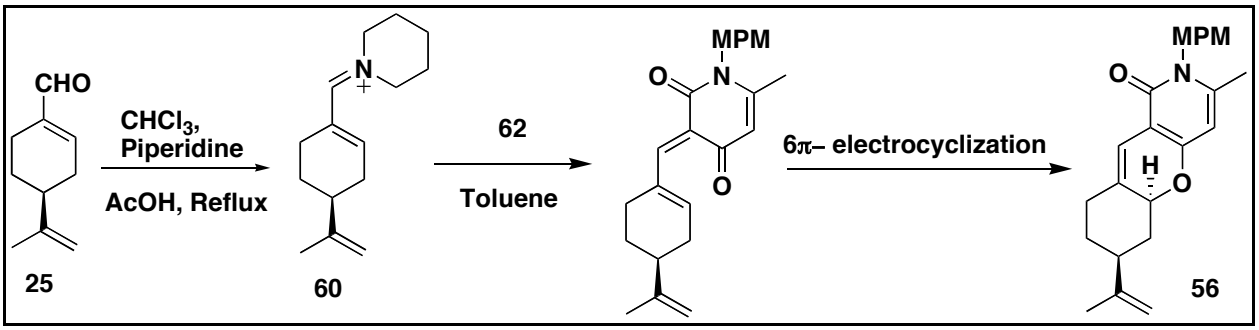

Scheme 1.13. Proposed mechanism for the synthesis of tricyclic pyrone molecule **56.**

4-hydroxy-6-methyl-2-pyrone (**24**) was heated in the presence of a 28% NH_4OH solution for 6 h, resulting in the formation of yellow precipitate, which was filtered and crystallized from ethanol to afford **61** in an 80% yield as a yellow solid.[86] A mixture of pyridinone (**61)**, perialdehyde (**25**), piperidine and glacial acetic acid was refluxed overnight in chloroform to yield **62** in a 91% yield.[85] Protection of the pyridinone nitrogen was achieved by its treatment with triethylamine base followed by addition of di-tert-butyldicarbonate $(Boc)_2O$ at 0°C overnight to afford **63** in 97% yield. Selective hydroxylation of the terminal double bond was obtained by treating **63** with BH_3•THF in THF at –20°C followed by oxidation with H_2O_2 and NaOH, which resulted in the formation of compound **64** in 65% yield as two diasteromers in 1:1 ratio. Mesylated product **65** was obtained by treating the alcohol with triethylamine and methanesulfonyl chloride in a 79% yield. Displacement of the mesyl functional group with adenine was achieved by heating the reaction mixture in distilled DMA at 150°C for 8 h. Compounds **66** and **67** were purified by column chromatography. Because of high reaction temperature, the Boc protecting group was removed during the course of the reaction (**Scheme 1.14**). The N3 and N9 regiochemistry of **66** and **67** was unequivocally assigned using 2D NOESY spectroscopy and was in agreement with compound **2** and **29**.

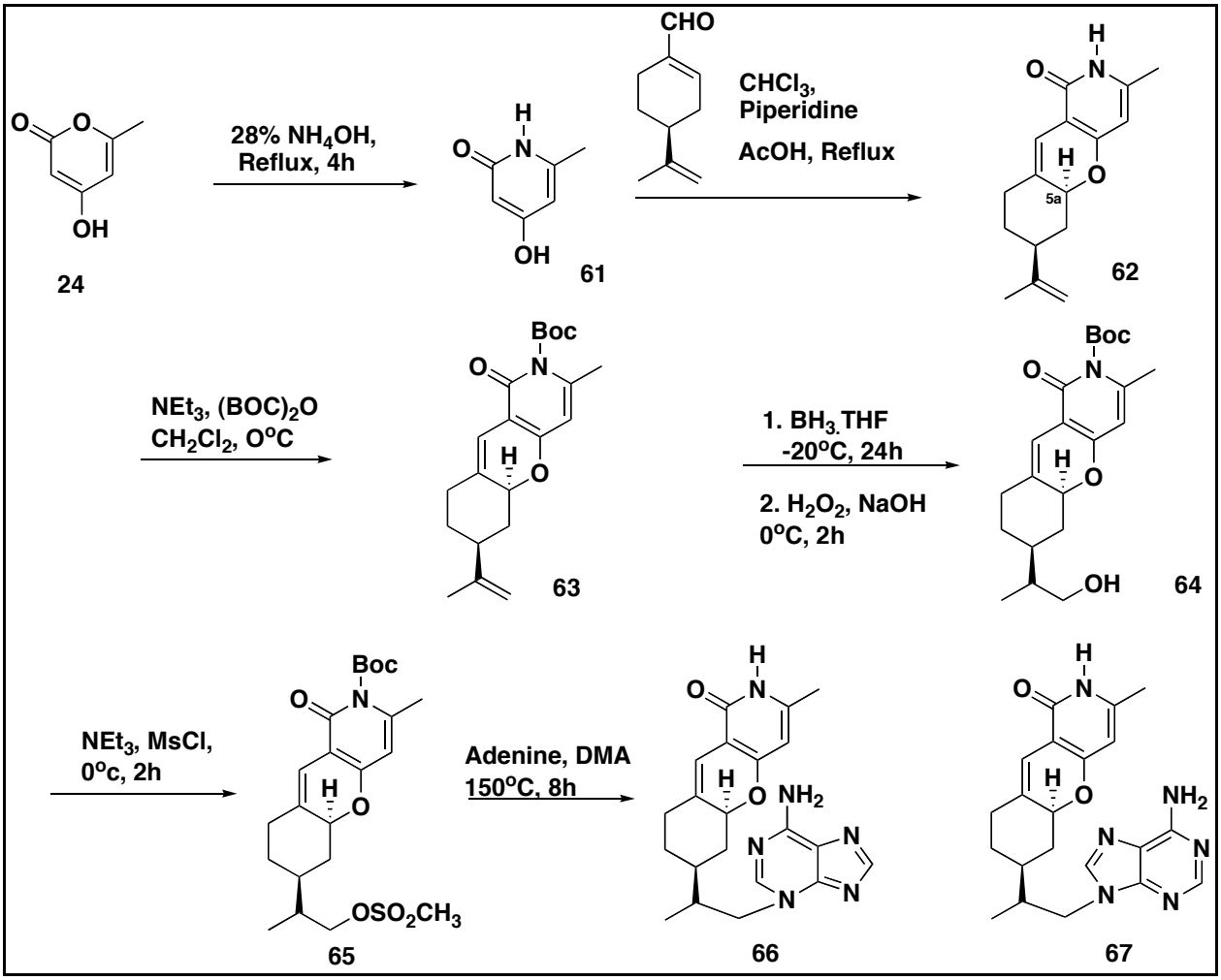

Scheme 1.14. Synthesis of novel pyridinone compounds.

The nitrogen atom at position 2 was successfully installed using ammonium hydroxide. The condensation reaction was used for the synthesis of tricyclic pyridinone core structure and a single diasteromer was obtained. The stereochemistry at C5a carbon was unambiguously determined through the X-ray crystallography analysis.

1.3.6. Synthesis of bicyclic pyrone and pyridinones analogs

More recently, we focused our attention on the synthesis of an array of bicyclic compounds with different substituents attached to them and in the screening of their anti-AD

activity. Pyridinone **61** was treated with triethylorthoformate and aniline in DMF:Acetic acid (3:1) mixture and refluxed for two hours. After the aqueous work up, **68** was obtained in 72% yield.[87] Aldehyde **69** was obtained from **68** by refluxing it in 5% aqueous potassium carbonate solution for one hour in an open reaction vessel.[88] Ethanol was used as a crystallization solvent to obtain aldehyde product in 95% yield as yellow solid. Treatment of **69** with [(methoxycarbonyl)methylene]triphenyl phosphorane in refluxing toluene for 2 hours led to the formation of 3,4-unsubstituted pyranopyridine **70** in 60% yield (**Scheme 1.15**).[89]

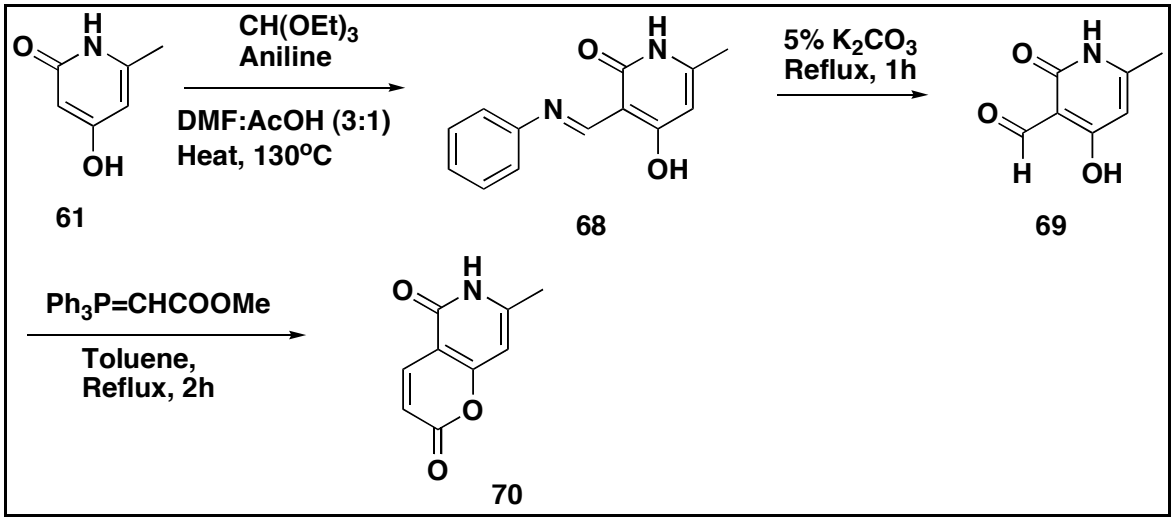

Scheme 1.15. Synthesis of novel bicyclic pyridinone compounds using a Wittig reagent.

1.4 Conclusion and future work

Neurodegenerative diseases mainly occur because of protein misfolding. There is no cure for AD. In our laboratory, we are currently synthesizing different tricyclic pyrones and pyridinones, modifying L-shape fused pyranoisoquinolinone, and synthesized tricyclic pyridinones containing a nitrogen atom at 2 position as well as analogs having a nitrogen atom at position 5. CP2 has a structural scaffold that is accessible for optimization and for further synthesization for more CP2 analogs by modification at positions C11 and C13. These potentially position modifications remains a part of our future work.

1.5 Experimental Section

(5a*S*,7*S*)-7-Isopropenyl-3-methyl-1*H*,7*H*-5a,6,8,9-tetrahydro-1-oxopyrano[4,3-b][1] benzopyran (24)

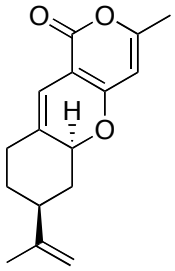

To a solution of 5 g (0.04 mol) of **24** in 200 ml of ethyl acetate under argon at room temperature was added 6.55 g (0.04 mol) of aldehyde **25** and 2.28 g (0.02 mol) of L-proline. The reaction mixture was heated to reflux for 5 h. The progress of the reaction was monitored using TLC using hexane and ethyl acetate as a developing solvent. The reaction mixture was washed with water and brine. The organic layer was extracted with ethyl acetate. The organic layer was dried with anhydrous sodium sulfate, filtered and concentrated. Column chromatographic on silica gel using gradient mixture of hexane and ethyl acetate afforded to give a yellow solid of **26** in 78% yield. Purification can also be performed by recrystallization using ethyl acetate as a solvent. $[\alpha]^{22}_{D}$ = +31.9^{0} (*c* 0.75, $CHCl_3$); ^{1}H NMR ($CDCl_3$) δ 6.1 (s, 1H, C10H), 5.72 (s, 1H, C4H), 5.1 (dd, *J* = 11 Hz, 5Hz, 1H, C5a H), 4.75 (m, 1H, =CH), 4.73 (m, 1H, =CH), 2.48 (ddd, *J*=14Hz, 4Hz, 2.4Hz, 1H), 2.22-2.02 (m, 3H), 2.19 (s, 3H, C4-Me), 1.88-1.72 (m, 2H), 1.74(s, 3H, MeC=), 1.31 (ddd, *J* = 25Hz, 12.8Hz, 4Hz, 1H); ^{13}C NMR δ 163.4, 162.6, 161.7, 147.9, 132.3, 109.8, 109.6, 99.9, 97.5, 79.4, 43.6, 40.0, 32.5, 32.1, 20.9, 20.3.; MS FAB, m/z 259 (M + 1).

(5a*S*,7*S*)-7-[(1*R*) and (1*S*)-2-Hydroxy-1-methylethyl]- 3-methyl-1*H*,7*H*-5a,6,8,9-tetrahydro-1-oxopyrano[4,3-b][1]benzopyran (27)

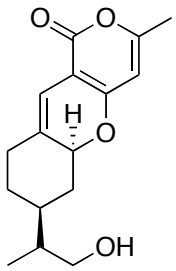

To a cold solution (-20ºC) of 3 g (11.74 mmol) of **26** in 25 mL of THF under argon, was added 5.85 mL (5.85 mmol) of BH_3·THF complex (1.0 M in THF). After stirring the solution at -20ºC for 1 h, kept in the refrigerator for 48 h at -20ºC. Warm to 0ºC and added 15 mL of 0.5% aqueous NaOH and 8 mL of 30% hydrogen peroxide were added. The solution was stirred for 2 h, diluted with 200 mL of water, and extracted three times with dichloromethane. The combined organic layer was washed with 100 mL of brine, dried ($MgSO_4$), concentrated, and column chromatographed on silica gel using a gradient mixture of hexane and diethyl ether as eluents to give 1.72 g (63% yield; based on reacted **26**) of **27** as a mixture of two diastereomers at C12 (1:1; based on 13C NMR spectrum) and 0.43 g (14% recovery) of **27**. ^{1}H NMR ($CDCl_3$) δ 6.08 (s, 1H, C4H), 5.71 (s, 1H, C10H), 5.07 (t, *J*= 5.2 Hz, 1H, C5aH), 3.62 – 3.52 (m, 2H, CH_2O), 2.46 (m,1H), 2.19 (s, 3H, Me), 2.13 – 1.99 (m, 2H), 1.73 – 1.51 (m, 3H), 1.19 – 1.12 (m, 2H), 0.92 (d, *J*=7 Hz, 3H, Me); ^{13}C NMR (two diastereomers) δ 163.5, 162.8, 161.6, 133.0, 109.0, 100.0, 97.4, 79.7, 79.6, 65.6, 39.9, 39.8, 39.4, 37.2, 37.1, 36.9, 32.4, 32.3, 31.1, 30.4, 28.5, 20.1, 13.2 (Me for a diastereomer), 13.1 (Me for another diastereomer).

(5a*S*,7*S*)-3-Methyl-7-[(1*R*) and (1*S*)- 2-(methanesulfonyloxy)-1-methylethyl]-1*H*,7*H*-5a,6,8,9-tetrahydro-1-oxopyrano[4,3-b][1]benzopyran (28)

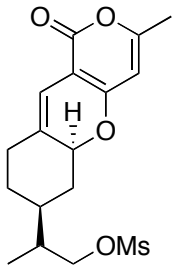

To a cold (0ºC) solution of 1.72 g (6.23 mmol) of **27** in 20 mL of methylene chloride under argon, were added 2.62 mL (18.69 mmol) of triethylamine and 0.72 mL (9.35 mmol) of dimethylacetamide chloride. The solution was stirred for 3h, diluted with 50 mL of $NaHCO_3$, and extracted three times with methylene chloride. The combined dichloromethane layer was washed with washed with brine, dried ($MgSO_4$), concentrated, and column chromatographed on silica gel using a gradient mixture of hexane and ether as eluents to give 2.16g (94% yield) of **28** as a mixture of two diastereomers (1:1; based on ^{13}C NMR spectrum). ^{1}H NMR δ 6.08 (s, 1H, C4H), 5.71 (s, 1H, C10H), 5.06 (m, 1H, CHO), 4.18 – 4.08 (m, 2H, CH_2O), 3.03 (s, 3H, MeS), 2.49 (d, *J*=2.8 Hz, 1H), 2.19 (s, 3H, Me), 2.14 – 1.11 (m, 7H), 0.98 (d, *J*=6.8 Hz, 3H, Me); ^{13}C NMR δ 163.2, 162.4, 161.7, 132.1, 109.6, 105.2, 99.8, 79.2, 79.1, 72.3, 38.9, 37.5, 37.4, 37.3, 37.2, 36.9, 32.2, 32.1, 30.8, 28.6, 20.2, 13.3 (Me for a diastereomer), 13.2 (Me for another diastereomer).

(5a*S*,7*S*)-7-[(1*R*) and (1*S*)-2-Bromo-1-methylethyl]- 3-methyl-1*H*,7*H*-5a,6,8,9-tetrahydro-1-oxopyrano[4,3-b][1]benzopyran (39)

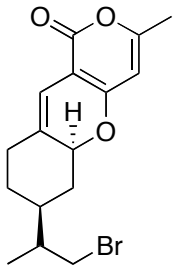

To a cold (0ºC) solution of 0.50 g (1.83 mmol) of **27** (2 diastereomers at C12) and 0.96 g (3.65 mmol) of triphenyl phosphine in 10 mL of dichloromethane under argon was added 1.52 g

(4.56 mmol) of carbon tetrabromide in small portions. The reaction was stirred at 0°C for one hour. The solvent was removed using a rotary evaporator and the residue was subjected to a silica gel column (the silica gel was pre-treated with 1% triethylamine before packing the column) using a gradient mixture of hexane and diethyl ether as eluents to give 0.56 g (91% yield) of **39**. ^{1}H NMR δ 6.09 (s, 1 H), 5.71 (s, 1 H), 5.08 (dt, *J* = 12, 7 Hz, 1 H, C5aH), 3.41 (d, *J* = 4 Hz, 2 H, CH_2Br), 2.47 (dd, *J* = 14, 4 Hz, 1 H), 2.19 (s, 3 H, Me), 2.18 – 2.10 (m, 1 H), 2.03 (q, *J* = 11 Hz, 1 H), 1.80-1.70 (m, 3 H), 1.60 – 1.50 (m, 1 H), 1.20 – 1.16 (m, 1 H), 1.03 (d, *J* = 7 Hz, 3 H, Me); ^{13}C NMR δ (2 diasteromers) 163.4, 162.6, 161.8, 132.4, 109.5, 99.9, 97.5, 79.4, 79.3, 39.6, 39.5, 39.2, 39.1, 38.8, 38.7, 37.0, 32.2, 32.1, 31.0, 28.7, 20.3, 15.9, 15.8. HRMS calcd for $C_{16}H_{20}BrO_3$ ($M+H^+$) 339.0596, found 339.0597.

(5a*S*,7*S*)-7-[(1*R*) and (1*S*)- 2-(N3-adenyl)-1-methylethyl]-3-methyl-1*H*,7*H*-5a,6,8,9-tetra hydro-1-oxopyrano[4,3-b][1]benzopyran (2)

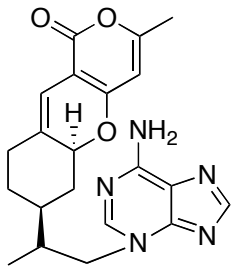

(5a*S*,7*S*)-7-[(1*R*) and (1*S*)-2-(N9-Adenyl)-1-methylethyl]-3-methyl-1*H*,7*H*-5a,6,8,9-tetra hydro-1-oxopyrano[4,3-b][1]benzopyran (29)

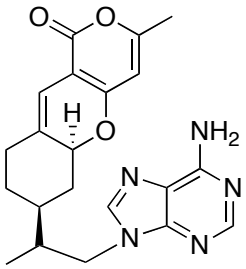

In a round bottom flask fitted with reflux condenser, taken 1.0 g of mesylate **28** (2.7 mmol) and 0.36 g of adenine (2.7 mmol) together and vacuum dried, purge argon and added 8 mL of DMA (dried over CaH_2) and reflux at 140°C overnight. TLC showed no starting material.

Cool to RT, dilute sodium bicarbonate and extract twice with methylene chloride and with 5% methanol in methylene chloride. Combined organic layer washed with brine, dried over sodium sulfate and column chromatographed on silica using methylene chloride and methanol as eluent to afford CP2 (**2**) in 21% yield and TP2 (**29**) in 6% yield. Compound **29** (less polar; two diastereomers at C12); ^{1}H NMR δ 8.36 (s, 1H, C2'H), 7.78 (s, 1H, C8'H), 6.09 (s, 1H, C4H), 5.89 (bs, 2H, NH_2, 5.72 (s, 1H, C10H), 5.01 (m, 1H, C5aH), 4.24 (dd, J= 14, 7 Hz, 1H, CHN), 4.01 (dd, J = 14, 7 Hz, 1H, CHN), 2.5–1.2 (a serious of m, 8H), 2.19 (s, 3H, Me), 0.90 (d, *J* = 7 Hz, 3H, Me); ^{13}C NMR δ 163.4, 162.7, 161.9, 155.6 (adenine moiety), 153.5 (adenine moiety), 150.6 (adenine moiety), 140.9 (adenine moiety), 132.1, 119.8 (adenine moiety), 109.9, 99.9, 97.5, 79.4, 79.2, 47.9, 39.3, 38.4, 38.3, 38.1, 38.0, 36.2, 32.3, 32.1, 31.1, 27.8, 20.3, 13.8. Compound **2** (more polar; 2 diastereomers at C12); ^{1}H NMR δ 8.07 (s, C8 H of adenine), 7.98 and 7.97 (2 s, 1H, C2H of adenine; 2 diastereomers), 6.10 (s, 1H, C10H), 5.72 and 5.71 (2s, 1H, C4H), 5.02 (m, 1H, C5aH), 4.50 (dd, J = 14, 7 Hz, 1H, CHN), 4.08 (2dd, J =14, 8 Hz, 1H, CHN; 2 diastereomers), 2.46 (m, 2H), 2.20 and 2.19 (2s, 3H, Me; 2 diastereomers), 2.10–1.22 (a series of m, 6H), 0.91 (d, J1/47.0 Hz, 3H, Me). ^{13}C NMR (2 diastereomers) δ 163.2 and 163.1, 162.4, 161.7, 154.4,154.0, 150.7, 142.3, 131.7 and 131.6, 121.0, 199.8, 99.7, 97.3, 79.0, 78.8, 54.5 and 54.4, 38.9, 38.1 and 38.0, 37.1 and 36.9, 36.1, 32.0 and 31.9, 30.7, 27.6, 20.1, 13.3 and 13.2. HRMS calculated for $C_{21}H_{24}N_5O_3$ (M+H) 394.1881, found 394.1875.

((2-hydroxyethyl)-7-isopropenyl-1*H*,7*H*-5a,6,8,9-tetrahydro-1-oxopyrano[4,3b][1]benzo pyran (30)

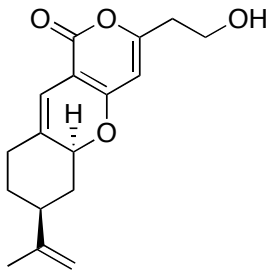

To a solution of 0.4 mL of diisopropylamine in 28 mL of THF was cooled to –20°C. To this solution 1.8 mL of 1.6M *n*BuLi was added and stirred for 30 minutes. Thus obtained solution is the freshly prepared LDA and the reaction vessel is maintained at –20°C to reduce the decomposition. In another flask, to a solution of 250 mg (0.969 mmol) of **26** in 5 mL THF was

cooled to –78°C. To this solution 19.4 mL (1.9372 mmol) of freshly prepared LDA was added via syringe. After five minutes of stirring at –78°C the solution turned deep blue in color indicating the formation of anion. This solution was stirred at –78°C for 2 h. In another flask a suspended solution of 290 mg (9.6899 mmol) of paraformaldehyde in 10 mL THF was taken and cooled to 0°C. The anion formed in another flask is transferred to the paraformaldehyde-THF mixture via cannula and allowed to stir at 0°C and slowly warmed to room temperature. The color of the solution turned reddish brown after reaching to room temperature. The progress of the reaction was monitored using TLC using hexane and diethylether as a developing solvent. The reaction mixture was washed with water and extracted using methylene chloride. The organic layer was washed with aqueous sodium bicarbonate solution and brine, dried over anhydrous sodium sulfate, filtered and concentrated. Column chromatographic on silica gel using gradient mixture of hexane and diethyl ether afforded to give a moderate yield 28% of **30** and 15% of starting material **26**. $[\alpha]_D^{23}$ = +23.7° (C 3.5, $CHCl_3$); ^{1}H NMR $CDCl_3$ δ 6.06 (s, 1 H), 5.86 (s, 1 H), 5.11 (dd, *J* = 11, 4.4 Hz, 1 H, C5a-H), 4.75 (s, 1 H, =CH_2), 4.73 (s, 1 H, =CH_2), 3.90 (t, *J* = 6.2 Hz, 2 H, CH_2O), 2.69 (t, *J* = 6.2 Hz, CH_2), 2.48 (m, 1 H), 2.20 ~ 1.70 (a series of m, 5 H), 1.73 (s, 3 H, Me), 1.34 ~ 1.25 (m, 1 H); ^{13}C NMR δ 163.3, 162.1, 148.0, 132.8, 109.9, 109.1, 101.1, 98.2, 79.6, 59.6, 43.6, 40.0, 37.3, 32.6, 32.1, 30.5, 20.9. HRMS calculated for $C_{17}H_{21}O_4$ (M+H) 289.1440, found 289.1411.

(5a*S*,7*S*)-3-(2-Acetoxyethyl)-7-isopropenyl-1*H*,7*H*-5a,6,8,9-tetrahydro-1-oxopyrano[4,3b][1] benzopyran (31)

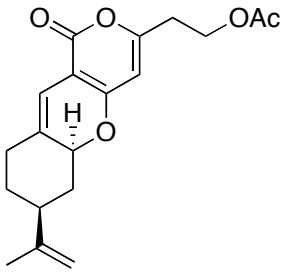

To a solution of 202 mg (0.7014 mmol) of **30** in 3 mL of distilled pyridine was added 143 mg (1.402 mmol) of acetic anhydride at 0°C. The reaction mixture was stirred at 0°C for 7 h. The progress of the reaction was monitored using TLC using hexane and diethylether as a developing

solvent. The reaction mixture was washed with water and extracted with ethyl acetate. The organic layer was washed with 1M HCl, aqueous sodium bicarbonate and brine, dried over anhydrous sodium sulfate, filtered and concentrated. Column chromatographic on silica gel using gradient mixture of hexane and diethyl ether afforded to give 140 mg of **31** in 62% yield. $[\alpha]_D^{23}$ = +16.9° (C 0.15, $CHCl_3$); ^{1}H NMR $CDCl_3$ δ 6.10 (s, 1 H), 5.79 (s, 1 H), 5.13 (dd, J = 11.2, 4.8 Hz, 1 H, C5a-H), 4.75 (s, 1 H, =CH_2), 4.73 (s, 1 H, =CH_2), 4.33 (t, *J* = 6.4 Hz, 2 H, CH_2O), 2.76 (t, *J* = 6.4 Hz, CH_2), 2.48 (m, 1 H), 2.20 ~ 1.70 (a series of m, 5 H), 1.74 (s, 3 H, Me), 1.28 (qd, *J* = 12.8, 4 Hz, 1 H); ^{13}C NMR δ 170.9, 163.0, 160.9, 147.9, 132.9, 110.0, 109.6, 100.8, 98.5, 79.6, 60.8, 43.6, 40.0, 33.6, 32.5, 32.1, 30.5, 20.1, 20.9. HRMS calculated for $C_{19}H_{23}O_5$ (M+H) 331.1545, found 331.1536.

(5a*S*,7*S*)-3-(2-Acetoxyethyl)-7-(2-hydroxy-1-methylethyl)-1*H*,7*H*-5a,6,8,9-tetrahydro-1-oxopyrano[4,3-b][1]benzopyran (32)

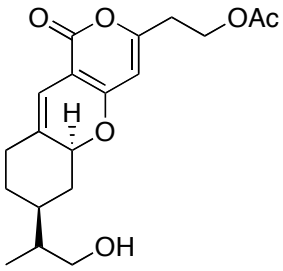

To a solution of 143 mg (0.433 mmol) of **31** in 3 mL THF under argon was added 0.43 mL (0.433 mmol) of 1M BH_3•THF and the solution was stirred at -78°C for 30 minutes and stirred at -20°C for two days. To the solution at 0°C, 1 mL of water, 0.5 mL of 0.1% NaOH aqueous solution, and 0.5 mL of 30% H_2O_2 were added, and the resulting solution was stirred for 1 h. The solution was washed with water and extracted with methylene chloride. The organic layer was washed with aqueous solution of ammonium chloride and brine, dried over anhydrous sodium sulfate, filtered and concentrated. Column chromatographic on silica gel using gradient mixture of hexane and diethyl ether afforded to give 72 mg of **32** in 56% yield along with 14% recovery of starting material **31**. ^{1}H NMR $CDCl_3$ δ 6.07 (s, 1 H), 5.78 (s, 1 H), 5.10 (m, 1 H, C5a-H), 4.32 (t, *J* = 6.2 Hz, 2 H, CH_2O), 3.56 (m, 2 H, CH_2OH) 2.76 (t, *J* = 6.2 Hz, CH_2), 2.47 (m, 1 H), 2.17 ~ 1.10 (a series of m, 7 H), 0.91 (d, *J* = 7 Hz, 1 H); ^{13}C NMR δ 170.9, 163.0,

160.9, 133.4, 118.1, 109.3, 100.8, 98.5, 79.9, 66.0, 60.8, 40.2, 39.5, 37.6, 37.5, 37.3, 33.6, 31.2, 21.0. HRMS calculated for $C_{19}H_{25}O_6$ (M+H) 349.1651, found 349.1649.

(5a*S*,7*S*)-3-(2-Acetoxyethyl)-7-[(2-methanesulfonyloxy)-1-methylethyl]-1*H*,7*H*-5a,6,8,9-tetrahydro-1-oxopyrano[4,3-b][1]benzopyran (33)

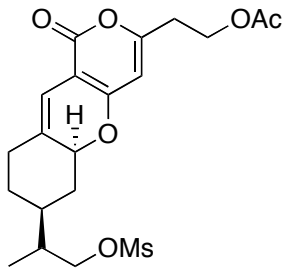

To a solution of 85 mg (0.2442 mmol) of **32** in 3 mL of methylene chloride was added 0.11 mL (0.7326 mmol) of triethylamine at 0°C. To the above solution 28 μL (0.3664 mmol) of methanesulfonyl chloride was added at 0°C, the resulting mixture was stirred at room temperature for 3 h. The progress of the reaction was monitored using TLC using hexane and diethyl ether as a developing solvent. The reaction mixture was washed with water and extracted with methylene chloride. The organic layer was washed with aqueous solution of sodium bicarbonate and brine, dried over anhydrous sodium sulfate, filtered and concentrated. Column chromatographic on silica gel using gradient mixture of hexane and diethyl ether afforded to give 94 mg of **33** in 90% yield. ^{1}H NMR $CDCl_3$ δ 6.05 (s, 1 H), 5.76 (s, 1 H), 5.07 (m, 1 H, C5a-H), 4.29 (t, *J* = 6.3 Hz, 2 H, CH_2O), 4.10 (m, 2 H, CH_2OS), 3.00 (s, 3 H, CH_3S), 2.73 (t, *J* = 6.3 Hz, CH_2), 2.47 (d, *J* = 14 Hz, 1 H), 2.17 ~ 1.10 (a series of m, 7 H), 2.02 (s, 3 H, CH_3CO), 0.96 (d, *J* = 7 Hz, 1 H); ^{13}C NMR δ 170.9, 162.9, 162.3, 161.1, 132.7, 109.7, 100.7, 98.4, 79.4, 72.3, 60.8, 39.1, 37.6, 37.5, 37.4, 33.6, 32.3, 30.9, 13.3. HRMS calculated for $C_{20}H_{27}O_8S$ (M+H) 427.1426, found 427.1434.

(5a*S*,7*S*)-3-(2-Acetoxyethyl)-7-[(1*R*) and (1S)- 2-(N3-adenyl)-1-methylethyl]-1*H*,7*H*-5a,6,8,9-tetrahydro-1-oxopyrano[4,3-b][1]benzopyran (34)

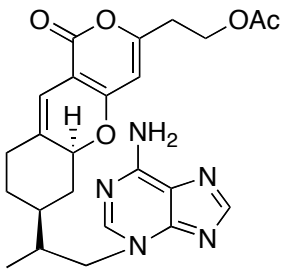

To a solution of 94 mg (0.22 mmol) of **33** in 1.5 ml of DMA was added 33 mg (0.2442 mmol) of adenine and the resulting mixture was heated to 150°C for 7 h. The reaction mixture was cooled to room temperature and 50 mg (0.59 mmol) of sodium bicarbonate was added and DMA was distilled out under reduced pressure to obtain a brown residue. This residue was made to dissolve in minimum amount of methanol and applied to column directly. Column chromatographic on silica gel using gradient mixture of chloroform and methanol afforded to give 5 mg of **34** in low yields. The product was further purified by HPLC using acetonitrile, water and 0.1% trifluoro acetic acid as solvents to give pure **34**. ^{1}H NMR $CDCl_3$ δ 8.07 (s, C8'H of adenine), 8.01 & 8.00 (2s, 1 H, C2'H of adenine; 2 diastereomers), 6.10 (s, 1 H, C10H), 5.79 & 5.78 (2s, 1 H, C4H), 5.05 (m, 1 H, C5aH), 4.54 (2dd, *J* = 13.5, 6.5 Hz, 1 H, CHN; 2 diastereomers), 4.34 & 4.33 (2t, *J* = 6.2 Hz, 2 H, CH_2O; 2 diastereomers), 4.07 (dd, *J* = 13.5, 8 Hz, 1 H, CHN), 2.78 & 2.76 (2t, *J* = 6.2 Hz, 2 H, CH_2; 2 diastereomers), 2.07 & 2.06 (2s, 3 H, Me; 2 diastereomers), 2.60 ~ 1.22 (a series of m, 8 H), 0.91 (d, *J* = 7.0 Hz, 3 H, Me). ^{13}C NMR 182.0, 181.6, 164.8, 163.3, 161.1, 155.8, 152.9, 148.0, 141.6, 131.1, 129.6, 129.1, 121.3, 100.7, 79.1, 78.9, 63.8, 59.2, 50.5, 33.6, 29.9, 21.1, 15.1. HRMS calculated for $C_{24}H_{28}N_5O_5$ (M+H) 466.2090, found 466.2081.

(5a*S*,7*S*)-7-[(3-acetoxy-1-propen-2-yl)]-3-methyl-1*H*,7*H*-5a,6,8,9-tetrahyro-1-oxopyranol [4,3-b][1]benzopyran (35)

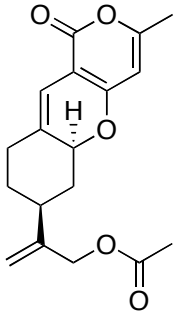

A solution of 200 mg (0.78 mmol) of **26**, 17 mg (78 μmol) of palladium acetate, 0.25 g (2.3 mmol) of benzoquinone, and 25 mg (0.16 mmol) of diethyl malonate in 5 mL of acetic acid under argon was stirred and heated to 75°C for 2 h and 47°C for 24 h. The reaction solution was cooled to 25°C, filtered through celite, washed with aqueous $NaHCO_3$, water, and brine, dried (anhydrous Na_2SO_4), concentrated and column chromatographed on silica gel using a mixture of hexane: ethyl acetate as eluent to give 0.15 g (60% yield) of **35** (5a*S*, 7*S*)-7-[(3-acetoxy-1-propen-2-yl)]-3-methyl-1*H*, 7*H*-5a,6,8,9-tetrahyro-1-oxopyranol[4,3-b][1]benzopyran. $[\alpha]^{22}_D$ = +24.3° (c 0.07, $CHCl_3$); ^{1}H NMR δ 6.12 (s, 1 H), 5.73 (s, 1 H), 5.12 (s, 1 H, $=CH_2$), 5.10 - 5.09 (m, 1 H, CHO), 5.02 (s, 1 H, $=CH_2$), 4.58 (s, 2 H, CH_2OAc), 2.51 (dt, *J* = 14, 4 Hz, 1 H), 2.28 - 2.24 (m, 2 H), 2.20 (s, 3 H, Me), 2.11 (s, 3 H, CH_3CO), 2.11 ~ 2.05 (m, 1 H), 1.93 – 1.89 (m, 1 H), 1.77 (dd, *J* = 12, 11 Hz, 1 H), 1.36 – 1.31 (m, 1 H); ^{13}C NMR δ 170.9, 163.4, 162.7, 161.9, 146.4, 131.8, 112.9, 110.0, 99.9, 97.5, 79.2, 66.1, 40.0, 39.5, 32.4, 32.3, 21.2, 20.3. HRMS calculated for $C_{18}H_{21}O_5$ ($M+H^+$) 317.1389, found 317.1396.

(5a*S*,7*S*)-7-[(3-Hydroxy-1-propen-2-yl)]-3-methyl-1*H*,7*H*-5a,6,8,9-tetrahyro-1-oxopyrano [4,3-b][1]benzopyran (36)

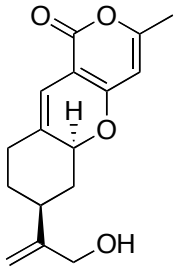

A solution of 0.59 g (1.9 mmol) of the above acetoxy tricyclic pyrone **35** and 0.51 g (3.7 mmol) of potassium carbonate in 5 mL of methanol was stirred at 0°C for 1 h. The solution was neutralized with 1 N HCl, and extracted with dichloromethane three times. The combined extract was washed with aqueous NH_4OH, water, and brine, dried ($MgSO_4$), concentrated, and column chromatographed on silica gel using a gradient mixture of hexane and ether as eluents to give 0.42 g (82% yield) of compound **36**. $[\alpha]^{22}_D$ = +20.0^o (c 0.05, $CHCl_3$); ^{1}H NMR δ 6.12 (s, 1 H), 5.73 (s, 1 H), 5.13 – 5.12 (m, 1 H, CHO), 5.11 (s, 1 H, $=CH_2$), 4.94 (s, 1 H, $=CH_2$), 4.15 (d, *J*

= 7 Hz, 2 H, CH_2O), 2.51 (dt, *J* = 14, 4 Hz, 1 H), 2.34 - 2.23 (m, 2 H), 2.20 (s, 3 H, Me), 2.18 ~ 2.08 (m, 1 H), 1.93 – 1.83 (m, 1 H), 1.77 (q, *J* = 12 Hz, 1 H), 1.40 – 1.28 (m, 1 H); ^{13}C NMR δ 163.5, 162.7, 161.7, 151.4, 132.2, 109.5, 109.4, 99.9, 97.4, 79.3, 64.9, 40.2, 38.9, 32.4 (2 C), 20.2; HRMS calculated for $C_{16}H_{19}O_4$ ($M+H^+$) 275.1283, found 275.1305.

(5a*S*,7*S*)-7-[(3-methanesulfonyloxy-1-propen-2-yl)]-3-methyl-1*H*,7*H*-5a,6,8,9-tetrahyro-1-oxopyranol[4,3-b][1]benzopyran (37)

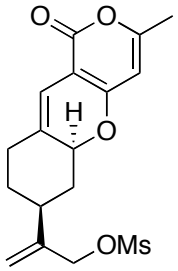

A cold (0°C) solution of 0.15 g (0.54 mmol) of alcohol **36**, 92 mg (0.80 mmol) of methanesulfonyl chloride, 0.20 mL (1.61 mmol) of triethylamine in 5 mL of methylene chloride was stirred under argon for 2 h. The reaction solution was diluted with dichloromethane (30 mL) and washed with aqueous $NaHCO_3$, water, and brine, dried (anhydrous Na_2SO_4), concentrated, column chromatographed on silica gel using a gradient mixture of hexane, diethyl ether and ethyl acetate as eluents to give 77 mg (41% yield) of **37.** $[\alpha]^{22}_D$ = +21.1^o (c 0.09, $CHCl_3$); ^{1}H NMR δ 6.10 (s, 1 H), 5.71 (s, 1 H), 5.26 (s, 1 H, $=CH_2$), 5.14 (s, 1 H, $=CH_2$), 5.11 (dd, *J* = 12, 5 Hz, 1 H, CHO), 4.70 (s, 2 H, CH_2O), 3.03 (s, 3 H, SCH_3), 2.51 (dt, *J* = 14, 3 Hz, 1 H), 2.37 - 2.20 (m, 2 H), 2.19 (s, 3 H, Me), 2.15 ~ 2.03 (m, 1 H), 1.95 – 1.89 (m, 1 H), 1.77 (dd, *J* = 12, 11 Hz, 1 H), 1.32 (qd, *J* = 13, 4 Hz, 1 H); ^{13}C NMR δ 163.4, 162.6, 161.9, 144.8, 131.5, 116.1, 110.1, 99.9, 97.5, 78.9, 71.5, 39.8, 38.7, 38.1, 32.2, 32.1, 20.3; HRMS calculated for $C_{17}H_{21}O_6S$ ($M+H^+$) 353.1059, found 353.1044.

(5a*S*,7*S*)-7-{[3-(6-Amino-9*H*-purin-3-yl)-1-propen-2-yl]}-3-methyl-1*H*,7*H*-5a,6,8,9-tetrahydro-1-oxopyrano[4,3-b][1]benzopyran (38)

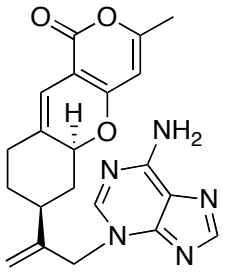

A solution of 77 mg (0.22 mmol) of mesylate **37** and 30 mg (0.22 mmol) of adenine in 1.5 mL of DMA was heated at 150°C under argon for 10 h. DMA was removed via distillation under vacuum (0.1 mm Hg), and the residue was subjected to silica gel column chromatography using a gradient mixture of hexane, ethyl acetate, and methanol as eluents to give 19 mg (26% yield) of compound **38**. $[\alpha]^{22}_{D}$ = -24.7° (c 0.09, $CHCl_3$) ^{1}H NMR δ 8.07 (s, 1 H, C2'H), 8.02 (s, 1 H, C8'H), 6.11 (s, 1 H), 5.72 (s, 1 H), 5.14 (s, 1 H, CH_2N), 5.05 (s, 2 H, $=CH_2$), 5.03 – 5.00 (m, 1 H, CHO), 4.92 (s, 1 H, CH_2N), 2.50 – 2.42 (m, 1 H), 2.32 - 2.29 (m, 1 H), 2.26 – 2.12 (m, 1 H), 2.20 (s, 3 H, Me), 2.08 ~ 1.93 (m, 2 H), 1.80 (q, *J* = 12 Hz, 1 H), 1.36 (qd, *J* = 12, 4 Hz, 1 H); ^{13}C NMR δ 163.4, 162.6, 162.0, 154.5, 154.2, 151.1, 145.9, 142.6, 131.3, 120.8, 114.2, 110.2, 99.9, 97.5, 78.8, 53.1, 39.9, 39.5, 32.3, 32.2, 20.3; HRMS calculated for $C_{21}H_{22}N_5O_3$ ($M+H^+$) 392.1723, found 392.1715.

(5a*S*,7*S*)-7-[(1*R*) and (1S)-2-(6-chloropurin-9-yl)-1-methylethyl]-3-methyl-1*H*,7*H*-5a,6,8,9-tetrahydro-1-oxopyrano[4,3-b][1]benzopyran (40)

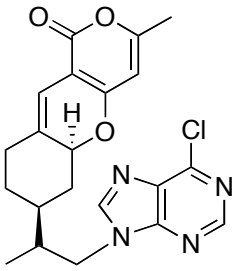

To a solution of 3.0 mg (0.15 mmol) of NaH in 1.5 mL of DMF under argon was added 23 mg (0.15 mmol) of 6-chloropurine at 25°C, and the solution was stirred for 1 h. This solution was then added to a solution of 50 mg (0.15 mmol) of bromide **39** in 1.5 mL of DMF via

cannula. The reaction solution was stirred at 25°C for 24 h and 80°C for 20 h, diluted with aqueous NH_4Cl, and extracted twice with diethyl ether. The combined organic layer was washed with brine, dried ($MgSO_4$), concentrated and column chromatographed on silica gel using a gradient mixture of dichloromethane and methanol as eluents to give 50 mg (82% yield) of compound **40** (as two diastereomers at C12). ^{1}H NMR δ 8.69 & 8.68 (2 s, 1 H, C2'H), 8.04 & 8.03 (2 s, 1 H, C8'H), 6.03 (s, 1 H), 5.66 & 5.64 (2 s, 1 H), 5.00 – 4.90 (m, 1 H, C5aH), 4.28 (ddd, J = 14, 7, 2 Hz, 1 H, CH_2N), 4.04 (ddd, J = 14, 9, 3 Hz, 1 H, CH_2N), 2.48 – 2.38 (m, 1 H), 2.13 & 2.12 (2 s, 3 H, Me), 2.20 - 2.02 (m, 2 H), 1.96-1.78 (m, 1 H), 1.79 – 1.56 (m, 1 H), 1.50 – 1.40 (m, 1 H), 1.34 - 1.18 (m, 2 H), 0.91 (d, J = 7 Hz, 3 H, Me); ^{13}C NMR δ 163.4 & 163.3, 162.7 & 162.6, 161.9, 152.2, 151.4, 145.5, 131.8, 110.0, 99.8, 97.5, 79.2 & 79.0, 48.4 & 48.3, 39.1, 38.4 & 38.3, 38.26 & 38.2, 36.6, 36.4, 32.2 & 32.0, 31.6, 30.9, 28.0, 20.3, 13.94 & 13.91. HRMS calculated for $C_{21}H_{22}ClN_4O_3$ ($M+H^+$) 413.1380, found 413.1372. 2D NOESY spectrum shows correlation of δ C8'-H (δ7.21 ppm) signal with CH_2N (δ 3.93 and 3.39 ppm) peaks.

(5a*S*,7*S*)-7-[(1*R*) and (1*S*)-2-(N1-cytosinyl)-1-methylethyl]-3-methyl-1*H*,7*H*-5a,6,8,9 tetrahyro-1-oxopyrano[4,3-b][1]benzopyran (41)

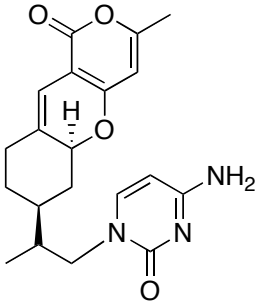

(5a*S*,7*S*)-7-((*R*)-1-(4-amino-1,2-dihydropyrimidin-2-yloxy)propan-2-yl)-6,7,8,9-tetrahydro-3-methylpyrano[4,3-b]chromen-1(5a*H*)-one (42)

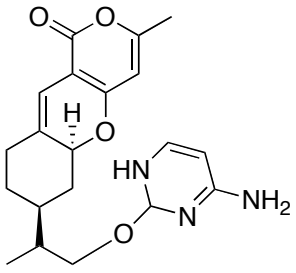

To a solution of 24 mg (0.59 mmol) of NaH in 3 mL of DMF under argon was added 66 mg (0.59 mmol) of cytosine at 25°C, and the solution was stirred for 1 h. This solution was then added to a solution of 0.20 g (0.59 mmol) of bromide **39** in 2 mL of DMF via cannula, and the resulting solution was stirred at 25°C for 24 h and 85°C for 24 h. The reaction solution was diluted with dichloromethane and washed with water, and brine, dried (anhydrous Na_2SO_4), concentrated, and column chromatographed on silica gel using a gradient mixture of dichloromethane and methanol as eluents to give 21 mg (10% yield) of compound **42** (less polar; 2 diastereomers (-O compound) and 62 mg (28% yield) of compound **41** (more polar; 2 diastereomers) along with 25 mg of tricyclic pyrone **26** (from dehydrobromination reaction). Compound **41**: (more polar) ^{1}H NMR δ 7.21 (d, *J* = 7 Hz, 1 H, C6'H), 6.04 (s, 1 H), 5.87 (d, *J* = 7 Hz, 1 H, C5'H), 5.72 (s, 1 H), 5.06 – 5.00 (m, 1 H, C5aH), 3.98 – 3.84 (m, 1 H, CH_2N), 3.42 – 3.33 (m, 1 H, CH_2N), 2.48 – 2.38 (m, 1 H), 2.30 – 2.10 (m, 1 H), 2.19 (s, 3 H), 2.08 – 1.92 (m, 2 H), 1.78 – 1.52 (m, 3 H0, 1.30 – 1.12 (m, 1 H), 0.84 (d, *J* = 6 Hz, 3 H); ^{13}C NMR δ 165.5, 163.6, 162.7, 161.9, 156.9, 146.0, 132.5, 109.4, 100.0, 97.4, 95.2, 79.46 & 79.40, 53.9, 38.3, 37.1 & 36.5, 32.3, 31.8 & 31.0, 29.9 & 28.0, 20.3, 13.5. 2D NOESY spectrum shows correlation of δ 7.21ppm signal with δ 3.93 and 3.39 ppm. Compound **42** (less polar): ^{1}H NMR δ 8.02 (d, *J* = 7 Hz, 1 H, C6'H), 6.10 (d, *J* = 7 Hz, 1 H, C5'H), 6.07 (s, 1 H), 5.70 (s, 1 H), 5.08 (m, 1 H, C5aH), 4.97 (s, 2 H, NH_2), 4.22 - 4.13 (m, 2 H, CH_2N), 2.46 (d, *J* = 14 Hz, 1 H), 2.19 (s, 3 H, Me), 2.15 - 1.54 (m, 5 H), 1.34 - 1.10 (m, 2 H), 1.01 (d, *J* = 7 Hz, 3 H, Me); ^{13}C NMR δ 165.4, 164.9, 163.5, 162.8, 161.7, 157.6, 133.0, 109.3, 100.0, 99.7, 97.5, 79.8 & 79.6, 69.7, 39.4, 37.4 & 37.3, 37.2 & 37.1, 36.9, 32.5 & 32.4, 31.2 & 28.5, 20.3, 13.5 & 13.4. HRMS calcd for $C_{20}H_{24}N_3O_4$ ($M+H^+$) 370.1767, found 370.1760. 2D NOESY spectrum shows no correlation between δ 8.02 and 4.22 – 4.13 ppm.

(5a*S*,7*S*)-7-[(1*R*) and (1*S*)-2-Amino-1-methylethyl)- 3-methyl-1*H*,7*H*-5a,6,8,9-tetrahydro-1-oxopyrano[4,3-b][1]benzopyran (48)

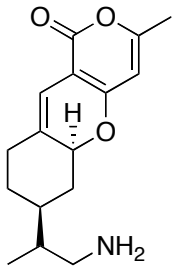

To a cold (-20°C) solution of 500mg (1.94 mmol) of **26** in 2 mL THF was added 0.64mL (0.64 mmol) of BH_3•THF complex (1.0 M in THF). After stirring the solution from -20ºC to 0°C over a period of 30 minutes was added the hydroxylamine-*O*-sulfonic acid and refluxed the reaction mixture for 3 h. Cool down to the room temperature and diluted with 1N HCl and extracted with ethyl acetate twice. Combined organic layer was washed with brine, dried ($MgSO_4$) and concentrated to recover 310 mg (62%) the starting material **26**. The aqueous layer was basified using 3 M NaOH and extracted with ethyl acetate twice. Organic layer was washed with brine, dried ($MgSO_4$), concentrated to give 125 mg (62%; based on reacted **26**) of **48** as a mixture of two diastereomers at C12 (1:1; based on 13C NMR spectrum). ^{1}H NMR δ 6.07 (s, 1H, C4H), 5.71 (s, 1H, C10H), 5.07 (m, 1H, C5aH), 2.73 (m, 1H, 2 isomer, CHN), 2.58 (m, 1H, 2 isomers, CHN), 2.46 (d, 1H), 2.19 (s, 3H, Me), 2.15–1.10 (m, 7H), 0.91 (d, J = 7 Hz, 3H, Me); ^{13}C NMR δ 163.4, 162.7, 161.7, 132.9, 109.3, 100.0, 97.5, 79.8 and 79.7 (2 isomers), 66.0, 46.0 and 45.9 (2 isomers), 40.9, 39.1, 38.5 and 38.4 (2 isomers), 37.1, 32.6 and 32.4 (2 isomers), 31.3, 31.2, 28.6, 20.3, 15.5, 14.3. HRMS calculated for $C_{17}H_{22}NO_3$ (M+1) 276.1601, found 276.1610.

(5a*S*,7*S*)-7-[(1*R*) and (1*S*)-2-(3-amino-4-cyanopyrazol-1-yl)-1-methylethyl]-3-methyl-1*H*,7*H*-5a,6,8,9-tetrahyro-1-oxopyrano[4,3-b][1]benzopyran (43)

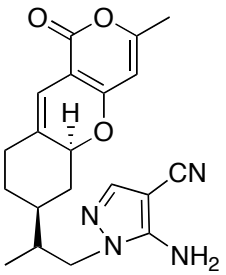

To a mixture of 16 mg (0.15 mmol) of 3-aminopyrazole-4-carbonitrile and 6 mg (0.15 mmol; 40% oil) of sodium hydride under argon was added 0.5 mL of DMF, and the solution was stirred at 25°C for 1 h. To it was added a solution of 50 mg (0.15 mmol) of bromide **39** in 1 mL of DMF via cannula, and the solution was stirred at 25°C for 24 h and 85°C for 24 h. The reaction solution was cooled to 25°C, diluted with dichloromethane, washed with water, and brine, dried ($MgSO_4$), concentrated, and column chromatographed on silica gel using a gradient mixture of hexane and ethyl acetate as eluents to give 23 mg (43% yield) **43**. ^{1}H NMR δ 7.51 and 7.48 (2s, 1 H, C5'H), 6.10 (s, 1 H), 5.72 (s, 1 H), 5.10 – 5.00 (m, 1 H, C5aH), 4.26 (bs, 1 H, NH), 4.11 (bs, 1 H, NH), 3.95 (dd, *J* = 14, 6 Hz, 1 H, CH_2N), 3.69 (dd, *J* = 14, 8 Hz, 1 H, CH_2N), 2.56 – 2.42 (m, 1 H), 2.20 (s, 3 H, Me), 2.16 – 1.90 (m, 3 H), 1.80 - 1.50 (m, 3 H), 1.34 – 1.12 (m, 1 H), 0.89 & 0.84 (2d, *J* = 7 Hz, 3 H, Me; 2 diastereomers); ^{13}C NMR δ 163.5 & 163.4, 162.8 & 162.7, 161.9, 157.0, 140.3, 134.7, 132.3 & 132.1, 114.5 & 113.8, 109.8 & 109.7, 99.9 & 97.5, 79.4 & 79.3, 56.5 & 51.6, 39.1 & 39.06, 38.1 & 37.9, 37.5 & 37.4, 36.7 & 36.4, 32.3 & 32.1, 28.1 & 27.9, 20.3, 13.7 & 13.6. HRMS calculated for $C_{20}H_{22}N_4O_3Na$ ($M+Na^+$) 389.1590, found 389.1593. 2D NOESY spectrum shows correlation betweenC5'-H of pyrazole (δ 7.51 and 7.48 ppm, two diastereomers) with 3.95 and 3.69 ppm signals.

(5a*S*,7*S*)-7-[(1*R*) and (1*S*)-2-(pyrimidino-2-thio)-1-methylethyl]-3-methyl-1*H*,7*H*-5a,6,8,9-tetrahyro-1-oxopyrano[4,3-b][1]benzopyran (44)

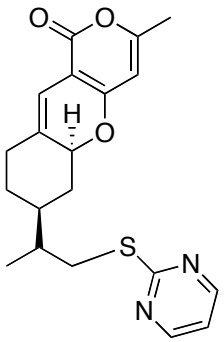

To a mixture of 17 mg (0.15 mmol) of 2-mercaptopyrimidine and 6 mg (0.15 mmol) of NaH (in 40% oil) under argon was added 0.5 mL of DMF, and the solution was stirred at 25°C

for 1 h. To it was added a solution of 50 mg (0.15 mmol) of bromide **39** in 1.5 mL of DMF via cannula, and the solution was stirred at 25°C for 48 h, diluted dichloromethane, washed with water, and brine, dried ($MgSO_4$), concentrated, and column chromatographed on silica gel using a gradient mixture of hexane and ethyl acetate as eluents to give 49 mg (90% yield) of compound **44**. ^{1}H NMR δ 8.51 (d, *J* = 5 Hz, 1 H, C4'H), 6.97 (t, *J* = 5 Hz, 1 H, C5'H), 6.09 (s, 1 H), 5.71 (s, 1 H), 5.11 – 5.02 (m, 1 H, C5aH), 3.31 (dd, *J* = 13, 7 Hz, 1 H, CH_2S), 3.02 (dd, *J* = 13, 6 Hz, 1 H, CH_2S), 2.52 – 2.44 (m, 1 H), 2.20 (s, 3 H, Me), 2.08 – 1.95 (m, 1 H), 1.90 - 1.56 (m, 4 H), 1.34 – 1.10 (m, 2 H), 1.04 (d, *J* = 6 Hz, 3 H, Me); ^{13}C NMR δ 172.7, 163.4 & 163.3, 162.6, 161.7, 157.3 (2 C), 132.7, 116.6, 109.4, 100.0, 97.5, 79.7 & 79.5, 39.9 & 39.8, 39.2, 37.5 & 37.4, 35.6 & 35.5, 32.4 & 32.3, 31.0 & 28.5, 20.2, 16.0 & 15.9. HRMS calculated for $C_{20}H_{23}N_2O_3S$ ($M+H^+$) 371.1429, found 371.1443.

(5a*S*,7*S*)-7-[(1*R*) and (1*S*)-2-(N2-Acetyl-N9-guaninyl)-1-methylethyl]-3-methyl-1*H*,7*H*-5a,6,8,9-tetrahyro-1-oxopyrano[4,3-b][1]benzopyran (46)

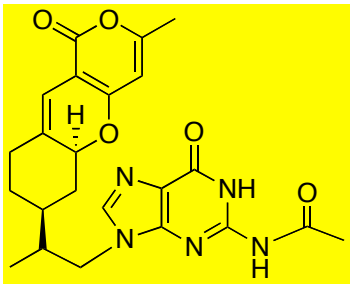

To a solution of 57 mg (0.29 mmol) of N^2-acetylguanine in 1 mL of DMF under argon was added 13 mg (40% oil; 0.32 mmol) of sodium hydride, and the solution was stirred at 25°C for 30 min. To it, a solution of 0.10 g (0.29 mmol) of bromide **39** in 2 mL of DMF was added via cannula under argon, and the solution was stirred at 25°C for 24 h and 60°C for 48 h. The solution was diluted with dichloromethane and washed with water, and brine, dried ($MgSO_4$), concentrated, and column chromatographed on silica gel using a gradient mixture of chloroform and methanol to give 20 mg (15% yield) of compound **46** along with 30 mg of compound **26** (tricyclic pyrone). Compound **53**: ^{1}H NMR δ 12.23 (bs, 1 H, NH), 10.49 (bs, 1 H, NH), 7.73 (s, 1 H, C8'H), 6.11 (s, 1 H), 5.73 & 5.71 (2s, 1 H, 2 diastereomers at C12), 5.08 – 5.02 (m, 1 H,

C5aH), 4.45 (dd, *J* = 13, 6 Hz, 1 H, CH_2N), 4.03 (dd, *J* = 13, 9 Hz, 1 H, CH_2N), 2.50 (t, *J* = 14 Hz, 1 H), 2.39 (s, 3 H, COMe), 2.20 (s, 3 H, Me), 2.06 – 1.94 (m, 2 H), 1.86 – 1.56 (m, 3 H), 1.36 – 1.22 (m, 2 H), 0.87 (d, *J* = 7 Hz, 3 H, Me); ^{13}C NMR δ 173.4, 163.45 & 163.41, 162.7, 161.9, 157.0, 153.4, 148.2, 143.6, 132.1, 112.5, 109.9, 99.9, 97.5, 79.4 & 79.2, 51.4 & 51.3, 39.2 & 39.17, 38.5 & 38.4, 36.7, 32.3 & 32.2, 30.8 & 28.3, 24.8, 20.3, 13.6 & 13.5. HRMS calcd for $C_{23}H_{26}N_5O_5$ ($M+H^+$) 452.1934, found 452.1917. 2D NOESY spectrum shows correlation between δ 7.73 with 4.45 and 4.03 ppm signals.

(5a*S*,7*S*)-7-[(1*R*) and (1*S*)-2-[(N1-thyminyl)-1-methylethyl]-3-methyl-1*H*,7*H*-5a,6,8,9-tetrahyro-1-oxopyrano[4,3-b][1]benzopyran (45)

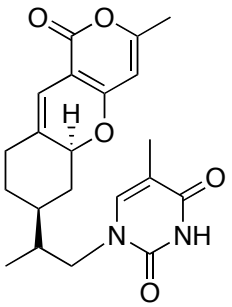

To a solution of 14 mg (0.35 mmol) of NaH in 2 mL of DMF under argon was added 45 mg (0.35 mmol) of thymine at 25°C, and the solution was stirred for 1 h. To it was added a solution of 0.10 g (0.29 mmol) of bromide **39** in 1 mL of DMF via cannula. The reaction solution was stirred at 25°C for 24 h and 80°C for 24 h, cooled to 25°C, and added 9 μL of acetic acid. DMF was removed under vacuum at 50°C, and the resulting solid was column chromatographed on silica gel using a gradient mixture of dichloromethane and methanol as eluent to give 45 mg (42 % yield) of compound **45**. ^1H NMR δ 9.17 (bs, 1 H, NH), 6.94 (s, 1 H, C6'H), 6.07 (s, 1 H), 5.70 (s, 1 H), 5.10 – 5.00 (m, 1 H, C5aH), 3.82 (dd, *J* = 13, 6 Hz, 1 H, CH_2N), 3.40 (dt, *J* = 13, 9 Hz, 1 H, CH_2N), 2.50 – 2.42 (m, 1 H), 2.18 (s, 3 H, Me), 2.10 - 1.50 (m, 5 H), 1.91 (s, 3 H, Me), 1.34 - 1.12 (m, 2 H), 0.89 (d, J = *7* Hz, 3 H, Me); ^{13}C NMR δ 164.2, 163.4, 162.7, 161.8, 151.1, 140.7 & 140.6, 132.1, 110.9 & 110.8, 109.84 & 109.80, 99.9, 97.5, 79.4 & 79.2, 52.3 & 52.1, 39.1, 38.4 & 38.2, 37.5 & 37.4, 36.7 & 36.4, 32.3 & 32.2, 30.9 & 28.1, 20.3, 13.5 & 12.5. HRMS calculated for $C_{21}H_{25}N_2O_5$ ($M+H^+$) 385.1763, found 385.1760. 2D NOESY spectrum shows correlation between C6'-H of thymine (δ 6.94) with CH_2N (3.82 and 3.40) signals.

(5a*S*,7*S*)-7-[(1*R*) and (1*S*)-2-(2-Amino-9*H*-purin-9-yl)-1-methylethyl]-3-methyl 1*H*,7*H*- 5a,6,8,9-tetrahydro-1-oxopyrano[4,3-b][1]benzopyran (47)

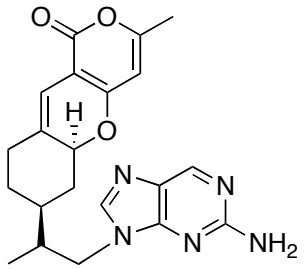

To a solution of 96 mg (0.29 mmol) of Cs_2CO_3 in 1 mL of DMF under argon at 25°C was added 40 mg (0.29 mmol) of 2-aminopurine, and the solution was stirred for 1 h. This solution was then added to a solution of 0.10 g (0.29 mmol) of bromide **39** in 2 mL of DMF via cannula. The reaction solution was stirred at 25°C for 24 h, and DMF was removed under vacuum distillation at 50°C/0.1 mm Hg. The resulting residue was subjected to a silica gel column and eluted with a gradient mixture of methylene chloride and methanol to give 56 mg (48% yield) of compound **47** (as two diastereomers at C12). Compound **47:** ^{1}H NMR δ 8.66 (s, C6'H), 7.72 & 7.71 (2s, C8'H, 2 diastereomers), 6.07 (s, 1 H), 5.70 (s, 1 H), 5.29 (2, 2 H, NH_2), 5.00 (dt, J = 11, 5 Hz, 1 H, C5aH), 4.09 (dd, J = 8, 6 Hz, 1 H, CH_2N), 3.90 (m, 1 H, CH_2N), 2.46 (t, J = 14 Hz, 1 H), 2.18 & 2.17 (2s, 3 H, Me), 2.13 - 1.80 (m, 2 H), 1.73 - 1.42 (m, 3 H), 1.38-1.16 (m, 2 H), 0.87 (d, J = 7 Hz, 3 H, Me); ^{13}C NMR δ 163.3 & 163.2, 162.5, 161.8, 160.0, 153.64 & 153.61, 149.7, 142.9, 132.0, 128.1, 109.7 & 109.6, 99.8, 97.4, 79.3 & 79.1, 47.1, 39.1, 38.1 & 38.0, 37.9 & 37.88, 36.2, 32.2 & 32.0, 31.0, 29.8, 27.8, 21.5, 20.2, 13.8 & 13.7. HRMS calcd for $C_{21}H_{24}N_5O_3$ ($M+H^+$) 394.1879, found 394.1879. 2D NOESY spectrum shows correlation between δ 7.72 with 4.09 and 3.90 ppm signals.

4-bromo-6-methyl-2H-pyran-2-one (49)

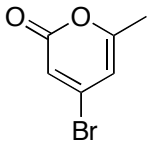

To 10 mL of dry DMF under argon atmosphere was dropwise added the solution of PBr_3 in ether (8.734 g, 32 mmol in 18 mL ether) at 0°C. Then, a solution of 1.0 g (8.0 mmol) of 4-hydroxy-6-methyl-2-pyrone **24** in 8 mL DMF was transferred to the above PBr_3 solution. The resultant solution was heated to 60°C for 12 h. The resultant solution was cooled to 0°C and quenched with water, extracted with diethyl ether three times. Combined organic layer was washed with brine and dried over $MgSO_4$ and concentrated. Column chromatography on silica gel using the gradient mixture of hexane and diethyl ether gave 1.251g of **49** (83% yield). ^{1}H NMR ($CDCl_3$) δ 6.33 (bs, 1 H), 6.13 (bs, 1 H), 2.16 (s, 3 H); ^{13}C NMR δ 162.1, 160.4, 141.1, 114.5, 108.3, 19.6.

4-azido-6-methyl-2*H*-pyran-2-one (50)

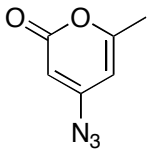

To the vacuum dried mixture of 0.32 g (11.561 mmol) of bromide **49** and 0.152 g ((2.34 mmol) of NaN_3 was added 5 mL of DMF and stirred at room temperature for 3 h under argon atmosphere. Water was added to the reaction and extracted with diethyl ether three times. Combined organic layer was washed with brine and dried over $MgSO_4$ and concentrated. Column chromatography on silica gel using the gradient mixture of hexane and diethyl ether gave 0.204 g of **50** (87% yield). ^{1}H NMR ($CDCl_3$) δ 5.76 (s, 2 H), 2.26 (s, 3 H) ^{13}C NMR δ 163.9, 162.6, 156.4, 99.1, 96.9, 19.9.

4-amino-6-methyl-2H-pyran-2-one (51)

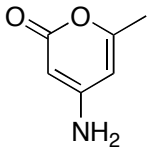

In a round bottom flask, taken 0.204 g of azide **50** (1.35 mmol) and vacuum flame dried thoroughly, purge argon and added 6 mL of dry ethanol via syringe. If not completely soluble, warm a little. Open under stream of argon and added 0.021 g of 10% Pd/C. Hydrogen balloon was fitted on top and stir the reaction mixture for 2 h. Reaction was monitored was TLC. The

reaction was filtered through celite and further washed with ethanol. Organic solvent was removed through rotary evaporator to give 0.168 g of amine (**51**) (100%). ^{1}H NMR ($CDCl_3$) δ 5.58 (s, 1 H), 5.14 (s, 1 H), 4.25 - 4.4 (bs, 2H), 2.19 (s, 3H); ^{13}C NMR (DMSO) δ 163.69, 161.47, 159.84, 98.68, 80.47, 19.54.

(5a*S*,7*S*)- 3-Methyl-7-(prop-1-en-2-yl)-6,7,8,9-tetrahydro-1*H*-pyrano[4,3-b]quinolin-1-one (52)

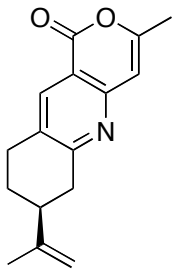

(5a*S*,7*S*)- 3-methyl-9-(prop-1-en-2-yl)-7,8,9,10-tetrahydro-1*H*-pyrano[4,3- c]isoquinolin-1-one (53)

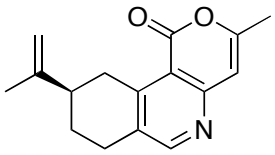

A solution of 0.17 g (1.34 mmol) of 4-amino-6-methyl-2-pyrone (**51**), 0.34 g (2.28 mmol) of (*S*)-perillaldehyde (**25**), and 35 mg (0.15 mmol) of 10-camphorsulfonic acid in 12 mL of toluene was stirred at 85°C under argon for 3 days. The reaction solution was cooled to 25°C, diluted with ethyl acetate, washed with aqueous NH_4OH, and brine, dried ($MgSO_4$), concentrated, and column chromatographed on silica gel using a gradient mixture of hexane and diethyl ether as eluents to give 63 mg (18% yield) of compound **52** and 62 mg (18% yield) of compound **53**, along with 0.11 g of (*S*)- perillaldehyde. Compound **52**: $[\alpha]^{22}_{D}$ = -59.0° (c 0.10, $CHCl_3$); ^{1}H NMR δ 8.17 (s, 1 H, C10H), 6.45 (s, 1 H, C4H), 4.82 (s, 1 H, $=CH_2$), 4.77 (s, 1 H, $=CH_2$), 3.18 (dd, *J* = 18, 5 Hz, 1 H), 3.00 - 2.82 (m, 3 H), 2.60 – 2.42 (m, 1 H), 2.32 (s, 3 H, Me),

2.15 ~ 2.02 (m, 1 H), 1.83 (s, 3 H, Me), 1.78 – 1.62 (m, 1 H); ^{13}C NMR δ 165.6, 163.2, 158.0, 152.6, 147.9, 137.3, 131.8, 114.3, 110.2, 105.7, 41.0, 38.8, 28.3, 27.3, 21.1, 20.2. HRMS calculated for $C_{16}H_{18}NO_2$ ($M+H^+$) 256.1338, found 256.1351. Compound **53**: $[\alpha]^{22}_D$ = -76.5° (c 0.09, $CHCl_3$); ^{1}H NMR δ 8.76 (s, 1 H, C10H), 6.83 (s, 1 H, C4H), 4.89 (s, 1 H, =CH_2), 4.77 (s, 1 H, =CH_2), 3.82 (dd, *J* = 21, 5 Hz, 1 H), 3.22 (dd, *J* = 21, 5 Hz, 1 H), 3.06 - 2.92 (m, 1 H), 2.58 – 2.37 (m, 1 H), 2.40 (s, 3 H, Me), 2.20 ~ 2.03 (m, 2 H), 1.86 (s, 3 H, Me), 1.80 – 1.65 (m, 1 H); ^{13}C NMR δ 162.3, 157.5, 156.2, 154.5, 151.0, 148.3, 132.1, 114.5, 110.3, 106.5, 41.1, 33.8, 27.3, 26.3, 20.9, 19.8. HRMS calculated for $C_{16}H_{18}NO_2$ ($M+H^+$) 256.1338, found 256.1337.

4-hydroxy-1-(4-methoxybenzyl)-6-methylpyridin-2(1*H*)-one (55)

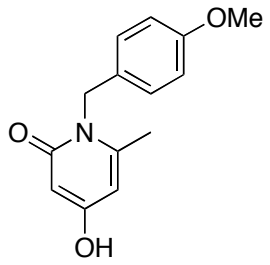

A solution of 2.0 g (16 mmol) of pyrone **24** and 2.2 g (16 mmol) of 4-methoxybenzylamine (**54**) in 30 mL of ethanol was reflux for 24 h, cooled to 25°C, and ethanol was removed under vacuum. Crystallization the resulting solid in ethyl acetate gave 1.65 g of 4-hydroxy-1-(4-methoxybenzyl)-6-methylpyridin-2(1H)-one (**55**). The mixture was dissolved in ethyl acetate (70 mL) and washed with 2 N HCl (20 mL), water, and brine, dried ($MgSO_4$), concentrated to give 1.01 g (26% yield) of pure **55**. This material was used in the following step without further purification. Compound **55**: ^{1}H NMR δ 7.08 (d, *J* = 8 Hz, 2 H), 6.83 (d, *J* = 8 Hz, 2 H), 6.08 (s, 1 H), 5.86 (s, 1 H), 5.24 (s, 2 H, CH_2N), 3.77 (s, 3 H, OMe), 2.24 (s, 3 H, Me); ^{13}C NMR (DMSO-d_6) δ 165.9, 164.1, 158.2, 147.7, 129.6, 127.7 (2 C), 114.0 (2 C), 100.5, 96.0, 55.0, 44.8, 19.9. HRMS calculated for $C_{14}H_{16}NO_3$ ($M+H^+$) 246.1125, found 246.1133.

(5a*S*,7*S*)-2-(4-methoxybenzyl)-3-methyl-7-(prop-1-en-2-yl)-6,7,8,9-tetrahydro-2*H*chromeno[3,2-c]pyridin-1(5a*H*)-one (56)

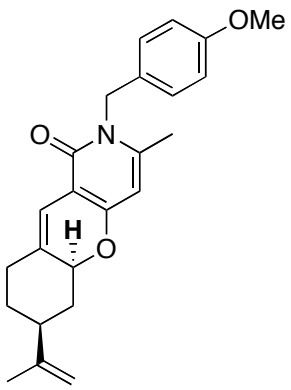

A solution of 1.0 g (4.1 mmol) of compound **55**, 0.61 g (4.1 mmol) of (*S*)-perillaldehyde (**25**), 0.35 g (4.1 mmol) of piperidine, and 0.24 g (4.1 mmol) of acetic acid in 30 mL of chloroform was reflux for 12 h, cooled to 25°C, diluted with ethyl acetate, washed with aqueous NH_4Cl, and brine, dried ($MgSO_4$), concentrated, and column chromatographed on silica gel using a gradient mixture of hexane and ethyl acetate as eluents to give 1.38 g (90% yield) of compound **56**. $[\alpha]^{22}_D = +5.7^o$ (c 0.18, $CHCl_3$); ^{1}H NMR δ 7.10 (d, *J* = 8 Hz, 2 H), 6.82 (d, *J* = 8 Hz, 2 H), 6.38 (s, 1 H), 5.67 (s, 1 H), 5.21 (s, 2 H, CH_2N), 5.10 – 5.00 (m, 1 H, C5aH), 4.74 (s, 2 H, $=CH_2$), 3.77 (s, 3 H, OMe), 2.58 – 2.47 (m, 1 H), 2.22 (s, 3 H, Me), 2.20 – 2.00 (m, 2 H), 1.90 - 1.61 (m, 2 H), 1.74 (s, 3 H, Me), 1.44 – 1.22 (m, 2 H); ^{13}C NMR δ 161.5, 159.8, 158.8, 148.2, 145.3, 131.7, 129.1, 127.9 (2 C), 114.1 (2 C), 111.3, 109.5, 103.7, 100.3, 78.2, 55.3, 46.3, 43.4, 39.9, 32.4, 31.9, 20.8, 20.7. HRMS calculated for $C_{24}H_{28}NO_3$ ($M+H^+$) 378.2069, found 378.2050.

(5a*S*,7*S*)-2-(4-methoxybenzyl)-3-methyl-7-[(1*R*) and (1*S*)-1-hydroxypropan-2-yl]-6,7,8,9-tetrahydro-2*H*-chromeno[3,2-c]pyridin-1(5a*H*)-one (57)

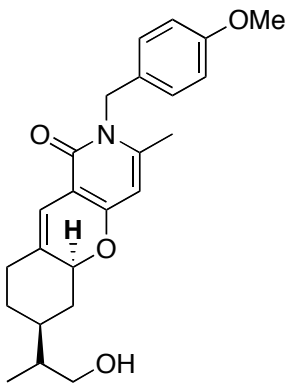

To a cold (-20°C) solution of 1.15 g (3.06 mmol) of compound **56** in 20 mL of THF under argon was added 1.53 mL (1.53 mmol) of BH_3•THF (1.0 M in THF). After standing at -20°C for 4 days, the reaction solution was stirred at 0°C, and 10 mL of 0.5% aqueous NaOH and 5 mL of 30% H_2O_2 were added. The solution was stirred at 0°C for 2 h, diluted with ethyl acetate, washed with aqueous NH_4Cl, and brine, dried ($MgSO_4$), concentrated, and column chromatographed on silica gel using a gradient mixture of hexane and ethyl acetate as eluents to give 0.79 g (69% yield; based on reacted **56**) of **57**. Compound **57**: ^{1}H NMR δ 7.08 (d, *J* = 8 Hz, 2 H), 6.81 (d, *J* = 8 Hz, 2 H), 6.33 (s, 1 H), 5.64 (s, 1 H), 5.19 (s, 2 H, CH_2N), 5.15 – 4.96 (m, 1 H, C5aH), 3.75 (s, 3 H, OMe), 3.58 – 3.44 (m, 2 H, CH_2O), 2.47 (d, *J* = 12 Hz, 1 H), 2.24 – 2.18 (m, 1 H), 2.19 (s, 3 H, Me), 2.11 – 1.94 (m, 3 H), 1.75 - 1.46 (m, 2 H), 1.22 – 1.02 (m, 1 H), 0.88 (d, *J* = 7 Hz, 3 H, Me); ^{13}C NMR δ 161.7, 160.0, 158.9, 145.3, 132.5, 129.2, 128.0 (2 C), 114.3 (2 C), 111.1, 103.9, 100.5, 78.7 & 78.6 (2 diastereomers), 66.0 & 65.9, 55.5, 46.5, 40.25 & 40.21, 39.5 & 37.1, 37.5 & 37.3, 32.6 & 32.5, 31.3 & 28.7, 20.9, 13.4 & 13.3. The signal intensities indicate the ratio of two diastereomers is 1:1. HRMS calculated for $C_{24}H_{30}NO_4$ ($M+H^+$) 396.2175, found 396.2192.

(5a*S*,7*S*)-2-(4-methoxybenzyl)-3-methyl-7-[(1*R*) and (1*S*)-(2-methanesulfonyloxy)-1-methylethyl]-6,7,8,9-tetrahydro-2*H*-chromeno[3,2-c]pyridin-1(5a*H*)-one (58)

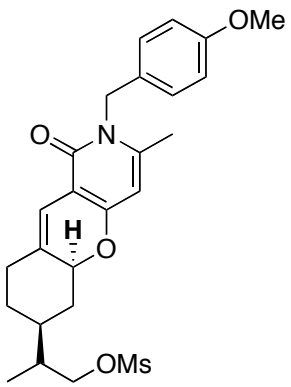

To a cold (0°C) solution of 0.13 g (0.33 mmol) of alcohol **57** and 0.14 mL (0.97 mmol) of triethylamine in 4 mL of dichloromethane was added 38 μL (0.49 mmol) of methanesulfonyl chloride under argon. The reaction solution was stirred at 0°C for 2 h, diluted with dichloromethane, washed with aqueous $NaHCO_3$, and brine, dried ($MgSO_4$), concentrated, and column chromatographed on silica gel using a gradient mixture of hexane and ethyl acetate as eluents to give 0.12 g (79% yield) of mesylate **58**. ^{1}H NMR δ 7.10 (d, *J* = 8 Hz, 2 H), 6.83 (d, *J* = 8 Hz, 2 H), 6.38 (s, 1 H), 5.66 (s, 1 H), 5.21 (bs, 2 H, CH_2N), 5.06 – 4.98 (m, 1 H, C5aH), 4.21 – 4.08 (m, 2 H, CH_2O), 3.78 (s, 3 H, OMe), 3.03 (s, 3 H, MeS), 2.52 (d, *J* = 14 Hz, 1 H), 2.22 (s, 3 H, Me), 2.20 – 2.18 (m, 2 H), 1.94 – 1.85 (m, 1 H), 1.78 - 1.52 (m, 3 H), 1.32 – 1.12 (m, 1 H), 1.00 (d, *J* = 7 Hz, 3 H, Me); ^{13}C NMR δ 161.6, 159.8, 158.8, 145.5, 131.6, 129.1, 128.0 (2 C), 114.2 (2 C), 111.5, 103.6, 100.2, 78.1 & 78.0 (2 diastereomers), 72.4, 55.4, 46.4, 38.9, 37.5 & 37.4, 37.35, 37.2 & 37.1, 37.0, 32.2 & 32.1, 30.8 & 28.6, 20.8, 13.3 & 13.2. The signal intensities indicate the ratio of two diastereomers is 1:1. HRMS calculated for $C_{25}H_{32}NO_6S$ ($M+H^+$) 474.1950, found 474.1945.

(5a*S*,7*S*)-2-(4-Methoxybenzyl)-7-((2*R*) and (2*S*)-1-(6-amino-3*H*-purin-3-yl)propan-2-yl)-3-methyl-6,7,8,9-tetrahydro-2*H*-chromeno[3,2-c]pyridin-1(5a*H*)-one (59)

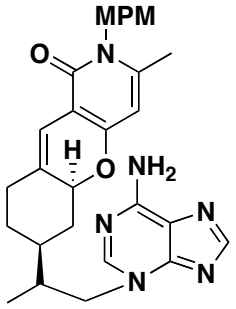

A solution of 0.12 g (0.25 mmol) of mesylate **58** and 34 mg (0.25 mmol) of adenine in 2 mL of DMA was heated at 150°C under argon for 10 h, cooled to 25°C, diluted with dichloromethane and washed with water, and brine, dried (anhydrous Na_2SO_4), concentrated, and column chromatographed on silica gel using a gradient mixture of hexane, ethyl acetate, dichloromethane, and methanol as eluents to give 23 mg (18% yield) of **59**. ^{1}H NMR δ 8.06 (s, 1 H, C2'H), 7.99 (s, 1 H, C8'H), 7.10 (d, *J* = 8 Hz, 2 H), 6.82 (d, *J* = 8 Hz, 2 H), 6.39 (s, 1 H), 5.66 (s, 1 H), 5.21 (bs, 2 H, CH_2N), 5.06 – 4.94 (m, 1 H, C5aH), 4.51 (dd, *J* = 13, 6 Hz, 1 H, CH_2N), 4.08 (dd, *J* = 13, 9 Hz, 1 H, CH_2N), 3.77 (s, 3 H, OMe), 2.60 – 2.30 (m, 2 H), 2.11 (s, 3 H, Me), 2.20 – 2.18 (m, 2 H), 1.98 – 1.55 (m, 2 H), 1.50 - 1.20 (m, 2 H), 0.90 (d, *J* = 7 Hz, 3 H, Me); ^{13}C NMR δ 161.7, 159.9, 158.9, 154.6, 152.8, 150.4, 145.6, 143.2, 131.5, 129.1, 128.0 (2 C), 119.7, 114.3 (2 C), 111.7, 103.7, 100.4, 78.2, 55.5 & 54.7, 46.6, 39.1 & 36.2, 38.3, 37.2, 32.1 & 31.0, 29.9 & 27.8, 22.7 & 21.8, 21.0 & 20.8, 13.4. The signal intensities indicate the ratio of two diastereomers is 1:1. HRMS calculated for $C_{29}H_{33}N_6O_3$ ($M+H^+$) 513.2614, found 513.2627. 2D NOESY spectrum shows NOE correlation between C2'-H (δ 8.08 ppm) and CH_2N (4.51 and 4.08 ppm) signals.

4-hydroxy-6-methyl-2-pyridone (61)

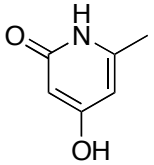

In a 10 ml round bottom flask, taken 250 mg (1.98 mmol) of pyrone **24** dissolved in 1 mL of 28% NH_4OH and mixture was refluxed at 100°C for 6 h. Reaction was allowed to cool to

room temperature. Solid was separated by filtration and recrystallized from ethanol in 81% yield as a yellow solid **61**. M.P. 322°C; ^{1}H NMR (400 MHz, DMSO-d_6) δ ppm 10.87 (bs, 1H), 5.7 (s, 1H), 5.3 (s, 1H), 2.1 (s, 3 H); ^{13}C NMR δ 167.6, 164.8, 146, 98.2, 95.8, 18.5.

(7*S*)-6,7,8,9-tetrahydro-3-methyl-7-(prop-1-en-2-yl)-2*H*-chromeno[3,2-c]pyridin-1(5a*H*)-one (62)

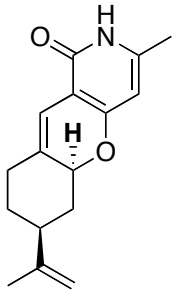

A solution of 250 mg (2.0 mmol) of compound **61**, 300 mg (2.0 mmol) of (*S*)-perillaldehyde **25**, 170 mg (2.0 mmol) of piperidine, and 120 mg (2 mmol) of acetic acid in 15 mL of chloroform was reflux for 12 h, cooled to 25°C, diluted with methylene chloride, washed with aqueous NH_4Cl, and brine, dried ($MgSO_4$), concentrated, and column chromatographed on silica gel using a gradient mixture of hexane and ethyl acetate as eluents to give 500 mg (97% yield) of compound **62**. ^{1}H NMR ($CDCl_3$, ^{1}H NMR ($CDCl_3$) δ 12.66 (bs, 1H), 6.3 (s, 1H), 5.64 (s, 1H), 5.1 (dd, *J* = 11 Hz, 5Hz, 1H), 4.75 (m, 1H, =CH), 4.73 (m, 1H, =CH), 2.48 (ddd, *J* =14Hz, 4Hz, 2.4Hz, 1H), 2.23 (s, 3H), 2.22-2.02 (m, 3H), 1.88-1.72 (m, 2H), 1.74(s, 3H, MeC=), 1.31 (ddd, *J* = 25Hz, 12.8Hz, 4Hz, 1H); ^{13}C NMR δ 163.2, 162.4, 148.4, 144.8, 131.7, 110.4, 109.6, 103.4, 99.1, 78.5, 43.6, 40.0, 32.5, 32.1, 20.9, 19.3.

(7*S*)-tert-butyl-6,7,8,9-tetrahydro-3-methyl-1-oxo-7-(prop-1-en-2-yl)-1*H*-chromeno[3,2-c]pyridine-2(5a*H*)-carboxylate (63)

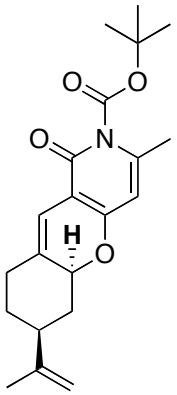

Taken 200 mg of pyridinone **62** (0.78 mmol) and 19 mg of DMAP (0.15 mmol) together in a round bottom flask and vacuum flame dried, purge argon and added 3 mL of acetonitrile. Added 273 μl of dry triethylamine (1.94 mmol) via syringe and cool to 0°C and stir for 30 minutes. Open quickly and added 340 mg of $(Boc)_2O$ (1.55 mmol) and warm to room temperature by stirring for 24 h. Dilute with water and extract ethyl acetate twice. Combine ethyl acetate washed with brine, dried over sodium sulfate, column chromatographed to give 268 mg of **63** (97%). ^{1}H NMR ($CDCl_3$) δ 6.3 (s, 1H), 5.95 (s, 1H), 5.1 (dd, *J* = 11 Hz, 5Hz, 1H), 4.75 (m, 1H, =CH), 4.73 (m, 1H, =CH), 2.48 (ddd, *J*=14Hz, 4Hz, 2.4Hz, 1H), 2.31 (s, 3H) 2.22-2.02 (m, 3H), 1.88-1.72 (m, 2H), 1.74(s, 3H, MeC=), 1.5 (s, 9H), 1.31 (ddd, *J* = 25Hz, 12.8Hz, 4Hz, 1H); ^{13}C NMR δ 161.9, 156.6, 152.13, 151.1, 147.7, 137.3, 109.7,109.0, 109, 106.2, 83.6, 78.0, 43.1, 39.9, 32.7, 31.7, 27.6, 24.1, 20.1.

(7*S*)-tert-butyl-6,7,8,9-tetrahydro-7-((*R*)-1-hydroxypropan-2-yl)-3-methyl-1-oxo-1*H*-chromeno[3,2-c]pyridine-2(5a*H*)-carboxylate (64)

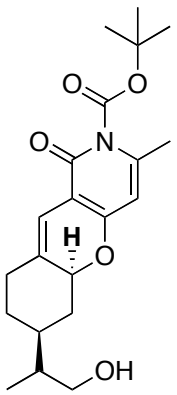

To a cold (-20°C) solution of 265 mg (0.74 mmol) of compound **63** in 6 mL of THF under argon was added 0.37 mL (0.37 mmol) of BH_3•THF (1.0 M in THF). After standing at -20°C for 2 days, the reaction solution was stirred at 0°C, and 2 mL of 0.5% aqueous NaOH and 1 mL of 30% H_2O_2 were added. The solution was stirred at 0°C for 2 h, diluted with ethyl acetate, washed with aqueous NH_4Cl, and brine, dried ($MgSO_4$), concentrated, and column chromatographed on silica gel using a gradient mixture of hexane and ethyl acetate as eluents to give 62 mg (65% yield; based on reacted **63**) of **64** as a mixture of two diastereomers at C12 (1:1; based on 13C NMR spectrum). ^{1}H NMR ($CDCl_3$) δ 6.38 (s, 1H), 5.96 (s, 1H), 5.05-5.00 (t, *J*= 5.2 Hz, 1H), 3.62 – 3.52 (m, 2H, CH_2O), 2.46 (m, 1H), 2.34 (s, 3H, Me), 2.13 – 1.99 (m, 2H), 1.73 – 1.51 (m, 3H), 1.54 (s, 9H), 1.19 – 1.12 (m, 2H), 0.90 (d, *J*=7 Hz, 3H, Me); ^{13}C NMR (two diastereomers) δ 162.1, 156.7, 152.2, 151.2, 138.1, 109.2, 108.8, 106.5, 83.9, 78.4, 65.7,40.0, 39.5, 37.2, 32.8, 31.01, 27.8, 24.2, 13.5 and13.2 (Me of two diastereomers).

(*R*)-2-((7*S*)-2-(*tert*-butoxycarbonyl)-2,5a,6,7,8,9-hexahydro-3-methyl-1-oxo-1*H*-chromeno[3,2-*c*]pyridin-7-yl)propyl methanesulfonate (65)

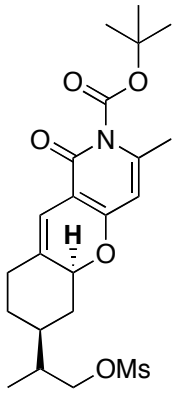

To a cold (0°C) solution of 400 mg (1.11 mmol) of alcohol **64** and 0.47 mL (3.34 mmol) of triethylamine in 8 mL of dichloromethane was added 129 μL (1.67 mmol) of methanesulfonyl chloride under argon. The reaction solution was stirred at 0°C for 2 h, diluted with dichloromethane, washed with aqueous $NaHCO_3$, and brine, dried ($MgSO_4$), concentrated, and column chromatographed on silica gel using a gradient mixture of hexane and ethyl acetate as eluents to give 382 mg (79% yield) of mesylate **65** as a mixture of two diastereomers at C12

(1:1; based on 13C NMR spectrum). ^{1}H NMR ($CDCl_3$) δ 6.31 (s, 1H), 5.89 (s, 1H), 5.05-5.00 (m, *J*= 5.2 Hz, 1H), 4.15 – 4.08 (m, 2H, CH_2O), 3.01 (s, 3H), 2.46 (m, 1 H), 2.27 (s, 3H, Me), 2.13 – 1.99 (m, 2H), 1.73 – 1.51 (m, 3H), 1.54 (s, 9H), 1.19 – 1.12 (m, 2H), 0.90 (d, *J*=7 Hz, 3H, Me); ^{13}C NMR (two diastereomers) δ 161.9, 156.5, 151.9, 150.9, 137.2, 108.9, 108.7, 106.0, 83.7, 77.7 and 77.77.61 (two diastereomers), 72.2, 38.71, 37.02 and 37.8 (two diastereomers), 36.7 and 36.6 (two diastereomers) 32.25 and 32.15 (two diastereomers), 31.48, 30.25, 28.1, 27.51, 23.9, 12.98.

(7*S*)-7-((*R*)-1-(6-amino-5,6-dihydropurin-3-yl)propan-2-yl)-6,7,8,9-tetrahydro-3-methyl-2*H*-chromeno[3,2-c]pyridin-1(5a*H*)-one (66)

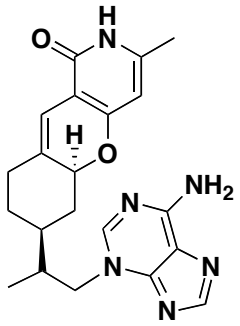

(7*S*)-7-((*R*)-1-(6-amino-4*H*-purin-9(8*H*)-yl)propan-2-yl)-6,7,8,9-tetrahydro-3-methyl-2*H*-chromeno[3,2-c]pyridin-1(5a*H*)-one (67)

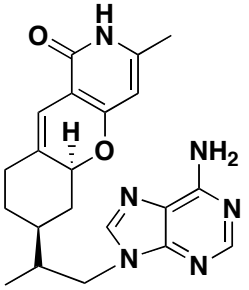

A solution of 0.12 g (0.25 mmol) of mesylate **65** and 34 mg (0.25 mmol) of adenine in 2 mL of DMA was heated at 150°C under argon for 10 h, cooled to 25°C, diluted with

dichloromethane and washed with water, and brine, dried (anhydrous Na_2SO_4), concentrated, and column chromatographed on silica gel using a gradient mixture of hexane, ethyl acetate, dichloromethane, and methanol as eluents to give 23 mg (18% yield) of **66** and 8 mg (6% yield) of **67**. Compound **66 (**more polar; 2 diastereomers at C12) ^{1}H NMR δ 8.08 (s, H of adenine), 7.98 and 7.97 (2s, 1H, H of adenine; 2 diastereomers), 6.30 (s, 1H), 5.63 and 5.62 (2s, 1H), 5.02 (m, 1H, C5aH), 4.50 (dd, *J*=13, 6 Hz, 1H, CHN), 4.08 (2dd, *J*=13, 8 Hz, 1H, CHN; 2 diastereomers), 2.46 (m, 2H), 2.25 and 2.24 (2s, 3H, Me; 2 diastereomers), 2.10–1.22 (a series of m, 6H), 0.91 (d, *J*=7Hz, 3H, Me); ^{13}C NMR (2 diastereomers) δ 163.2 and 163.1, 162.4, 161.7, 154.4,154.0, 150.7, 142.3, 131.7 and 131.6, 121.0, 199.8, 99.7, 97.3, 79.0, 78.8, 54.5 and 54.4, 38.9, 38.1 and 38.0, 37.1 and 36.9, 36.1, 32.0 and 31.9, 30.7, 27.6, 20.1, 13.3 and 13.2. HRMS calcd for $C_{21}H_{24}N_5O_3$ (M+H) 394.1881, found 394.1875.

4-hydroxy-6-methyl-3-((*E*)-(phenylimino)methyl)pyridin-2(1*H*)-one (68)

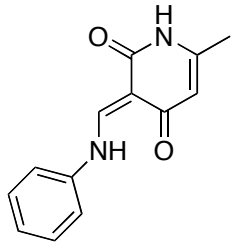

Taken 3.6 g of pyridinone **61** (23.98 mmol), 2.23 g of aniline (23.98 mmol), 15 mL of triethyl orthoformate together in a round bottom flask followed by addition of 20 mL of 3:1 DMF : AcOH and reflux at 130°C for 2 h. Color changes from yellow to brown. Cool to room temperature. Dilute brine and extract methylene chloride twice followed by extraction with 10% methanol in methylene chloride. Organic layer dried over sodium sulfate and crystallize from methylene chloride to obtain 3.81 g of **68** as yellow solid. ^{1}H NMR (DMSO-d_6) δ ppm 9.89 (bs, 1H), 8.91 (d, 1H, *E*/*Z* isomer), 7.2-7.6 (m, 5H), 5.7 (s, 1H), 2.2 (s, 3H); ^{13}C NMR ($CDCl_3$) 185.1, 166.9, 153.1, 150.3, 138.6, 130.2, 126.9, 118.6, 107.0, 20.2.

1,2-dihydro-4-hydroxy-6-methyl-2-oxopyridine-3-carbaldehyde (69)

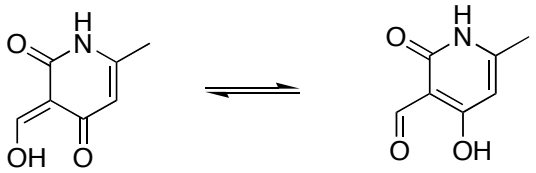

Taken 3.41 g of pyridinone **68** and added 50 mL of 5% K_2CO_3 in water and reflux in open for 1 h. Cool to room temperature. Acidify to pH ~1 by adding conc. HCl at 0°C. Filter the solid and crystallize from ethanol to yield 2.08 g of **69** (85%) as yellow solid. ^{1}H NMR (DMSO-d_6) δ ppm 13.52 (bs, 1H), 11.73 (bs, 1H), 9.83 (bs, 1H), 5.86 (s, 1H), 2.2 (s, 3H). ^{13}C NMR (DMSO-d_6) 193.3, 174.7, 163.3, 157.1, 105.3, 97.7, 19.6

7-methyl-6*H*-pyrano[3,2-c]pyridine-2,5-dione (70)

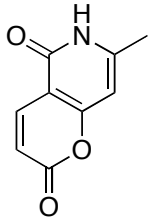

A mixture of 60 mg (.36 mmol) of aldehyde **69** and 146 mg (.43 mmol) of [(Methoxycarbonyl)methylene]triphenyl phosphorane (Wittig reagent) together in a round bottom flask and added freshly distilled toluene and reflux for 2 h. Color changes from yellow to purple. Cool to RT, precipitate formed, filter it, vacuum dried and crystallized from methanol to yield compound **70**. Yield 55% as yellow solid. ^{1}H NMR (400 MHz, DMSO-*d*6) d ppm 2.08 - 2.39 (m, 1 H) 2.39 - 2.63 (m, 1 H) 3.10 - 3.48 (m, 2 H) 5.84 - 6.47 (m, 1 H) 7.35 - 7.73 (m, 1 H) 7.92 (d, *J*=9.37 Hz, 1 H) 12.01(br. s, 1 H)

1.6 References

1. http://en.wikipedia.org/wiki/Neurodegenerative disease.
2. Berchtold, N. C.; Cotman, C. W., Evolution in the conceptualization of dementia and Alzheimer's disease: Greco-Roman period to the 1960s. *Neurobiol. Aging*, **1998**, *19*, 173–189.
3. Imarisio, S.; Carmichael, J.; Korolchuk, V.; Chen, C -W; Saiki, S; Rose, C; Krishna, G; Davies, J. E.; Ttofi, E.; Underwood, B. R.; Rubinsztein, D. C., Huntington's disease: from pathology and genetics to potential therapies. *Biochem. J.*, **2008**, *412*, 191-209.
4. Jankovic. J., Parkinson's disease: clinical features and diagnosis. *J. Neurol. Neurosurg. Psychiatr.*, **2008**, *79*, 368–76
5. http://en.wikipedia.org/wiki/Amyotrophic_lateral_sclerosis
6. Geula, C; Wu, C. K.; Saroff, D.; Lorenzo, A.; Yuan, M.; Yankner, B. A., Aging renders the brain vulnerable to amyloid beta-protein neurotoxicity. *Nature medicine,* **1998**, *4*, 827-31.
7. Ross, C. A.; Poirier, M. A., Protein aggregation and neurodegenerative disease. *Nature Medicine.,* **2004**, S10- S17
8. http://www.alz.org/alzheimers_disease_what_is_alzheimers.asp
9. Glenner, G. G.; Wong, C. W., Alzheimer's disease: initial report of the purification and characterization of a novel cerebrovascular amyloid protein. *Biochem. Biophys. Res. Commun.*, **1984**, *120*, 885-890.
10. Lee, V. M.; Balin, B. J.; Otvos, L.; Trojanowski, J. Q., Aβ: a major subunit of paired helical filaments and derivatized forms of normal Tau. *Science*, **1991**, *251*, 675-678.
11. Selkoe, D. J., Alzheimer's Disease-Genotypes, Phenotype, and Treatments. *Science*, **1997**, *275*, 630–631.
12. Weidemann, A.; Konig, O.; Bunke, D.; Fischer, P.; Salbaurn J. M.; Masters C. L.; Beyreutber K., Identification, biogenesis, and localization of precursors of Alzheimer's disease Aβ amyloid protein. *Cell*, **1998**, *57*, 115-126.

13. Oltersdorf, T.; Fritz, L.; Scheak, D. B.; Lieberburg, L.; Johnson-Wood K. L.; Beattie, E. C.; Ward, P. J.; Blacker, R. W.; Dovey, H. F.; Sinha, S., The secreted forms of the Alzheimer's amyloid precursor protein with the Kunitz domain is protease nexin-II. *Nature*, **1989**, *341*, 144-147.
14. Jin, L. –W.; Ninomia, H.; Roch, J. M.; Schubert, D.; Masliah, E.; Otem, D. A. C.; Saito, T., Peptides containing the RERMS sequence of amyloid beta/A4 protein precursor bind cell surface and promote neurite extension. *J. Neurosci.*, **1994**, *14*, 5461 –5470.
15. Mattson, M. P.; Cheng, B.; Culwell, A. R.; Esch, F. S.; Lieberburg, L.; Rydel, R., Evidence for excitoprotective and interneuronal calcium-regulating roles for secreted forms of the β-amyloid precursor protein. *Neuron*, **1993**, *10,* 243-254.
16. Chow, N.; Korenberg, I. R.; Chen, X. N.; Neve, R. L., APP-BPI, a novel protein that binds to the carboxy-terminal region of the amyloid precursor protein. *J. Biol. Chem*., **1996**, *271*, 11339-11346.
17. Selkoe, D. J. Alzheimer's disease: genes, proteins, and therapy. *Physiological Reviews* **2001**, *81*, 741-766.
18. Bitan, G.; Kirkitadze, M. D.; Lomakin, A.; Vollers, S.S.; Benedek, G. B.; Teplow, D. B., Amyloid beta -protein (Abeta) assembly: Abeta 40 and Abeta 42 oligomerize through distinct pathways. *Proc. Natl. Acad. Sci. U.S.A*., **2003**, *100*, 330.
19. Walsh, D. M.; Klyubin, I.; Fadeeva, J. V.; Cullen, W. K.; Aanwyl, R.; Wolfe, M. S.; Rowan, M. J.; Selkoe, D. J., Naturally secreted oligomers of amyloid beta protein potently inhibit hippocampal long-term potentiation in *vivo*. *Nature*, **2002**, *416*, 535-539.
20. Wirths, O.; Multhaup, G.; Bayer, T. A. A modified β-amyloid hypothesis: intraneuronal accumulation of the β -amyloid peptide - the first step of a fatal cascade *Journal of Neurochemistry* **2004**, *91*, 513-520.
21. Zhang, Y.; McLaughlin, R.; Goodyer, C.; LeBlanc, A. Selective cytotoxicity of intracellular amyloid β peptide$_{1–42}$ through p53 and Bax in cultured primary human neurons. *Journal of Cell Biology,* **2002**, *156*, 519-529.
22. Vieira, E. P.; Hermel, H.; Mohwald, H., Change and stabilization of the amyloid-β(1–40) secondary structure by fluorocompounds. *Biochimica et Biophysica Acta, Proteins and Proteomics,* **2003**, *1645*, 6-14.

23. Dewji, N. N.; Singer, S. J., The seven-transmembrane-spinning topography of the Alzheimer disease-related presenilin proteins in the plasma membranes of cultured cells. *Proc Nat. Acad. Sci.,* **1997,** *94*: l4025- 14030.
24. Sisodia S. S.; Kim S. H.; Thinakaran, G., Function and dysfunction of the presenilins. *Am. J. Hum.Genet.*, **1999,** *65*, 7–12.
25. Borchelt, D. R.; Thinakaran, G.; Eckman, C. B.; Lee, M. K.; Davenport, F.; Ratovitsky, T.; Prada, C. M.; Kim, G.; Seekins, S.; Yager, D.; Slunt, H. H.; Wang, R.; Seeger, M.; Levey, A. I.; Gandy, S. E.; Copeland, N. G.; Jenkins, N. A.; Price, D. L.; Younkin, S. G.; Sisodia, S. S., Familial Alzheimer's disease-linked presenilin 1 variants elevate Abeta1–42/1–40 ratio in vitro and in vivo. *Neuron*, **1996**, *17*,1005–1013.
26. Lorenzo, A.; Yuan, M. L.; Zhang, Z. H.; Paganetti, P. A.; Sturchler-Pierrat, C.; Staufenbiel, M.; Mautino, J.; Sol Vigo, F.; Sommer, B.; Yankner, B. A., Amyloid beta interacts with the amyloid precursor protein: a potential toxic mechanism in Alzheimer's disease. *Nat. Neurosci*. **2000**, *3*, 460–464.
27. Matsuoka, Y.; Gray, A. J.; Hirata-Fukae, C.; Minami, S. S.; Waterhouse, E. G.; Mattson, M. P.; LaFerla, F. M.; Gozes, I.; Aisen, P. S., Intranasal NAP administration reduces accumulation of amyloid peptide and tau hyperphosphorylation in a transgenic mouse model of Alzheimer's disease at early pathological stage. *J. Mol Neurosci.,* **2007,** *31*, 165–170.
28. Miranda, S.; Opazo, C.; Larrondo, L.F.; Muñoz, F. J.; Ruiz, F.; Leighton, F.; Inestrosa, N. C., The role of oxidative stress in the toxicity induced by amyloid β-peptide in Alzheimer´s disease. *Prog. Neurobiol*., **2000**, *62*, 633-648.
29. Schubert, D.; Chevion, M., The role of iron in Abeta amyloid toxicity. *Biochem. Biophys. Res. Commun.*, **1995**, *216*, 702.707
30. Taniguchi, A.; Sohma, Y.; Hirayama, Y.; Mukai, H.; Kimura, T.; Hayashi, Y.; Matsuzaki, K.; Kiso, Y., "Click peptide": pH-triggered in situ production and aggregation of monomer Aβ 1-42. *ChemBioChem*, **2009**, *10*, 710-715.
31. Castano, E. M.; Prelli, F.; Wisiniewski, T.; Golabek, A.; Kumar, R. A.; Soto, C.; Frangione, B., Fibrillogenesis in Alzheimer's disease of amyloid beta peptides and apolipoprotein E. *Bichem. J*., **1992**, *306*, 599-604.

32. Ma, J.; Yee, A.; Brewer, H. B.; Das, S.; Potter, H., Amyloid-associated proteins alpha 1-antichymotrypsin and apolipoprotein E promote assembly of alzheimer beta-protein into filaments. *Nature*, **1994**, 372, 92-94.
33. LaDu, M. J.; Stine, W. B. Jr., Narita, M.; Getz, G. S.; Reardon, C. A.; Bu. G., Self-Assembly of HEK Cell-Secreted ApoE Particles Resemble ApoE-Enrichment of Lipoproteins as a Ligand for the LDL Receptor-Related Protein. *Biochemistry*, **2006**, *45*, 381-390.
34. Strittmatter, W. J.; Saunders, A. M.; Schmechel, D.; Pericak-vance., M.; Enghild, J.; Salvesen, G. S.; Roses, A. D., Apolipoprotein E: high-avidity binding to beta-amyloid and increased frequency of type 4 allele in late-onset familial Alzheimer disease . *Proc. Natl. Acad. Sci. U.S.A.,* **1993**, *90*, 1977-1981.
35. Gearing, M.; Mori, H.; Mirra, S. S.; Aβ-peptide length and apolipoprotein E genotype in Alzheimer's disease. *Ann. Neurol*., **1996**, *39*, 395-399.
36. Cho, H. S., Hyman, B. T.; Greenberg, S.M.; Rebeck, G.W., Quantitation of ApoE domains in Alzheimer disease brain suggests a role for ApoE in Abeta aggregation. *J. Neuropathol. Exp. Neurol.*, **2001**, *60*, 342-349.
37. Mann, D. M.; Iwatsubu, T.; Pickering Brown, S. M.; Owen, F.; Saido, T. C.; Perry, R. H., Preferential deposition of amyloid beta protein (Abeta) in the form Abeta40 in Alzheimer's disease is associated with a gene dosage effect of the apolipoprotein E E4 allele. *Neurosci. Lett*., **1997**, *221*, 81-84
38. Ishii, K.; Tamaoka, A.; Mizusawa, H.; Shoji, S.; Ohtake, T.; Fraser, P. E.; Takahashi, H.; Tsuji, S.; Gearing, M.; Mizutani, T.; Yamada, S.; Kato, M.; St. George-Hyslop. P. H.; Mirra, S. S., Mori, H., Abeta1-40 but not Abeta1-42 levels in cortex correlate with apolipoprotein E epsilon4 allele dosage in sporadic Alzheimer's disease. *Brain Res*. **1997**, *748*, 250-252.
39. Jin, L.-W.; Hua, D. H.; Shie, F, -S.; Maezawa, I.; Sopher, B.; Martin, G. M., Novel Tricyclic Pyrone Compounds Prevent Intracellular APP C99-Induced Cell Death. *J. Mol. Neurosci.*, **2002**, *19*, 57-61
40. Omura, S.; Tomoda, H.; Kim, Y. K.; Nishida, H. Pyripyropenes, highly potent inhibitors of acyl-CoA:cholesterol acyltransferase produced by Aspergillus fumigatus. *Journal of Antibiotics* **1993**, *46*, 1168-9.

41. Simons, M.; Keller, P.; Dichgrans, J.; Schulz J. B., Cholesterol and Alzhimer: Is there a link? *Neurology*, **2001**, *57*, 1089-1093.
42. Wolozin B., cholesterol and the biology of alzheimer disease. *Neuron*, **2004**, *41*, 7-10.
43. Sparks, D.L., Intraneuronal beta amyloid immunoreactivity in the CNS. *Neurobiol. Aging.* **1999**, *17*, 291-299.
44. Refolo, L. M.; Malester, M. B.; LaFrancois, J.; Bryant-Thomas, T.; Wang, R.; Tint, G. S.; Sambamurti, K.; Duff, K.; Pappolla, M. A., Hypercholesterolaemia accelerates the alzheimer's amyloid pathology in a transgenic mouse model. *Neurobiol. Dis.*, **2000**, *7*, 321-331.
45. Wood, W. G.; Schroeder, F.; Avdulov, N. A.; Chochina, S. V.; Igbavboa, U., Recent advances in brain cholesterol dynamics: transport, domains, and Alzheimer's disease. *Lipids*, **1999**, *34*, 225-234.
46. Avdulov, N. A., Chochina, S. V.; Igbavboa, U.; Warden, C. S.; Vassiliev, A. V.; Wood, W. G., Lipid binding to the amyloid β-peptide aggregates: preferential binding of cholesterol as compared with phosphatidylcholine and fatty acids. *J Neurochem.*, **1997**, *69*, 1746-1752.
47. McLaurin, J.; Darabie, A. A.; Morrison, M. R., Cholesterol, a modulator of membrane-associated Aβ-fibrillogenesis. *Ann. N. Y. Acad. Sci.*, **2002**, *977*, 376-383.
48. Yip, C. M.; Elton, E. A.; Darabie, A. A.; Morrison, M. R.; McLaurin, J., Cholesterol, a modulator of membrane-associated Aβ-fibrillogenesis and neurotoxicity. *J. Mol. Biol.*, **2001**, *311*, 723-734.
49. Kirsch, C.; Eckert, G. P.; Mueller, W. E., Cholesterol attenuates the membrane perturbing properties of β-amyloid peptides. *Amyloid*, **2002**, *9*, 149-159.
50. Probst, A.; Langui, D.; Ipsen, S.; Robakis, N.; Ulrich, J., Deposition of β/A4 protein along neuronal plasma membrane in diffuse senile plaques. *Acta. Neuropathol. (Berl)*, **1991**, *83*, 21-29.
51. Mori, T.; Paris, D.; Town, T.; Rojaini, A. M.; Sparks, D. L.; Delledonne, A.; Crawford, F.; Abdullah, A. I.; Humphrey, J. A.; Dickson, D. W.; Mullan, M. J., Cholesterol accumulates in senile plaques of Alzheimer disease patients and in transgenic APP(SW) mice. *J. Neuropathol. Exp. Neurol.*, **2001**, *60*, 778-785.

52. Hua, D. H.; Huang, X.; Tamura, M.; Chen, Y.; Woltkamp, M.; Jin, L.-W.; Perchellet, E. M.; Perchellet, J.-P.; Chiang, P. K.; Namatame, I.; Tomoda, H., Synthesis and bioactivities of tricyclic pyrones. *Tetrahedron*, **2003**, *59*, 4795- 4803.
53. Maezawa, I.; Hong, H. -S.; Wu, H. -C.; Battina, S. K.; Rana, S.; Iwamoto, T.; Radke, G. A.; Pettersson, E.; Martin, G. M.; Hua, D. H.; Jin, L.-W., A novel tricyclic pyrone compound ameliorates cell death associated with intracellular amyloid-β oligomeric complexes. *J. Neurochem.*, **2006**, *98*, 57-67.
54. Hong, H. -S.; Rana, S.; Barrigan, L.; Shi, A.; Zhang, Y.; Zhou, F.; Jin, L.-W.; Hua, D. H., Inhibition of Alzheimer's amyloid toxicity with the tricyclic pyrone molecule in vitro and in vivo., *J. Neurochem.*, **2009**, *108*, 1097-1108.
55. Lashuel, H. A.; Hartley, D. M.; Balakhaneh, D.; Aggarwal, A.; Teichberg, S.; Callaway, D. J. E., New Class of Inhibitors of Amyloid-beta Fibril Formation. Implications for the mechanism of pathogenesis in Alzheimer's disease. *J. Biol. Chem.,* **2002**, *277*, 42881-42890
56. Yang, F.; Lim, G. P; Begum, A. N; Ubeda O. J.; Simmons M. R.; Ambegaokar, S. S; Chen, P. P.; Kayed, R.; Glabe C. G.; Frautschy S. A.; Cole, G. M., Curcumin inhibits formation of amyloid beta oligomers and fibrils, binds plaques, and reduces amyloid in vivo. *J. Boil. Chem*., **2005**, *280*, 5892-901.
57. Taniguchi, S.; Suzuki, N.; Masuda, M.; Hisanaga, S.; Iwatsubo, T.; Geodert, M.; Hasegawa, M., *J. Biol. Chem*., **2004**, *280*, 7614-7623.
58. Pollack, S. J.; Sadler, I. I. J.; Hawtin, S. R.; Tailor, V. J.; Shearman, M. S., Sulfonated dyes attenuate the toxic effects of β -amyloid in a structure-specific fashion. *Neurosci. Lett.*, **1995**, *197*, 211-14.
59. Bush, A. I., Metal complexing agents as therapies for Alzheimer's disease. *Neurobiol. Aging*, **2002**, *23*, 1031-8.
60. Yang, F.; Lim, G. P.; Begum, A. N.; Ubeda, O. J.; Simmons, M. R.; Ambegaokar, S. s.; Chen, P.; Kayed, R.; Glabe, C. G.; Frautschy, S. A.; Cole, G. M., Curcumin inhibits formation of amyloid β oligomers and fibrils, binds plaques, and reduces amyloid in vivo. *J. Biol. Chem*. **2005**, *280*, 5892-5901.

61. Cheng, Y.; Feng, Z.; Zhang, Q. -Z.; Zhang, J. -T., Beneficial effects of melatonin in experimental models of Alzheimer disease. *Acta Pharmacologica Sinica,* **2006**, *27*, 129-139.

62. Lovell, M. A.; Robertson, J. D.; Teesdale, W. J., Copper iron and Zinc in Alzheimer disease senile plaque. *J. Neurol. Sci*., **1998**, *158*, 47-52

63. Schubert ,D.; Chevion, M., The role of iron in Abeta amyloid toxicity, *Biochem. Biophys. Res. Commun.*, **1995**, *216*, 702-707

64. Bush, A. I.; Pettinghel, W. H.; Multhaup, G., Rapid induction of alzheimer Aβ amyloid formation by zinc. *Science*, **1994**, *265*, 1464-67

65. Multhaup, G.; Schlicksupp, A.; Hesse, L., The amyloid precursor protein of alzheimer disease in the reduction of copper II to copper I., *Science*, **1996**, *271*, 1406-1407

66. Behl, C.; Davis, J.B.; Lesley, R.; Schubert, D., Hydrogen peroxide mediates amyloid β protein toxicity. *Cell*, **1994**, *77*, 817-827

67. Cherny R. A.; Legg, J. T.; McLean, C. A., Aqueous dissolution of Alzheimer disease Aβ amyloid deposits by biometal depletion. *J. Biol. Chem.*, **1999**, *274*, 23223-28

68. Omura, S.; Kuno, F.; Otoguro, K.; Sunazuka, T.; Shiomi, K.; Mamuma, R.; Iwai, Y., Arisugacin, a Novel Selective Inhibitor of Acetylcholinesterase from Penicillium sp. FO-4259. *J. Antibiot.*, **1995**, *48*, 745–746.

69. Gu, X.; Li, C.; Wei, W.; Lo, V.; Gong, S.; Li, S. -H.; Iwasato, T.; Itohara, S.; Li, X –J.; Mody, I.; Heintz, N.; Yang, W., Pathological Cell-Cell Interactions Elicited by a Neuropathogenic Form of Mutant Huntingtin Contribute to Cortical Pathogenesis in HD Mice. *Neuron*, **2005**, *46*, 433- 444.

70. Ridley, C. P.; Khosla, C., Synthesis and biological activity of novel pyranopyrones derived from engineered aromatic polyketides. *ACS Chemical Biology*, **2007**, *2*, 104-108.

71. Hua, D. H., Chen, Y., Sin, H.-S., Maroto, M. J., Robinson, P. D., Newell, S. W., Perchellet, E. M., Ladesich, J. B., Freeman, J. A., Perchellet, J.-P., and Chiang, P. K., A one-pot condensation of pyrones and enals. Synthesis of 1H,7H-5a,6,8,9-tetrahydro-1-oxopyrano[4,3-b][1] benzopyrans. *J. Org. Chem.,* **1997**, *62*, 6888–6896.

72. Chen, Y., Synthetic studies toward the synthesis of tricyclic pyrone derivatives and chloropuuphenone. **1999**, 264 pp. CAN 134:178386

73. Trushina, E.; Rana, S.; McMurray, C.T.; Hua, D.H., Tricyclic pyrone compounds prevent aggregation and reverse cellular phenotypes caused by expression of mutant Huntington protein in striatal neurons. *BMC Neuroscience*, **2009,** *10,* E-ISSN:1471-2202.
74. McMurray, J. E.; Kocovsky, P., A method for the palladium-catalyzed allylic oxidation of olefins. *Tetrahedron*, **1984**, *25*, 4187.
75. Rana, S.; Hong, H. –S.; Barrigan, L.; Jin, L. –W, Hua, D.H., Synthesis of tricyclic pyrones and pyridinones and protection of Aβ-peptide induced MC65 neural cell death. *Bio. Org. Med. Chem*., **2009**. 19, 670-674.
76. Lim, M. -I.; Moyer, J. D.; Crysyk, R. L.; Marquez, V. E., Cyclopentenyluridine and cyclopentenylcytidine analogues as inhibitors of uridine-cytidine kinase. *J. Med. Chem.*, **1984**, *27*, 1536.
77. Wang, F.; Yang, Z. -J,; Jin, H. -W.; Zhang, L. -R.; Zhang, L. -H., A concise synthesis of 4,6-dideoxy-4-base-6-amino-2,5-anhydro-l-mannitols. *Tetrahedron: Asymmetry*, **2007**, *18*, 2139-2146.
78. Da Settimo, F.; Primofiore, G.; La Motta, C.; Taliani, S.; Simorini, F.; Marini, A. M.; Mugnaini, L.; Lovecchia, A.; Novellino, E.; Tuscano, D.; Martini, C.J., Novel, highly potent adenosine deaminase inhibitors containing the pyrazolo[3,4-d]pyrimidine ring system. Synthesis, structure-activity relationships, and molecular modeling studies. *J Med. Chem.*, **2005**, *48*, 5162-5174
79. Brown, D. J.; Grigg, G. W.; Iwai, Y.; McAndrew, K. N.; Nagamatsu, T.; Van Heeswyck, R., *Aust. J. Chem.,* **1979**, *32*, 2713
80. Wang, B.; Wang, M.; Zhang, H.; Sobal, N. S.; Tong. W. Gao, C.; Wang. Y.; Geirsig. M.; Wang. D.; Mohwald. H., Stepwise interfacial self-assembly of nanoparticales via specific DNA pairing. *Phys. Chem. Chem. Phys.*, **2007**, *9*, 6313
81. Papoulis, A.; Al-Abed, Y.; Bucala, R., Identification of N2-(1-carboxyethyl)guanine (CEG) as a guanine advanced glycosylation end product. *Biochemistry*, **1995**, *34*, 648
82. Li, Nan-Sheng; Piccirilli, Joseph A., Efficient Synthesis of 2'-C- β-Methylguanosine. *J. Org. Chem.*, **2006**, *71*, 4018-4020.
83. Busca, P.; McCort, I.; Prange, T.; Merrer, Y. L., Synthesis of C-Nucleosidic ATP Mimics as Potential FGFR3 Inhibitors. *Eur. J. Org. Chem.*, **2006**, *10*, 2403.

84. Hua, D. H., Chen, Y., Sin, H. -S., Robinson, P. D., Mayers, C.Y.; Maroto, M. J., Newell, S. W.; Perchellet, E. M.; Ladesich, J. B.; Freeman, J. A.; Perchellet, E. M.; Perchellet, J.-P.; Chiang, P. K.; Bielmann, J. –F., 6,7,8,9-tetrahydro-3-methyl-1H-pyrano-[4,3-b]quinolin -1-one. *Acta Cryst*., **1999**, *C55*, 1698-1701.

85. Wang, J.; Swidorski, J. J.; Sydorenko, N.; Hsung, R. P.; Coverdale, H. A.; Kuyava, J. M.; Liu, J., Aza-[3 + 3] annulations. Part 6. total synthesis of putative (-)-cylindrincine C., *Heterocycles*, **2006**, *70*, 423-459.

86. Wang, C. -S., Structure and chemistry of 4-hydroxy-6-methyl-2-pyrone. *Heterocycles*, **1970**, 389-392.

87. Castillo, S.; Ouadahi, H.; Herault, V., Reaction of 4-hydroxy-6-methyl-2-pyrone with primary amines: synthesis of N-substituted 2-pyridinones and hexanamide intermediates. *Bulletin de la Societe Chimique de France*, **1982**, 7-8, 257-61.

88. Ollinger, P.; Wolfbeis, O. S.; Junek, H., Darstellung, E/Z- Isomeric und gehinderte rotation an N-substituierten Aminomethylen-chromandionen, -pyrandionen und –pyridionene. *Monotshefte fur chemie*, **1975**, *106*, 963-971.

89. Stoyanov, E. V.; Ivanov, I. C., Synthesis of some substituted 2H-pyrano[3,2-c]pyridine-2,5(6H)-Diones. Reaction of their 3-acetyl derivatives with methyl 3-amino-2-butenoate. *Syn. Commun.*, **1998**, *28*, 1755-1767.

CHAPTER 2 - Insight into the inhibition of aggregation of Alzheimer's Aβ peptides and disaggregation of Aβ oligomers using various biophysical techniques

2.1 Introduction

Neurodegenerative disease such as Alzheimer's disease and Huntington's disease involve the neuronal damage caused by the deposition of protein aggregates both extracellularly and intracellularly, which leads to abnormal brain function. The neurotoxicity of amyloid beta- (Aβ) peptide has been widely accepted as one of the fundamental causes of Alzheimer's disease. Our goal is to study the inhibition of aggregation and disaggregation of oligomers and protofibrils using different tricyclic pyrone molecules such as CP2, in solution. In this chapter, I will discuss different biophysical techniques such as atomic force microscopy (AFM), surface plasmon resonance (SPR) spectroscopy, circular dichroism (CD) spectroscopy and protein quantification assay and use them to study the kinetics of aggregation of amyloid Aβ peptide and disaggregation of Aβ42 oligomers and protofibrils. Also, our objective is to search for the role of TP molecules in the counteraction of Aβ toxicity.

2.2 Background

Alzheimer's disease (AD) is a cerebral degenerative disorder characterized by gradual loss of memory, impaired judgment etc. and is affecting 1% of the world population. AD involves two kinds to protein aggregates; (I) Extracellular aggregates, also known as neuritic plaques are composed of Aβ peptide aggregates, which are derived from the proteolytic processing of a transmembrane amyloid precursor protein (APP), by β- and γ- secretase enzymes. These Aβ aggregates tend to adopt β-sheet conformation.[1] Amyloid plaque is deposited in cerebral blood vessels and cortex. (II) Intercellular aggregates, also known as

neurofibrillary tangles (NFT) is composed of phophorylated microtubule-associated tau protein and Aβ.[2] In addition to that, the pathogenesis of AD is also related to genetic mutations responsible for familial forms of AD. The mutations could be in APP itself or in presenilin 1 (PS1) and presenilin II (PS II).[3] Although the detailed mechanism of Aβ aggregation is not fully resolved, a general hypothesis of Aβ aggregation is widely accepted and is as shown in **Figure 1.2**.[4] Aβ42 monomers rapidly oligomerize into paranuclei. Paranuclei themselves then can oligomerize to form larger, beaded protofibrils and fibrils. Monomers, paranuclei, and large oligomers are predominately unstructured but do contain β-sheet/ β-turn and helical (α) elements.[4]

Amyloid fibrils are insoluble filamentous structures with width ~10 nm and length of 0.1-10 μm. Using Solid State Nuclear Magnetic Resonance Spectroscopy, the β-sheet structure of Aβ(10-35) was revealed to have anti-parallel a β-sheet organization.[5] Subsequently, it was found that full length Aβ(1-42) forms β-sheet structure with the same registry and orientation as shown in **Figure 2.1**.[6]

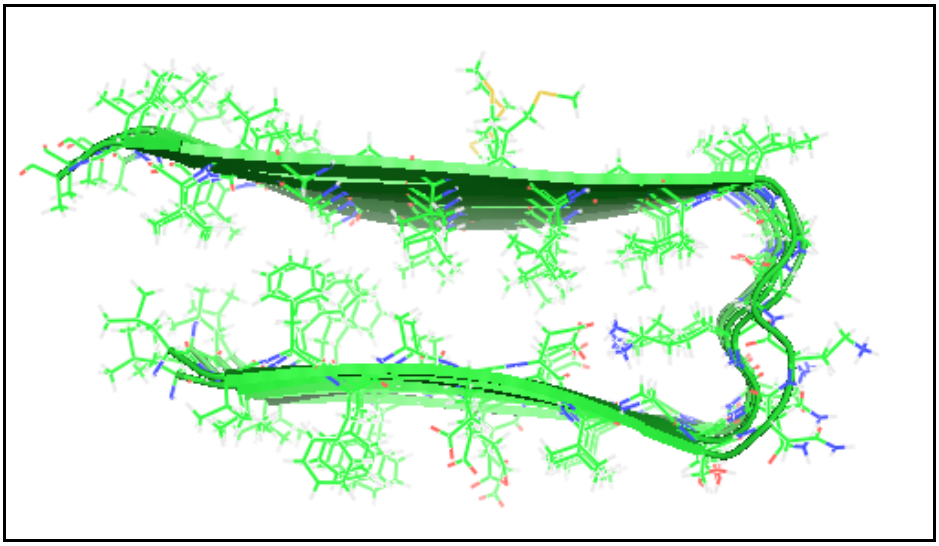

Figure 2.1 Structural model for Aβ42 fibrils, (Taken from protein data bank, provided by Luhrs *et al.*).[6]

Recent studies have suggested that intracellular Aβ oligomers rather than protofibrils or fibrils are the primary toxic species leading to the AD.[7-8] It has been found that intracellular Aβ

aggregates are more toxic then the extracellular Aβ aggregates.[9] Utilization of compounds that reduce the level of Aβ, prevent Aβ aggregation, and disaggregate existing Aβ aggregates has been proposed as a therapeutic strategy for AD. Different biophysical techniques including atomic force microscopy (AFM), circular dichroism (CD) spectroscopy, surface plasmon resonance (SPR) spectroscopy, and a protein quantification assays were used to study to study the mechanism of aggregation of Alzheimer Aβ peptide in solution phase as described in detail in the following sections.

2.3 Biophysical experiments conducted to study the inhibition of aggregation of amyloid Aβ peptides and disaggregation of Aβ oligomers and protofibrils

2.3.1 Use of atomic force microscopy to study the inhibition of aggregation and disaggregation of Aβ peptide

Atomic force microscopy (AFM) is a powerful tool to study the growth/kinetics and morphology of amyloid beta peptide, both in air/solid phase and in solution phase. AFM is used for the screening of small organic molecules as amyloid inhibitors along with other analytical techniques.

2.3.1.1 Introduction and background

AD involves the transformation of non-toxic soluble α-helical monomers into insoluble β-sheet fibrils. These insoluble fibrils are deposited in the extracellular part of the brain and along the walls of cerebral blood vessels as amyloid plaque.[9] A significant amount of evidence suggests that these amyloid plaques play a central role in AD pathogenesis.[9] Although electron microscopy and X-ray diffraction studies revealed the structure and morphology of beta sheet fibrils, they were unsuccessful in providing any insight on the structure and mechanism of aggregation.[11,12] On the other hand, AFM studies have shown the presence of different

intermediates such as small soluble oligomers, large oligomers and protofibrils. In 1990s, AFM was used by Oda *et al.* to study the inhibition of Aβ fibrils formation by clusterin.[13] Lansbery *et al.* used the AFM and showed the formation and structure of Aβ protofibrils.[14-15] Recently, McLaurin *et al.* published an extensive data on the structure of soluble Aβ 40 oligomers.[16] Using AFM, Liu *et al.* reported that amino acid residues 17-20 and 30-35 play a critical role in the formation of oligomers and protofibrils.[17] Our primary focus is to make use of AFM spectroscopy and study the effect of TP compounds on Aβ inhibition of aggregation and disaggregation of soluble oligomers and protofibrils.

2.3.1.2 Preparation of Aβ40 stock solution

A stock solution was prepared by dissolving 0.2 mg of Aβ40 (0.046 μmol) in 50 μL of DMSO (purchased from BACHEM, Bachem California Inc. Torrance, CA). 10 μL of Aβ40 was taken and diluted it with 90 μL of phosphate buffer (50 mM Na_2HPO_4 and 100 mM NaCl, pH 7.4, filtered through "Fischer brand PTFE 0.2 μm) and 100 μL of deionized distilled water (filtered through "Fischer brand PTFE 0.2 μm) to make the total volume to 200 μL. Solution was ultra centrifuged and filtered through a 10,000 molecular weight cutoff ("microcon centrifugal filter devices" purchased from Millipore Corporation, Bedford, MA) at 13,000 r.p.m and 4ºC for 30 minutes and was used for different experiments.[18]

2.3.1.3 Preparation of Aβ42 stock solution

A stock solution was prepared by dissolving 0.25 mg of Aβ42 in 150 μL (0.055 μmol) of DMSO (purchased from CALBIOCHEM, CAT# PP69)). A small aliquot, 20 μL of Aβ42 (0.0073 μmol) was taken and diluted it with 80 μL of phosphate buffer (50 mM Na_2HPO_4 and 100 mM NaCl, pH 7.4, filtered through "Fischer brand PTFE 0.2 μm pore size) and 100 μL of deionized distilled water (filtered through "Fischer brand PTFE 0.2 μm pore size) to make the total volume up to 200 μL. Solution was ultra centrifuged and was filtered through a 10,000 molecular weight cutoff ("microcon centrifugal filter devices" purchased from Millipore Corporation, Bedford, MA) at 13,000 r.p.m and 4ºC for 30 minutes and was used as is for different experiments.[18]

2.3.1.4 AFM instrumentation and sample preparation

A Nanoscope IIIa SPM AFM (Digital Instruments Inc., Santa Barbara, CA, USA) workstation equipped with a multimode head using E-series or J-series piezoceramic scanner (Digital Instruments, Santa Barbara, CA). AFM probes were silicon nitride microcentilevers with 300kHz resonance frequency and 40 N/m spring constant model images were acquired at scan rate of 0.5-1 Hz. Prior to sample preparation, all the stock solutions were vortexed for 30-45 seconds. From the aliquot, 10 μL sample was removed and immediately spotted on freshly

cleaved micas. After waiting for 60-90 seconds, unbound Aβ peptide was washed with water twice (80 μL each), and dried with argon. AFM images were collected using a tapping mode with a high-aspect ration tip (Veeco Nanoprobe TM tips, Model TESP-HAR; Nanoscience Instruments, Inc., Phoenix, AZ, USA). Image J software at an 8-bit resolution was used to carry out grain analysis to collect quantitative data. The image was adjusted by setting a threshold so that no noise on the image was present. The same threshold was used for all other images in the same independent experiment. The drive amplitude and force constant were adjusted, to minimize the force of interaction between the tip and the mica surface, thus limiting the sample deformation. For each experiment, 25 μm^2 images from three independent AFM scans were used to determine the density (particles/field) of monomers/ oligomers and protofibrils.[18]

2.3.1.5 Inhibition of aggregation of Aβ40 with several compounds

In vitro MC65 cell assay demonstrated the efficacy of CP2 as an amyloid inhibitor.[19,20] We studied the inhibition effect of two equivalents of CP2 and compared it with thioflavin T, curcumin and Congo red. A stock solution of 200 μL as explained in **2.3.1.2** was prepared and divided into five different vials (30 μL, 37 μM) and two equivalents of different compounds such as CP2, TP17, curcumin, congo red and TP17 (**Figure 2.2**) were added. After 24 h and 48 h, a small aliquot was taken and AFM images were captured. Different areas of the mica were scanned and representative images are shown in **Figure 2.3**.[18]

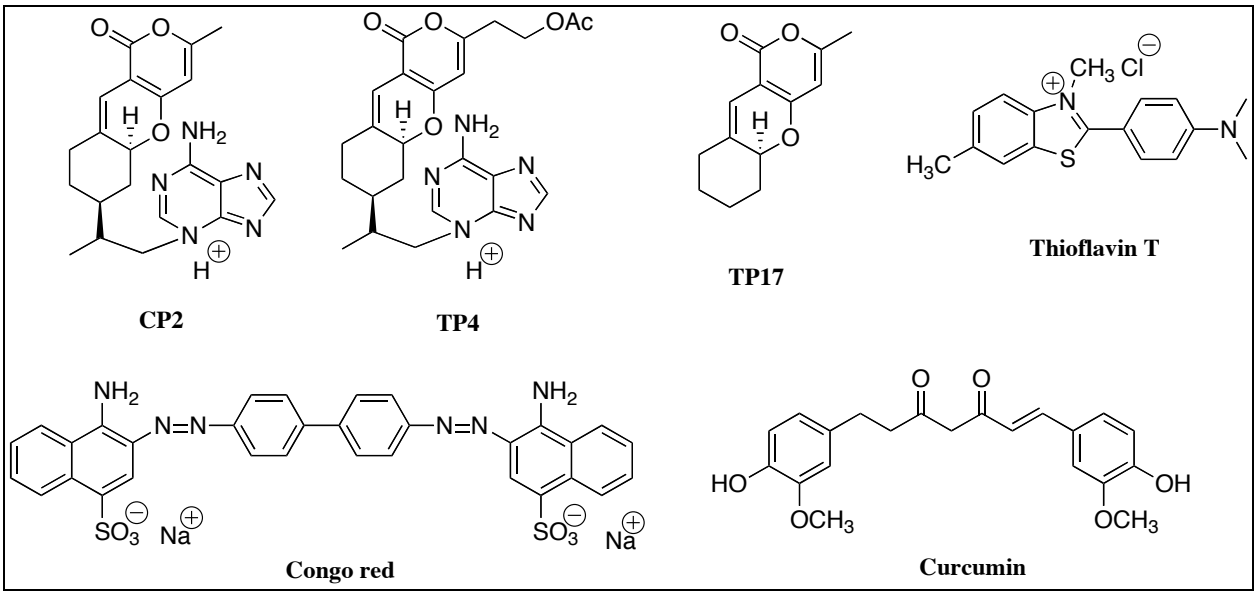

Figure 2.2. Structure of CP2, TP4, TP17, thioflavin T, Congo red and curcumin.

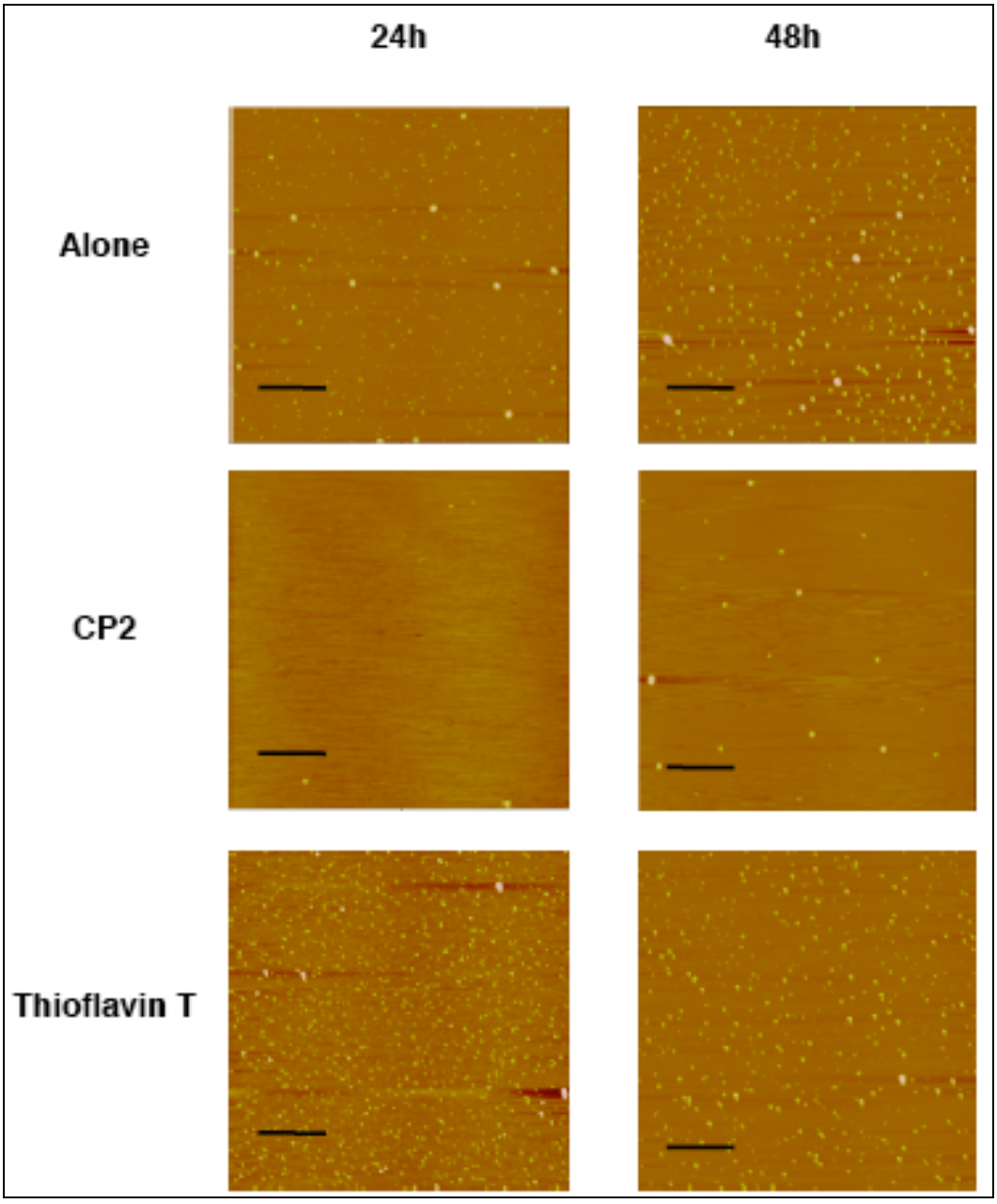

Continued….

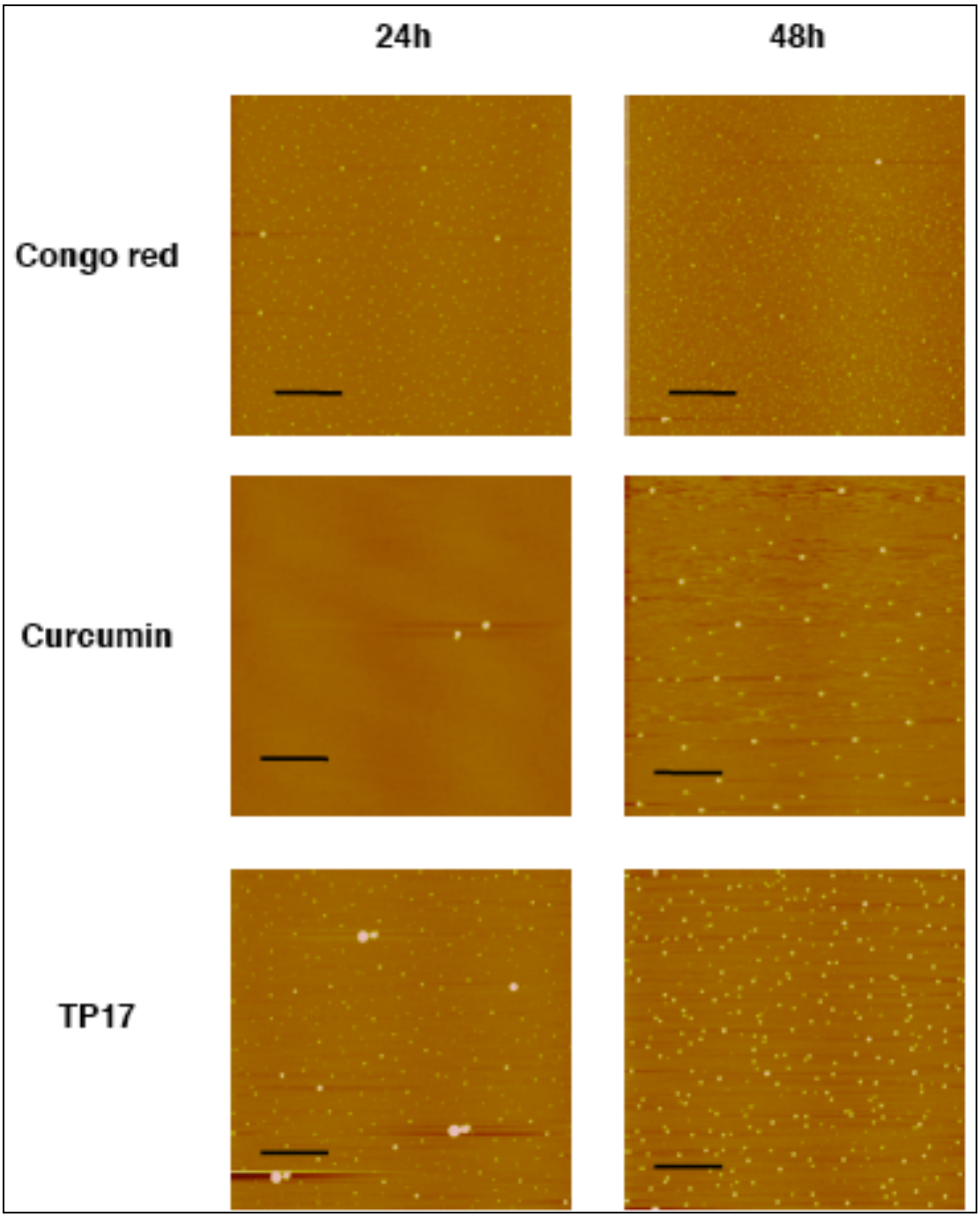

Figure 2.3. AFM images of inhibition of aggregation of Aβ40 monomers (Scale bar 1 μm).

2.3.1.6 Inhibition of aggregation of Aβ42 with several compounds

Since the hydrophobicity of Aβ42 is more than Aβ40, it aggregates fast in buffer solution and is thus more toxic. Similar to Aβ40 inhibition of aggregation studies, we studied Aβ42 inhibition of aggregation. A stock solution of 200 μL as explained in **2.3.1.3** was prepared and divided into five different vials (30 μL, 37 μM) and two equivalents of different compounds such as CP2, TP17, curcumin, Congo red etc. were added. After 24 h and 48 h, a small aliquot was taken and AFM images were captured. Different areas were scanned and representative images are shown in **Figure 2.4.** CP2, Congo red and curcumin have similar inhibitory activities, while TP17 and thioflavin T are inactive.[18]

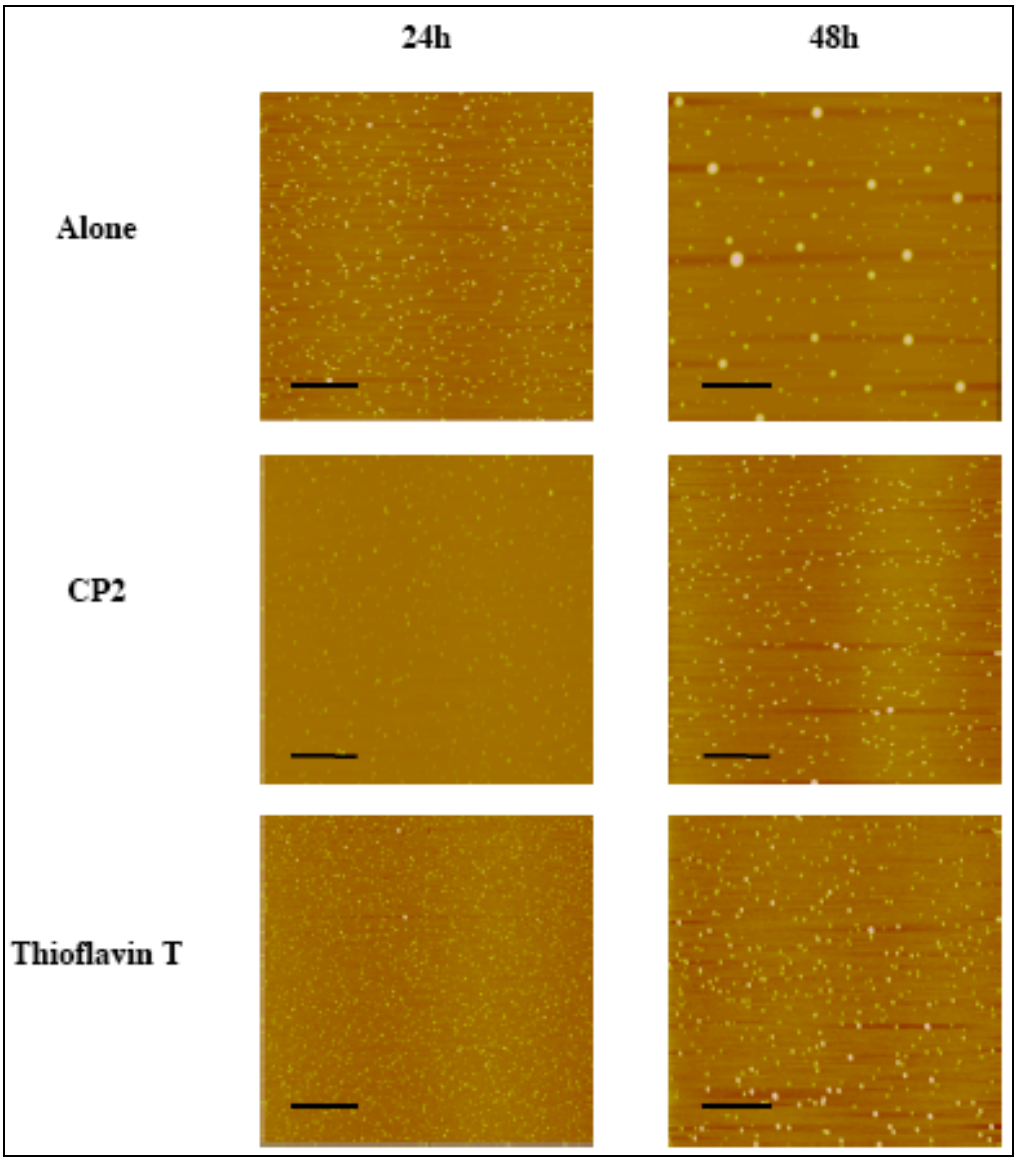

Continued….

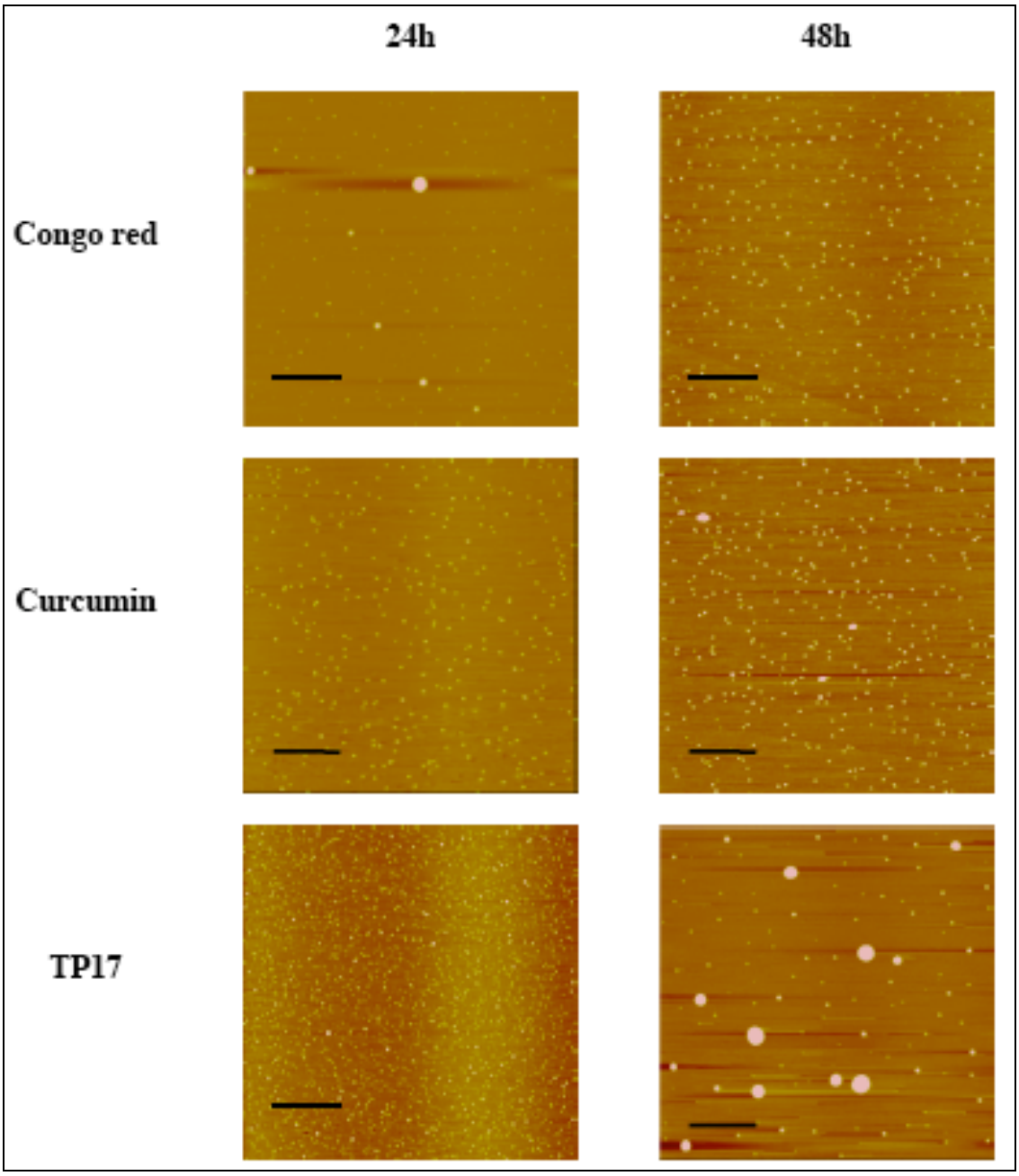

Figure 2.4. AFM images of inhibition of aggregation of Aβ42 monomers.

2.3.1.7 Disaggregation of Aβ42 oligomers with several compounds

A stock solution of 200 μL as explained in **2.3.1.3** was prepared. Stock solution was kept at 4ºC for 24 h and small aliquot was taken. AFM confirms the formation of small oligomers. Once oligomers formed, stock solution was divided into five different vials (30 μL, 37 μM) and two equivalents of different compounds such as CP2, TP17, curcumin, congo red etc. were added. Samples were stored at 4ºC to slow down the speed of aggregation. After 24 h and 48 h, a small aliquot was taken and AFM images were captured. Different areas were scanned and representative images are shown in **Figure 2.5**) CP2, congo red and curcumin have similar inhibitory activities, while TP17 and Thioflavin T are inactive.[18]

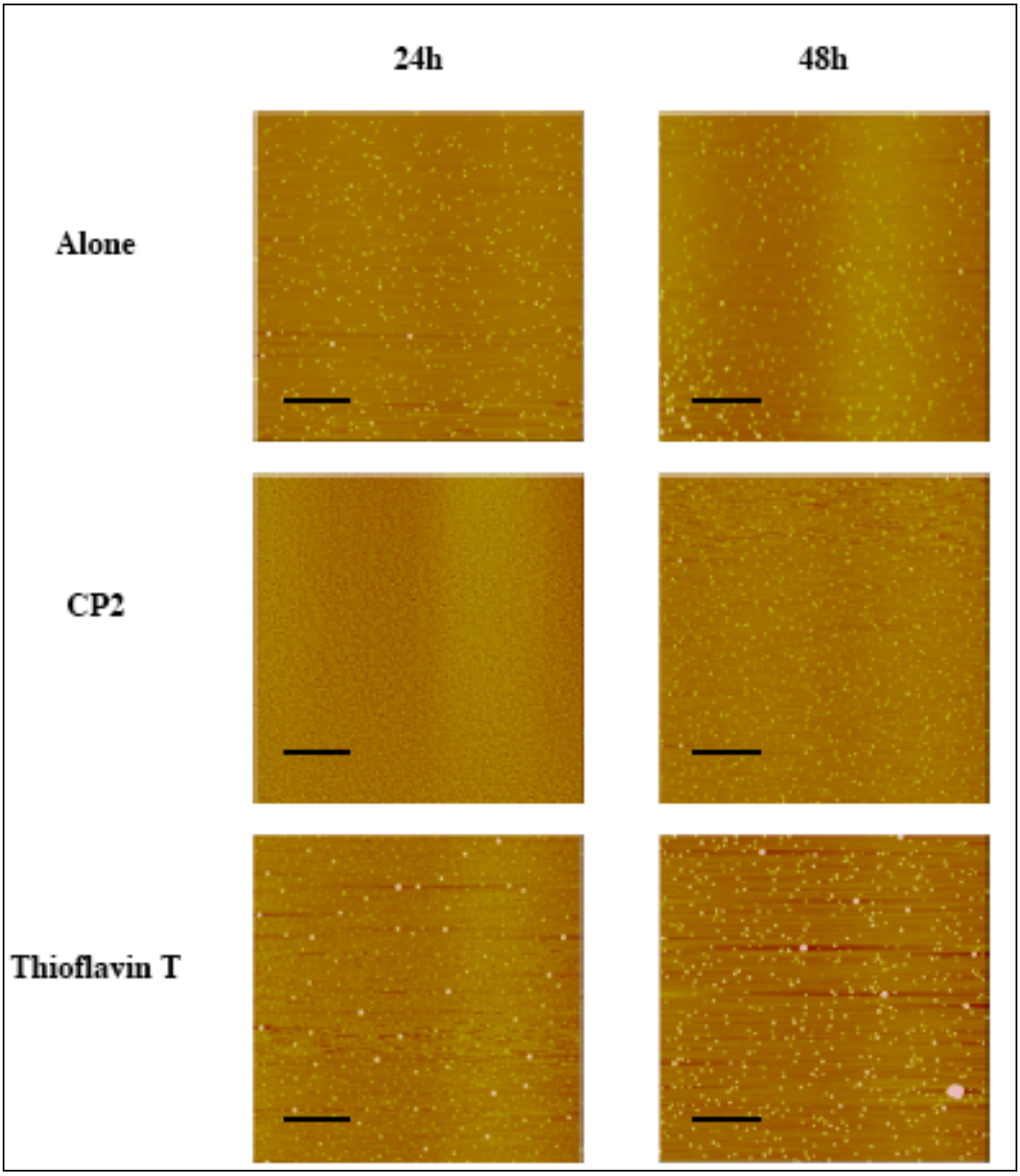
24h
48h
Alone
CP2
Thioflavin T

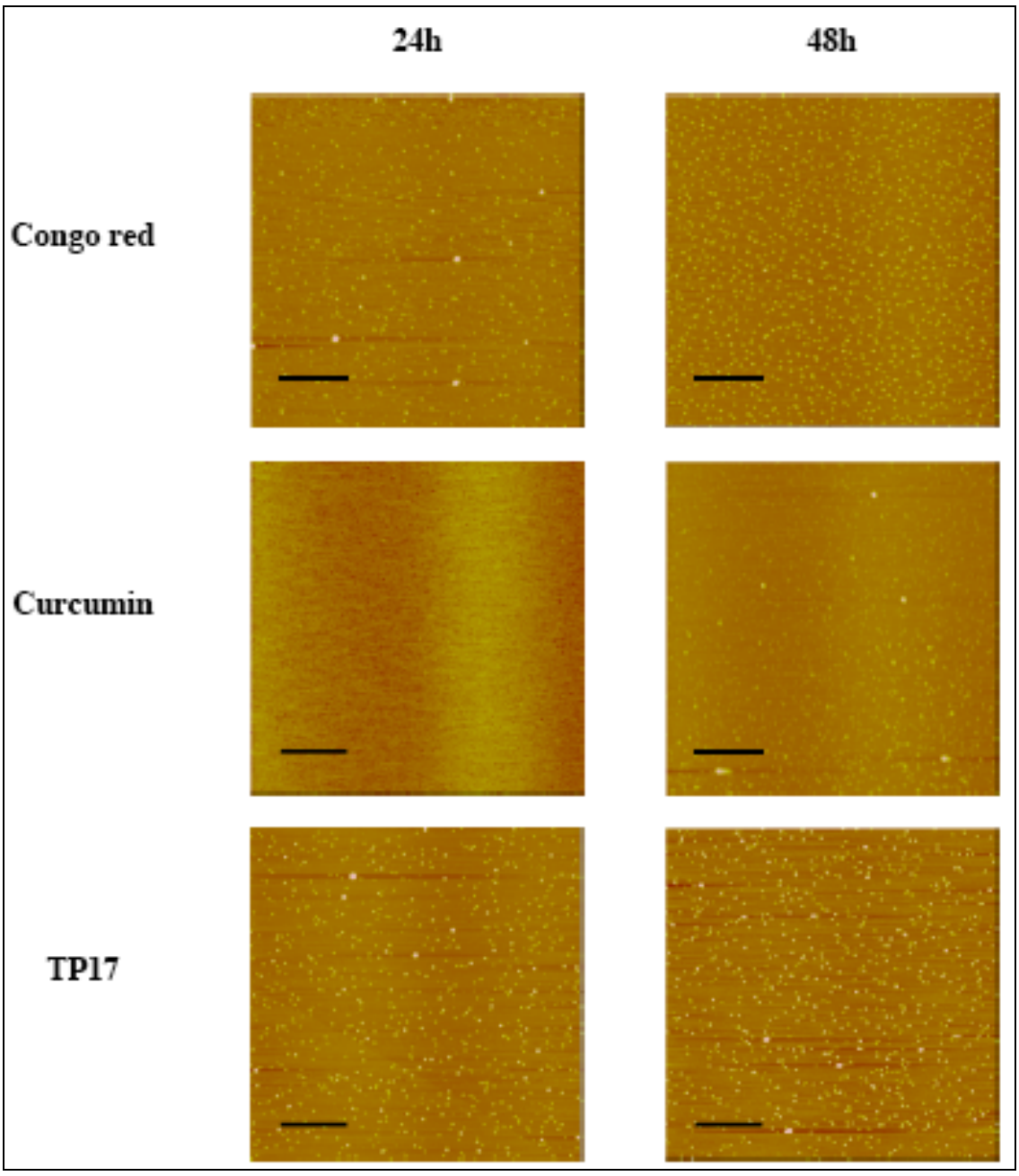

Figure 2.5. AFM images of disaggregation of Aβ42 oligomers.

2.3.1.8 Disaggregation of Aβ42 protofibrils with CP2

According to the proposed aggregation hypothesis, Aβ42 monomers tend to aggregate to form the soluble oligomers. If untreated, soluble oligomers aggregate further to form long protofibrils and fibrils. We studied the efficacy of CP2 on Aβ42 protofibril disaggregation. A stock solution of 200 µL was prepared as explained in **2.3.1.3**. The stock solution was stored at

4°C for 4 days and AFM image was taken to confirm the formation of Aβ protofibrils. Once the protofibrils had formed, 30 μL of Aβ42 (37 μM) was taken and to it was added two equivalents of CP2. After the addition of CP2, the sample was stored at 25ºC for 24 h. After 24 h, a small aliquot was taken and AFM was recorded. Different areas were scanned and a representative image is shown in **Figure 2.6**.[18]

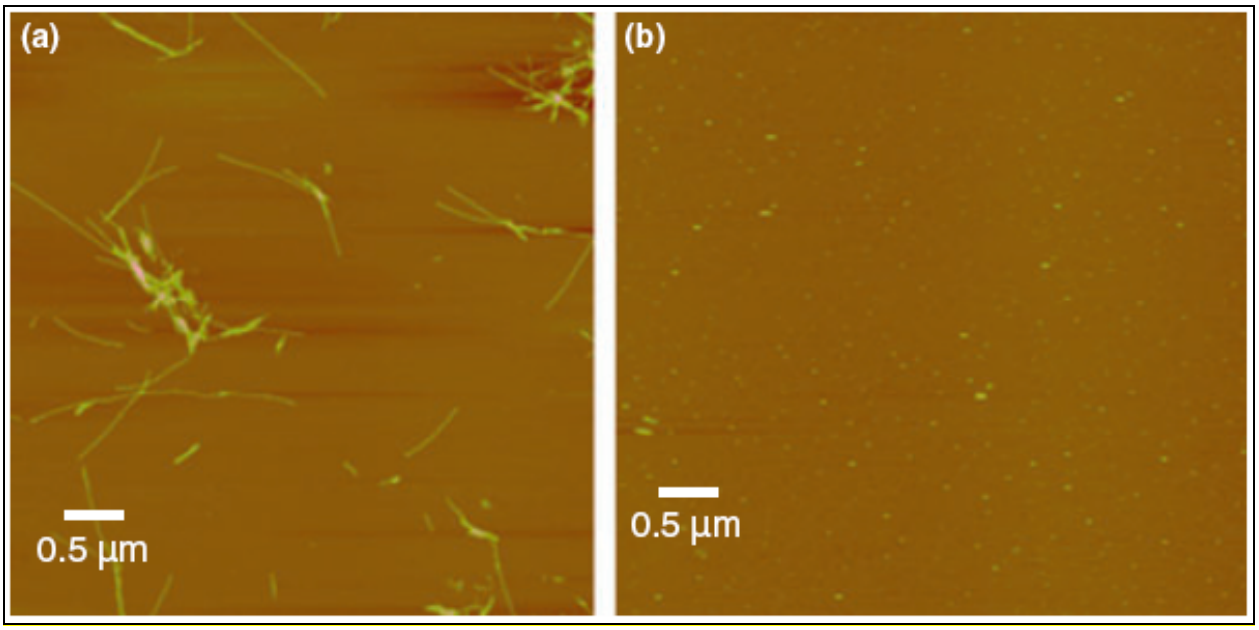

Figure 2.6. AFM images of disaggregation of Aβ42 protofibrils; (a) Aβ42 protofibrils formed form the incubation of Aβ42 monomer (37 μM) at 4ºC for 4 days. (b) Incubation of Aβ42 protofibrils with CP2 (two equivalents) for 24 h at room temperature.

2.3.1.9 Disaggregation of Aβ42 oligomers with CP2 over the period of five days

While performing the disaggregation of Aβ42 oligomers experiment, we found that the disaggregated Aβ42 monomers tend to re-aggregate to oligomers over time. We studied how much CP2 is needed to maintain the Aβ42 in monomeric form. Aβ42 (37 μM) oligomers were treated with 2, 5, and 10 equivalents of CP2 over a period of five days. Each day, a small aliquot (10 μL) was removed from the stock and AFM images were taken. Three representative images are used to calculate the particle density using Image J software and the results are summarized in **Figure 2.7**.[18]

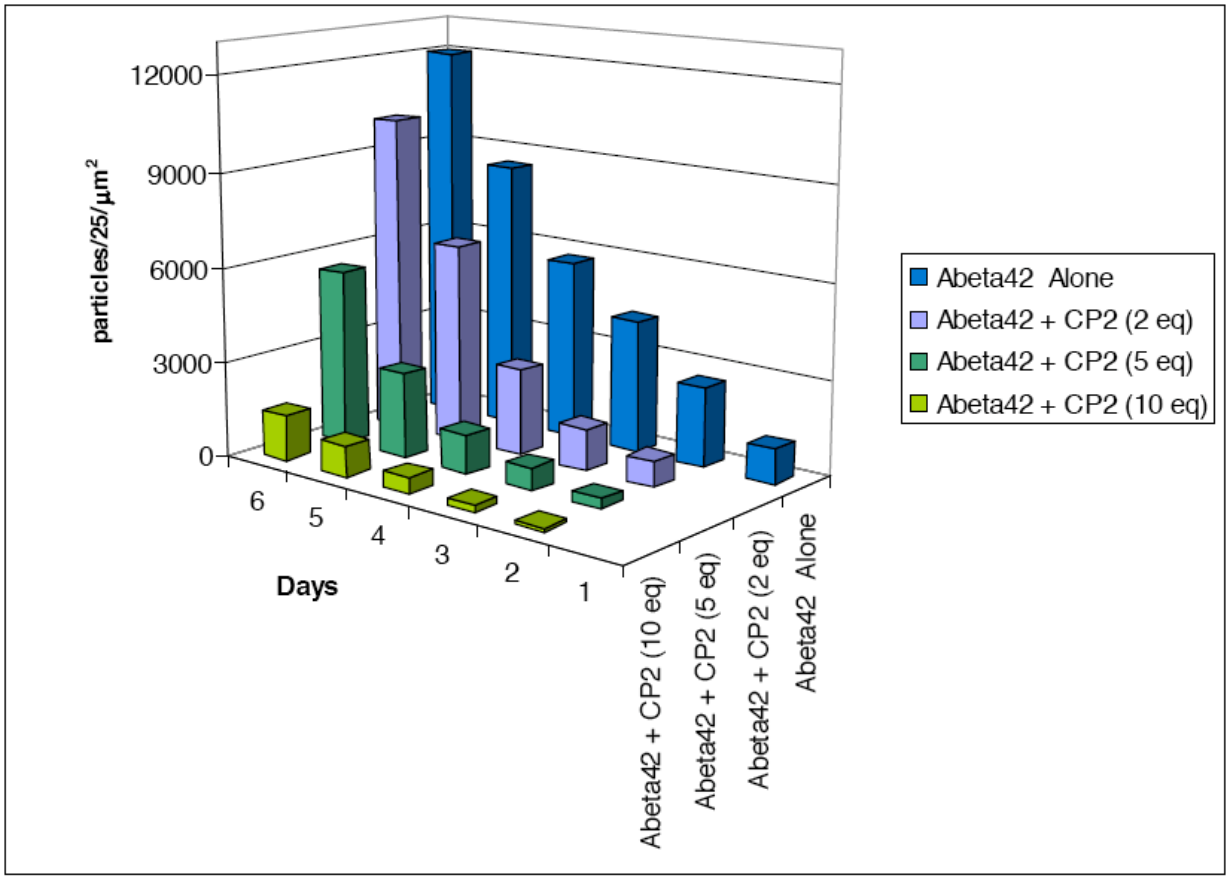

Figure 2.7. Disaggregation of Aβ42 oligomers with different equivalents of CP2 over the period of five days. Quantitative analysis of particle density in 25 μm^2. Aβ oligomeric density from three independent AFM scans was calculated using Image J program.

2.3.1.10 Result and discussion

Using AFM spectroscopy, we studied the efficacy of some compounds such as CP2 and TP4 synthesized in our laboratory and compared it with different commercially available amyloid beta inhibitors such as thioflavin T[21], congo red[22] and curcumin.[23] Tricyclic pyrone molecule TP17 was used as a negative control.[20] Different areas of the mica surface were scanned and a few representative pictures of the result of inhibition of aggregation of Aβ40 (**Figure 2.3**) and Aβ42 (**Figure 2.4**), disaggregation of Aβ42 oligomers (**Figure 2.5**), disaggregation of Aβ42 protofibrils (**Figure 2.6**) with CP2, Thioflavin T, congo red, curcumin, TP17 were captured. Based on our previous results[20], we predicted low affinities of thioflavin T

and TP17 to the Aβ oligomers and consistent results were obtained (**Figure 2.5**). Since Aβ40 is less hydrophobic than Aβ42, lower amounts of aggregates were formed (**Figure 2.3**). Bioactive compounds CP2, congo red and curcumin inhibits the extent of aggregation by about 50% over a period of 48 h, whereas no such inhibitory effect was observed for TP17 and thioflavin T (**Figure 2.8**). Also, when compared to the control, two equivalents of CP2, Congo red and curcumin are sufficient enough to slow down the speed of aggregation (**Figure 2.9**).[18]

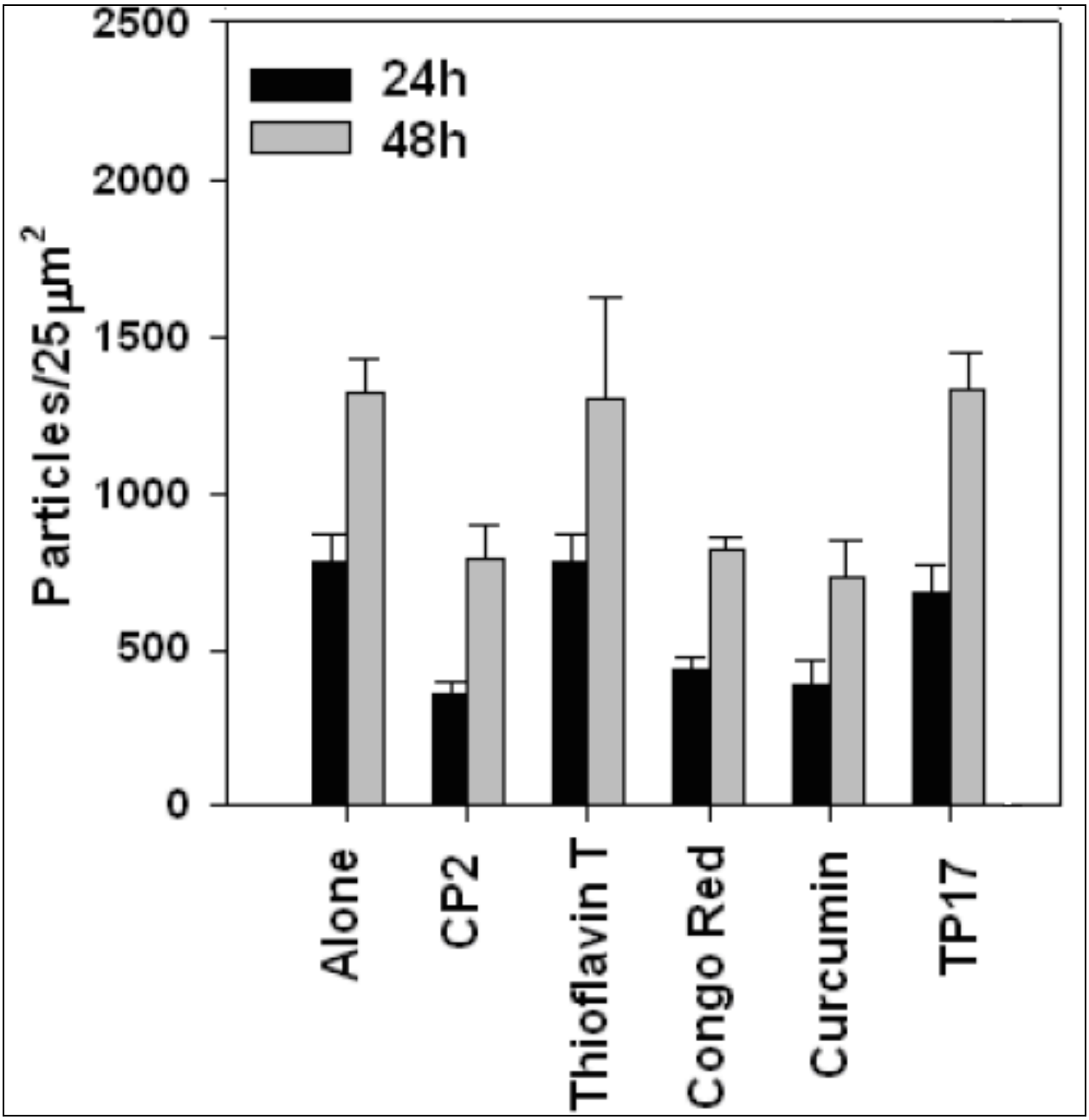

Figure 2.8. Inhibition of aggregation of Aβ40 with two equivalents of CP2, TP17, thioflavin T, curcumin and congo red separately over 24 h and 48 h. Quantitative analysis of particle density in 25 μm^2 AFM scans. Aβ oligomeric density from three independent AFM scans was calculated using Image J program. Error bars represent standard deviation.

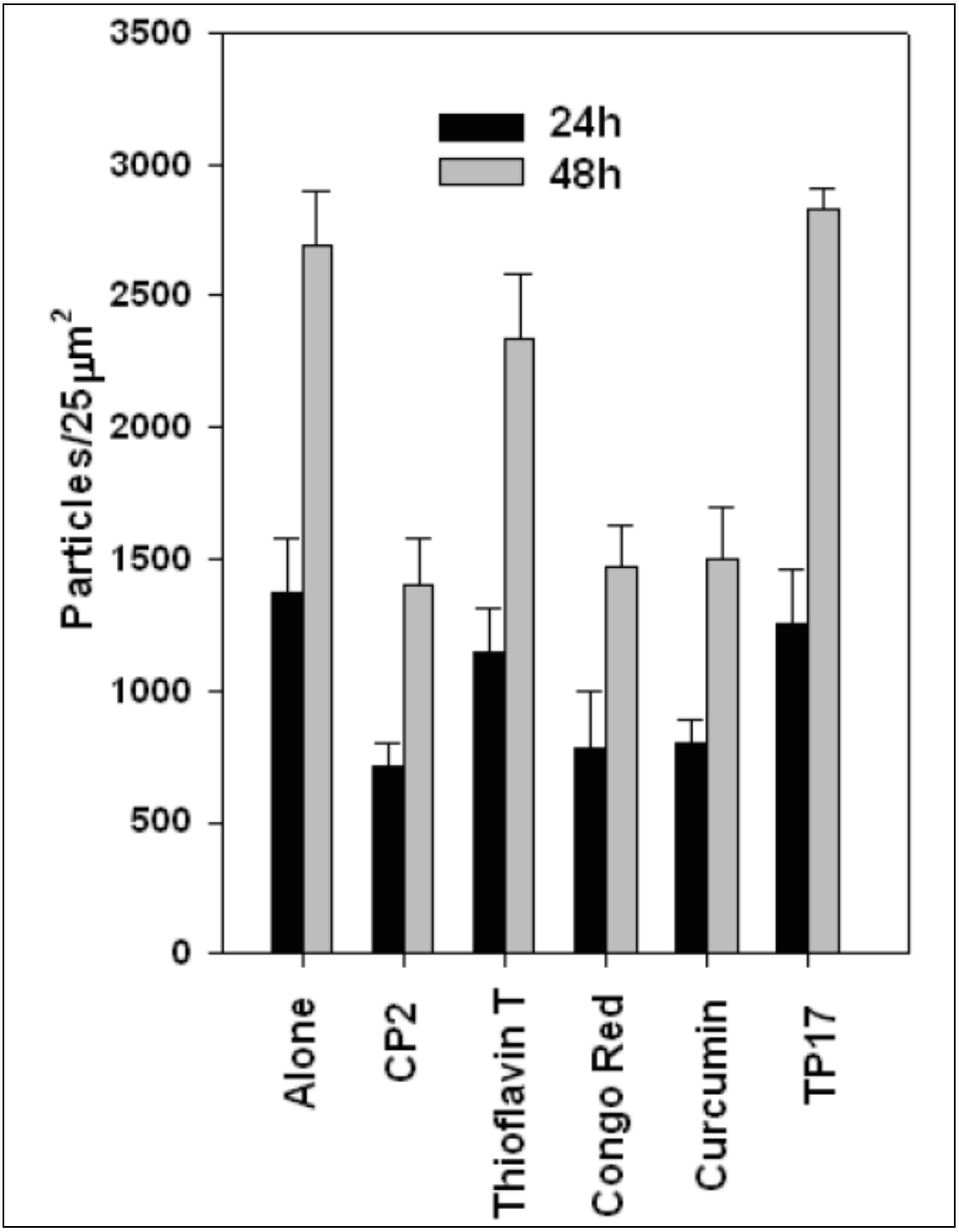

Figure 2.9. Inhibition of aggregation of Aβ42 with two equivalents of CP2, TP17, thioflavin T, curcumin and congo red separately over 24 h and 48 h. Quantitative analysis of particle density

in 25 μm^2 AFM scans. Aβ oligomeric density from three independent AFM scans was calculated using Image J program. Error bars represent standard deviation.

It is widely accepted that Aβ oligomers are toxic to neurons and play a critical role in AD progression.[7] Also, compared to Aβ42, Aβ40 is less toxic and thus we focused our studies on toxic Aβ42 oligomers and protofibrils.[19] We investigated whether CP2, curcumin and congo red have similar effects on Aβ42 disaggregation of the toxic oligomers to non-toxic monomers. Aβ42 oligomers were grown based on a published protocol.[24] Aβ42 oligomers were treated with two equivalents of different compounds such as CP2, thioflavin T, congo red, curcumin and TP17 and AFM images were recorded after 24 h and 48 h (**Figure 2.5**). Due to the size limitation of AFM, Aβ42 monomers and dimers (< 2 nm diameter) were too small to be observed. Different areas were scanned and image J software was used to calculate the peptide density (average three images) and the results are summarized in **Figure 2.10**. After 24 h and 48 h of incubation of different compounds in Aβ42 oligomers at 4°C, a 50% decrease in aggregates was observed for CP2, Congo red and curcumin. After 48 h, CP2 showed the greatest disaggregating ability. Curcumin had a greater disaggregation activity than congo red. Thioflavin T and TP17 did not show disaggregation activities.[18]

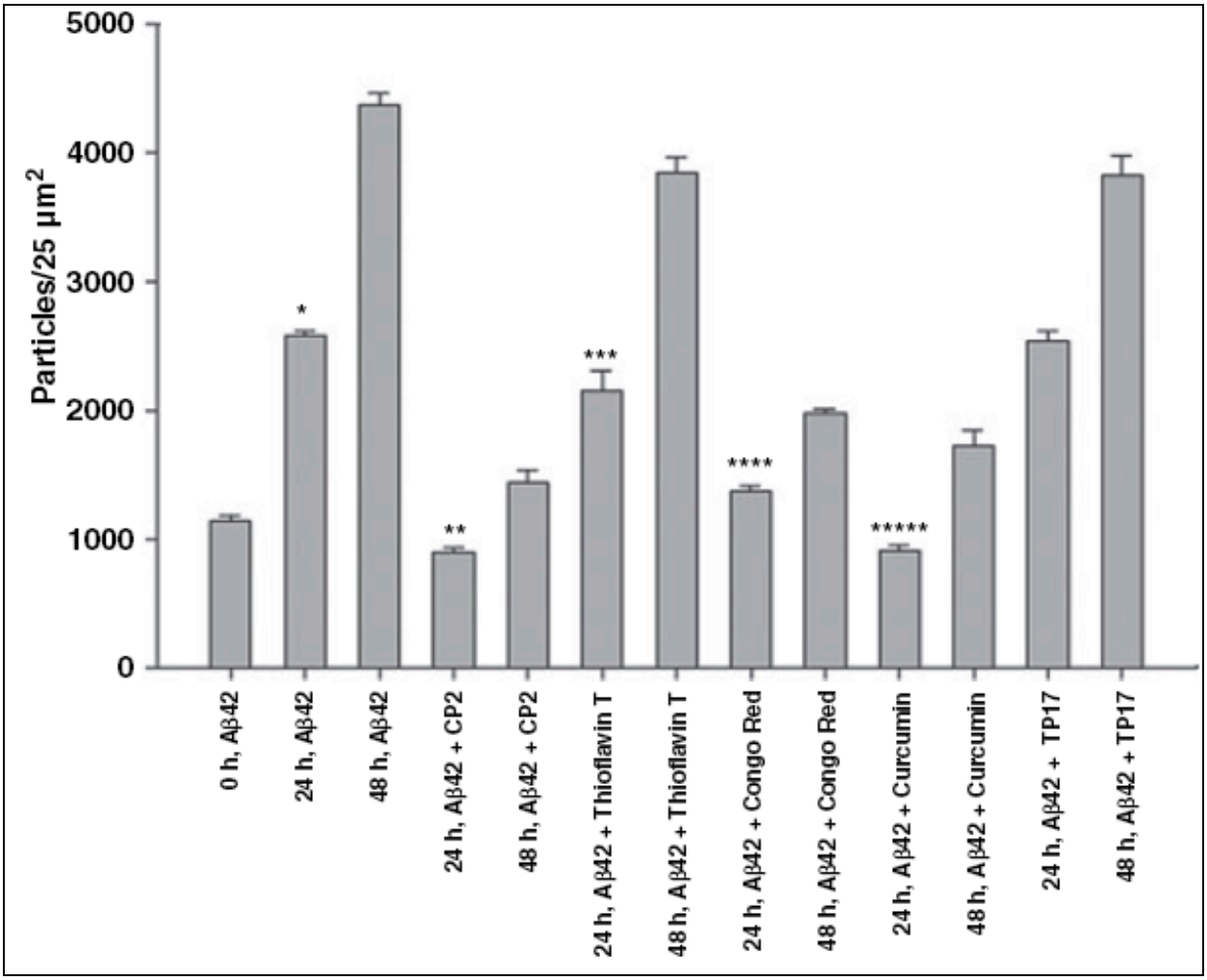

Figure 2.10. Disaggregation of Aβ42 oligomers with two equivalents of CP2, TP17, thioflavin T, curcumin and congo red separately over 24 h and 48 h. Quantitative analysis of particle density in 25 μm^2 AFM scans. Aβ oligomeric density from three independent AFM scans was calculated using Image J program. Error bars represent standard deviation. n =3, *p, **p, ***p, ****p, *****p < 0.01 compared with their respective controls.

Surprisingly, after 24 h, disaggregated Aβ42 tends to re-aggregate over time and more aggregates were observed for CP2, curcumin and congo red over time (**Figure 2.10**). We studied the amount to CP2 required to maintain Aβ42 peptide in monomeric form (derived from the disaggregation of oligomers) without aggregation over 5 days. Hence, Aβ42 oligomers (37 μM) in pH 7.4 PBS solution were prepared (confirmed by AFM) and treated with various amounts of

CP2 and incubated at 4°C over 5 days (days 2–6). Each day, an aliquot was removed and AFM images were taken (in various locations of the mica), and three representative images were used to calculate the peptide particle density. The results are summarized in **Figure 2.7**. On day 4, protofibrils were observed in the Aβ42 solution without CP2, and on day 6, protofibrils predominated. It was observed that Aβ42 solutions incubated with 2 and 5 equivalents of CP2 showed lesser amounts of oligomers after 24 h and 48 h but the oligomers size increased after 5 days. On the other hand, in the presence of 10 equivalent of CP2, only ~8% of oligomers were observed compared with zero equivalent of CP2 after 5 days. The results suggest that disaggregated Aβ42 monomer and smaller oligomers tend to aggregate and can recombine to form larger oligomers over time It is suggestive that CP2 binds to Aβ oligomers and breaks apart the oligomers into small monomer and dimer. The binding of CP2 with monomeric Aβ and Aβ oligomers is reversible and Aβ42 monomer re-aggregates to form oligomers over time in a closed compartment.[18]

Also, based on Aβ aggregation pathway (**Figure 1.2**) Aβ oligomers undergo nucleation polymerization and aggregate to form protofibrils, which have been revealed to be toxic to neuronal cells and to affect learning in mice.[25,26] We studied the disaggregation of Aβ42 protofibrils with CP2. Aβ42 protofibrils were produced by incubation of Aβ42 monomer in PBS for 4 days (confirmed by AFM). To preformed Aβ42 protofibrils, two equivalents of CP2 was added and incubated at 25°C for 24 h. After 24 h, a small aliquot was taken and AFM images revealed the disappearance of protofibrils and presence of small amounts of oligomers (**figure 2.6**).

Detailed AFM studies were conducted in our laboratory and the results have shown that CP2 inhibits the Aβ aggregation formation, disaggregates soluble oligomers to non-toxic monomers and protofibrils to small oligomers.[18]

2.3.2 Use of surface plasmon resonance spectroscopy to study the interaction of tricyclic pyrone and Aβ peptide

2.3.2.1 Introduction and background

Surface plasmon resonance (SPR) is one of the most sensitive tools to detect the mass change above the gold-coated metal surface.[27] SPR used to study the direct binding of protein-protein, protein-compound, ligand-receptor, host-guest, and protein-antibody etc. interactions. In SPR spectroscopy, a change in the mass above the metal surface can be quantified in situ by monitoring a shift in SPR angle (**Figure 2.11**). A SPR spectrometer can sense the change in pg/mm^2.[28]

Aβ monomers polymerize to form insoluble fibrils, which are toxic to neurons. Previous studies indicate that Aβ polymerization involves interactions between the Aβ peptides.[29] A pharmacological approach to prevent the amyloid formation is to use drugs that specifically disrupts the Aβ - Aβ interactions. Tjernberg *et al.* reported a small peptide ligands that can bind to the full length Aβ, and hinder Aβ-Aβ interaction thus inhibits aggregation. Their aim was to find a region of Aβ peptide, which is crucial for Aβ aggregation. Using SPR spectroscopy, they arrest the Aβ fibril formation by a pentapeptide ligand (beta sheet breakers) and confirmed it by AFM spectroscopy.[30] Our goal is to study the binding affinity of TP compound CP2 to Aβ40 and Aβ42 monomers and small soluble oligomers (confirmed by AFM).

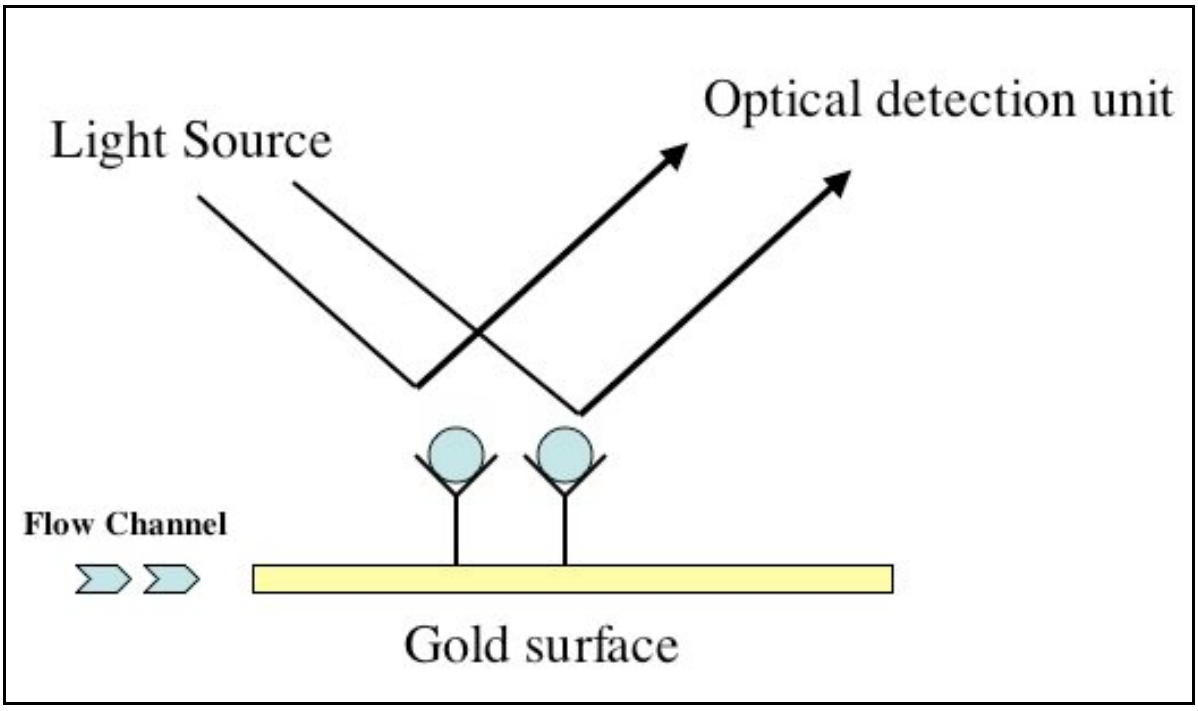

Figure 2.11. Schematic representation of SPR principle.[28] (This picture is modified from the manufacturer's handbook)

2.3.2.2 Binding of CP2 and TP17 to Aβ40 and Aβ42 monomers

A Biacore 3000 (Biacore Inc., Piscataway, NJ, USA), equipped with four flow cells in one sensor chip (CM5), was used for real-time binding studies. The Aβ40 and Aβ42 peptides were separately immobilized on gold sensor CM5 chips as described.[31] First, carboxymethylated dextran of CM5 was activated with N-hydroxysuccinimide in pH 7.4 buffer, followed by the coupling with Aβ peptides. Free activated unreacted chip surface was blocked by ethanolamine. The resulting Aβ-bound sensor chip was used in the SPR studies, and the amounts of bound Aβ were measured from the SPR graph. The reference cells were prepared following the same procedure but without addition of Aβ peptides (**Figure 2.12**).

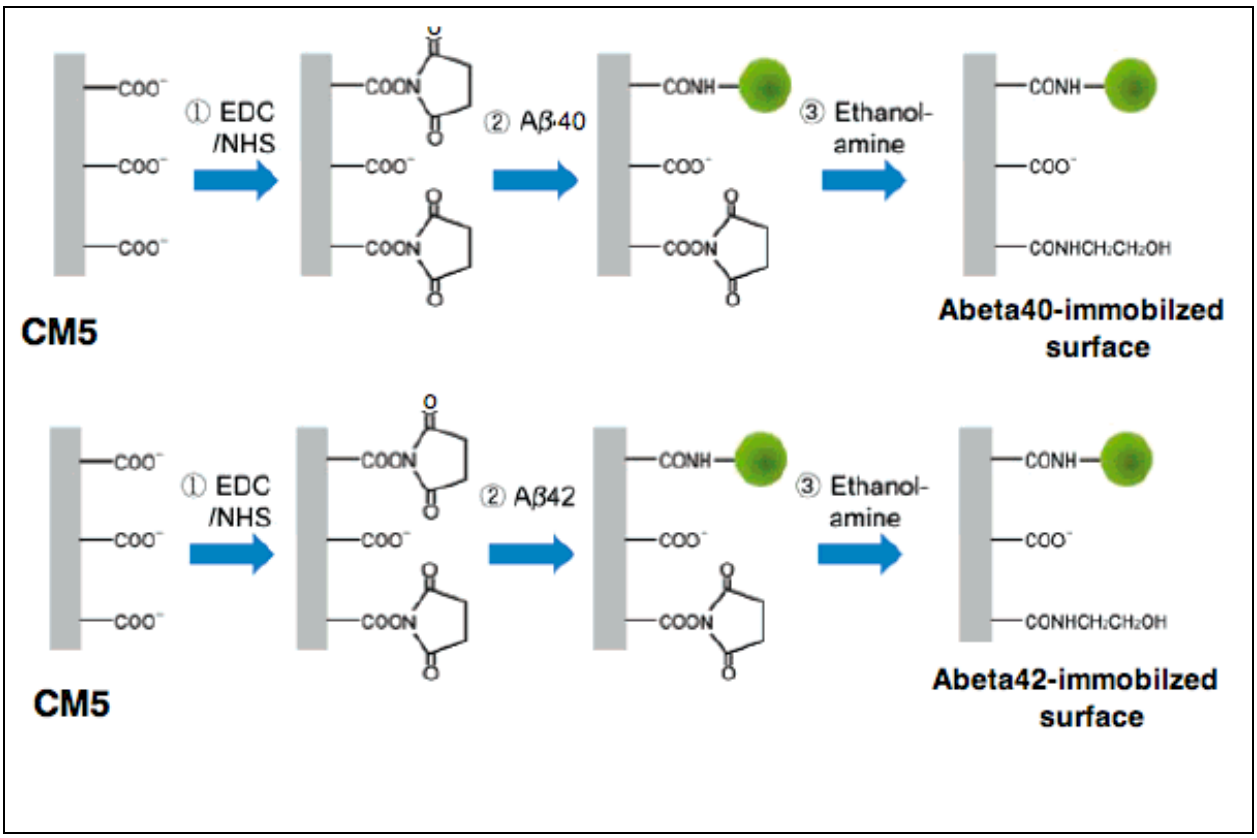

Figure 2.12. Immobilization of Aβ on to CM5 gold chip. (1) Activation and immobilization of Aβ on gold CM5 sensor chip. (2) The surface activated by EDC/NHS was exposed to a fresh Aβ40/ Aβ42 solution to form a peptide bond between the amine group on the peptide and the carboxylic group on the CM5 surface. (3) The deactivation of unreacted sites was achieved by blocking NHS-activations with ethanolamine.[31]

CP2 and TP17 were dissolved in 50 mM Tris buffer to a concentration of 800 μM and injected into flow cells. The chip surface was exposed to compounds for 60 s, then to running buffer (10 mM HEPES, 150 mM NaCl, 3.4 mM EDTA, 0.05% surfactant P20, pH 7.4) for 180 s. The response unit (RU) was recorded, converted to pmol bound compound, and analyzed (1RU = 1 pmol). The flow cells were then regenerated with regenerating buffer containing urea, while leaving the immobilized Aβ peptides intact. The same chips with the same amounts of bound Aβ peptides were used for consecutive analysis of different compounds and comparisons were made only between the bindings to the same chips. The amounts of bound compounds were calculated by the ΔRU value, obtained by subtracting the RU at the time before compound injection from

the RU at the time just after the injection of running buffer. The ΔRU obtained from the reference cell was considered the background binding and was subtracted before the analysis (**Figure 2.13**).[20]

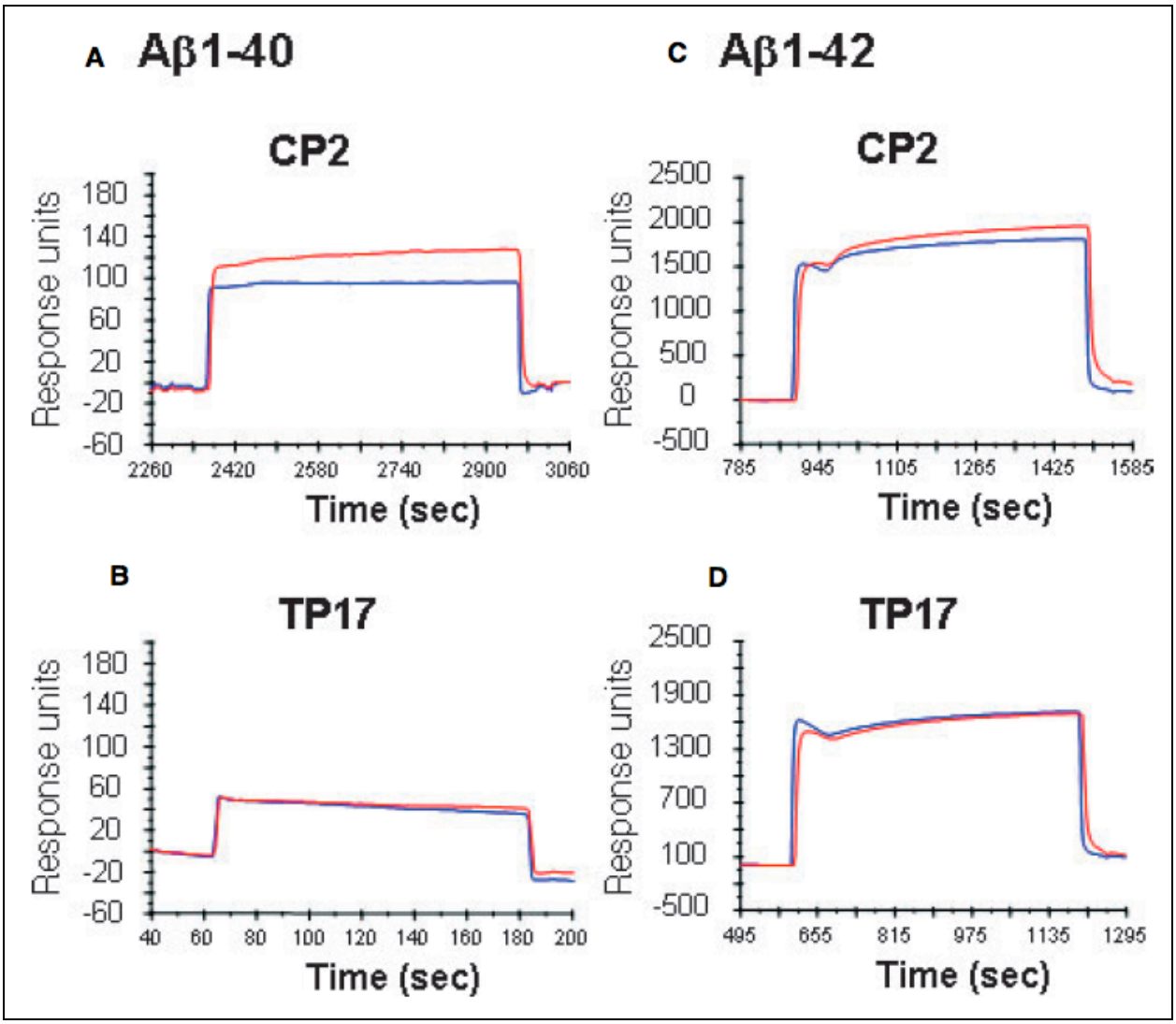

Figure 2.13. Real-time detection of the binding of tricyclic pyrone to Aβ40 (A and B) and Aβ42 (C and D) by SPR. The results from a typical experiment are shown. Color code: Blue is cell surface without immobilized Aβ and Red is cell surface with immobilized Aβ.

2.3.2.3 Binding of CP2 to Aβ42 oligomers using anti-oligomer antibody (AB9234)

We have shown that in real time binding studies, CP2 binds to Aβ peptide. Also, AFM studies have shown that CP2 disaggregates Aβ42 oligomers to monomers but the mechanism of disaggregation is still unknown. In order to shed some light, we are interested in knowing if CP2 binds to Aβ42 oligomers. For real time binding studies using SPR, injecting Aβ42 oligomers to the flow cell does not confirm the binding of the oligomers as it could be only the monomers that bound to the surface. We therefore modified our experiment and used AB9234 antibody as a host that binds to the activated gold surface of CM5 sensor chip.[32] AB9234 is an anti amyloid oligomer antibody that specifically binds to all types of Aβ oligomers.[33] A Biacore 3000 (Biacore Inc., Piscataway, NJ, USA), equipped with four flow cells in one sensor chip (CM5), was used for real-time binding studies. Carboxymethylated dextran (CM5) of sensor chip is activated by injecting 200 μL of 1:1 mixture of *N*-ethyl-*N*'-[(dimethylamino)-propyl]carbodiimide (EDC) and *N*-hydroxysuccinimide (NHS) in pH 7.4 buffer solution for 30 min, followed by the injection of antibody AB9234 (10 μL of AB9234 was diluted with 600 μL of pH 5.0 sodium acetate buffer, injected at the rate of 10 μL per minute). Anti-amyloid oligomer antibody AB9234 was immobilized on the first gold sensor CM5 chip flow cell, and the second flow cell is used as a reference (without immobilization of AB9234). Antibody cdk5, a negative control, was immobilized on the third flow cell, and the fourth flow cell had no immobilization (used as a reference). The resulting AB9234 bound sensor chip (and the cdk5 bound chip) was used in the SPR studies. The reference cells were prepared similarly but without the addition of AB9234 or cdk5 for correction of background bindings. A running buffer solution consisting of 10 mM HEPES, 150 mM NaCl, 3.4 mM EDTA, 0.05% surfactant P20, pH 7.4, was used as a washing solvent between injections of reagents, antibody, Aβ42 oligomers, and CP2. After immobilization of the antibody, a solution of Aβ42 oligomers (prepared by incubation of a 10 μM solution of Aβ42 monomer in pH 7.4 PBS buffer for 24 h at 4^{o}C; formation of small Aβ42 oligomers were confirmed by AFM) was injected to the cell, and binding was observed. To the bound AB9234-Aβ42 oligomer, a solution of CP2 (40 μM in the aforementioned running buffer) was injected followed by washing with the running buffer solution. The amounts of immobilized antibody, bound Aβ42 oligomers and CP2 were determined based on the amounts of response

units obtained from the sensograms. The amounts of immobilization and bindings were calculated by the ΔRU value, obtained by subtracting the RU at the time before compound injection from the RU at the time just after injection of running buffer (**Figure 2.14**). RUs are equivalent to picograms and can be converted into picomol. One RU is defined to be 1 pg/mm^2 of bound protein molecules and can be converted into pmol/mm^2.[34]

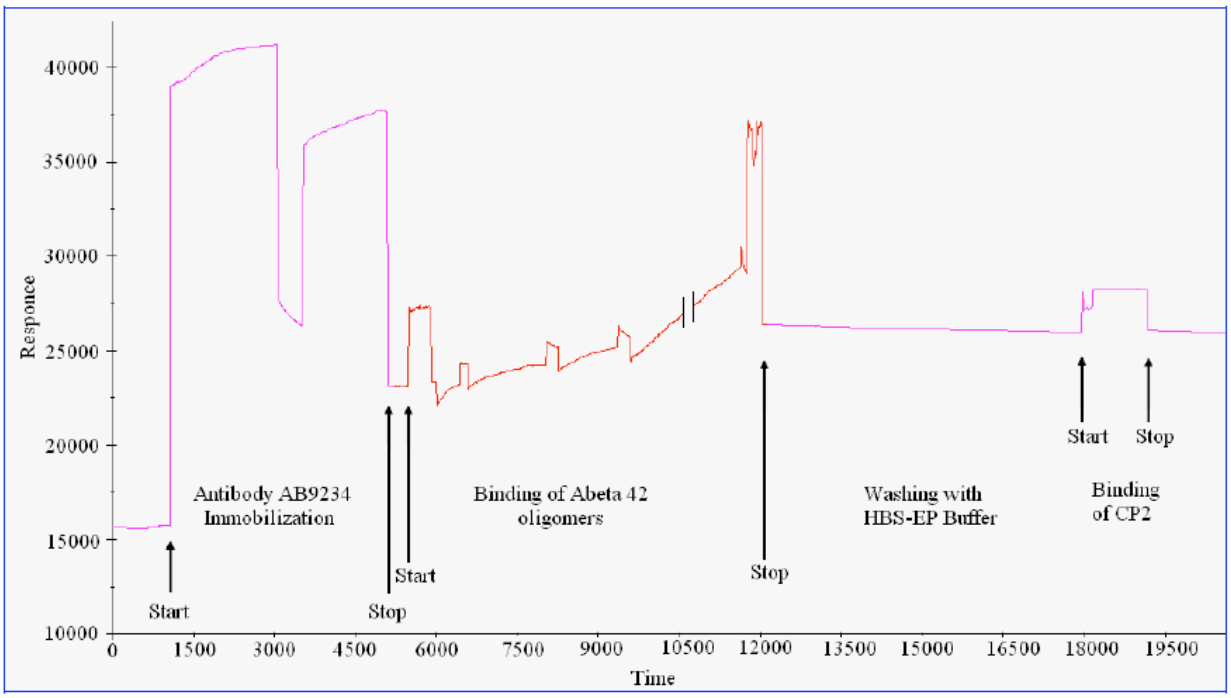

Figure 2.14. SPR sensogram of the in real-time binding of CP2 to Aβ42 oligomers-AB9234 antibody complex. The first two injections showed the immobilization of anti-amyloid oligomer antibody, the following five injections were Aβ42 oligomers, and the last injection was CP2. Lower concentrations of Aβ42 were used in the first four injections and higher concentration of Aβ was used in the fifth injection to ensure that the immobilized antibody was bound with the oligomer.

2.6.2.4 Result and discussion

SPR has been used extensively to study the interaction of peptides and proteins with other peptides and small organic molecules. In search of potential amyloid beta inhibitors, Tjernberg *et al.* studied the binding of small peptides (called beta sheet breakers) to full length Aβ40

peptide.[30] In general, Aβ peptide was immobilized from a solution of very low concentration (~ pmol/L) on a sensor chip and maintained in a pH 7.4 buffer solution. When a drug molecule/peptide flows through the chip and a binding occurs between the drug/peptide and Aβ-peptide, the refractive index of the medium next to the chip will change. This is represented by a response unit (RU) that is equivalent to the mass of bound drug in picograms.[34] We observed less binding of Aβ42 over Aβ40 (**Figure 2.13**) because of faster aggregation of Aβ42 during the course of the experiment. CP2 was injected and binding of TP compounds onto the gold chip having Aβ was observed (ΔRU). TP17 was used as a negative control. Using Biaevaluation software, version 3.0, analysis of sensograms was performed. The kinetic result fits the binding curves to a 1:1 Langmuir binding model. Whereas, 1.5 equivalents of CP2 bind to 1 equivalent of Aβ40 monomers and 1 equivalent of CP2 binds to Aβ42 monomers. No interaction was observed for inactive TP17-Aβ peptide. The dissociation constant K_D (M) is derived from the equation, K_D = kd/ka, where kd and ka are dissociation- and association-rate constants, respectively. CP2 binds to Aβ40 with a high affinity (K_D= 5.05 nM) as compared to Aβ42 (K_D = 269 nM).[20]

On the other hand, for CP2 to Aβ42 oligomer binding studies, anti-amyloid oligomer antibody (AB9234, ~150 KDa MW) was immobilized onto the CM5 gold chip. Based on the sensogram (**Figure 2.14**), after two injections of the antibody, there were 0.052 pmol of antiamyloid oligomer antibody immobilized. After eluting the flow cells with running buffer for 20 min to remove all unbound antibody, preformed 10 μM Aβ42 oligomers were injected (four injections over 100 min) into the flow cells and 0.426 pmol of Aβ42 oligomers were found to bind to the antibody. After washing the flow cell with running buffer for 100 min to remove any unbound Aβ oligomer, a solution of CP2 (40 μM) was injected and then washed with running buffer, 0.21 pmol of CP2 was found to bind to the antibody–Aβ oligomer complex. The data suggests that for each antibody, there are eight molecules of Aβ42 (based on MW of the monomer; ~4530) bound to the antibody, and 4 molecules of CP2 (MW ~510) bind to each Aβ42 oligomer-antibody. Similar binding studies were also carried out by immobilizing anti-Cdk5 antibody in one of the flow channels as a negative control, and no bindings of Aβ42 oligomers were found. We also found that CP2 did not bind to anti-amyloid oligomer antibody alone when CP2 was injected to a separate flow cell immobilized with the antibody alone. The real-time

binding study using SPR shows Aβ42 oligomers bind to anti-amyloid oligomer antibody and CP2 binds to the Aβ oligomer–antibody complex.[18]

2.3.3 Use of protein quantification assay to study the inhibition of aggregation of Aβ with and without tricyclic pyrone molecule CP2

2.3.3.1 Introduction and background

Conversion of soluble, non-toxic Aβ monomers aggregate to insoluble toxic, beta sheet fibrils play a crucial role in pathology of AD. Any compound that either inhibits or slows down the kinetics of aggregation can be screened as a potential therapeutic agent for AD. Studies have shown that in terms of toxicity, concentration plays a very crucial role and Aβ is toxic even in nanomolar range.[20] The Pierce Micro BCA^{TM} protein assay reagent kit has been used for quantitation of amyloid beta protein.[35] The micro BCA reagent kit can quantify protein up to 0.5-20 μg/mL of the sample.[36] This quantification experiment utilized bicinchoninic acid (BCA) as a detection reagent for Cu^{+1} which is formed, when Cu^{+2} is reduced by the protein in alkaline environment. A purple colored solution is formed when two molecules of BCA chelates with one molecule of Cu^{+1} and this complex exhibits a strong absorbance at 530-590 nm wavelength.

2.3.3.2 Inhibition of aggregation of Aβ40 and Aβ42 with CP2

A Micromax RF refrigerated microcentrifuge (Thermo Electron Co., Fisher Scientific, Pittsburgh, PA) and a UV-Vis spectrometer (Shimadzu UV-120-02; Columbia, MD) were used for the experiment. Prior to the experiment, synthetic Aβ40 and Aβ42 (0.2 mg in 200 μL) were dissolved in hexafluoroisopropanol (HFIP), a low polar solvent that stabilizes the α-helix structure and disrupts inter-strand hydrogen bonding between the beta sheets. Sample was kept at 25°C for 48 h, and after which HFIP was allowed to evaporate at 25°C. Four different concentrations of Aβ peptides, 30, 40, 50, 60 μM for Aβ40, and 10, 20, 30, 40 μM for Aβ42 were freshly dissolved in pH 7.4 PBS buffer (500 μL) and treated each with 500 μL of freshly prepared Micro BCA^{TM} reagent. The solutions were incubated at 60ºC for 30 minutes, cooled to

25ºC, and absorbance was measured using a UV spectrometer at 569 nm wavelength (a BCA reagent was used as a reference) within 10 minutes. Linear correlations (Aβ40 & 42 with and without CP2; 2 equivalents) between the absorbance and concentration were obtained (**Graph 2.1**).[18] Once the linear correlation was observed, Monomeric Aβ40 and Aβ42 peptides were treated with 2 equivalents of CP2 separately for 1 week at 25ºC, and each day the concentrations of Aβ40 and Aβ42 peptides were quantified using a micro BCA™ protein assay reagent kit and results are summarized in **Figure 2.15**.[18]

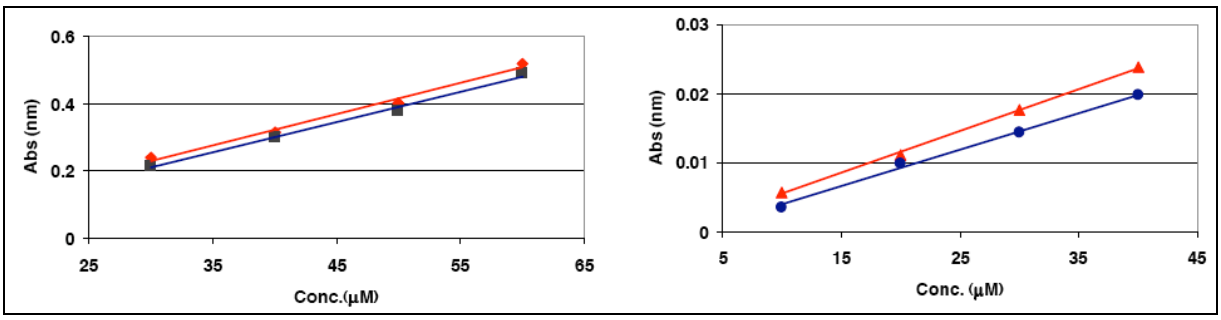

Graph 2.1. Correlations of concentrations of monomeric Aβ40 and Aβ42 separately versus UV absorbance with and without CP2 using Micro BCA™ protein assay reagent kit. Left panel: Aβ40, diamond is Aβ40 with CP2 and square is Aβ40 without CP2; Right panel: Aβ42, triangle is Aβ42 with CP2 and circle is Aβ42 without CP2.

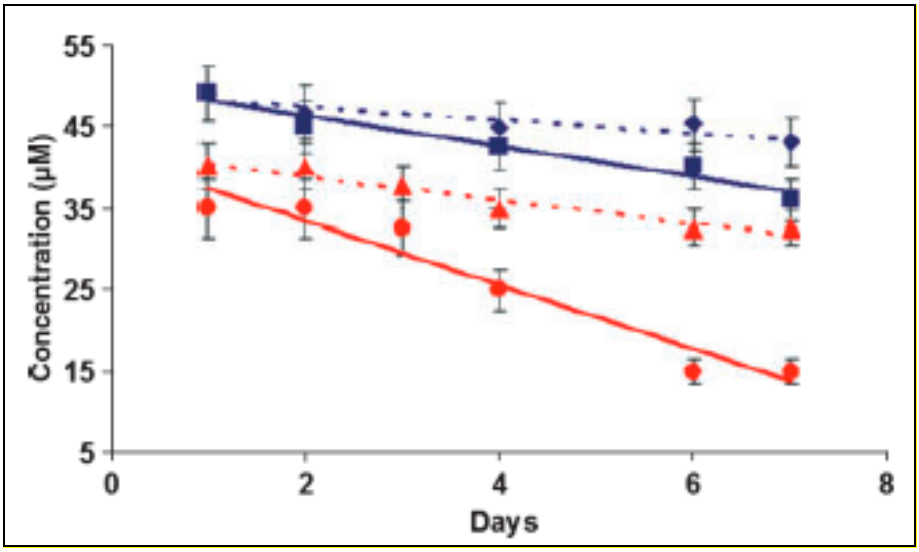

Figure 2.15. Quantification of soluble Aβ40 and Aβ42 peptide separately in PBS buffer (pH 7.4) at 25°C over 7 days using a micro BCA™ protein assay reagent kit in the absence (marked in square for Aβ40 and circle for Aβ42) and presence (marked in diamond for Aβ40 and triangle for Aβ42) of 2 equivalents of CP2.

2.6.3.3 Result and discussion

We have already observed, by AFM and SPR spectroscopy, that CP2 binds to Aβ monomers and inhibit its aggregation. Also, CP2 binds to toxic Aβ oligomers and protofibrils and disaggregates them to non-toxic monomers (by AFM). Using Micro BCA™ protein assay kit, we investigated whether CP2 inhibits Aβ fibril formation in PBS buffer solution (pH 7.4) over time at 25ºC. In the absence of CP2, we found ~73% of Aβ40 and ~43% of Aβ42 in the solution after 1 week. On the other hand, in the presence of two equivalents of CP2, there was ~88% and ~81% of Aβ40 (**Table 2.1**) and Aβ42 (**Table 2.2)**, respectively that remained in the solution after 1 week of incubation. The data shows that CP2 inhibits the fibril formation, which is in agreement with the results of the inhibitions of aggregation of Aβ peptides (vide supra), as further aggregation of oligomers leads to protofibrils and fibrils.[18]

Days	Day 1	Day 2	Day 4	Day 6	Day 7
Aβ40 (μM)	49	45	42.5	40	36
Aβ40 + CP2 (μM)	49	46.7	44.9	45.2	43

Table 2.1. Amount of Aβ40 peptide (μM) over 7 days at 25ºC in PBS buffer (pH 7.4) at 25ºC with and without CP2 (two equivalents) determined by micro BCA™ protein assays.

Days	Day 1	Day 2	Day 3	Day 4	Day 6	Day 7
Aβ42 (μM)	35	35	32.5	25	15	15
Aβ42 + CP2 (μM)	40	40	37.5	35	32.5	32.5

Table 2.2. Amount of Aβ40 peptide (μM) over 7 days at 25ºC in PBS buffer (pH 7.4) at 25ºC with and without CP2 (two equivalents) determined by micro BCA™ protein assays.

2.3.4 Use of circular dichroism (CD) spectroscopy to study the inhibition of aggregation of Aβ with and without tricyclic pyrone molecule CP2

2.3.4.1 Introduction and background

Circular dichroism helps in studying the real time secondary structure of the protein (**Figure 2.16**).[37] It is known that Aβ aggregation involves the transformation of soluble unordered α-helix/ random coil to β-sheet rich conformation. Numerous reports have shown the use of CD spectroscopy to study the kinetics of Aβ aggregation pathway.[38-40] In general, most CD studies performed so far have used fluorinated solvents such as trifluoroethanol (TFE) and hexafluoroisopropanol (HFIP). Since fluorinated solvents promote intramolecular hydrogen bonding, which indicates that stable α-helix conformation is intramolecular and β-sheet structure are intermolecular. TFE and HFIP are weaker proton donors than water and thus promote structure formation by intramolecular hydrogen bonding rather than intermolecular hydrogen bonding with the solvent. Barrow *et al*. performed detailed studies into the structure and kinetics of Aβ(39-43) aggregation in solution phase and concluded that the Aβ peptide adopts a mixture of random coil, α-helix and β-sheet with the relative ratio depending on the solvent composition, concentration of peptides, temperature, pH etc.[41] It was observed that increasing the percentage

of TFE favors the formation of α-helix and random coil and a maxima was observed in 90% trifluoroethanol (TFE). Similar results were obtained in hexafluoroisopropanol (HFIP). We also obtained the similar results for Aβ42 as shown in **Figure 2.17**.

However, for real time *in vitro* inhibitors studies, use of fluorinated solvent (HFIP) is not a suitable solvent due to its low volatility. It was also found that the morphology and stability of soluble oligomers are different in HFIP when compared with aqueous buffer.[42] Recently, Andrisano *et al*. developed a highly reproducible *in vitro* assay and validated it by studying different synthesized and commercially available amyloid inhibitors.[43] We used their published protocol to study the kinetics of Aβ42 aggregation and effect of CP2 on the inhibition/stabilization of α-helix/ random coil secondary conformation of Aβ42.

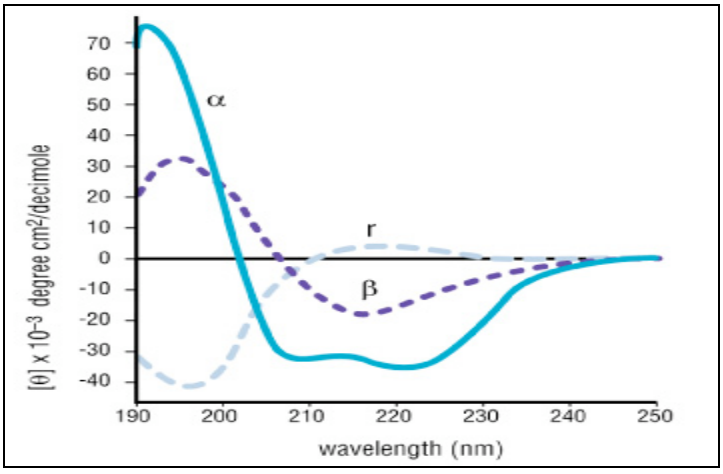

Figure 2.16. CD spectrum of different conformations of Aβ peptide.[37]

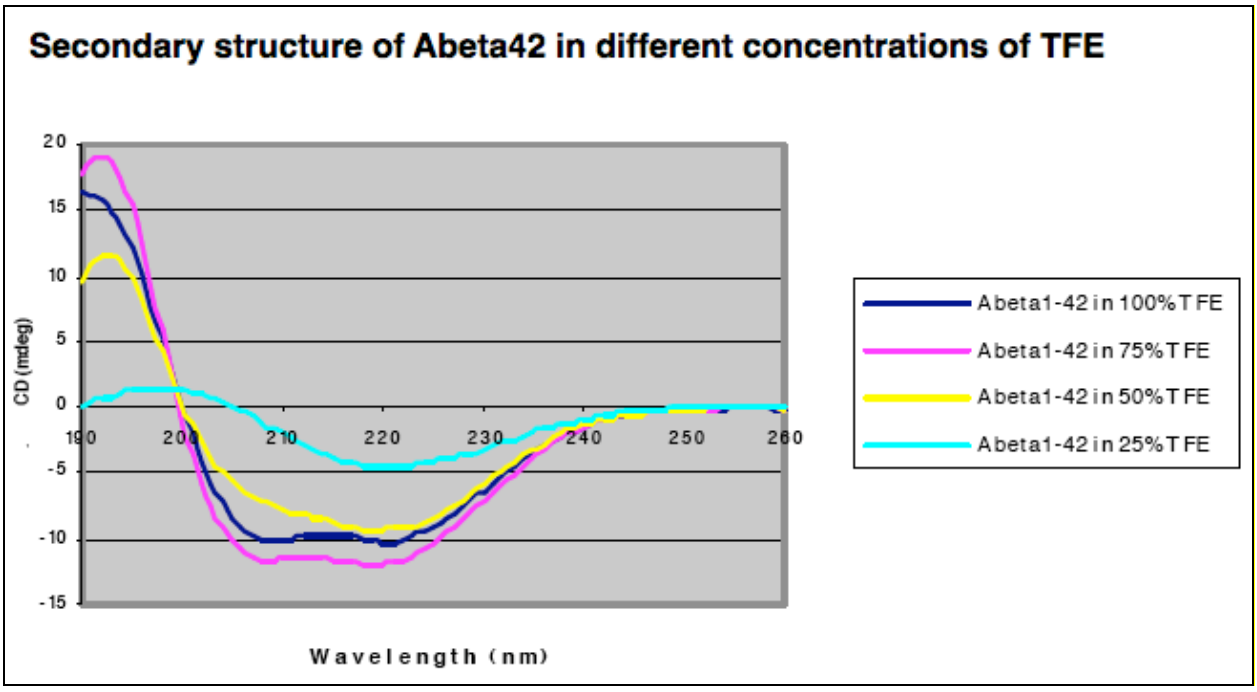

Figure 2.17. CD spectrum showing the effect of TFE on Aβ42 peptide.

2.3.4.2 Study of inhibition of aggregation of Aβ42 with CP2 (1.25 equivalents)

A Jasco J-815 Spectropolarimeter CD instrument (JASCO; Easton, MD) and a quartz cell (0.1 cm length; 200 μL internal volume) were used to record CD spectra in a spectral range of 190 – 260 nm, 1 nm data pitch, 1 nm bandwidth, and at 50 nm/min scan speed. A solution of Aβ42 (40 μM) in phosphate buffer solution containing NaCl, Na_2CO_3, NaOH, and acetonitrile was prepared according to the reported method[43] to monitor Aβ42 solution structure in the absence and presence of 1.25 equivalents of CP2 over 48 h at 25ºC in a time course manner. In order to remove already preformed aggregates, Aβ42 (0.12 mg) was dissolved in hexafluoroisopropanol (HFIP; 200 μL), a low polar solvent that stabilizes the a-helix structure and disrupts inter-strand hydrogen bonds between of the beta sheet, by brief sonication and vortexing, kept at 25°C for 48 h, and HFIP was evaporated at 25°C. The resulting Aβ42 was re-dissolved in a freshly prepared mixture (70 μL) of CH_3CN/Na_2CO_3 (0.3 mM)/NaOH (0.25 M) (48.3:48.3:3.4, v/v/v) by brief sonication and vortexing providing an alkaline solution of Aβ42 (0.38 mM). An aliquot (30 μL) of the Aβ42 solution was diluted with phosphate buffer saline (PBS; 0.25 mL) solution to give a 40 μM solution of Aβ42 in phosphate buffer (7.7 mM) that

contained NaCl (8.9 mM), Na2CO3 (15.5 mM), NaOH (0.91 mM), and 5.1% acetonitrile. CP2 (1.25 equivalents; 10 μL of 1.5 mM in PBS-ethanol, 9:1) was added to 280 μL of the above Aβ42 (40 μM) solution, and CD spectra were recorded at regular interval over 48 h. The control solutions that contained the above incubation buffer with and without CP2 were prepared and their contributions were subtracted in the CD spectra of Aβ42 with and without CP2, respectively (**Figure 2.18**). Although CP2 can interfere with the experiments, 1.25 equivalents of CP2 alone showed only a small absorption and did not change the overall shape of Aβ42. To follow Aβ42 conformational changes and inhibition studies with CP2, the CD wavelength at 215 nm (beta sheet structure) was plotted verses the time of incubation (**Figure 2.19**).[18]

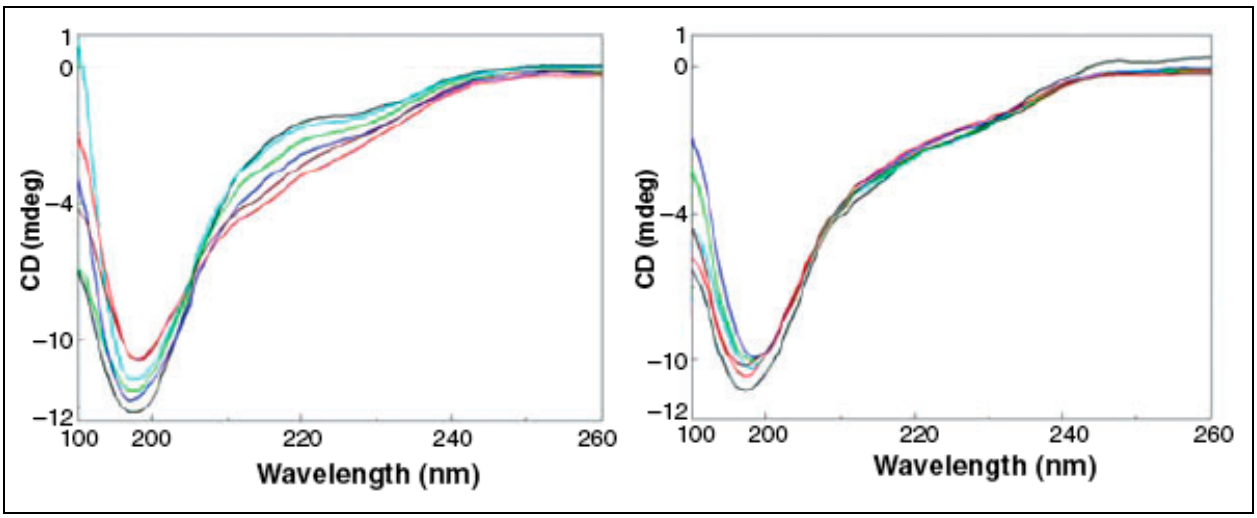

Figure 2.18. CD spectra of Aβ42 (40 μM) in phosphate buffer (7.7 mM) containing NaCl (8.9 mM), Na_2CO_3 (15.5 μM), NaOH (0.91 mM), and 5.1% acetonitrile solution with and without CP2 over 48 h. The control solutions that contained the above incubation buffer with and without CP2 were prepared and their contribution was subtracted in the CD spectra. Left panel: Aβ42 alone; 0 h: black; 9 h: light blue; 19 h: green; 21 h: dark blue; 45 h: brown; and 48 h: red. Right panel: Aβ42 + CP2 (1.25 equivalents); 0 h: black; 9.5 h: light blue; 15.5 h: green; 20 h: dark blue; 23 h: brown; and 48 h: red.

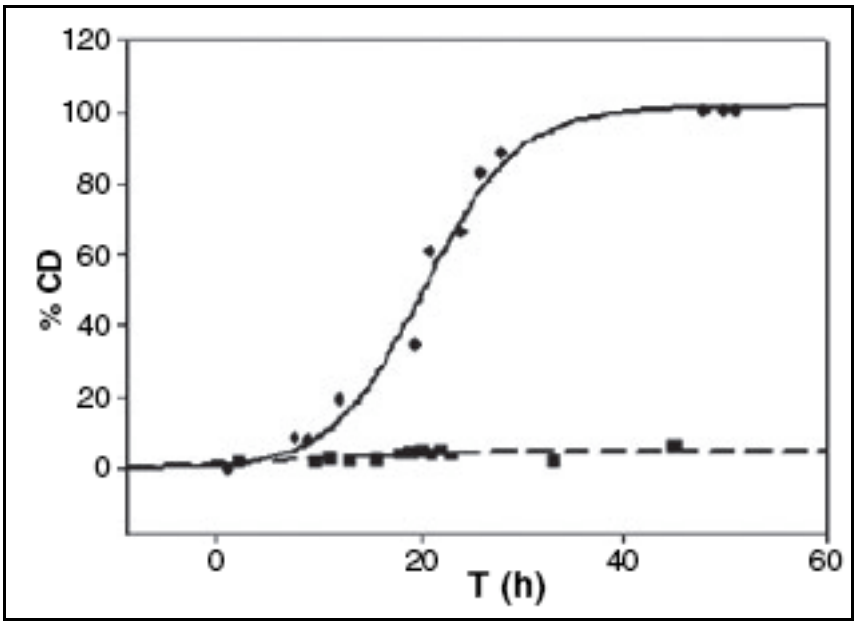

Figure 2.19. Trend of β-sheet content over time: circle is Aβ42 alone and square is Aβ42 + CP2.

2.3.4.3 Results and discussion

It is accepted that Aβ undergoes conformational changes or misfolding from random coil/α-helix to β-sheet structure, resulting in oligomerization and insoluble fibrils formation.[43,44] CD spectroscopy offers a real-time monitoring of protein conformations in aqueous solution.[44] A PBS buffer solution containing Na_2CO_3-NaOH-acetonitrile was established[43] recently to study Aβ conformational changes in the presence of Aβ42 inhibitors and marketed drugs for AD treatment using CD. Hence, the same buffer solution was used to examine whether CP2 maintains Aβ42 random coil/α-helix structures and blocks β-sheet formation over times using CD spectroscopy. **Figure 2.18**, left panel, shows Aβ42 conformational changes in the absence of CP2 over 48 h, in which CD value at 198 nm (random coil structure) gradually decreased over time and 215 nm (β-sheet) value increased. On the other hand, in the presence of 1.25 equivalents of CP2 (**Figure 2.18, right panel**), although band at 198 nm decreased slightly due to some unknown reason, CD value at 215 nm remains unchanged. In term of the kinetics of self-aggregation, a plot of CD values at 215 nm versus time is shown in **Figure 2.19**. Kinetics proceeds in three phases: a lag phase with significant conformation change (until 0-9 hours), an exponential phase where there is rapid increase in aggregation (10-32 hours) followed by a

plateau phase (after 32 h), where majority of the conformation is beta sheet. No such aggregation pattern was observed in the presence of CP2. The results imply that CP2 stabilizes Aβ42 random coil/α-helix structures and blocks β-sheet formation. The intensity at 198 nm of Aβ42 peptide plus CP2 is weaker than that of Aβ42 alone because the solution of Aβ-CP2 is slightly diluted compared with that of Aβ alone (from the addition of a solution of CP2 in PBS) and the contribution of the CD graph of CP2 (control) was subtracted from the observed Aβ-CP2 graph.[18]

2.4 Conclusion

Amyloid Aβ aggregation is the main culprit in AD. Reducing the levels of intracellular Aβ, preventing Aβ aggregation, and eliminating the existing Aβ aggregates have been proposed for treatment of AD. AFM studies demonstrated that tricyclic pyrone compound CP2 inhibits Aβ aggregation and disaggregates Aβ40 and Aβ42 oligomers and protofibrils as well. SPR spectroscopy and protein quantification assay studies showed that CP2 binds to Aβ42 monomer and oligomers. CD studies revealed that CP2 stabilizes the random coil/α-helix structures of monomeric Aβ42 peptide in PBS buffer, which leads to the inhibition of aggregate formation. Protein quantification assay results suggested that CP2 not only disaggregates Aβ oligomers but also inhibit fibril formation.

2.5 References

1. Glenner, G. G.; Wong, C.W. Alzheimer's disease: initial report of the purification and characterization of a novel cerebrovascular amyloid protein. *Biochem. Biophys. Res. Commun,* **1984**, *120*, 885-890.
2. Lee, V. M. -Y.; Balin, B. J.; Otvos Jr., L.; Hollosi, M.; Trojanowski, J. Q. A68: A major subunit of paired helical filaments and derivatized forms of normal Tau. *Science*, **1991**, *251*, 675-678.
3. Esler, W. P.; Wolfe, M. S., A portrait of Alzheimer secreatses-new features and new faces. *Science*, **2001**, *293*, 1449-1454.
4. Bitan, G.; Kirkitadze, M. D.; Lomakin, A.; Vollers, S. S.; Benedek, G. B.; Teplow, D., Amyloid beta-protein (Abeta) assembly: Abeta40 and Abeta42 oligomerize through distinct pathways. *Proc. Natl. Acad. Sci. USA*, 2003, *100*, 330-335.
5. Benzinger, T. L. S.; Gregory, D. M.; Burkoth, T. S.; Miller-Auer, H.; Lynn, D. G.; Botto, R. E.; Meredith, S. C., Propagating structure of Alzheimer's β-peptide (10-35) is parallel β-sheet with residues in exact register. *Proc. Natl. Acad. Sci. USA*, **1998**, *95*, 13407-13412.
6. Luhrs, T.; Ritter, C.; Adrian, M.; Riek-Loher, D.; Bohrmann, B.; Dobeli, H.; Schubert, D.; Riek, R., 3D structure of Alzheimer's amyloid β(1-42) fibrils. *Proc. Natl. Acad. Sci. U.S.A.*, **2005**, *102***,** 17342-17347.
7. Wirth, O.; Multhaup, G.; Bayer, T. A., A modified β-amyloid hypothesis: intraneuronal accumulation of the β-amyloid peptide-the first step of a fatal cascade. *J. Neurochem*., **2004**, *91*, 513-520.
8. Lambert, M. P.; Barlow, A. K.; Chromy, B. A.; Edwards, C.; Freed, R.; Liosatos, M.; Morgan, T. E.; Rozovsky, I.; Trommer, B.; Viola, K. L.; Wals, P.; Zhang, C.; Finch, C. E.; Krafft, G. A.; Klein, W. L., Diffusible, nonfibrillar ligands derived from Aβ1–42 are potent central nervous system neurotoxins. *Proc. Natl. Acad. Sci. USA.,* **1998***, 95,* 6448-6453.

9. Lansbury, P. T., A reductionist view of Alzheimer disease. Acc. Chem. Res., 1996, 29, 317-321.
10. Maggio, J. E.; Mantyh, P. W., Brain amyloid - a physicochemical perspective. *Brain pathol*., **1996**, *6*, 147-162.
11. Inouye, H.; Fraser, P. E.; Kirschner, D. A., Structure of β-crystallite assemblies formed by Alzheimer's β-amyloid protein analogues: analysis by x-ray diffraction. *Biophys. J.*, **1993**, *64*, 502-519.
12. Sunde, M.; Serpell, L. C. Bartlam, M.; Fraser, P. E.; Pepys, M. B.; Blake, C. C., Common core structure of amyloid fibrils by synchrotron X-ray diffraction. *J Mol Biol.*, **1997**, *273*, 729–739
13. Oda, T.; Wals, P.; Osterburg, H. H.; Johnson, S. A.; Pasinetti, G. M.; Morgan, T. E.; Rozovsky, I.; Stine, W. B.; Snyder, S. W.; Holzman, T. F.; Krafft, G. A.; Finch, C. E., Clusterin (apoj) alters the aggregation of amyloid β−peptide (Aβ1-42) and forms slowly sedimenting Aβ complexes that cause oxidative stress. *Exp. Neurol.*, **1995**, *136*, 22-31.
14. Harper, J. D.; Wong, S. S.; Lieber, C. M; Lansbery, P. T., Observation of metastable A beta amyloid protofibrils by atomic force microscopy. *Chem. Biol*., **1997**, *4*, 119-125.
15. Harper, J. D.; Wong, S. S.; Lieber, C. M; Lansbery, P. T., Assembly of Aβ amyloid protofibrils: An vitro model for a possibly early event in Alzheimer's disease. *Biochemistry*, **1999**, *38*, 8972-8980.
16. Huang, T. J. H.; Yang, D. –S.; Plaskos, N. P.; Go., S.; Yip, C. M.; Fraser, P. E.; Chakrabartty, A., Structure studies of soluble oligomers of the Alzheimer b-amyloid peptide. *J. Mol. Biol.*, **2000**, *297*, 73-87.
17. Liu, R.; McAllister, C.; Lyubchencko, Y.; Sierks, M. R., Residues 17-20 and 30-35 of beta-amyloid play a critical role in aggregation. *J. Neurosci. Res*., **2004**, *75*, 162-171.
18. Hong, H. -S.; Rana, S.; Barrigan, L.; Shi, A.; Zhang, Y.; Zhou, F.; Jin, L. -W.; Hua, D. H., Inhibition of Alzheimer's amyloid toxicity with a tricyclic pyrone molecule *in vitro* and *in vivo*. *J. Neurochem*. **2009**, *108*, 1097-1108.
19. Jin, L. -W.; Hua, D. H.; Shie, F. -S.; Maezawa, I.; Sopher, B.; Martin, G. M., Novel tricyclic pyrone compounds prevent intracellular APP C99-induced cell death. *J. Mol. Neurosci.*, **2002**, *19*, 57-61.

20. Maezawa, I.; Hong, H. -S.; Wu, H. -C.; Battina, S. K.; Rana, S.; Iwamoto, T.; Radke, G. A.; Pettersson, E.; Martin, G. M.; Hua, D. H.; Jin, L.-W., A novel tricyclic pyrone compound ameliorates cell death associated with intracellular amyloid-β oligomeric complexes. *J. Neurochem*. **2006**, *98*, 57-67.
21. LeVine H. III., Stopped-flow kinetics reveal multiple phases of thioflavin T binding to Alzheimer beta (1–40) amyloid fibrils. *Arch. Biochem. Biophys.,* **1997**, *342*, 306–316.
22. Lorenzo, A.; Yankner, B. A., β-Amyloid neurotoxicity requires fibril formation and is inhibited by Congo red. *Proc. Natl Acad. Sci. USA*. **1994**, *91*, 12243–12247.
23. Begum, A. N.; Jones, M. R.; Lim, G. P.; Morihara, T.; Kim, P.; Heath, D. D.; Rock, C. L.; Pruitt, M. A.; Yang, F.; Hudspeth, B.; Hu, S.; Faull, K. F.; Teter, B.; Cole, G. M.; Frautschy, S. A., Curcumin structure function, bioavailability, and efficacy in models of neuroinflammation and Alzheimer's disease. *J. Pharm. Exp. Ther.*, **2008**, *326*, 196–208.
24. Maezawa, I.; Hong, H. –S.; Liu, R.; Wu, C. –Y.; Cheng, R. H.; Kung, M. –P.; Kung, H. F.; Lam, K. S.; Oddo, S.; LaFerla, F. M.; Jin, L. –W., Congo red and thioflavin-T analogs detect Aβ oligomers. *J. Neurochem.*, **2008**, *104*, 457–468.
25. Hartley, D. M.; Walsh, D. M.; Ye, C. P.; Diehl, T.; Vasquez, S.; Vassilev, P. M.; Teplow D. B.; Selkoe, D. J., Protofibrillar intermediates of amyloid β-protein induce acute electrophysiological changes and progressive neurotoxicity in cortical neurons. *J. Neurosci.*, **1999**, *19*, 8876–8884.
26. Nilsberth, C.; Westlind-Danielsson, A.; Eckman, C. B.; Condron, M. M.; Axelman, K.; Forsell, C.; Stenh, C.; Luthman, J.; Teplow, D. B.; Younkin, S. G.; Näslund, J.; Lannfelt, L., The 'Arctic' APP mutation (E693G) causes Alzheimer's disease by enhanced Aβ protofibril formation. *Nat. Neurosci*., 2001, 4, 887-893 (2001).
27. Kasemo, B., Biological surface science. *Surface Science*, **2002**, *500*, 656-677.
28. http://www.fz-juelich.de/isb/isb-1/protein-protein_interaction
29. Jarrett, J. T.; Berger, E. P.; Lansbery, P. T.Jr., Biochemistry, 1993, 32, 4693-4697. Naslund, J.; Schierhorn, A.; Hellman, U. Lannfelt, L.; Roses, A. D.; Tjernberg, L. O.; Silberring, J.; Gandy, S. E.; Winblad, B.; Greengard, P.; Nordstedt, C.; Terenius, L., Relative abundance of Alzheimer A beta amyloid peptide variants in Alzheimer disease and normal aging. *Proc. Natl. acad. Sci. U.S.A.,* **1994**, *91*, 8378-8382.

30. Tjernberg, L. O.; Naslund, J.; Lindqvist, F.; Johansson, J.; Karlström, A. R.; Thyberg, J.; Terenius, L.; Nordstedt, C., Arrest of β-amyloid fibril formation by a pentapeptide ligand. *J. Biol. Chem.*, **1996**, *271*, 8545–8548.
31. Ryu, J.; Joung, H. –A.; Kim, M. -G.; Park, C. B., Surface plasmon resonance analysis of Alzheimer's β-peptide aggregation on a solid surface: From monomers to fully grown fibrils. *Anal. Chem.,* **2008**, *80*, 2400-2407.
32. Kayed, R.; Head, E.; Thompson, J. L.; McIntire, T. M.; Milton, S. C.; Cotman, C. W.; Glabe, C. G., Common Structure of Soluble Amyloid Oligomers Implies Common Mechanism of Pathogenesis. *Science*, **2003**, *300*, 486-489.
33. http://www.millipore.com/catalogue/item/ab9234
34. Van Wiggeren, G. D.; Bynum, M. A.; Ertel, J. P.; Jefferson, S.; Robotti, K. M.; Thrush, E. P.; Baney, D. M.; Killeen, K. P. A novel optical method providing for high-sensitivity and high-throughput biomolecular interaction analysis. *Sens. Actuators B*, **2007**, *127*, 341–349.
35. Konno, T., Amyloid-Induced Aggregation and Precipitation of Soluble Proteins: An Electrostatic Contribution of the Alzheimer's β(25-35) Amyloid Fibril. *Biochemistry*, **2001**, *40*, 2148-2154.
36. www.piercenet.com
37. http://www.mscwu.wur.nl/NR/rdonlyres/256B4909-D151-45EF-BA90 47A81D1F17A0/28328/cdprinc_1.jpg
38. Barrow, C. J.; Zagorski, M. G., Solution structures of beta peptide and its constituent fragments: relation to amyloid deposition. *Science*, **1991**, *253*, 179-182.
39. Barrow, C. J.; Yasuda, A.; Kenny, P. T.; Zagorski, M. G., Solution Conformations and Aggregational Properties of Synthetic Amyloid β-Peptides of Alzheimer's Disease: Analysis of Circular Dichroism Spectra. *J. Mol. Biol.*, **1992**, *225*, 1075-1093
40. Orvos, L.; Szendrei, G. I.; Lee, V. M.; Mantsch, H. H., Human and rodent Alzheimer β-amyloid peptides acquire distinct conformations in membrane-mimicking solvents. *Eur. J. Biochem.*, **1993**, *211*, 249-257.
41. Barrow, C. J.; Yasuda, A.; Kenny, P. T.; Zagorski, M. G., Solution Conformations and Aggregational Properties of Synthetic Amyloid β-Peptides of Alzheimer's Disease: Analysis of Circular Dichroism Spectra. *J. Mol. Biol.*, **1992**, *225*, 1075-1093.

42. Nichols, M. R.; Moss, M. A.; Reed, D. K.; Cratic- McDaniel, S.; Hoh, J. H.; Rosenberry, T. L., Amyloid-β Protofibrils Differ from Amyloid- β Aggregates Induced in Dilute Hexafluoroisopropanol in Stability and Morphology. *J. Biol. Chem.*, **2005**, *280*, 2471-2480.
43. Bartolini, M.; Bertucci, C.; Bolognesi, M.L.; Cavalli, A.; Melchiorre, C.; Andrisano, V., Insight into the kinetic of Amyloid β(1-42) peptide self-aggreagtion: Elucidation of inhibitors' mechanism of action. *ChemBioChem.*, **2007**, *8*, 2152-2161.
44. Fezoui, Y.; Teplow, D. B., Kinetic studies of amyloid β-protein fibril assembly. *J Biol. Chem.*, **2002**, *277*, 36948-36954.

CHAPTER 3 - Biological evaluation of tricyclic pyrone and pyridinone compounds: *in vitro* and *in vivo* studies

3.1 Introduction

Alzheimer disease (AD) is most common cause of dementia and is considered one of the leading causes of death worldwide. AD is a progressive neurodegenerative disorder characterized by memory loss and other cognitive disabilities. In AD patients, the cognitive decline is accompanied by impaired performances of daily activities, behavior, speech etc. AD affects patient's life at home and at work. The main pathophysiological hallmarks of AD are extracellular deposits of amyloid plaques formed by aggregated beta-amyloid (Aβ) peptide and intracellular neurofibrillary tangles (NFTs) composed of filamentous aggregates of hyperphosphorylated tau protein in the brain. This Aβ peptide is derived from the processing of large amyloid precursor protein (APP), a transmembrane protein by different enzymes. Although the etiology of AD is very complex and not yet fully resolved, numerous studies have shown that amyloid plays a central role in the neurodegeneration in AD. This hypothesis is supported by results indicating that amyloid aggregates are toxic to neuronal cell in culture and toxicity is directly linked to the extent of Aβ aggregation. Recently, it is reported that soluble small oligomeric intermediates rather then insoluble fibrils are primary toxic species in AD.[1] In this chapter, I will discuss *in vitro* biological activity of different tricyclic pyrone molecules using MC6 cell assay and effectiveness of tricyclic pyrone molecule CP2 *in vivo* activity on 5X FAD (familial alzheimer disease) transgenic mice.

3.2 Background

Aβ aggregation is widely accepted as the first pathological process in AD. Several findings support this theory. A number of genes found to be mutated in AD patients are related

to the biology of Aβ such as the gene for APP on chromosome 21, the gene for apoE4 on chromosome 19, and genes for PS1 and PS2 on chromosomes 14 and 1, respectively.[2] Also, Aβ is proved to be toxic to neuronal cell even in nanomolar concentration and causes death via membrane lipid peroxidation, which impairs the function of membrane ion-motive ATPases, glucose and glutamate transporters, leading to membrane depolarization, excessive Ca^{2+} influx, and mitochondrial dysfunction.[3] It is believed that any molecule that either inhibits aggregation or disaggregate preformed oligomers can serve as an attractive therapeutic target for AD. For successful screening of organic compounds, an efficient and reproducible screening model is a must. So far, limited cell culture models have shown a convincing and reproducible linkage between the intracellular Aβ aggregation and the cell death. This hinders the screening for various potentially therapeutic organic molecules. Recently, a screening model using primary neurons from Tg2576 APP transgenic mice has shown Aβ oligomer accumulations but preparation of this model is very time-consuming. Due to toxicity issues detection of aggregations is observed by electron microscopy.[4] On the other hand, MC65 cell line can be conveniently used to screen potential bioactive compounds.[5-7] MC65 is a human neuroblastoma cell line that conditionally expresses C99, a 99 amino acid residue carboxy terminal fragment derived from amyloid precursor protein after cleavage by the beta secretase enzyme. C99 is cleaved by γ-secretase enzyme leading to the generation of Aβ (**Figure 3.1**). Following the transgene induction, significant loss of cell viability was observed after 72 h. Compared with the method described by Takahashi *et al*. MC65 cells are easily propagated and cell toxicity is measured quantitatively by simple 3-(4,5-dimethylthiazol-2-yl)-2,5-diphenyltetrazolium bromide (MTT) assay.[6]

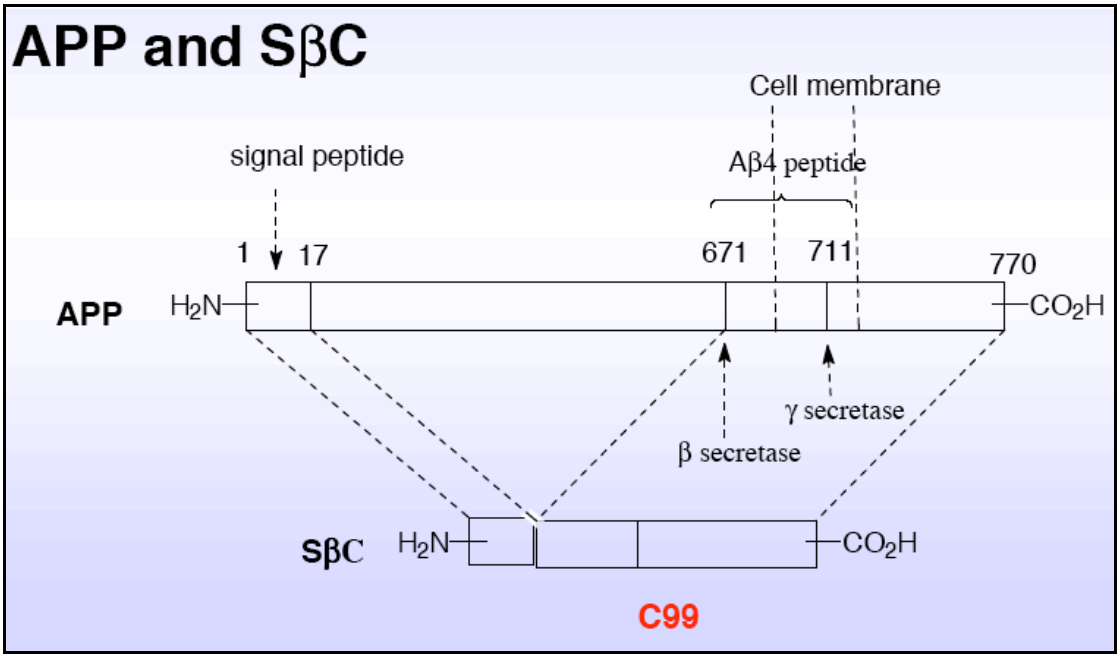

Figure 3.1. Schematic representation of C99 expression.

3.3 MC65 cell death is related to the intracellular generation and aggregation of Aβ

In neuronal cells, generation and aggregation of Aβ is believed to have the toxic effect. Intracellular aggregation of proteins is being linked to neurodegenerative processes. The mechanism by which intracellular Aβ protein misfolds, aggregates and become toxic is complex and is poorly understood. The MC65 cell model linked the neuronal cell death to the toxicity of intracellular Aβ generation. Western blot analysis demonstrated the predominant formation of dimer, tetramer and pentamer aggregates after 24 h as shown in **Figure 3.2**. No monomeric Aβ was observed by Tricine gel analysis. The C99 was induced by removal of Tetracycline (TC). At indicated times, the cells were homogenized. Cellular proteins (5 μg protein each) were subjected to Tris/tricine sodium dodecyl sulfate–polyacrylamide gel electrophoresis and western blot analysis with antibody 6E10 (for Aβ1–17). Aβ Standard, synthetic Aβ40 and Aβ42, served as standard Aβ monomer peptides.[8]

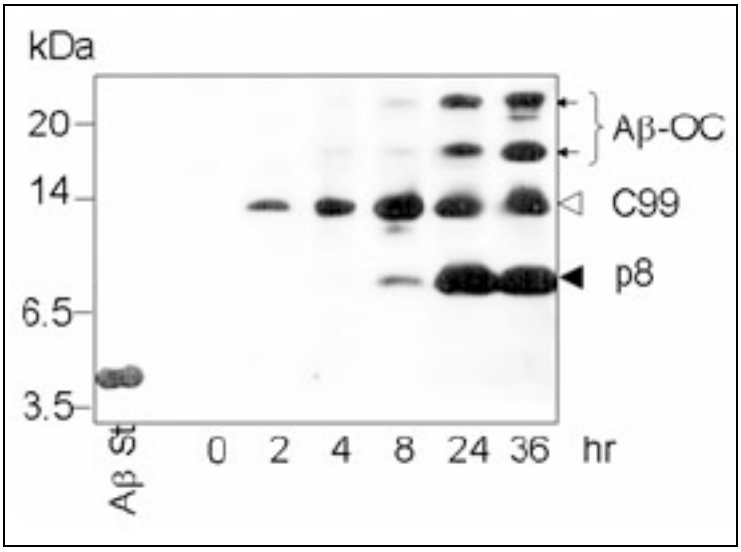

Figure 3.2. MC65 cell death is dependent upon Aβ generation and closely related to Aβ aggregation into Aβ-Oligomeric complexes.

In order to confirm the generation and toxicity of Aβ intracellularly, MC65 cells were treated with L-685 458, a highly specific γ-secretase inhibitor. No Aβ generation was observed (**figure 3.3A**). L-658 458 also inhibits the aggregate formation in a dose dependent manner (**Figure 3.3B**). Since the p8 (8 Kda) band is partially reduced by a γ-secretase inhibitor, it indicates that it is not entirely composed of Aβ peptide.[8] The γ-secretase results indicated that MC65 cell death is dependent on the production of Aβ. The ELISA quantification suggested that both L-685 458 and CP2 reduced Aβ oligomeric formation.

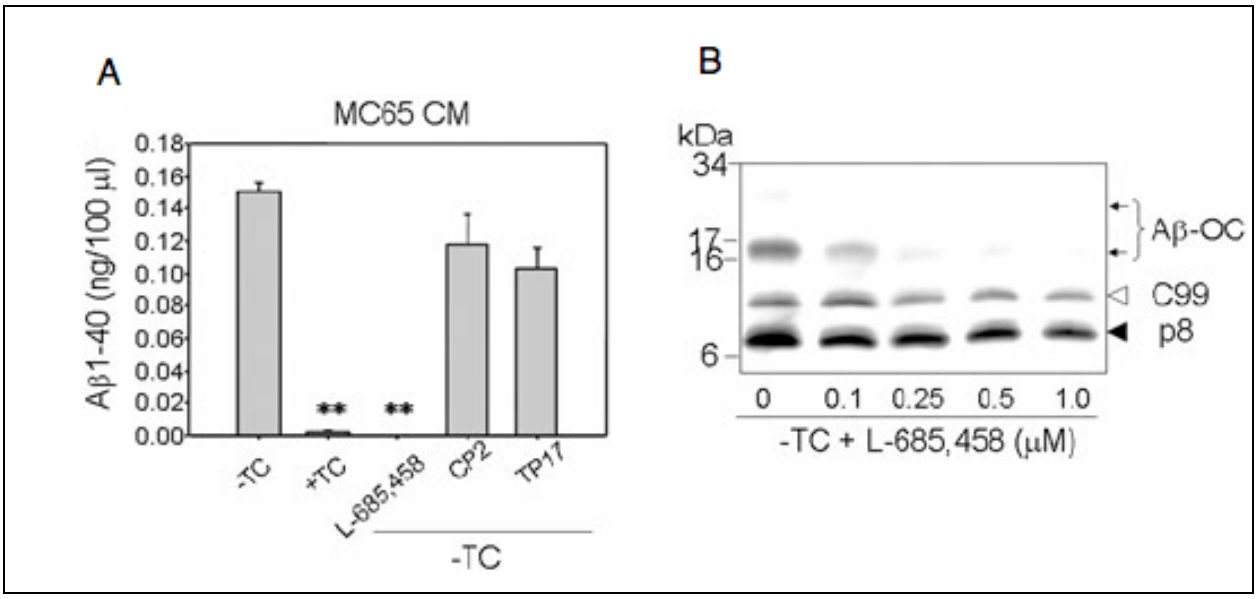

Figure 3.3. Treatment of MC65 cells with TP compounds and a γ-secretase inhibitor, L-685 458 (A) MC65 cells: –TC, without TC to induce C99 expression; +TC, with TC to suppress C99 expression. n = 3, **p < 0.001 compared with the –TC group. (B) L-685 458 of indicated concentrations was added at the same time as TC removal. Cellular proteins from 24 h cultures were analyzed by western blot using 6E10.

CP2 molecule target Aβ peptide and the dose independent effect of CP2 on Aβ was studied and was compared with TP17 (a negative control) (**Figure 3.5**). Without CP2, Aβ aggregates were observed. Whereas, the addition of CP2 lowered the formation of higher molecular weight cellular Aβ oligomer aggregates. A lower effect was observed for N9' analog and no effect was observed for TP17 (**Figure 3.4A**). In addition, a dose dependent study of CP2 was carried out by removal of TC and different concentrations of CP2 were added (**Figure 3.4B**).[8]

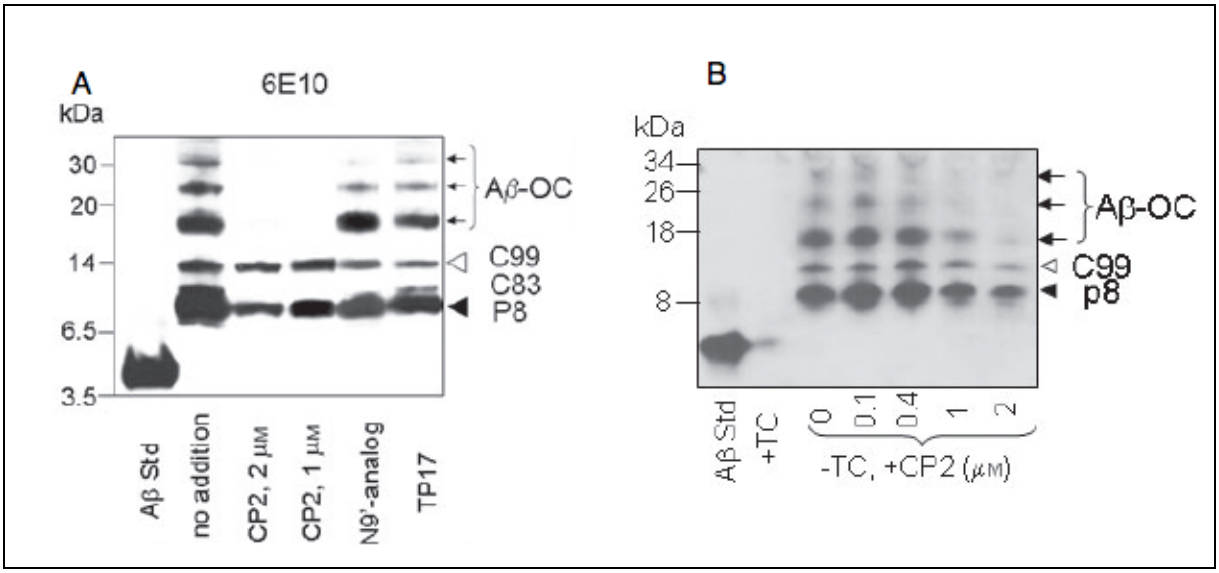

Figure 3.4. Dose dependent study of CP2. CP2 inhibits the formation of Aβ-OCs. (A) MC65 cells were treated with the indicated compounds for 24 h (2 μM N9'- analog and TP17 were used). Western blot of cellular proteins was analyzed with 6E10 (B) MC65 cells were treated with TC or without TC, but with the indicated concentrations of CP2 for 24 h. Cellular proteins were analyzed by western blots using 6E10.

We observed that tricyclic pyrone molecule CP2 ameliorates Aβ toxicity and reduces the levels of intracellular Aβ oligomers. Compound CP2 can be easily modified to produce a series of new compounds. Possible modifications include functionalization of methyl group, C10 double bond, substitute adenine with other heterocycles, replacement of oxygen at position 2 with nitrogen, pyranoquinoline and pyranoisoquinoline etc. (**Chapter 1**). This structure activity relationship (SAR) can help us elucidate the mechanism of inhibition of aggregation.

3.4 Tricyclic pyrone and pyridinone molecules inhibit the formation of Aβ oligomers and protect MC65 cell death

Compounds that protect cell death induced by the intracellular toxic Aβ oligomers can be further used for the drug development in Alzheimer's disease. We have screened several TP

compounds (**Figure 3.5** and **Figure 3.6**) using the MC65 cell assay (**Figure 3.7** and **Table 3.1**). MC65 cells were grown in the presence of 1 μg/ml tetracycline (TC).[5] The cell toxicity was induced by the removal of TC to induce C99 expression. To do so, the cells were washed extensively with phosphate buffer (PBS), and plated on a 96-well plate at a density of 2 x 10^5 cells/cm^2 in Opti-MEM (without phenol-red) from Gibco/BRL (Carlsbad, CA). For testing the protective effect of various TP analogs, various doses of TP compound were added to culture media without TC. After incubation for 72 h, the cell viability was determined using a colorimetric MTT [3-(4,5-dimethylthiazol-2-yl)-2,5-diphenyltetrazolium bromide] assay, the results of which were comparable to data obtained using counts of viable cells based on trypan blue exclusion and the LIVE/DEAD assay.[8-9] Different batches of MC65 cells produce small variations in the activities. Three batches were used to study these compounds and the average of the EC_{50} of different TP analogs is summarized in **Table 3.1.**[10]

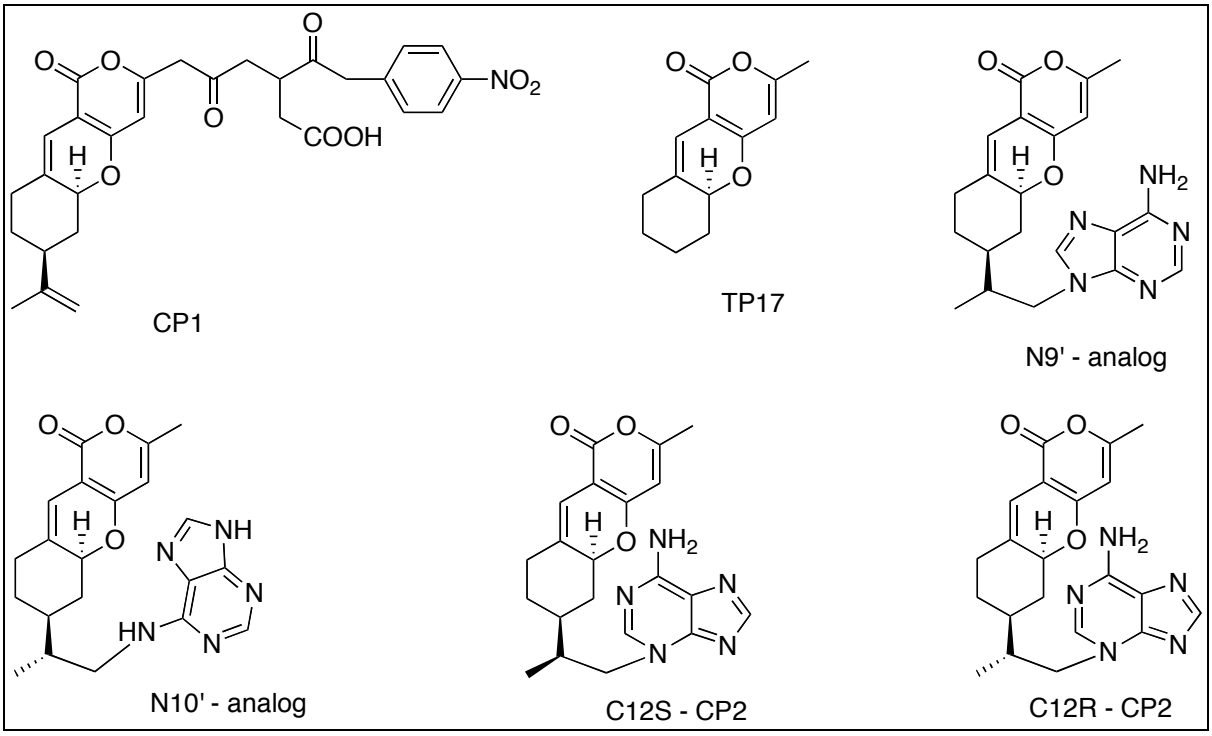

Figure 3.5. Structures of various tricyclic pyrone molecules.

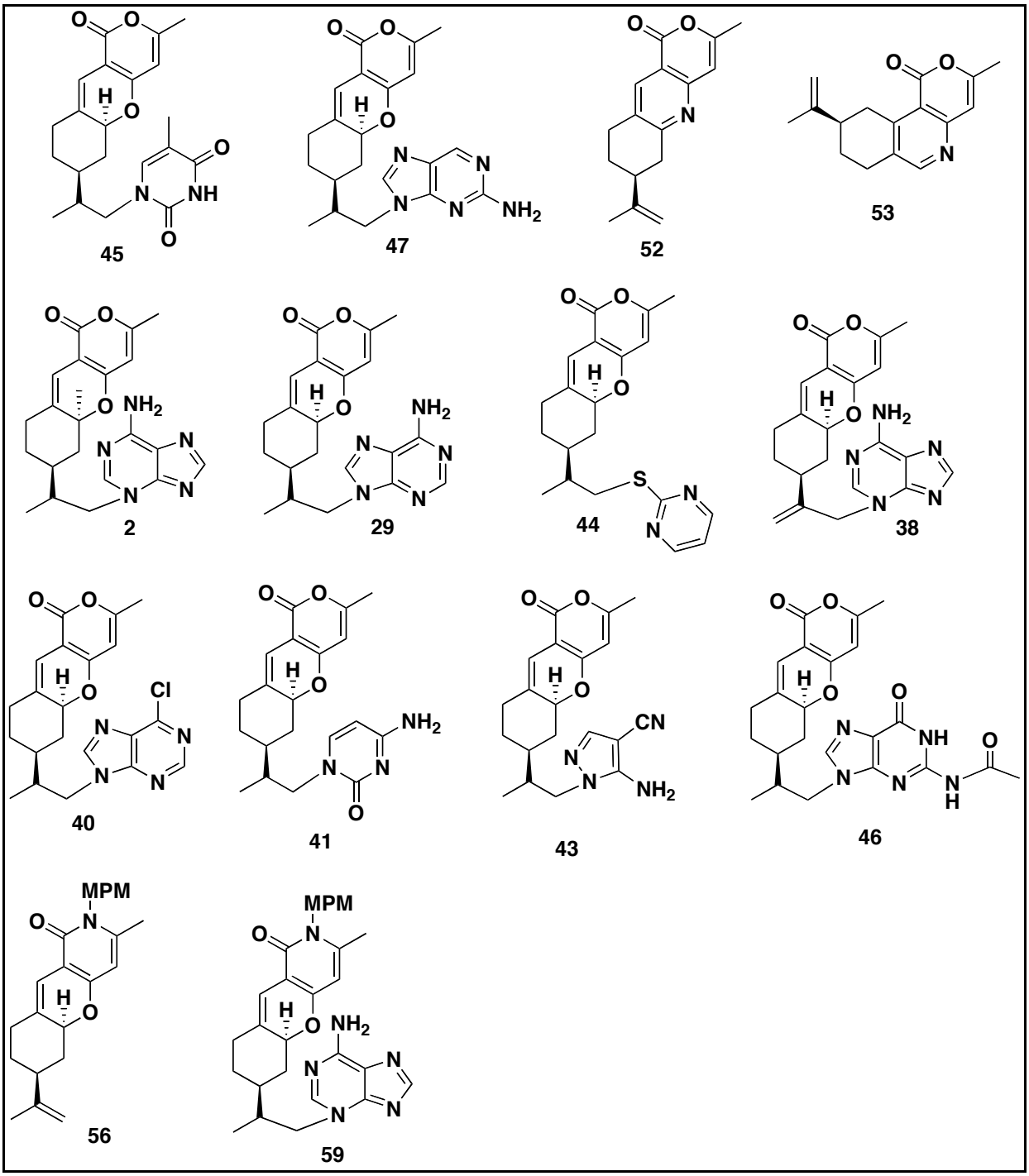

Figure 3.6. Synthesized tricylic pyrone and pyridinone compounds.

Tricyclic pyrone compound CP2 bearing a strong MC65 neuroprotective activity (EC_{50} = 0.15μM) and a low toxicity (**Figure 3.7**).[8] Both CP2 (R and S configuration, N3' analog)

have similar MC65 neuroprotective effect, whereas the N9' analog is less active with EC_{50} around 3.0 μM. N10' analog and TP17 are inactive thus can be used as a control for future experiments.

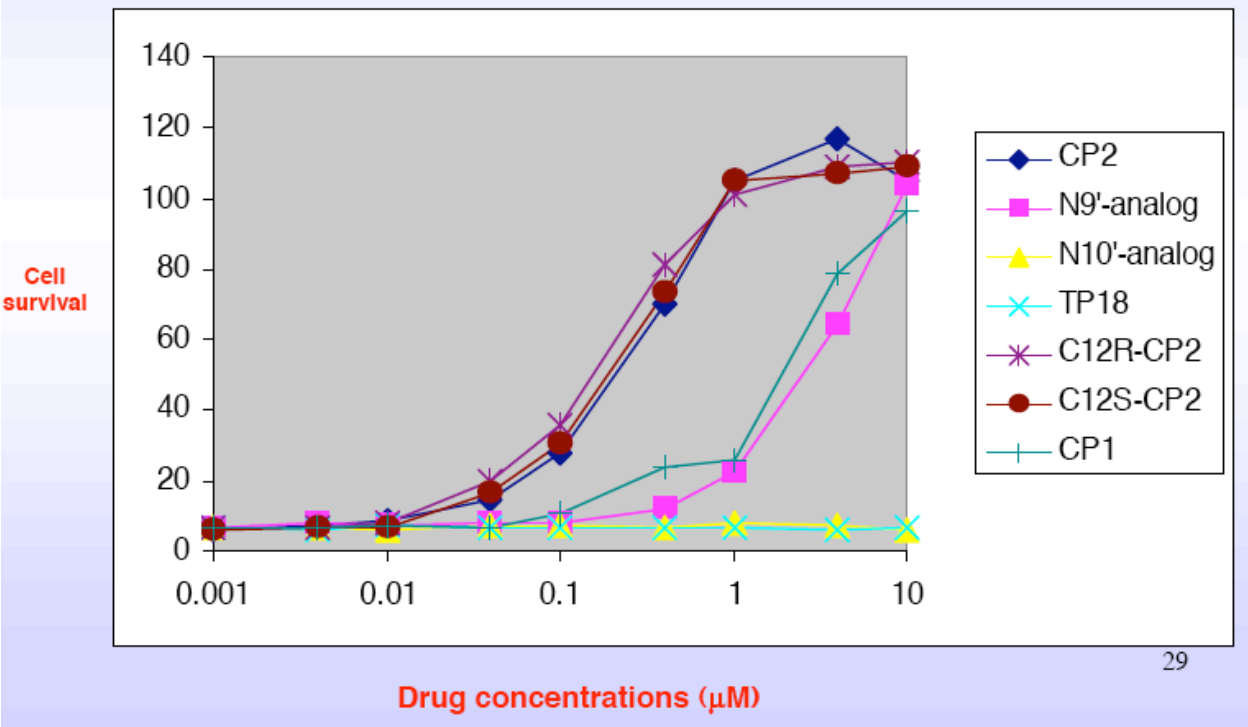

Figure 3.7. MC65 protection assay for different TP compounds. L-685 458 of indicated concentrations was added at the same time as TC removal. At 72 h, viability was assessed by MTT assay. Data are expressed as mean percentage viability (n = 7) with parallel +TC cultures set at 100% viability. Error bars represent standard error. ***p < 0.001, **p < 0.01, compared with untreated –TC controls.

Compound	EC_{50} (μM)	Compound	EC_{50} (μM)
2	0.31 ± 0.03	45	6.92 ± 0.69
29	3.0 ± 0.30	43	8.30 ± 0.83
38	1.95 ± 0.20	44	1.38 ± 0.14
40	0.93 ± 0.09	59	0.35 ± 0.03
47	0.86 ± 0.09	52	Inactive
41	Inactive	53	2.49 ± 0.25

46	Inactive	56	1.25 ± 0.13
34	0.31 ± 0.04		

Table 3.1. TP compounds and their IC50 inhibitory activities.

Compound **38** has a structure similar to **2** (CP2) containing a double at C12 is 6 folds less active. Substituting the adenine of CP2 with other heterocycles lowers the activity. Compounds **41** and **46** are surprisingly inactive. Simple tricyclic pyridinone **56**, which have a nitrogen atom at position 2, possesses an EC_{50} of 1.25 μM, and its adenine derivative **59** has similar EC_{50} activity as that of CP2. The Linear fused pyranoquinoline (**52**) is inactive however, the L-shape fused pyranoisoquinoline (**53**), lacking an adenine unit, is 8 fold less active then CP2. Further investigation is required on the synthesis of N2 and N5 containing tricyclic pyrones.

3.5 Tricyclic pyrone molecule CP2 penetrates MC65 cell

Previous experiments have shown that compound CP2 interacts with the intracellular and the extracellular Aβ. Rapid accumulation of CP2 was observed inside the cells as well as on the cell surface when we incubated the radiotracer [^{14}C]CP2 molecule to the MC65 cells (**figure 3.8**). Radiotracer [^{14}C]CP2 (0.04 μCi) was added to the cell culture wells of 2.5 X 10^6 cells and was incubated for the indicated period of time. The cells were scraped and spun down. Cell pellets were washed with ice-cold phosphate buffer and trypsinized. The supernatant was kept as 'trypsinizable cell surface', and pallets were called 'non-trypsinizable intracellular fraction'. Fractions were subjected to scintillation counting. Results showed that compound CP2 easily penetrated the cells, interacted/binded to the Aβ monomers and Aβ oligomers, and disrupted aggregation by either binding to the Aβ peptide or by changing the conformation of the peptide or by some unknown complex mechanism (**figure 3.8**).[8]

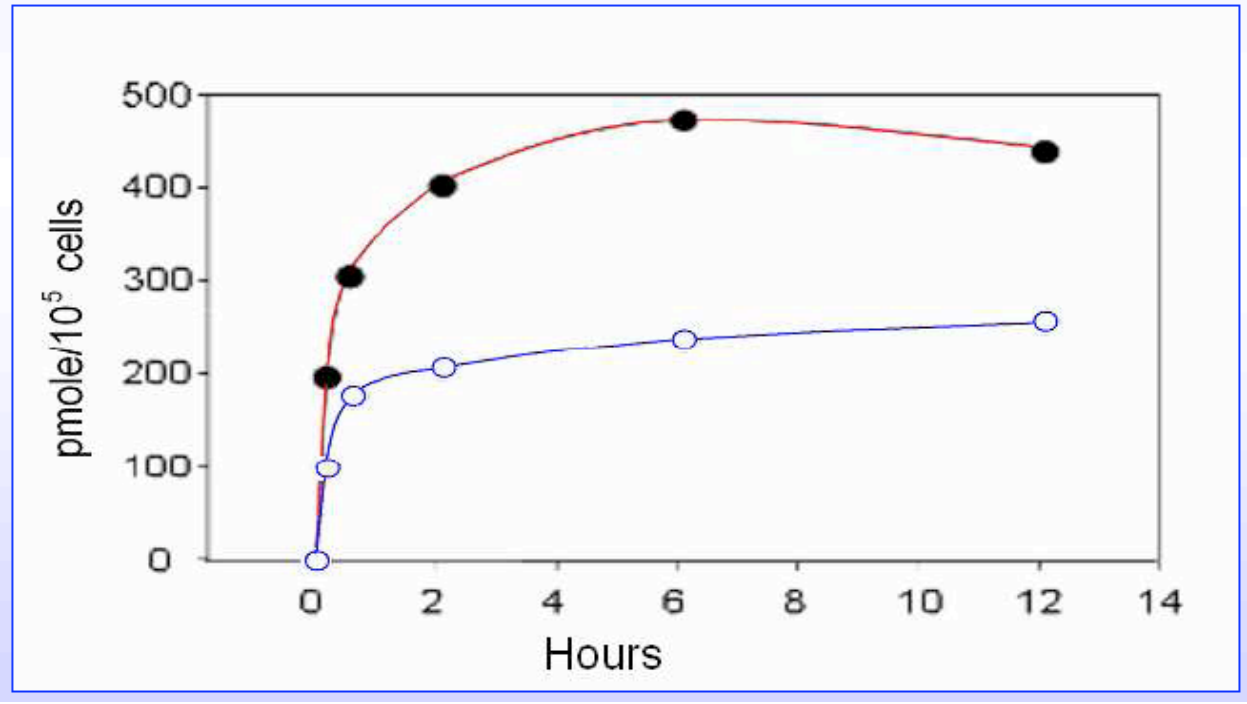

Figure 3.8. CP2 rapidly accumulates inside cells. MC65 cells were incubated with [^{14}C]CP2 for the indicated periods of time, washed, and the cell-associated counts that were trypsinizable from cell pellets (cell surface CP2, empty circles) and those remaining in cells after trypsinization (intracellular CP2, filled circles) were quantified. Expressed values are quantities of CP2 calculated from the radioactivity of 10^5 cells.

3.6 *In vivo* studies of CP2 on 5X FAD mice

3.6.1 Introduction and background

Amyloid plaque in the brain is mainly composed of Aβ peptide. Also, a strong genetic association between early-onset familial alzheimer disease (FAD) and Aβ peptides is well established.[11-13] Association of Aβ42 and FAD favors the causative role for Aβ42 in the etiology of AD.[14] Dr. Vasser *et al*. developed a rapid AD amyloid model of transgenic mice where five different FAD mutations were expressed [APP K670N, M67IL (Swedish) + I716V (Florida) + V717I (London) and human PS1 M146 l + L286V]. These "5X FAD" transgenic mice develop cerebral amyloid plaque and gliosis at 2 months of age. Aβ42 aggregates and reduced synaptic

markers are the characteristics of 5X FAD transgenic mice.[14] Interestingly, accumulation of intraneuronal Aβ42 was observed before the amyloid plaque formation.[14] Accumulation of intraneuronal Aβ was observed in the brain of AD mice.[15-16] We are interested in studying the efficacy of CP2 in 5X FAD transgenic model. Our collaborator Dr. Lee-Way Jin in UC Davis Health System, Sacramento, CA, has conducted all the *in vivo* experiments.

3.6.2 Experimental for in vivo *studies*

The UC Davis Animal Care and Use Committee approved all animal procedures followed on animals. 5X FAD mice were obtained from Dr. Robert Vassar, Department of Cell and Molecular Biology, Northwestern University.[12] Bioactive compound CP2 or an equivalent amount of DMSO (solvent; mock) was dissolved in 100 μL of artificial cerebrospinal fluid to make a working solution of 100μM concentration. The solution was transferred into osmotic mini-pumps (Alzet, Cupertino, CA). A reported procedure to implant the pump was followed.[17] Three-month-old 5x FAD transgenic mice were anesthetized with an intraperitoneal (i.p.) injection of Ketamin (100 mg/Kg body weight) with Xylazine (10 mg/Kg body weight). A brain-infusion cannula (brain infusion kit #3, Alzet) was stereotaxically positioned (antero-posterior, 0.7 mm; mediolateral, 1.5 mm; dorsoventral; 3 mm to Bregma) by cementing with Loctite 454 (Alzet, Cupertino, CA). This cannula was then connected to the subcutaneously implanted osmotic mini-pump (Alzet model 1002). Mice were infused (n = 6 for each group) at a flow rate of 0.25 μL/h for 2 weeks of CP2 or vehicle (DMSO). After 2 weeks, the mice were sacrificed and their brains were removed and snap frozen for Aβ42 ELISA.[18]

3.6.3 Aβ42 ELISA

The corresponding 1 mm-thick fresh frozen mouse brain sections containing hippocampus and subiculum were homogenized in 300 μL of radioimmune precipitation assay (RIPA) buffer containing protease inhibitors mixture solution. The homogenates were sonicated briefly then incubated for 20 min at 4°C. The RIPA insoluble fraction from brain homogenate

was obtained after centrifugation at 100,000 x *g*. The pellet was resuspended in 300 μL of 70% formic acid (FA) and then incubated for 30 min at 4°C. FA soluble fraction was obtained by 100,000 x *g* centrifugation. The FA extracts were neutralized by diluting 1:20 in 1 mole/L Tris buffer (pH 11). The Aβ42 concentration in each sample was determined by Aβ42 specific sandwich ELISA following the protocol of the manufacturer (IBL, Minneapolis, MN). All readings were in the linear range of the assay. The average of the duplicates was determined, and then the mean and standard error for each group of mice was calculated. The values were expressed in nanograms of Aβ per milligram of protein. The statistical significance of differences between groups was examined by t-test, using the SigmaStat 3.1 program (Systat Inc. Point Richmond, CA).[18]

3.6.4 Results and discussion

Neurons in these transgenic mice were engineered to generate a large amount of Aβ42, which results in robust Aβ accumulation and aggregation in brain.[14] Histologically detectable amyloid depositions begin by 2 months, especially in hippocampus and subiculum, and increase sharply between 2-4 months. We infused 100 μM CP2 or mock solution (DMSO alone) into cerebral ventricles of 3-month-old 5x FAD mice for two weeks at a speed of 0.25 μL/h (equivalent to approximately 370 ng per day). At the completion of this treatment, the mice were sacrificed and brains removed for quantification of Aβ levels by sandwich ELISA. The brains slices were extracted sequentially by RIPA and FA respectively. Previously, we found that the majority of Aβ in 5X FAD brain resides in the RIPA-soluble and FA-soluble fractions, which are roughly equivalent to the non-fibrillar and fibrillar Aβ species respectively.[19] CP2 treatment resulted in a 40% reduction of RIPA-soluble Aβ and a 50% reduction of FA-soluble Aβ (**Figure 3.9**). Thus, in a mouse model with perhaps the most robust Aβ42 production among all AD models, a short 2-week treatment of CP2 showed a promising anti-Aβ effect.[18]

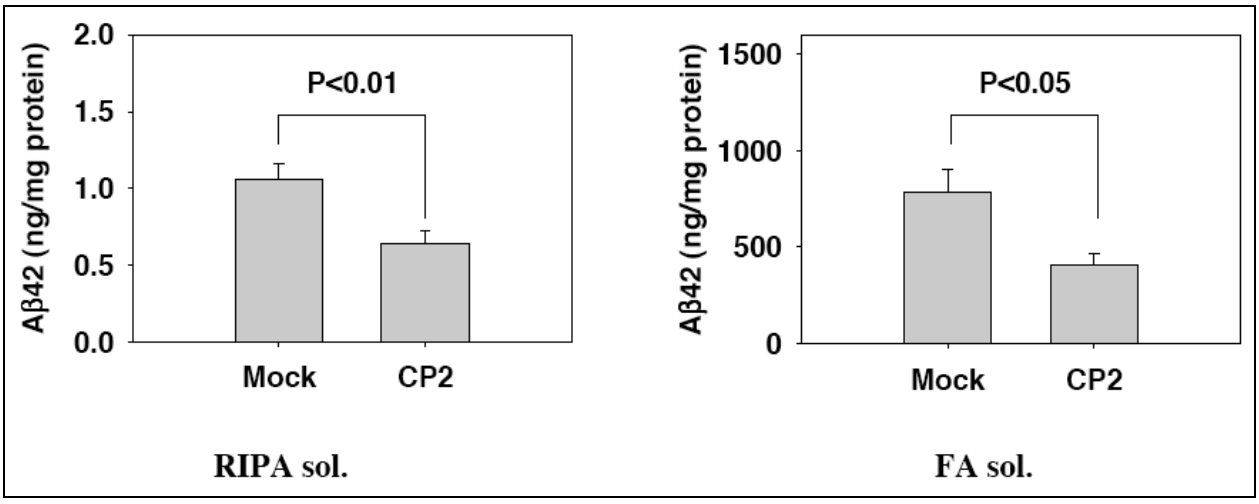

Figure 3.9. CP2 treatment reduces the level of cerebral Aβ. Brains from mice treated with CP2 or mock solution were sequentially extracted with RIPA and FA. Aβ42 levels in the RIPA and FA extracts (RIPA soluble and FA soluble, respectively) were measured by ELISA. Aβ levels were expressed in nanograms per milligram of brain protein. CP2 reduced the levels of both RIPA and FA soluble Aβ42. Error bars represent standard error. n = 6. The p values were obtained by comparing the two groups using t-test.

3.7 Conclusion

The neurotoxicity of amyloid β-protein is widely considered as one of the fundamental causes of neurodegeneration. In our laboratory, we synthesized a series of tricyclic pyrones and pyridinones and screened these compounds against Alzheimer's disease, which leads to the discovery of compound CP2, a small molecule that easily penetrates into the cells. Our data suggests that CP2 not only inhibits the Aβ aggregation but also disaggregates the preformed toxic small oligomers and protofibrils. Other than cell permeability character, CP2 also favors blood brain barrier passage. Our results strongly demonstrate that Aβ oligomeric complexes (Aβ-OC's, tetramers and pentamers) are the major culprit causing MC65 cell death. We believe that CP2 is a novel small compound, which has the ability to inhibit intracellular Aβ aggregation. Treatment of 5X familial Alzheimer's disease mice with CP2 over the period of two weeks resulted in 40% decrease in non-fibrillar aggregates and a 50% in decrease in fibrillar Aβ species.

3.8 References

1. Walsh, D. M.; Hartley, D.; Kusumoto, Y.; Fezoui, Y.; Condrom, M. M.; Lomakin, A.; Benedek, G. B.; Selkoe, D. J.; Teplow, D. B., Amyloid beta-protein fibrillosis. Structure and biological activity of protofibrillar intermediates. *J. Biol. Chem*. **1999**, *274*, 25945-25952
2. Selkoe, D. J., Alzheimer's disease: genes, proteins, and therapy. *Physiol Rev*, **2001**, *81*, 741-766.
3. Pereira, C., Ferreiro, E., Cardoso, S. M., de Oliveira, C. R., Cell degeneration induced by amyloid-beta peptides: implications for Alzheimer's disease. *J Mol Neurosci*, **2004**, *23*, 97-104.
4. Takahashi, R.H.; Almeida, C. G.; Kearney, P. F.; Yu, F.; Lin, M. T.; Milner, T. A.; Gouras, G. K., Oligomerization of alzheimer's β-amyloid within processes and synapses of cultured neurons and brain. *J. Neurochem.,* **2004**, *24*, 3592-3599.
5. Sopher, R. L.; Fukuchi, K.; Smith, A. C.; Leppig, K. A.; Furlog, C. E.; Martin, G. M., Cytotoxicity mediated by conditional expression of a carboxy-terminal derivative of the β -amyloid precursor protein. *Brain Res. Mol. Brain Res*., **1994**, *26*, 207-215.
6. Jin, L.-W.; Hua, D. H.; Shie, F, -S.; Maezawa, I.; Sopher, B.; Martin, G. M., Novel Tricyclic Pyrone Compounds Prevent Intracellular APP C99-Induced Cell Death. *J. Mol. Neurosci*., **2002**, *19*, 57-61.
7. Maezawa, I.; Jin, L. –W.; Woltjer, R. L.; Maeda, N.; Martin, G. M.; Montine, T. J.; Montine, K. S., Apolipoprotein E isoforms and apolipoprotein AI protect from amyloid precursor protein carboxy terminal fragment-mediated cytotoxicity through different mechanisms. *J. Neurochem*., **2004**, *91*, 1312-1321.
8. Maezawa, I.; Hong, H. -S.; Wu, H. -C.; Battina, S. K.; Rana, S.; Iwamoto, T.; Radke, G. A.; Pettersson, E.; Martin, G. M.; Hua, D. H.; Jin, L.-W., A novel tricyclic pyrone compound ameliorates cell death associated with intracellular amyloid-β oligomeric complexes. *J. Neurochem*. **2006**, *98*, 57-67.

9. Woltjer, R. L.; Nghiem, W.; Maezawa, I.; Milatovic, D.; Vaisar, T.; Montine, K. S.; Montine, T. J., Role of glutathione in intracellular amyloid-alpha precursor protein/carboxy-terminal fragment aggregation and associated cytotoxicity. *J Neurochem*. **2005**, *93*, 1047-1056.
10. Rana, S.; Hong, H. –S.; Barrigan, L.; Jin, L. –W, Hua, D. H., Synthesis of tricyclic pyrones and pyridinones and protection of Aβ-peptide induced MC65 neural cell death. *Bio. Org. Med. Chem*., **2009**. 19, 670-674.
11. Hutton, M.; Perez-Tur, J.; Hardy, J., Genetics of Alzheimer's disease. *Essays Biochem.*, **1998**, *33*, 117-131.
12. Sisodia, S. S.; Kim, S. H.; Thinakaran, G., Function and dysfunction of the presenils. *Am. J. Hum. Genet.*, **1999**, *65*, 7-12.
13. Younkin, S. G., The role of Abeta 42 in Alzheimer's disease. *J. Physiol. (Paris)*, **1998**, *92*, 289-292.
14. Oakley, H.; Cole, S. L.; Logan, S.; Maus, E.; Shao, P.; Craft, J.; Guillozet-Bongaarts, A.; Ohno, M.; Disterhoft, J.; Eldik, L. V.; Berry, R.; Vasser, R., Intraneuronal β-Amyloid aggregates, neurodegernation, and neuron loss in transgenic mice with familial alzheimer's disease mutations: potential factors in amyloid plaque formation. *J. Neurosci.*, **2006**, *26*, 10129-10140.
15. Cataldo, A. M.; Petanceska, S.; Terio, N. B.; Peterhoff, C. M.; Durham, R.; Mercken, M.; Mehta, P. D.; Buxbaum, J.; Haroutunian, V.; Nixon, R. A., Abeta localization in abnormal endosomes: association with earliest Abeta elevations in AD and Down syndrome. *Neuobiol. Aging.*, **2004**, *25*, 1263-1272.
16. Gouras, G. K.; Almeida, C. G.; Takahashi, R. H., Intraneuronal Abeta accumulation and origin of plaque in Alzheimer's disease. *Neurobiol. Aging*, **2005**, *26*, 1235-1244.
17. Dolev, I.; Michaelson, D. M., A nontrangenic mouse model shows inducible amyloid–β (Aβ) peptide deposition and elucidates the role apolipoprotein E in amyloid cascade. *Proc. Natl. Acad. Sci. USA*, **2004**, *101*, 13909-13914.
18. Hong, H. -S.; Rana, S.; Barrigan, L.; Shi, A.; Zhang, Y.; Zhou, F.; Jin, L. -W.; Hua, D. H., Inhibition of Alzheimer's amyloid toxicity with a tricyclic pyrone molecule *in vitro* and *in vivo*. *J. Neurochem*. **2009**, *108*, 1097-1108.

19. Hong, H. -S.; Maezawa, I.; Budamagunta, M.; Rana, S.; Shi, A.; Vassar, R.; Liu, R.; Lam, K.S.; Cheng, R.H.; Hua, D.H.; Voss, J.C.; Jin, L.-W., Candidate anti-Aβ fluorine compounds selected from analogs of amyloid imaging agents. *Neurobiol. Aging.*, **2008**, *In Press.*

Appendix: ^{1}H-NMR spectra, ^{13}C-NMR spectra, MS spectra, 2D-NOESY, 2D-COSY, 2D-HMBC, 2DHSQC

Formula $C_{21}H_{28}N_6O_3$	FW	393.4390		

Acquisition Time (sec)	2.0487	Comment	Std proton	Date	Mar 9 2009
Date Stamp	Mar 9 2009	File Name	C:\NMR 031009\400\SRANA\SR-9-118-CP2		
Frequency (MHz)	399.75	Nucleus	1H	Number of Transients	32
Original Points Count	13103	Points Count	16384	Pulse Sequence	s2pul
Receiver Gain	52.00	Solvent	CHLOROFORM-d		
Spectrum Offset (Hz)	2403.5376	Sweep Width (Hz)	6395.91	Temperature (degree C)	25.000

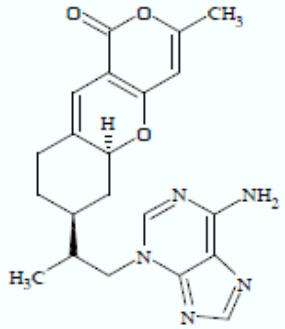

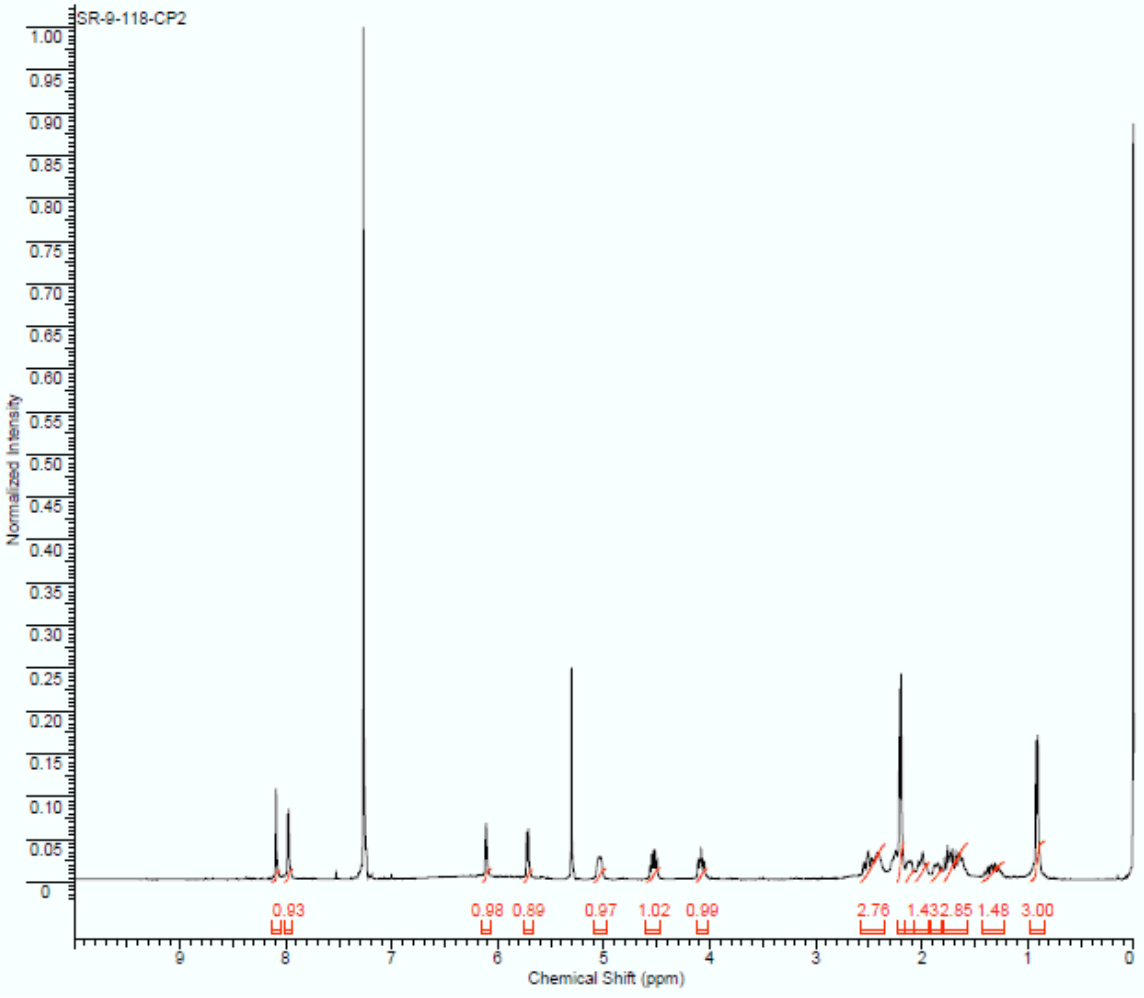

Formula $C_{22}H_{29}N_5O_3$	FW	391.4662

Acquisition Time (sec)	1.3005	Comment	Std proton	Date	Dec 17 2008
Date Stamp	Dec 17 2008	File Name	C:\NMR BACKUP\010609NMR BACKUP\400\SRANA\SRANA\SR-CP2-13C		
Frequency (MHz)	100.53	Nucleus	13C	Number of Transients	2000
Original Points Count	31375	Points Count	32768	Pulse Sequence	s2pul
Receiver Gain	30.00	Solvent	CHLOROFORM-d		
Spectrum Offset (Hz)	10543.4932	Sweep Width (Hz)	24125.45	Temperature (degree C)	25.000

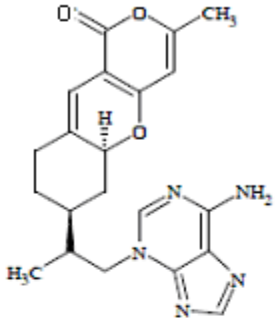

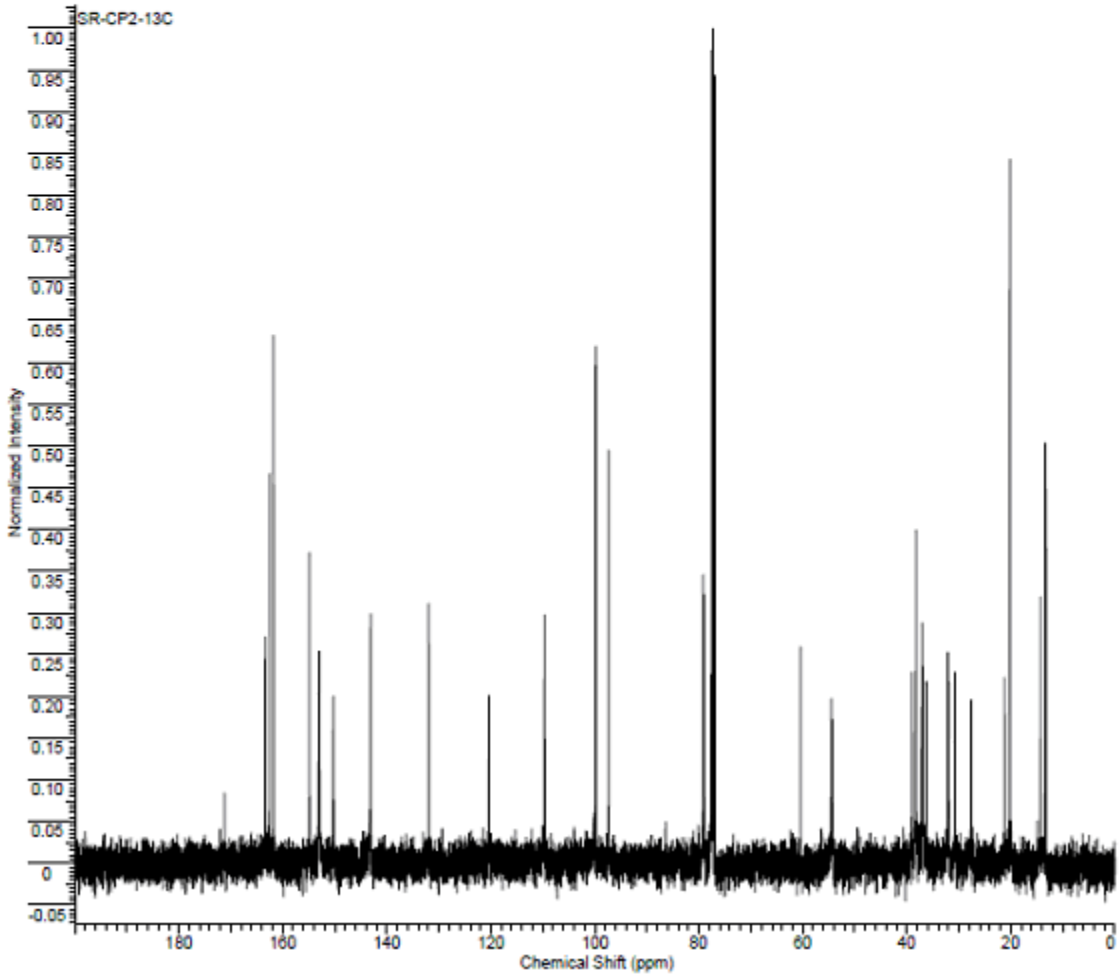

Formula $C_{16}H_{18}O_3$	FW	258.3123

Acquisition Time (sec)	2.0487	Comment	Std proton	Date	Dec 18 2008
Date Stamp	Dec 18 2008			File Name	C:\SANDEEP NMR\SR-TP-1H
Frequency (MHz)	399.75	Nucleus	1H	Number of Transients	4
Original Points Count	13103	Points Count	16384	Pulse Sequence	s2pul
Receiver Gain	14.00	Solvent	CHLOROFORM-d		
Spectrum Offset (Hz)	2404.3184	Sweep Width (Hz)	6395.91	Temperature (degree C)	25.000

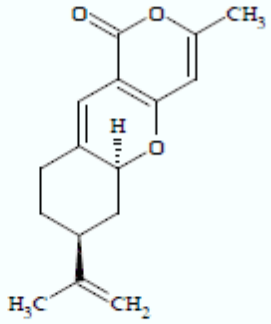

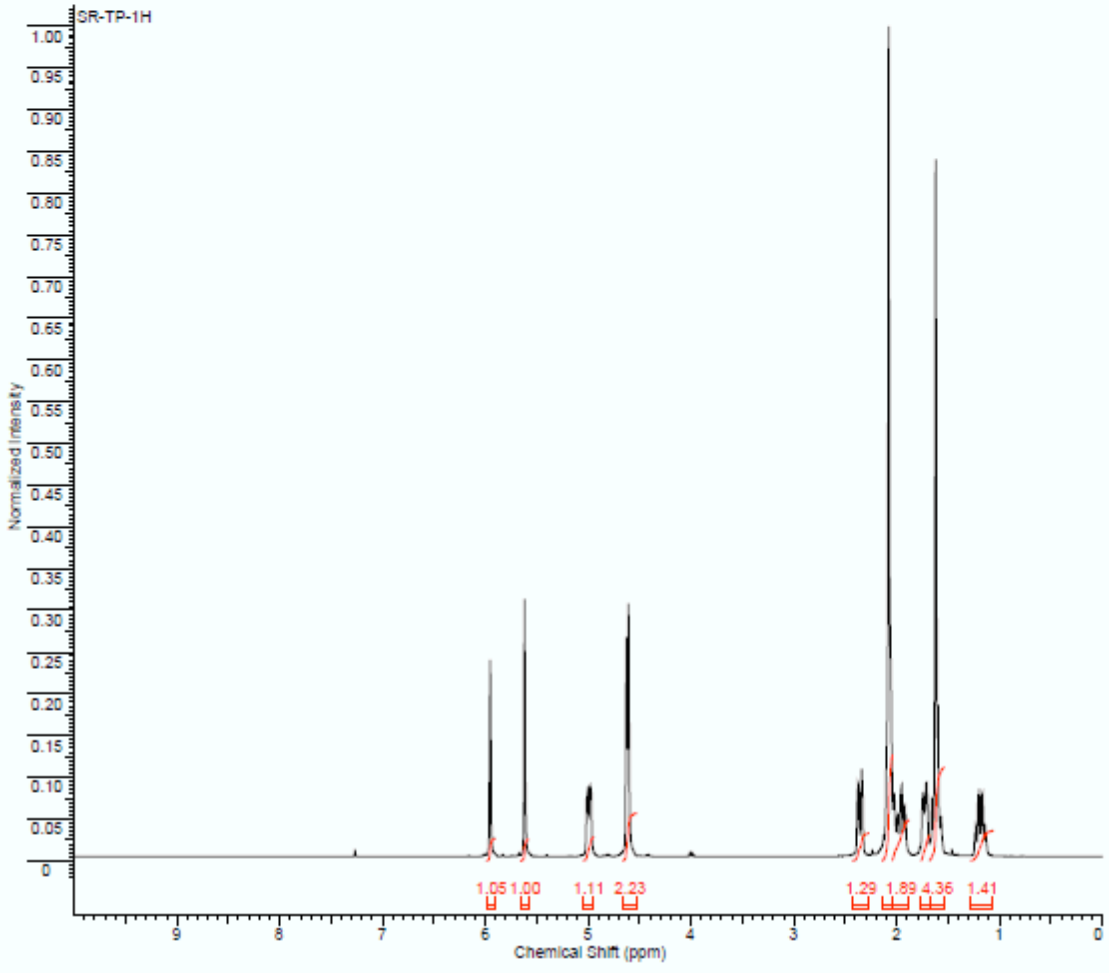

Formula $C_{15}H_{18}O_3$	FW	258.3123

Acquisition Time (sec)	1.3005	Comment	Std proton	Date	Dec 18 2008
Date Stamp	Dec 18 2008			File Name	C:\SANDEEP NMR\SR-TP-13C
Frequency (MHz)	100.53	Nucleus	13C	Number of Transients	500
Original Points Count	31375	Points Count	32768	Pulse Sequence	s2pul
Receiver Gain	30.00	Solvent	CHLOROFORM-d		
Spectrum Offset (Hz)	10529.5039	Sweep Width (Hz)	24125.45	Temperature (degree C)	25.000

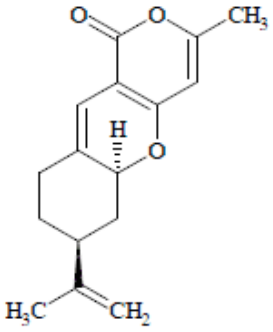

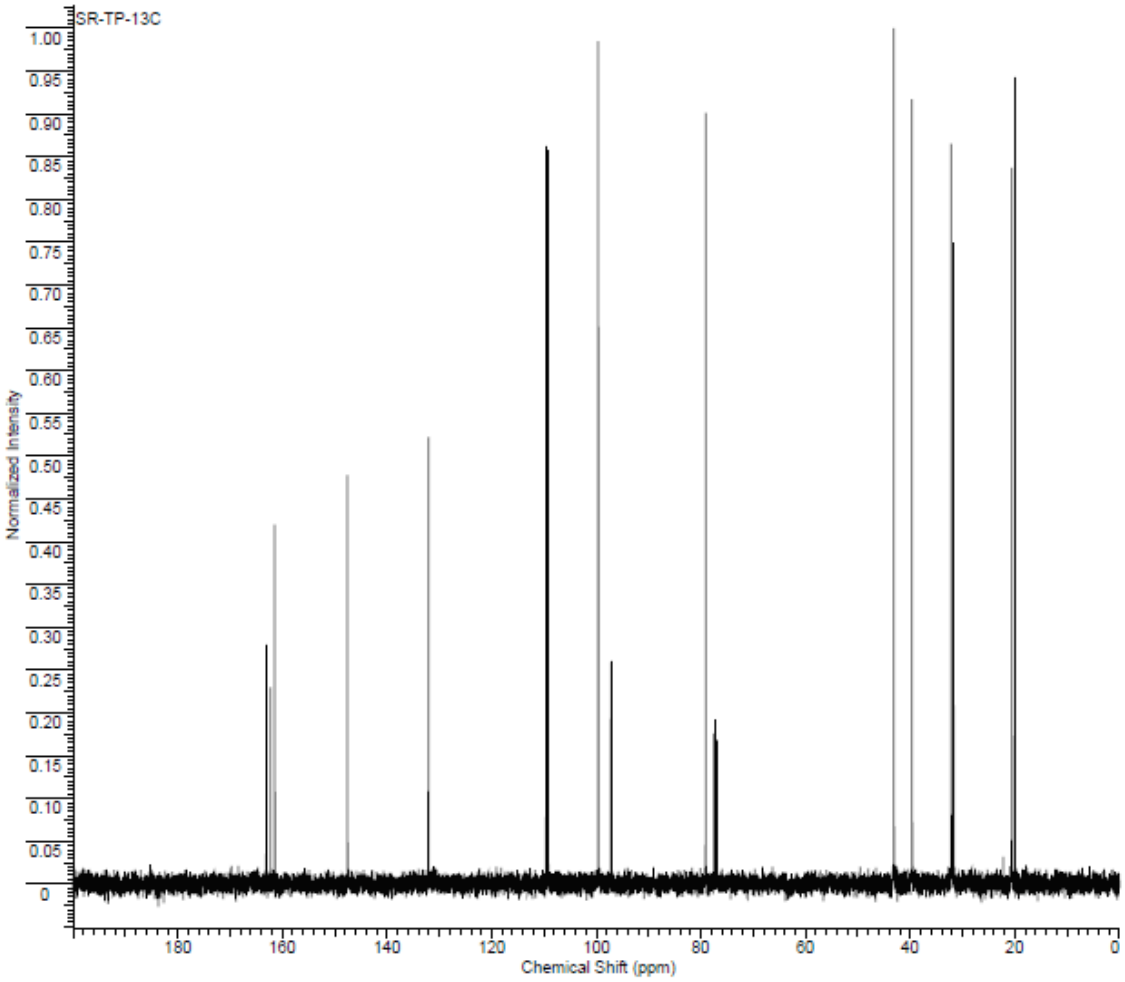

Formula $C_{15}H_{22}O_4$	FW	278.3435		
Acquisition Time (sec)	1.9945	Comment	STANDARD 1H OBSERVE	
Date	Oct 31 2007	Date Stamp	Oct 31 2007	
File Name	C:\NMR BACKUP\010609\NMR BACKUP\200\HUA-NEW\SANDEEP\BOOK5\SR-5-116-DP			
Frequency (MHz)	199.98	Nucleus	1H	Number of Transients 32
Original Points Count	5984	Points Count	8192	Pulse Sequence s2pul
Receiver Gain	4.00	Solvent	CHLOROFORM-d	
Spectrum Offset (Hz)	1004.2203	Sweep Width (Hz)	3000.30	Temperature (degree C) 29.000

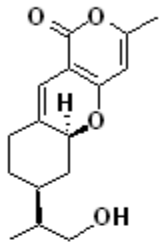

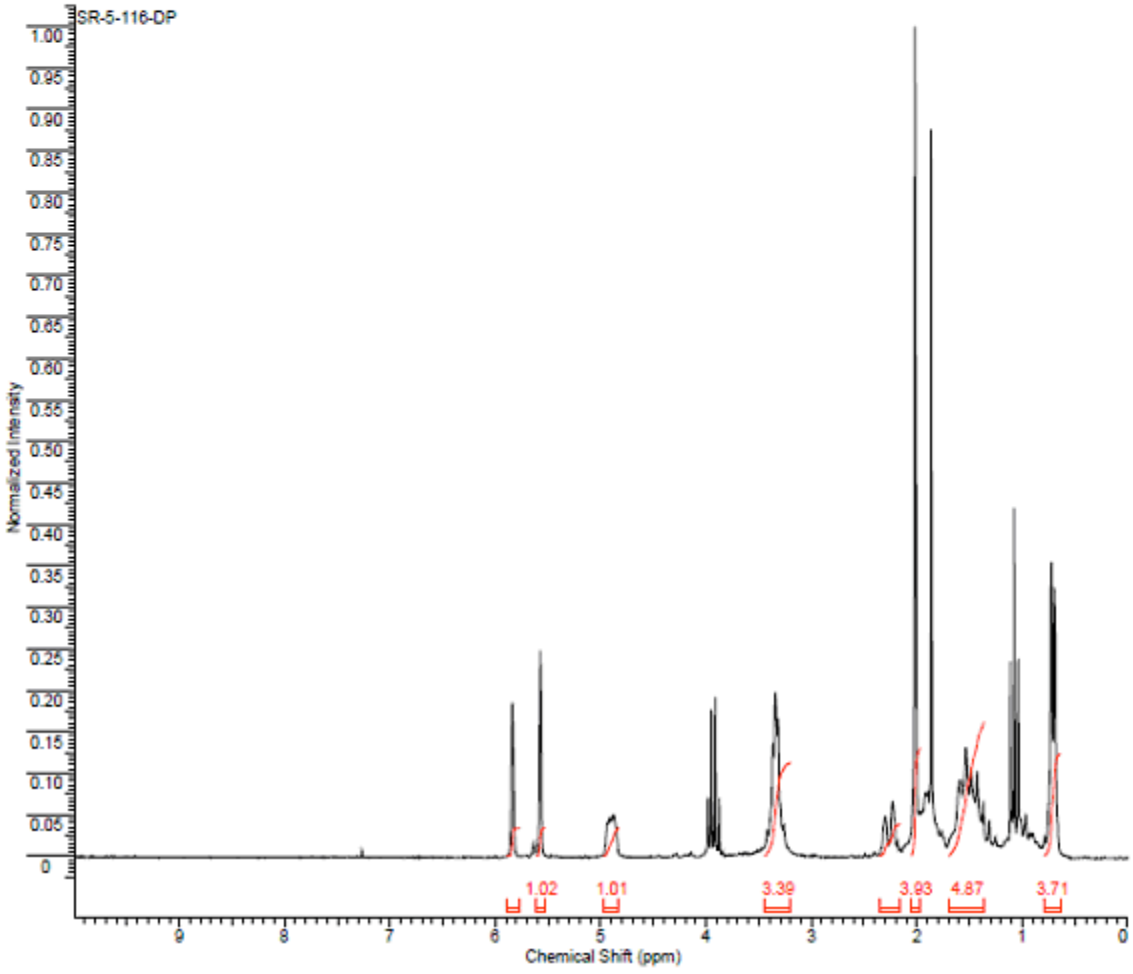

Formula $C_{16}H_{22}O_4$	FW	278.3435

Acquisition Time (sec)	1.3005	Comment	Std proton	Date	Oct 31 2007
Date Stamp	Oct 31 2007				
File Name	C:\NMR BACKUP\010609NMR BACKUP\400\SRANA\SRANA\SR-5-116-FR1D-15-13C				
Frequency (MHz)	100.53	Nucleus	13C	Number of Transients	2000
Original Points Count	31375	Points Count	32768	Pulse Sequence	s2pul
Receiver Gain	30.00	Solvent	CHLOROFORM-d		
Spectrum Offset (Hz)	10529.1475	Sweep Width (Hz)	24125.45	Temperature (degree C)	25.000

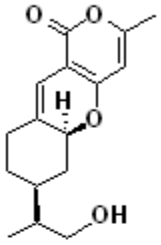

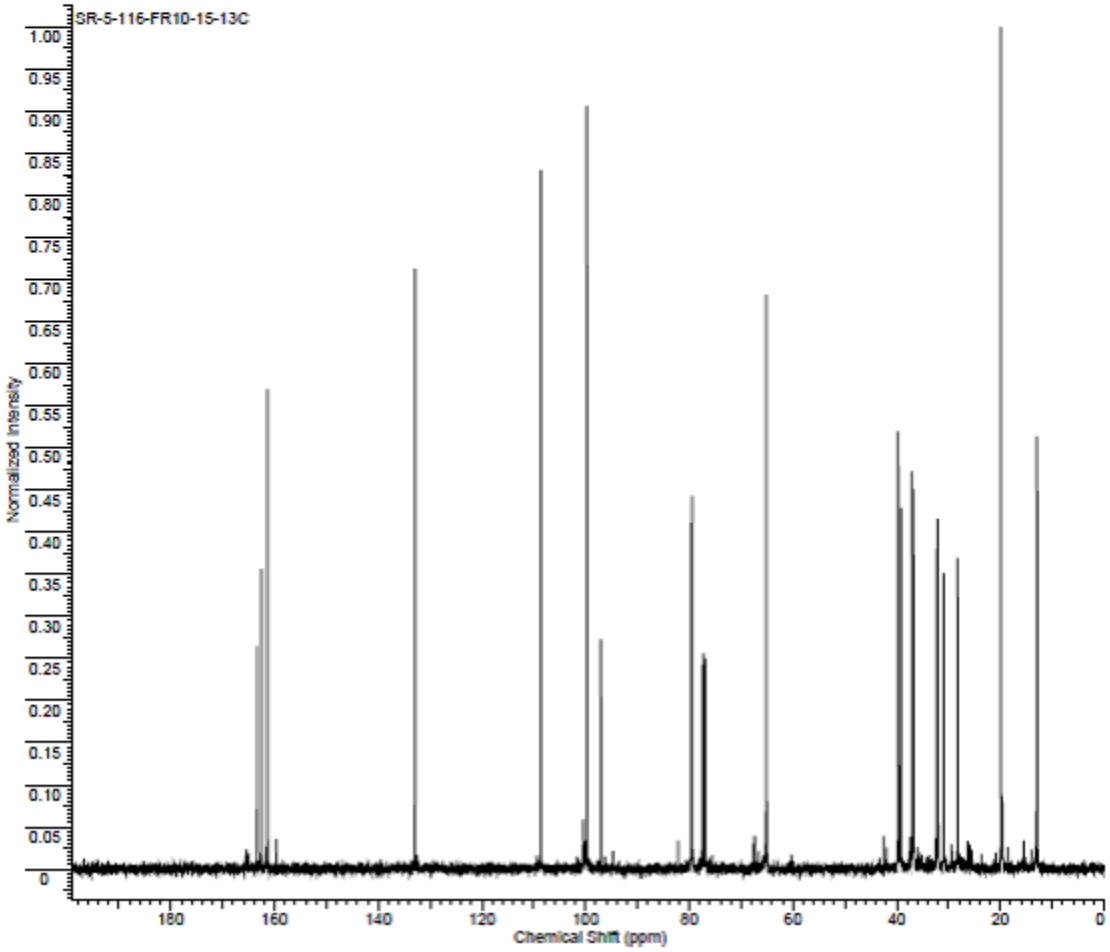

Formula $C_{16}H_{20}O_5$?	FW	261.3361+?

Acquisition Time (sec)	2.0486	Comment	Std proton	Date	Nov 1 2007
Date Stamp	Nov 1 2007	File Name	C:\NMR BACKUP\D10609NMR BACKUP\400\SRANA\SRANA\SR-7-11-FR8		
Frequency (MHz)	399.77	Nucleus	1H	Number of Transients	16
Original Points Count	13104	Points Count	16384	Pulse Sequence	s2pul
Receiver Gain	16.00	Solvent	CHLOROFORM-d		
Spectrum Offset (Hz)	2409.4956	Sweep Width (Hz)	6396.42	Temperature (degree C)	25.000

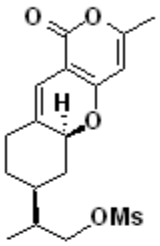

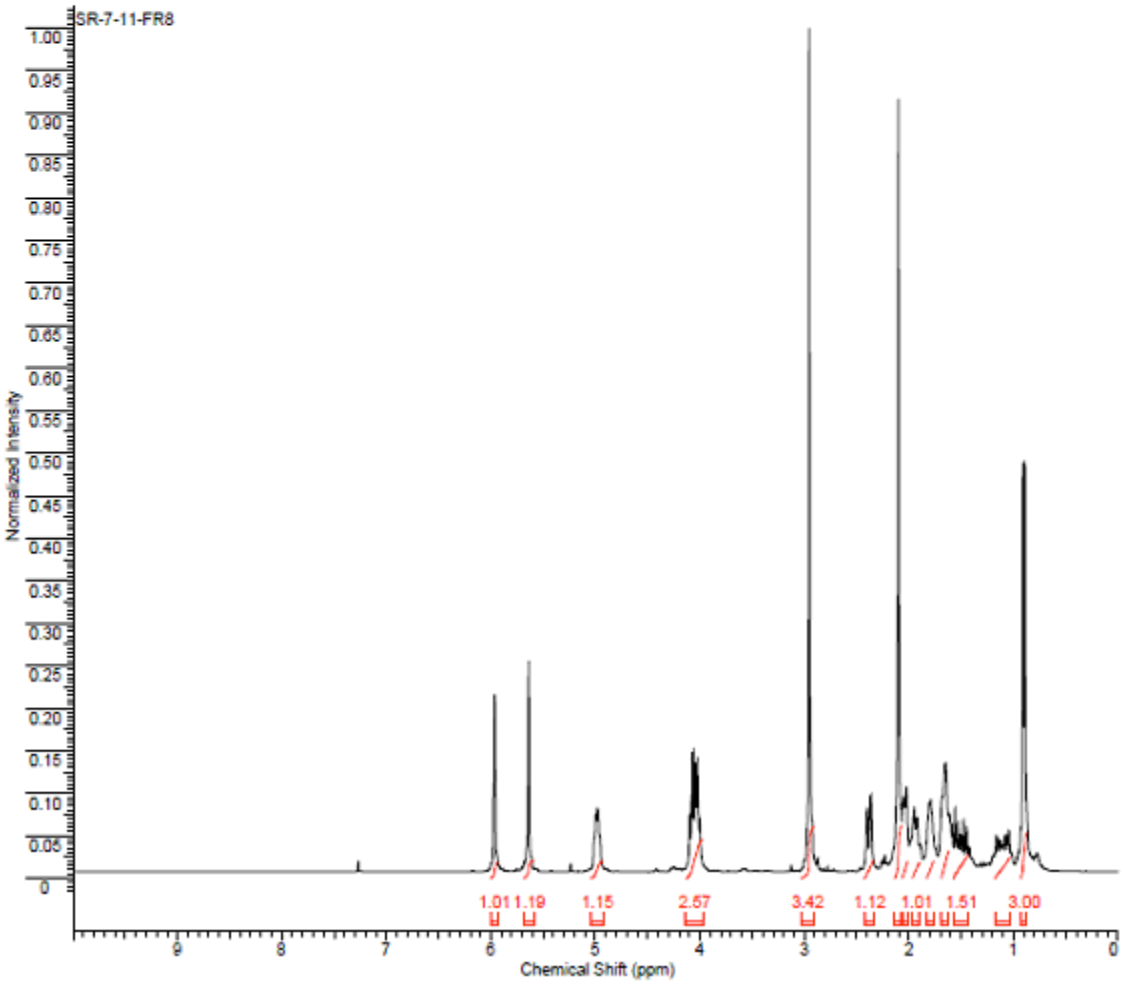

Formula $C_{16}H_{21}O_5$?	FW	261.3361+?			
Acquisition Time (sec)	1.3005	Comment	Std proton	Date	Nov 1 2007
Date Stamp	Nov 1 2007				
File Name	C:\NMR BACKUP\010609NMR BACKUP\400\SRANA\SRANA\SR-7-011-FR8-13C				
Frequency (MHz)	100.53	Nucleus	13C	Number of Transients	3000
Original Points Count	31375	Points Count	32768	Pulse Sequence	s2pul
Receiver Gain	30.00	Solvent	CHLOROFORM-d		
Spectrum Offset (Hz)	10532.0928	Sweep Width (Hz)	24125.45	Temperature (degree C)	25.000

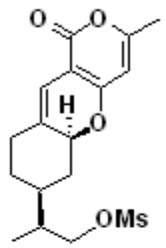

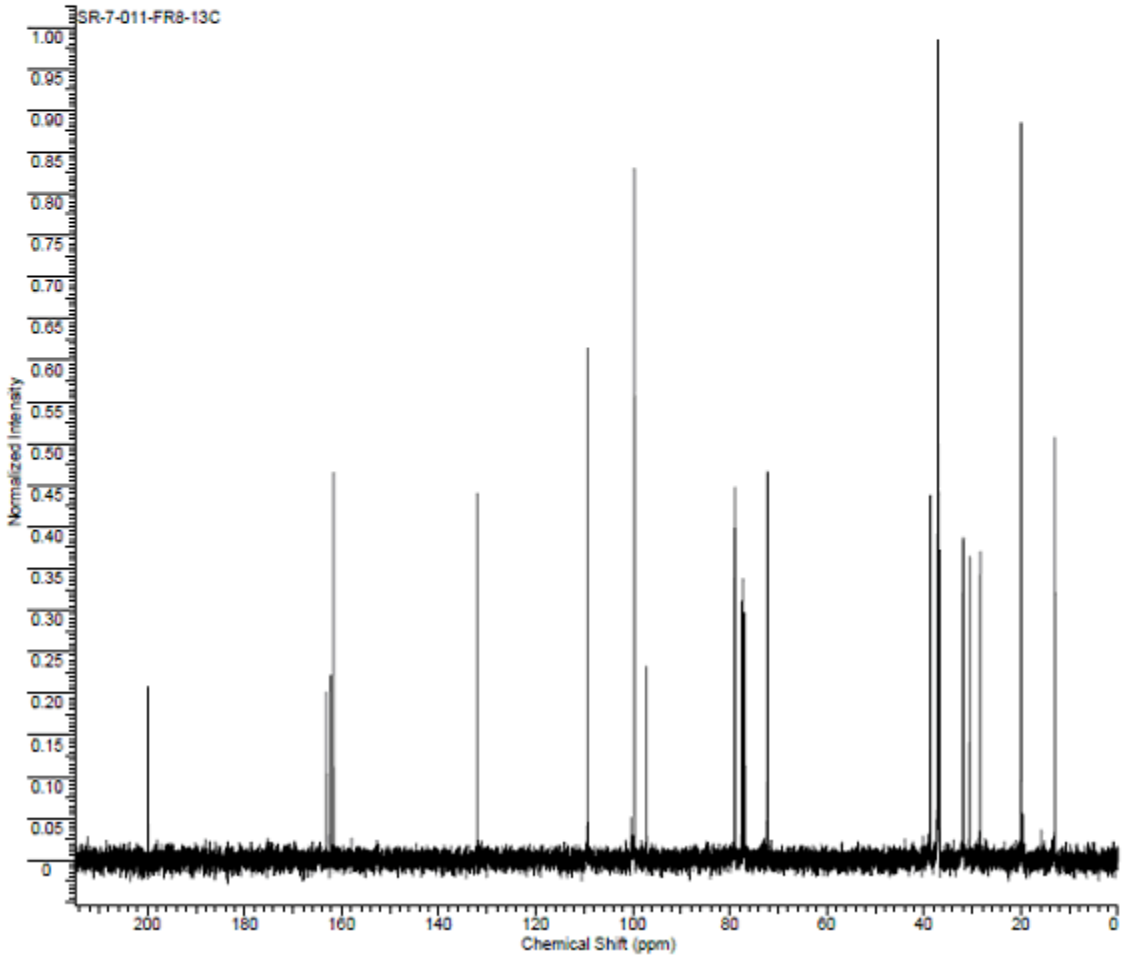

Formula $C_{17}H_{22}O_4$	FW	290.3542

Acquisition Time (sec)	1.9945	Comment	STANDARD 1H OBSERVE		
Date	Mar 17 2008	Date Stamp	Mar 17 2008		
File Name	C:\NMR BACKUP\010609NMR BACKUP\200\HUA-NEW\SANDEEP\BOOK 7\SR-7-104-FR7				
Frequency (MHz)	199.98	Nucleus	1H	Number of Transients	32
Original Points Count	5984	Points Count	8192	Pulse Sequence	s2pul
Receiver Gain	34.00	Solvent	CHLOROFORM-d		
Spectrum Offset (Hz)	1002.3889	Sweep Width (Hz)	3000.30	Temperature (degree C)	29.000

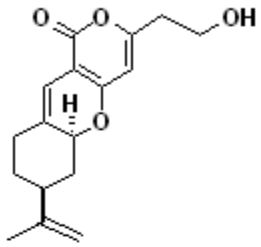

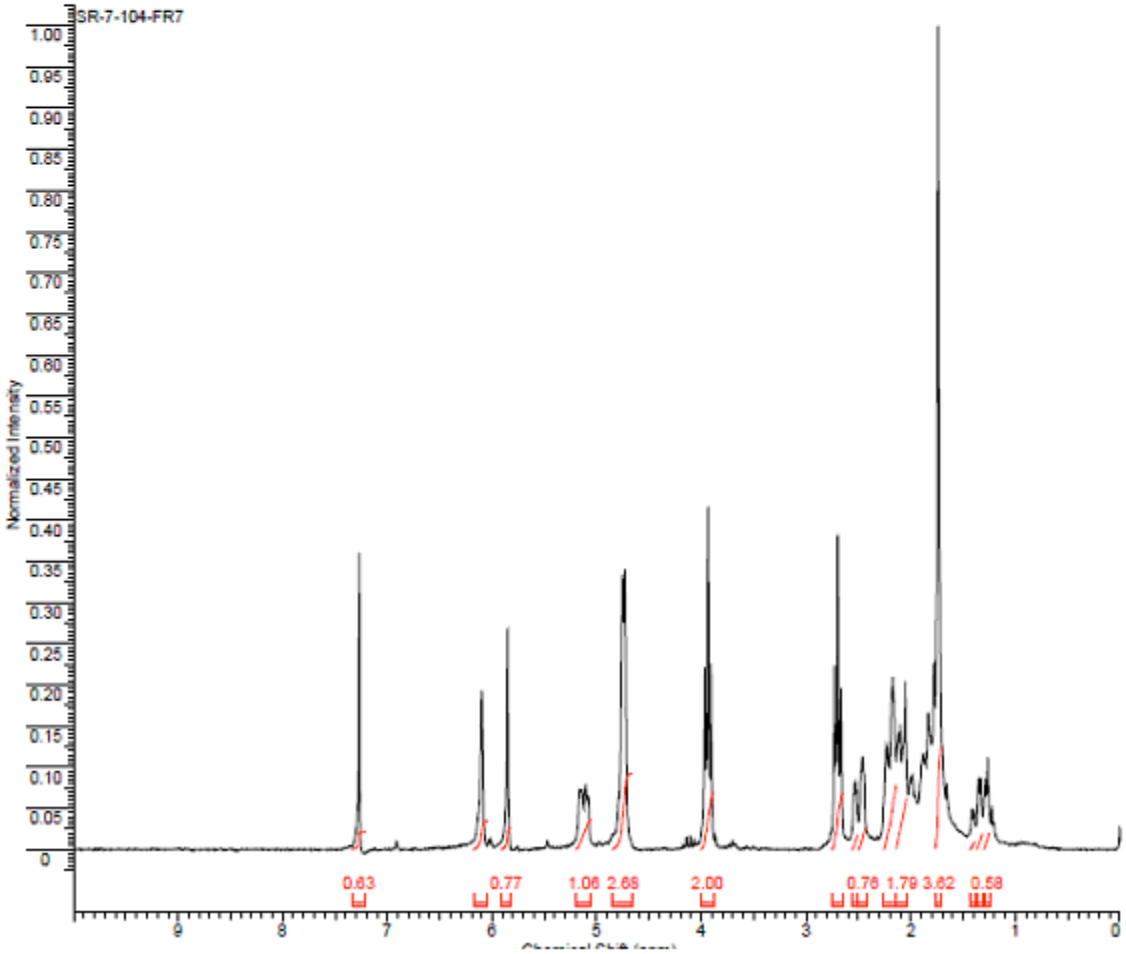

Formula $C_{17}H_{30}O_4$	FW 290.3542

Acquisition Time (sec)	1.3005	Comment	Std proton	Date	Dec 14 2007
Date Stamp	Dec 14 2007				
File Name	C:\NMR BACKUP\010609NMR BACKUP\400\SRANA\SRANA\SR-7-40-FR11-13C				
Frequency (MHz)	100.53	Nucleus	13C	Number of Transients	5000
Original Points Count	31375	Points Count	32768	Pulse Sequence	s2pul
Receiver Gain	30.00	Solvent	CHLOROFORM-d		
Spectrum Offset (Hz)	10548.2900	Sweep Width (Hz)	24125.45	Temperature (degree C)	19.000

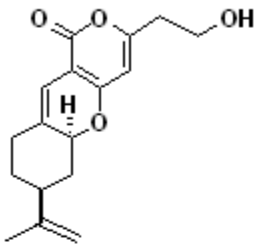

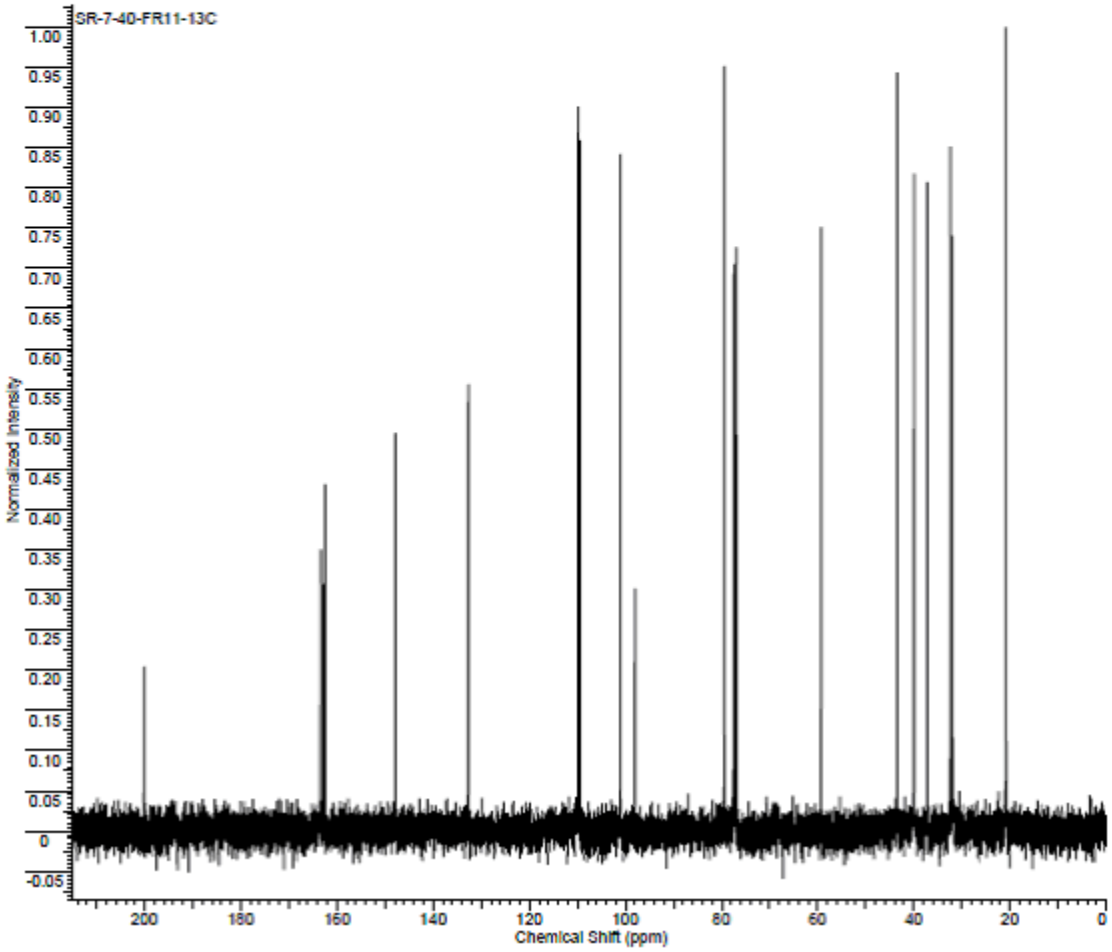

Formula $C_{20}H_{24}O_4$	FW	328.4022

Acquisition Time (sec)	2.0486	Comment	Std proton	Date	Apr 8 2008
Date Stamp	Apr 8 2008	File Name	C:\NMR 031009\400\SRANA\SR-TP4-ACETATE		
Frequency (MHz)	399.77	Nucleus	1H	Number of Transients	32
Original Points Count	13104	Points Count	16384	Pulse Sequence	s2pul
Receiver Gain	22.00	Solvent	CHLOROFORM-d		
Spectrum Offset (Hz)	2409.1055	Sweep Width (Hz)	6396.42	Temperature (degree C)	25.000

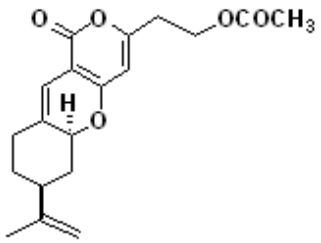

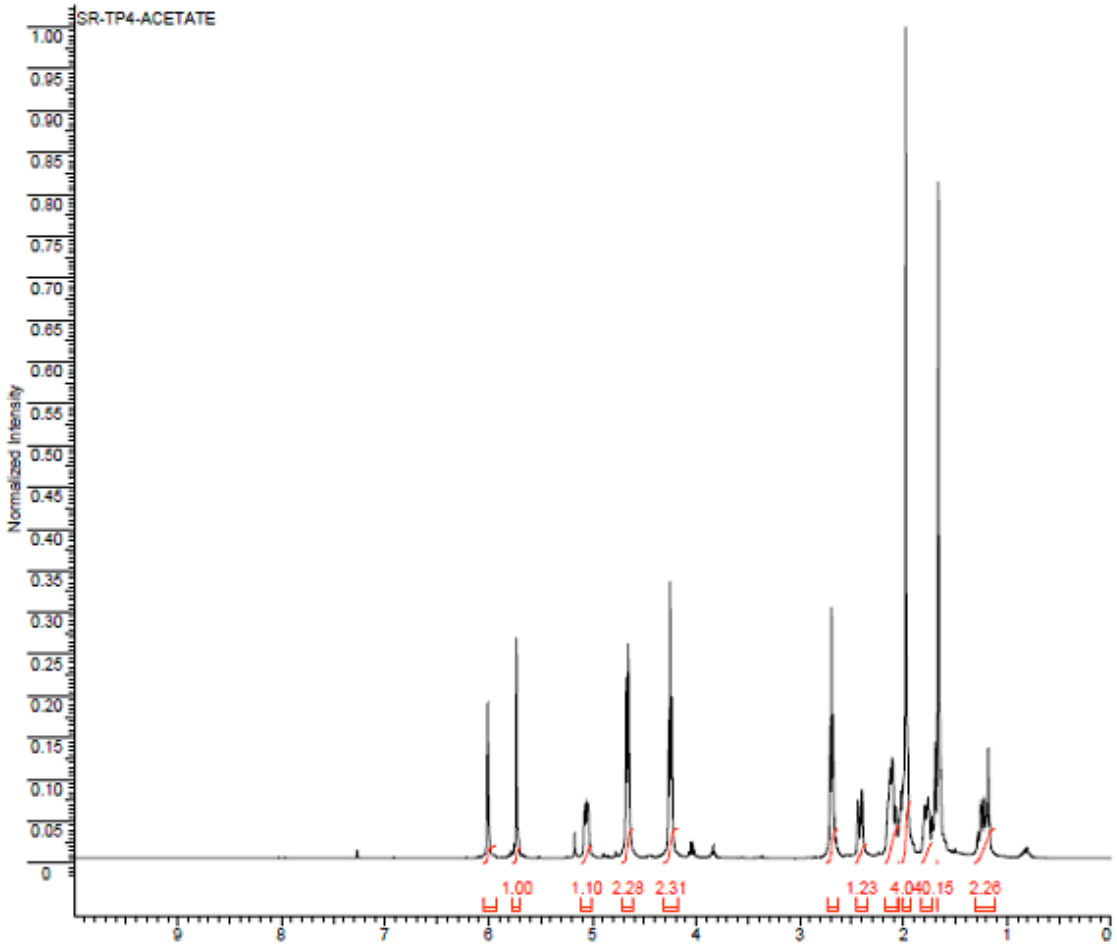

Formula $C_{19}H_{24}O_5$	FW	332.3909

Acquisition Time (sec)	1.3005	Comment	Std proton	Date	Dec 19 2007
Date Stamp	Dec 19 2007	File Name	C:\NMR BACKUP\010609NMR BACKUP\400\SRANA\SRANA\SR-7-43-DP-13C		
Frequency (MHz)	100.53	Nucleus	13C	Number of Transients	3000
Original Points Count	31375	Points Count	32768	Pulse Sequence	s2pul
Receiver Gain	30.00	Solvent	CHLOROFORM-d		
Spectrum Offset (Hz)	10542.3994	Sweep Width (Hz)	24125.45	Temperature (degree C)	19.000

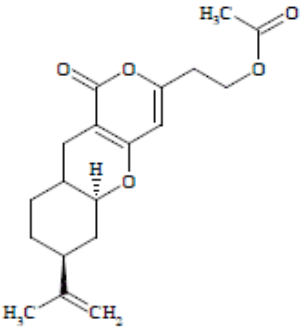

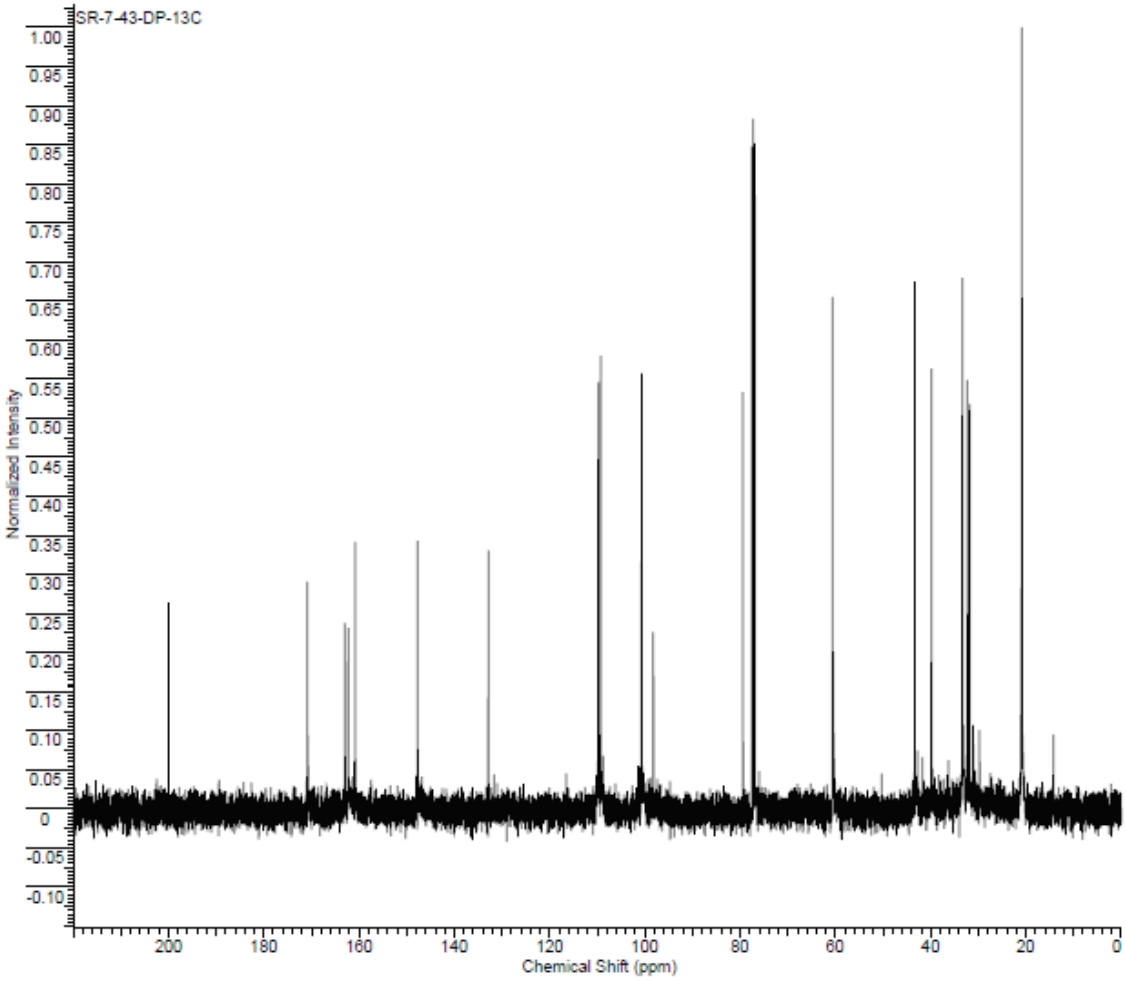

Formula $C_{19}H_{24}O_6$	FW	348.3903		
Acquisition Time (sec)	1.9945	Comment	STANDARD 1H OBSERVE	
Date	Aug 22 2008	Date Stamp	Aug 22 2008	
File Name	C:\NMR BACKUP\010609NMR BACKUP\200\HUA-NEW\SANDEEP\BOOK8\SR-8-112-DP			
Frequency (MHz)	199.98	Nucleus	1H	Number of Transients 32
Original Points Count	5984	Points Count	8192	Pulse Sequence s2pul
Receiver Gain	30.00	Solvent	CHLOROFORM-d	
Spectrum Offset (Hz)	1002.0226	Sweep Width (Hz)	3000.30	Temperature (degree C) 29.000

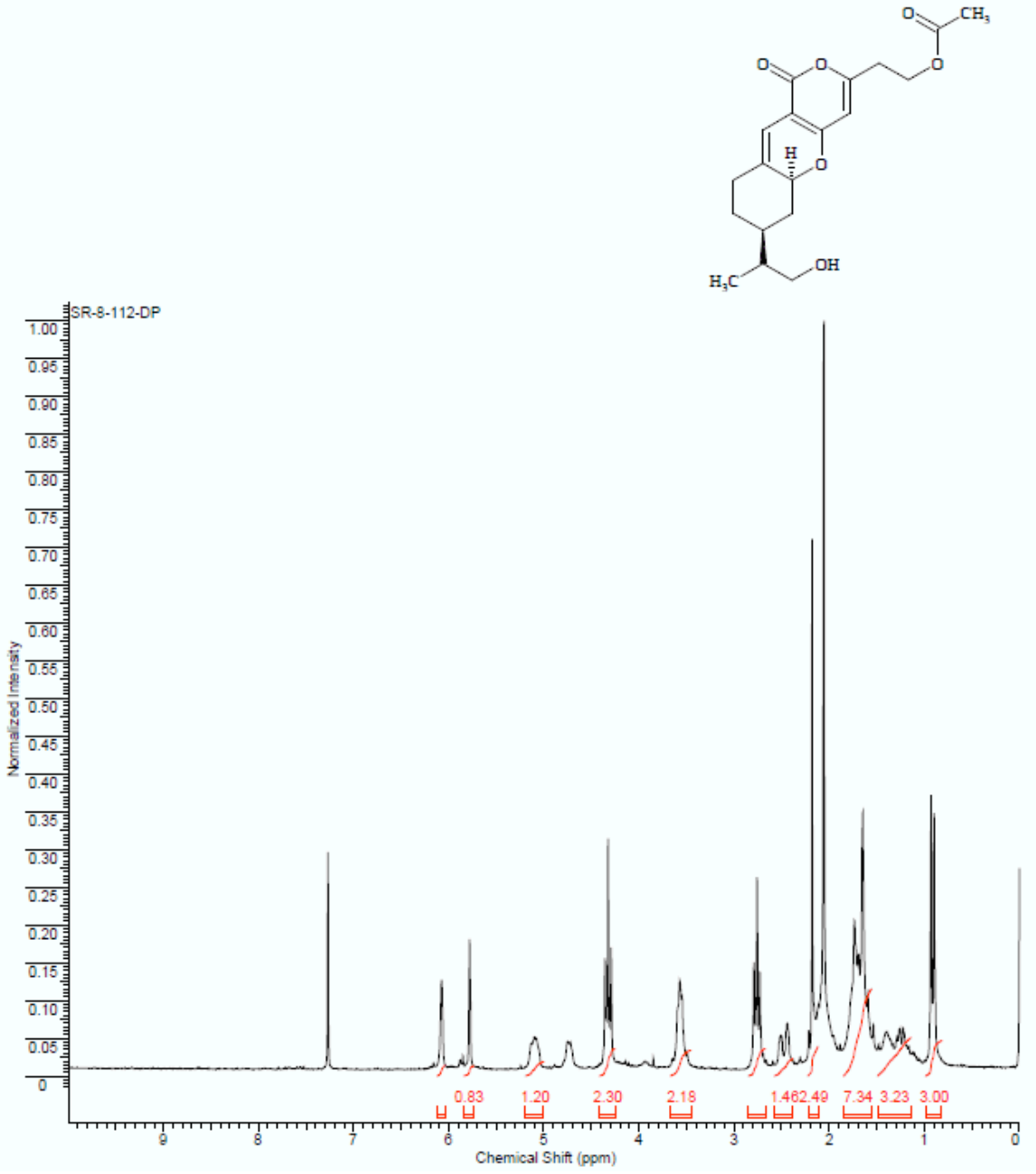

Formula $C_{15}H_{26}O_6$	FW	350.4061

Acquisition Time (sec)	1.3005	Comment	Std proton	Date	Feb 25 2008
Date Stamp	Feb 25 2008				
File Name	C:\NMR BACKUP\010609NMR BACKUP\400\SRANA\SRANA\SR-7-88-FR14-13C				
Frequency (MHz)	100.53	Nucleus	13C	Number of Transients	2000
Original Points Count	31375	Points Count	32768	Pulse Sequence	s2pul
Receiver Gain	30.00	Solvent	CHLOROFORM-d		
Spectrum Offset (Hz)	10549.7627	Sweep Width (Hz)	24125.45	Temperature (degree C)	25.000

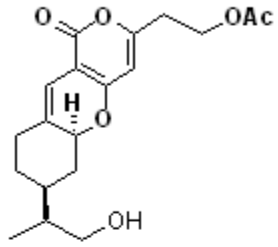

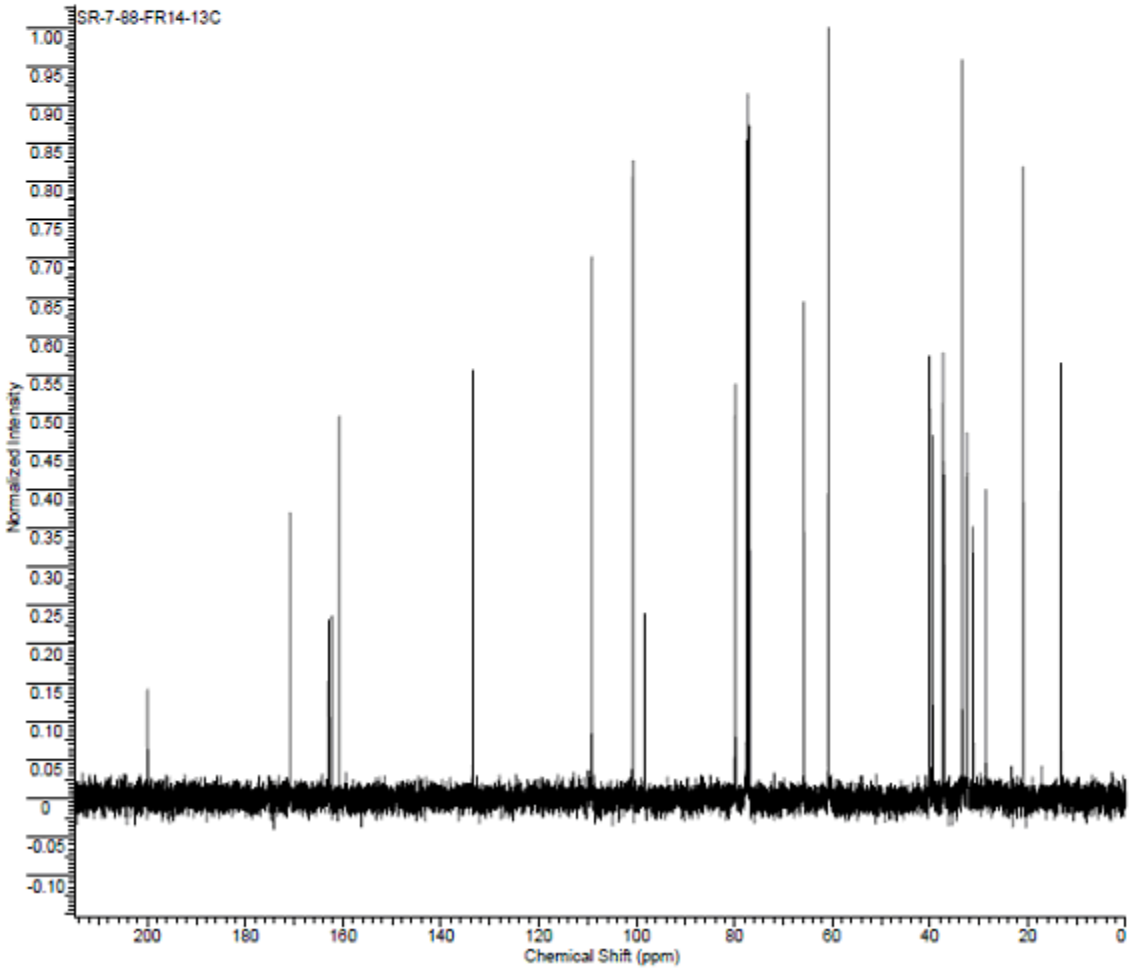

Formula $C_{19}H_{24}NO_7S$?	FW	332.4140+?		

Acquisition Time (sec)	1.9945	Comment	STANDARD 1H OBSERVE		
Date	Jun 5 2008	Date Stamp	Jun 5 2008		
File Name	C:\NMR BACKUP\010609NMR BACKUP\200\HUA-NEW\SANDEEP\BOOK8\SR-8-54-DP				
Frequency (MHz)	199.98	Nucleus	1H	Number of Transients	32
Original Points Count	5984	Points Count	8192	Pulse Sequence	s2pul
Receiver Gain	39.00	Solvent	CHLOROFORM-d		
Spectrum Offset (Hz)	1003.1215	Sweep Width (Hz)	3000.30	Temperature (degree C)	29.000

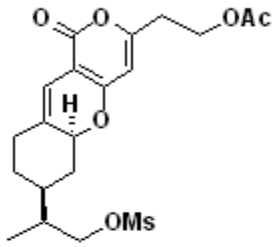

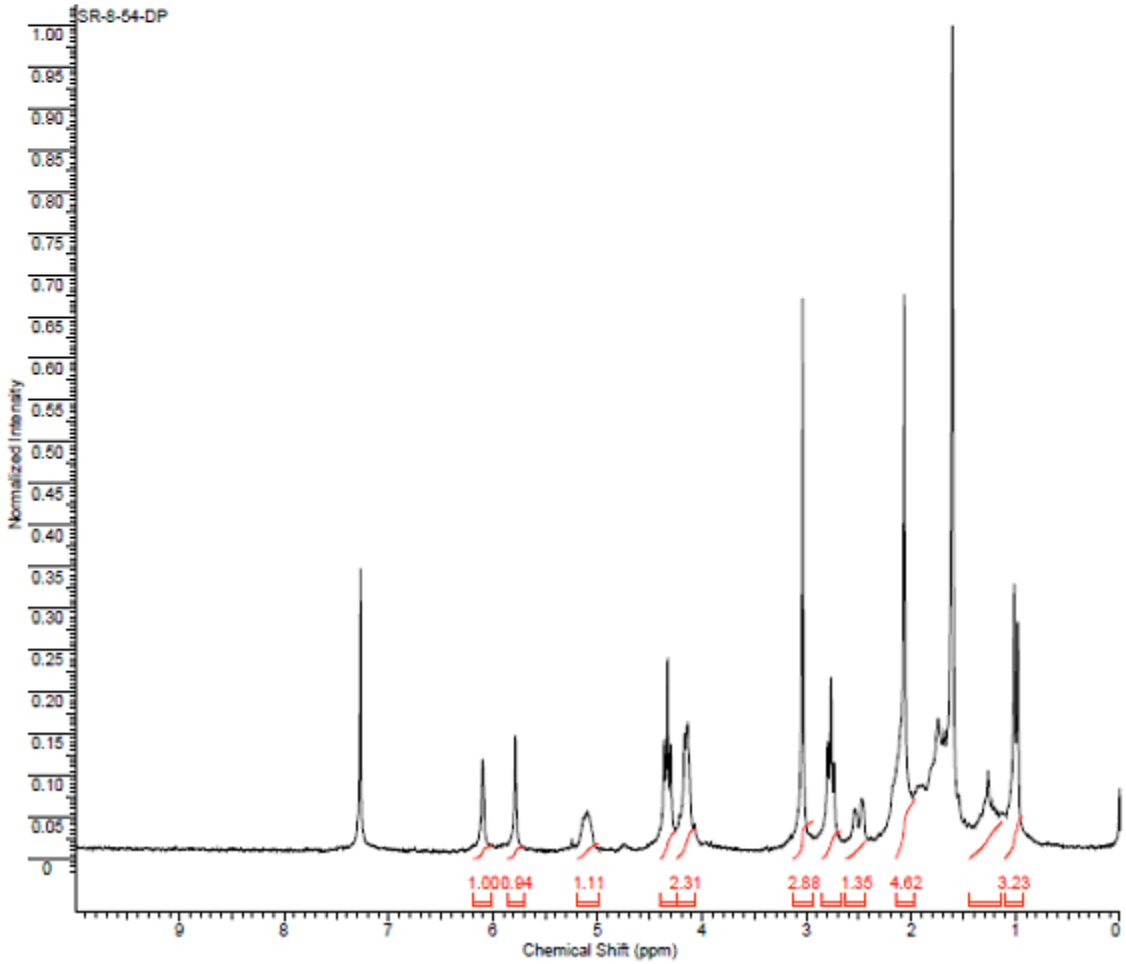

Formula $C_{24}H_{27}N_5O_6$	FW	465.5017

Acquisition Time (sec)	1.9945	Comment	STANDARD 1H OBSERVE		
Date	Apr 28 2008	Date Stamp	Apr 28 2008		
File Name	C:\NMR BACKUP\010609NMR BACKUP\200\HUA-NEW\SANDEEP\BOOK8\SR-8-TP4				
Frequency (MHz)	199.98	Nucleus	1H	Number of Transients	100
Original Points Count	5984	Points Count	8192	Pulse Sequence	s2pul
Receiver Gain	40.00	Solvent	CHLOROFORM-d		
Spectrum Offset (Hz)	1000.9237	Sweep Width (Hz)	3000.30	Temperature (degree C)	29.000

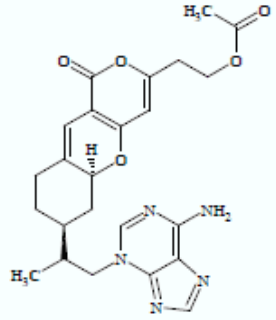

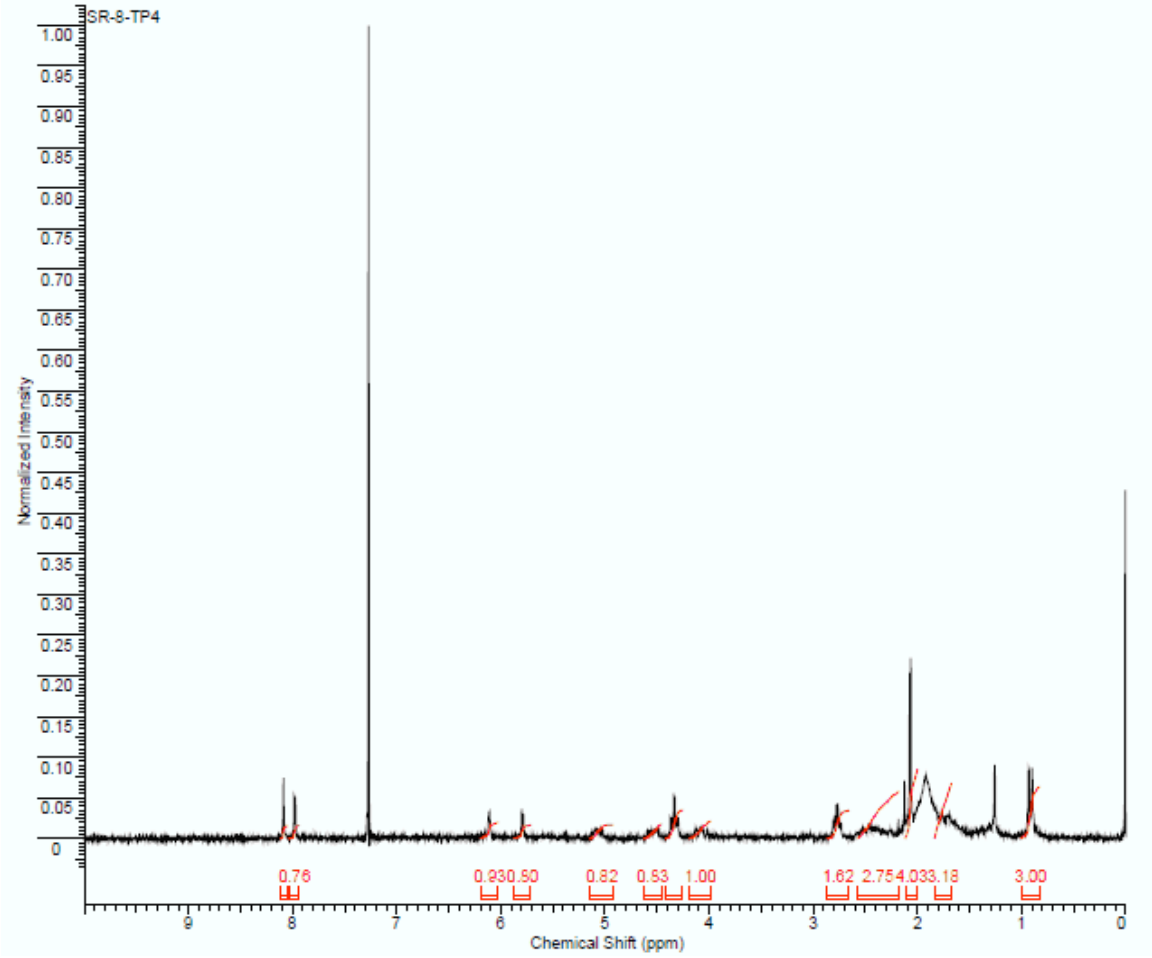

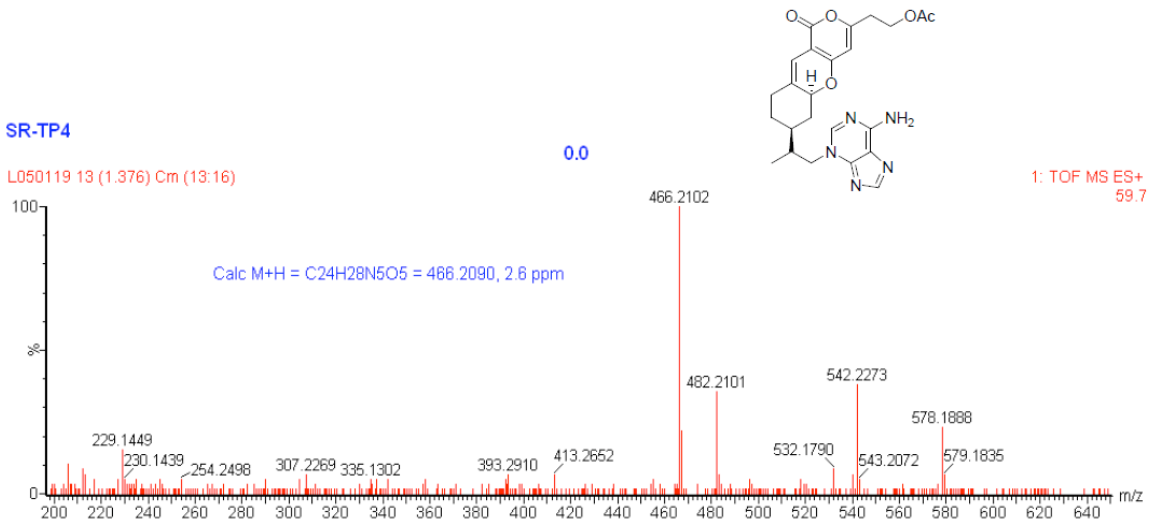
SR-TP4
0.0
L050119 13 (1.376) Cm (13:16)
1: TOF MS ES+
59.7
Calc M+H = C24H28N5O5 = 466.2090, 2.6 ppm
466.2102
482.2101
542.2273
578.1888
229.1449
230.1439
254.2498
307.2269
335.1302
393.2910
413.2652
532.1790
543.2072
579.1835
100
%
0
m/z
200 220 240 260 280 300 320 340 360 380 400 420 440 460 480 500 520 540 560 580 600 620 640

Formula $C_{19}H_{22}O_6$	FW	318.3643

Acquisition Time (sec)	2.0486	*Comment*	Std proton	*Date*	Sep 30 2008
Date Stamp	Sep 30 2008	*File Name*	C:\NMR 031009\400\SRANA\SR-9-21-RECOLUMN-FR23		
Frequency (MHz)	399.76	*Nucleus*	1H	*Number of Transients*	32
Original Points Count	9827	*Points Count*	16384	*Pulse Sequence*	s2pul
Receiver Gain	38.00	*Solvent*	CHLOROFORM-d		
Spectrum Offset (Hz)	2015.1156	*Sweep Width (Hz)*	4797.03	*Temperature (degree C)*	25.000

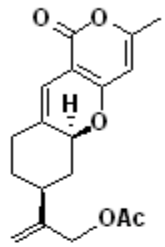

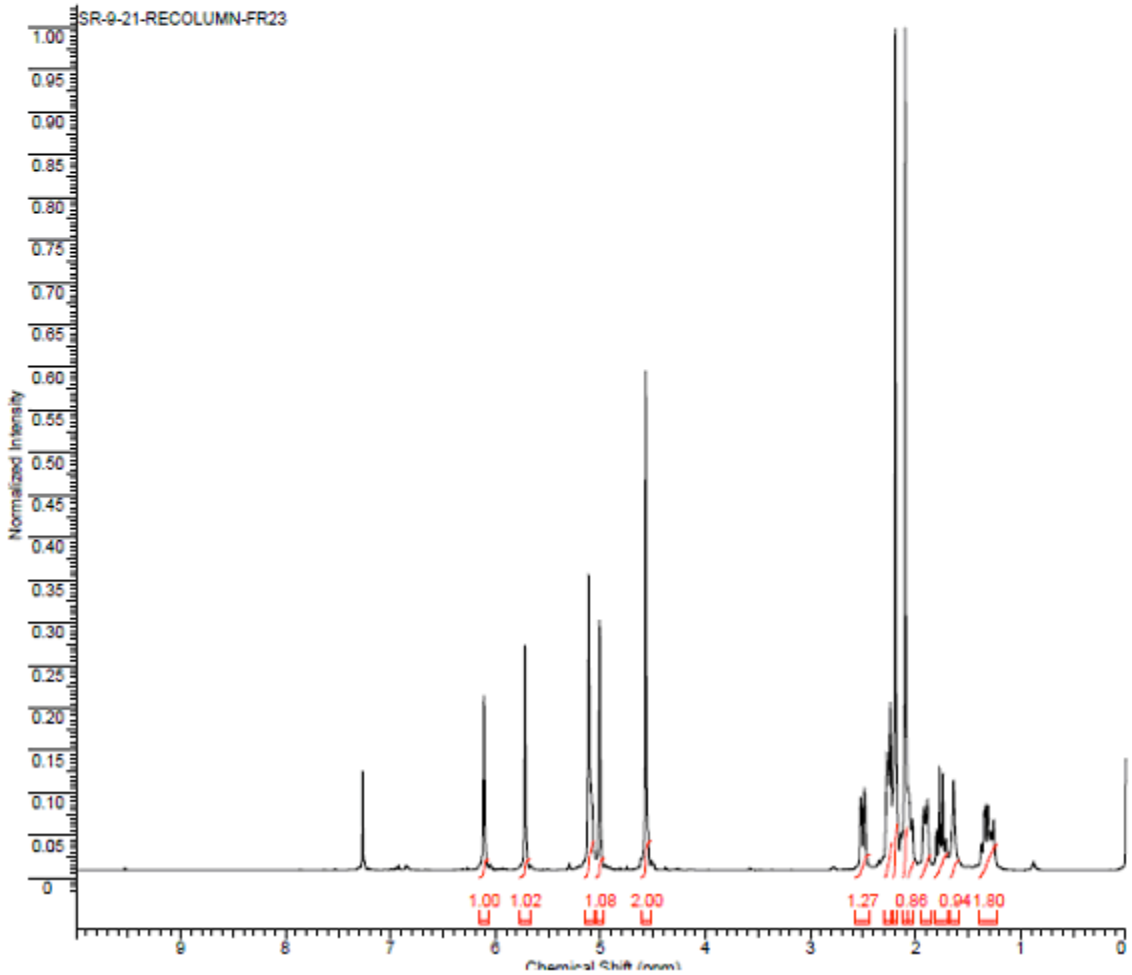

Formula $C_{19}H_{30}O_4$	FW	314.3756

Acquisition Time (sec)	1.3005	Comment	Std proton	Date	Sep 30 2008
Date Stamp	Sep 30 2008			File Name	C:\SANDEEP NMR\SR-9-21-FR23-13C
Frequency (MHz)	100.53	Nucleus	13C	Number of Transients	20000
Original Points Count	31375	Points Count	32768	Pulse Sequence	s2pul
Receiver Gain	30.00	Solvent	CHLOROFORM-d		
Spectrum Offset (Hz)	10556.2627	Sweep Width (Hz)	24125.45	Temperature (degree C)	25.000

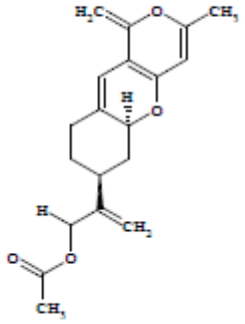

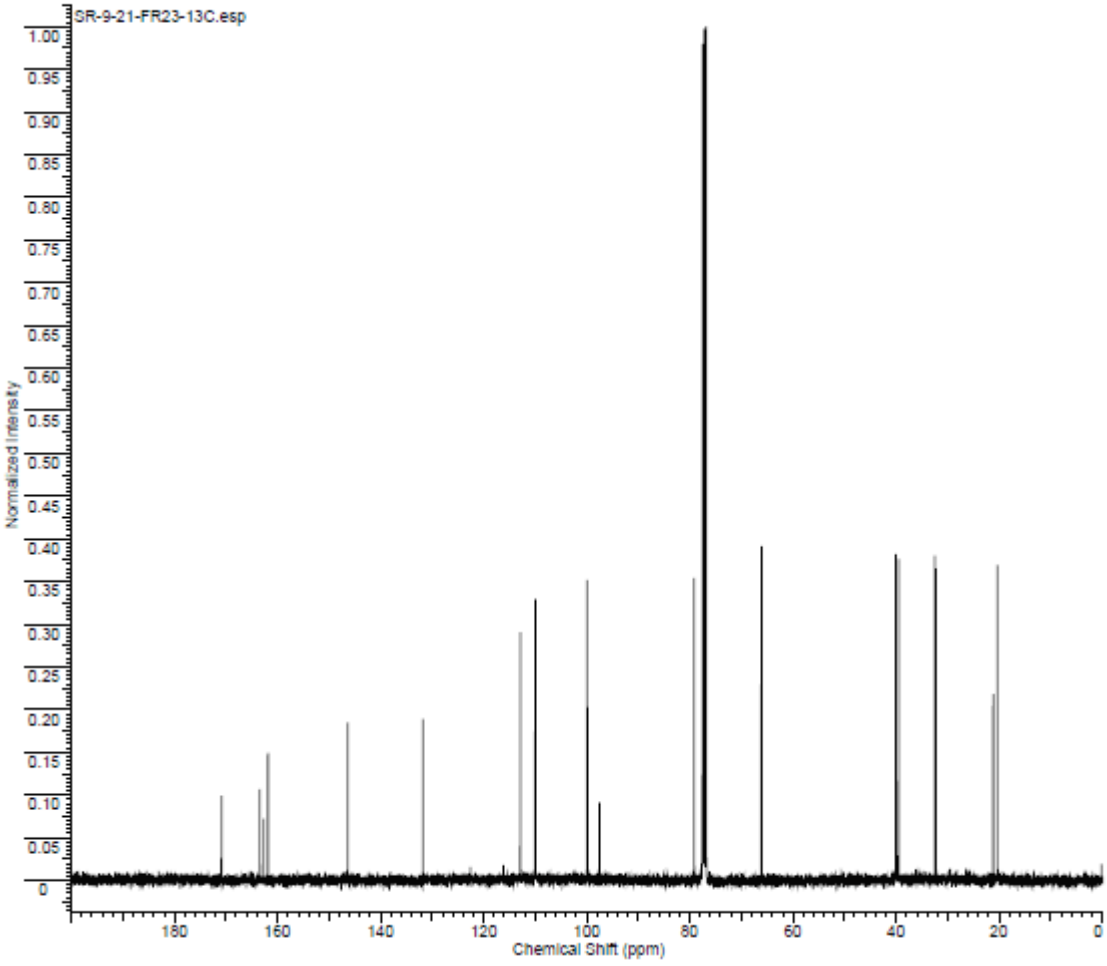

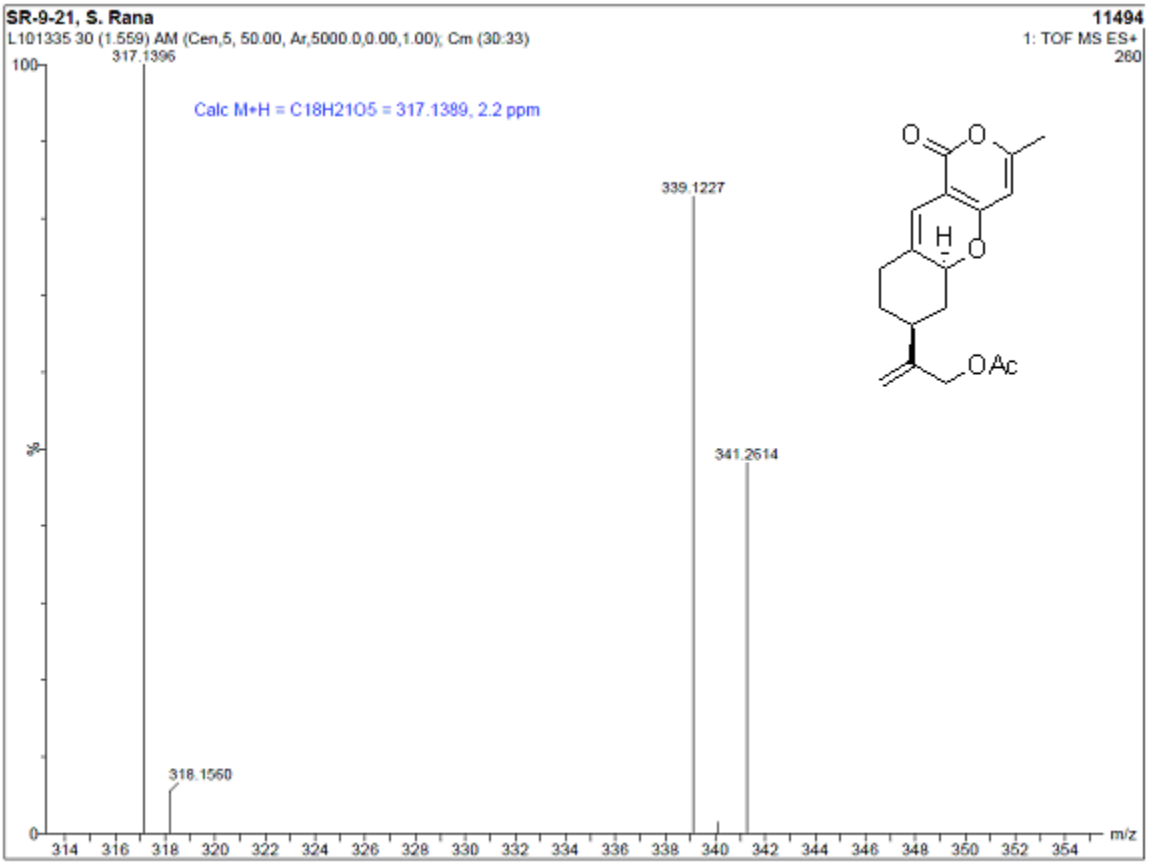
SR-9-21, S. Rana
11494
L101335 30 (1.559) AM (Cen,5, 50.00, Ar,5000.0,0.00,1.00); Cm (30:33)
1: TOF MS ES+
260
317.1396
Calc M+H = C18H21O5 = 317.1389, 2.2 ppm
339.1227
341.2614
318.1560
100
%
0
m/z
314 316 318 320 322 324 326 328 330 332 334 336 338 340 342 344 346 348 350 352 354
O
O
H
O
OAc

Formula $C_{17}H_{20}O_3$	FW	272.3389

Acquisition Time (sec)	1.3005	Comment	Std proton	Date	Jul 3 2008
Date Stamp	Jul 3 2008	File Name	C:\SANDEEP NMR\SR-8-73-FR22-13C		
Frequency (MHz)	100.53	Nucleus	13C	Number of Transients	15000
Original Points Count	31375	Points Count	32768	Pulse Sequence	s2pul
Receiver Gain	30.00	Solvent	CHLOROFORM-d		
Spectrum Offset (Hz)	10545.9541	Sweep Width (Hz)	24125.45	Temperature (degree C)	25.000

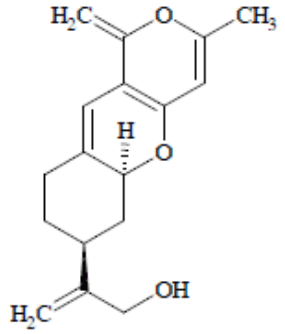

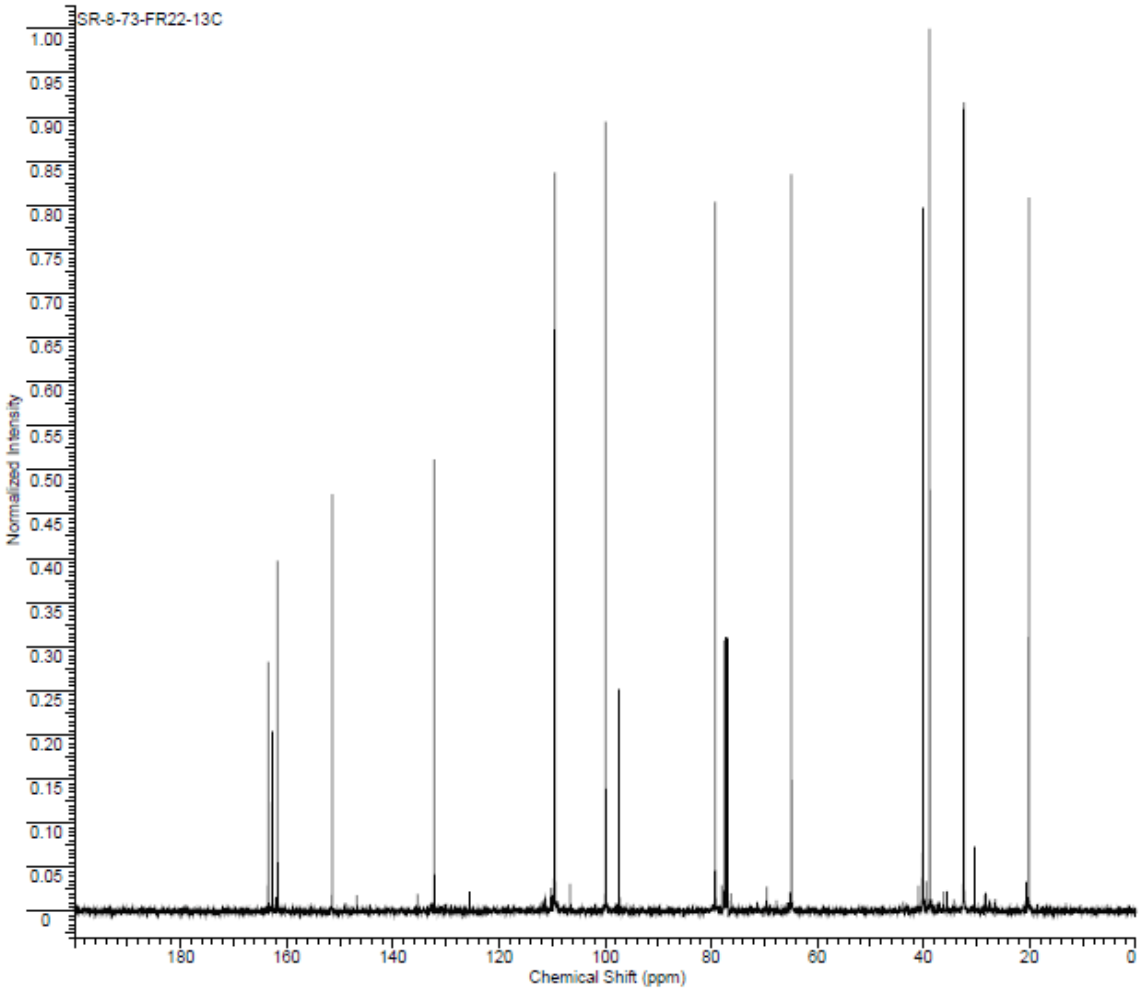

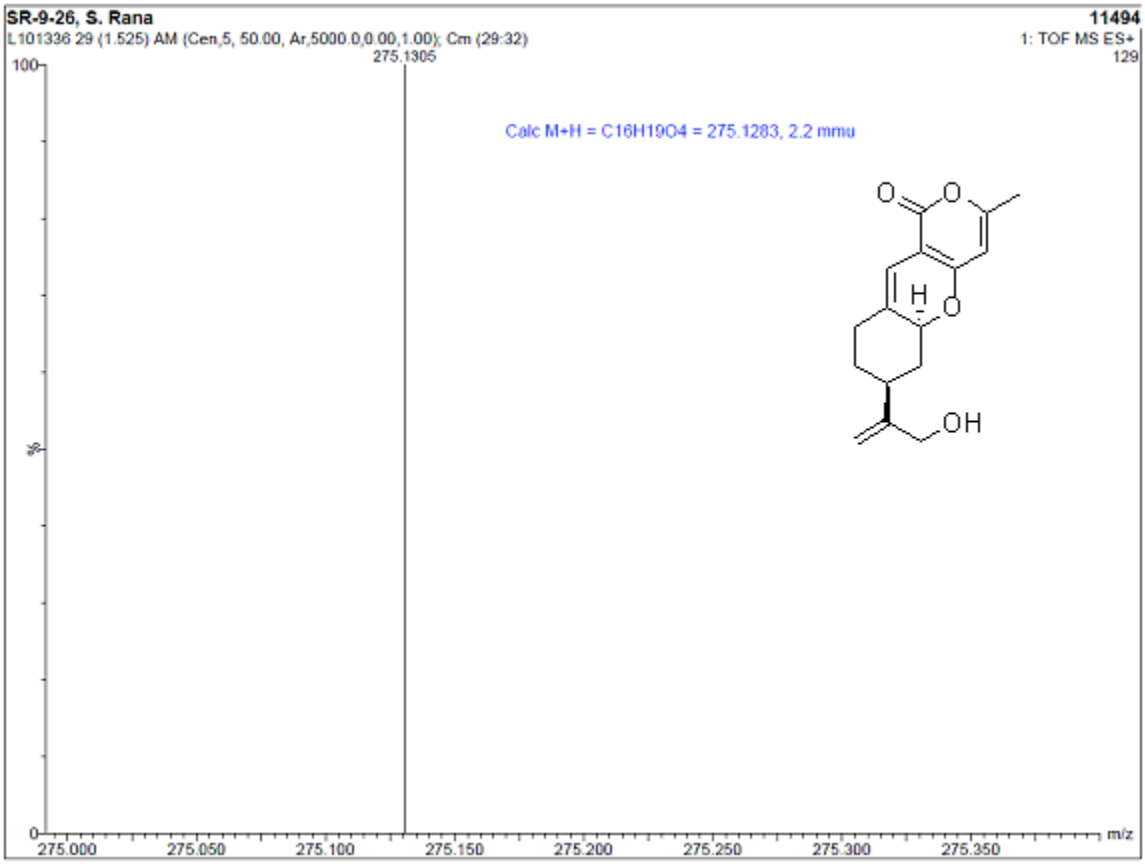
SR-9-26, S. Rana
11494
L101336 29 (1.525) AM (Cen,5, 50.00, Ar,5000.0,0.00,1.00); Cm (29:32)
1: TOF MS ES+
275.1305
129
100
%
0
Calc M+H = C16H19O4 = 275.1283, 2.2 mmu
O
O
H
O
OH
275.000
275.050
275.100
275.150
275.200
275.250
275.300
275.350
m/z

Formula $C_{17}H_{18}O_3$?	FW	255.3316+?

Acquisition Time (sec)	2.0486	Comment	Std proton	Date	Jul 8 2008
Date Stamp	Jul 8 2008	File Name	C:\SANDEEP NMR\SR-8-79-FR27		
Frequency (MHz)	399.76	Nucleus	1H	Number of Transients	32
Original Points Count	9827	Points Count	16384	Pulse Sequence	s2pul
Receiver Gain	30.00	Solvent	CHLOROFORM-d		
Spectrum Offset (Hz)	2016.8724	Sweep Width (Hz)	4797.03	Temperature (degree C)	25.000

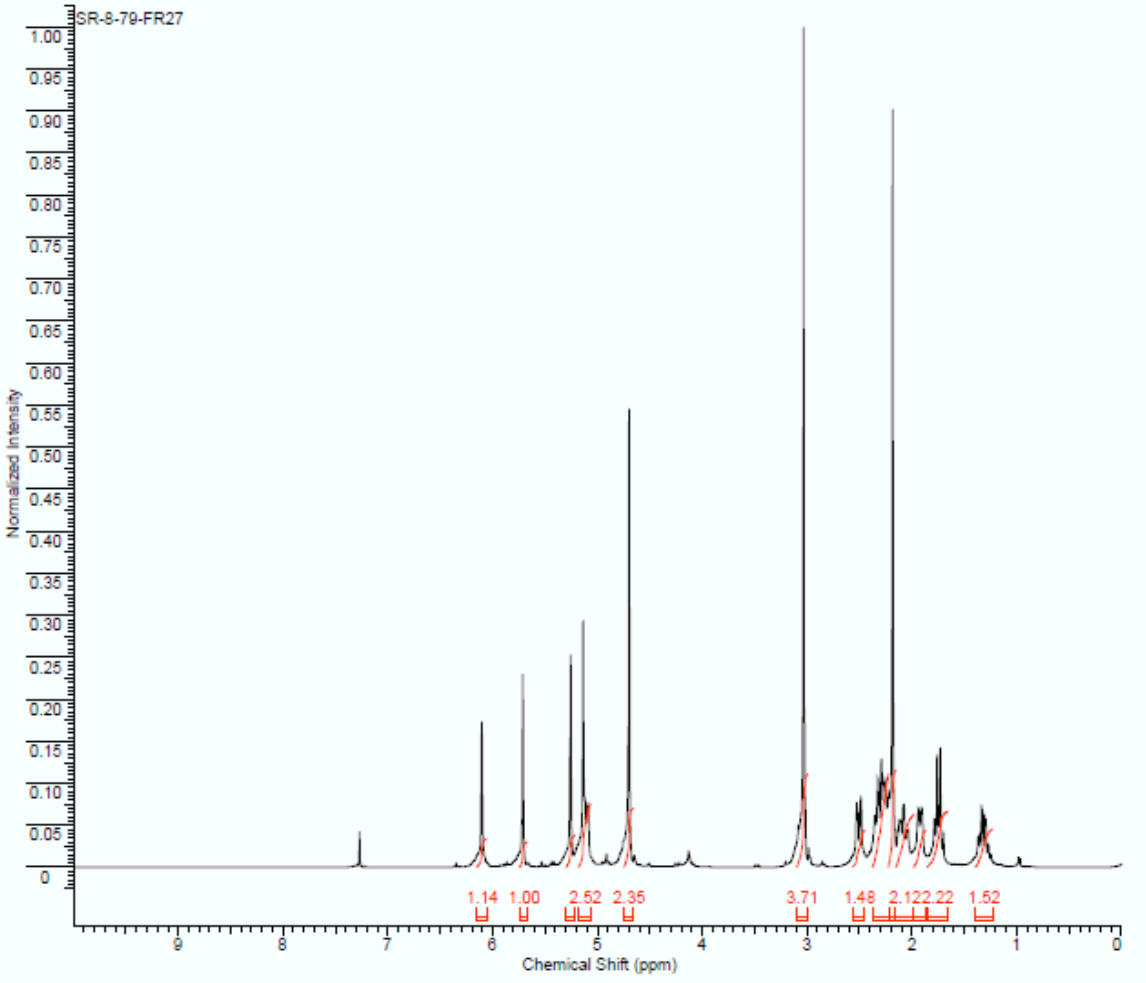

Formula $C_{17}H_{18}O_3$?	FW	255.3316+?

Acquisition Time (sec)	1.3005	Comment	Std proton	Date	Jul 8 2008
Date Stamp	Jul 8 2008	File Name	C:\SANDEEP NMR\SR-8-79-FR27-13C		
Frequency (MHz)	100.53	Nucleus	13C	Number of Transients	2000
Original Points Count	31375	Points Count	32768	Pulse Sequence	s2pul
Receiver Gain	30.00	Solvent	CHLOROFORM-d		
Spectrum Offset (Hz)	10552.5811	Sweep Width (Hz)	24125.45	Temperature (degree C)	25.000

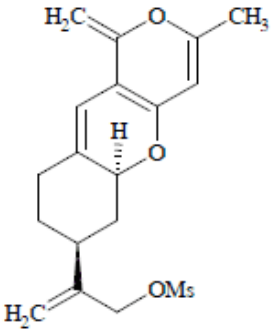

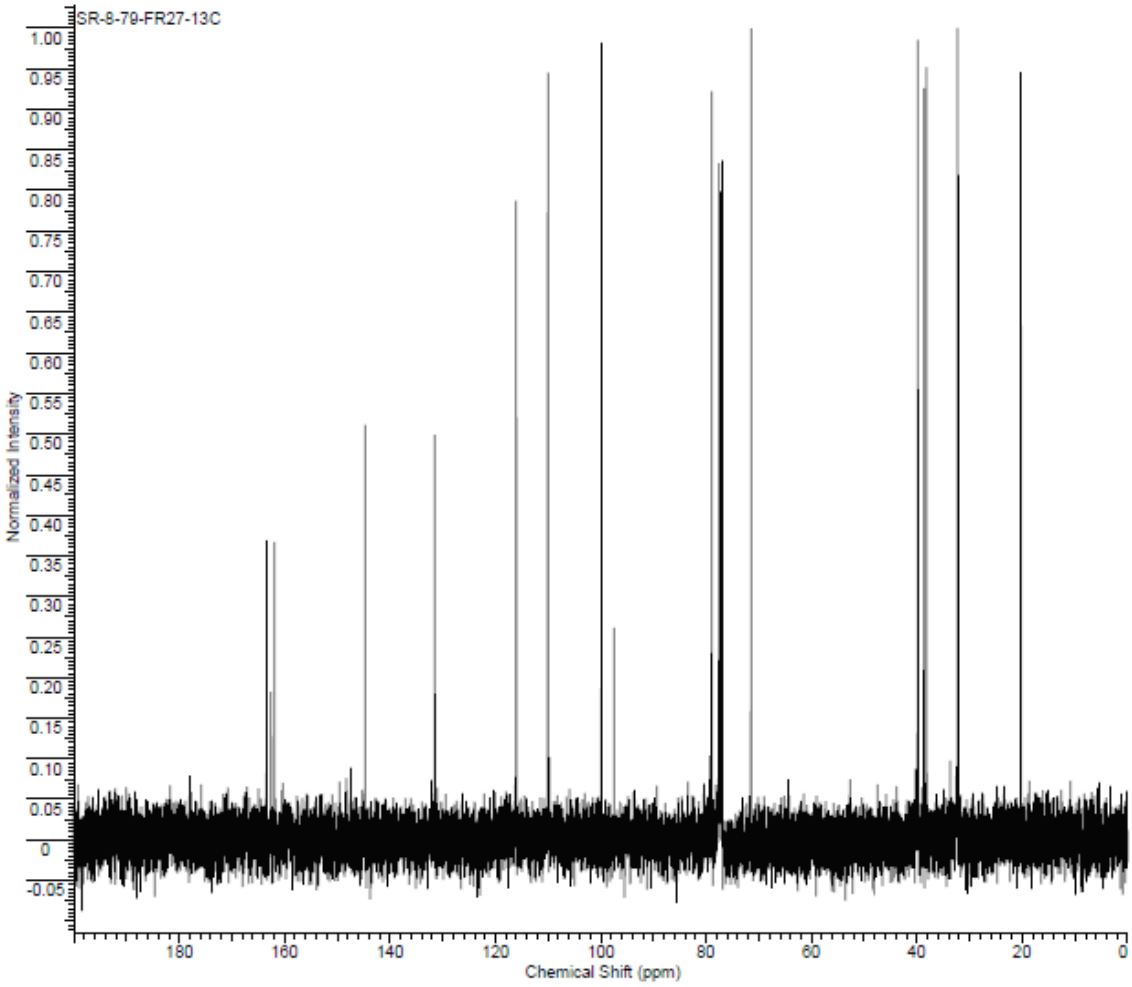

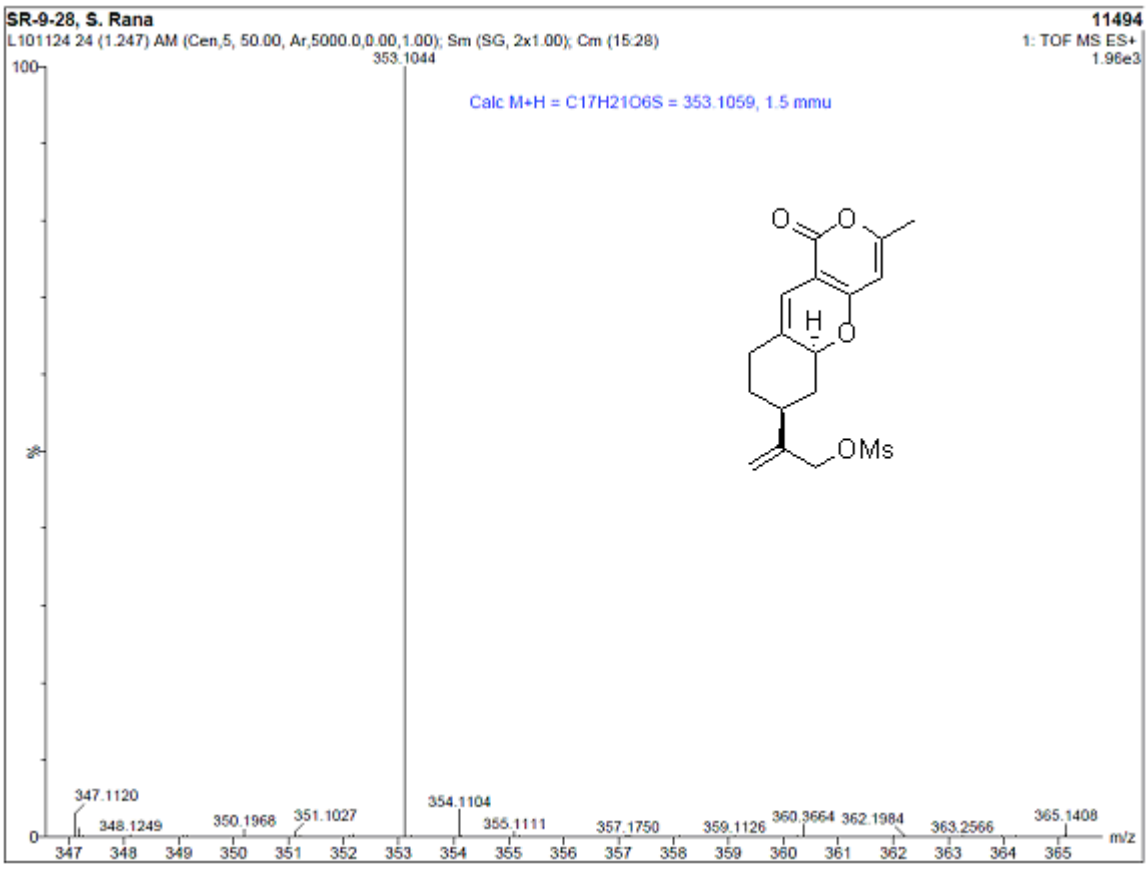
SR-9-28, S. Rana
11494
L101124 24 (1.247) AM (Cen,5, 50.00, Ar,5000.0,0.00,1.00); Sm (SG, 2x1.00); Cm (15:28)
1: TOF MS ES+
1.96e3
353.1044
Calc M+H = C17H21O6S = 353.1059, 1.5 mmu
OMs
100
%
0
347.1120
348.1249
350.1968
351.1027
354.1104
355.1111
357.1750
359.1126
360.3664
362.1984
363.2566
365.1408
347 348 349 350 351 352 353 354 355 356 357 358 359 360 361 362 363 364 365
m/z

Formula $C_{20}H_{28}N_6O_3$	FW	389.4503

Acquisition Time (sec)	2.0486	Comment	SR-8-82-dp		
Date	Jul 17 2008			Date Stamp	Jul 17 2008
File Name	C:\SANDEEP NMR\SR-8-82-DP			Frequency (MHz)	399.76
Nucleus	1H	Number of Transients	64	Original Points Count	9627
Points Count	16384	Pulse Sequence	s2pul	Receiver Gain	50.00
Solvent	CHLOROFORM-d			Spectrum Offset (Hz)	2016.2867
Sweep Width (Hz)	4797.03	Temperature (degree C)	25.000		

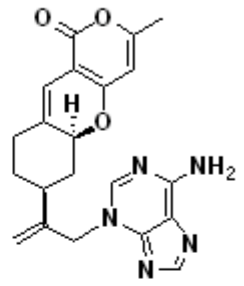

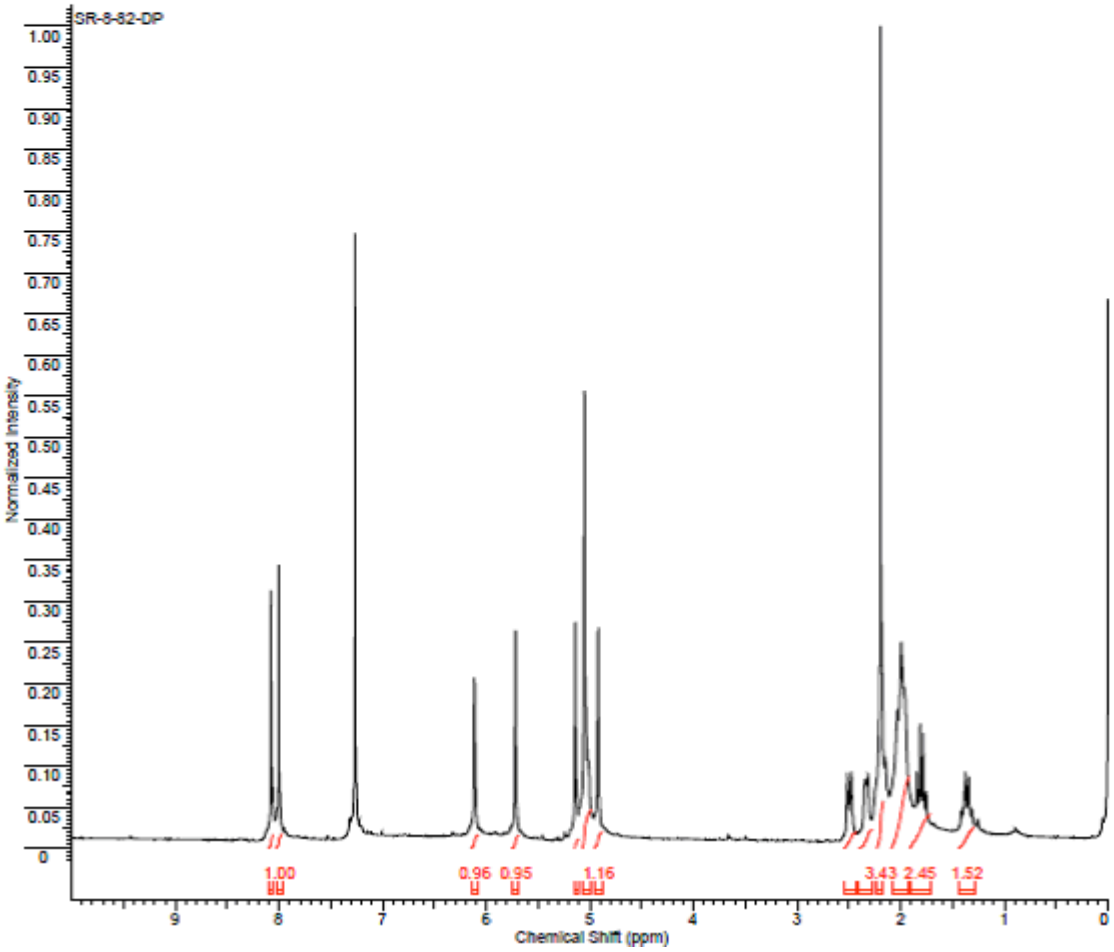

Formula $C_{20}H_{23}N_5O_5$	FW	389.4503

Acquisition Time (sec)	1.3005	Comment	SR-8-82-fr14-13C		
Date	Jul 19 2008	Date Stamp	Jul 19 2008	File Name	C:\SANDEEP NMR\SR-8-82-FR14-13C
Frequency (MHz)	100.53	Nucleus	13C	Number of Transients	20000
Original Points Count	31375	Points Count	32768	Pulse Sequence	s2pul
Receiver Gain	30.00	Solvent	CHLOROFORM-d		
Spectrum Offset (Hz)	10556.2627	Sweep Width (Hz)	24125.45	Temperature (degree C)	25.000

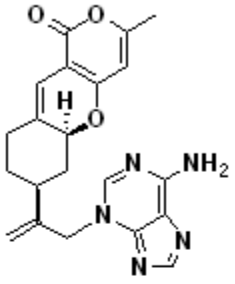

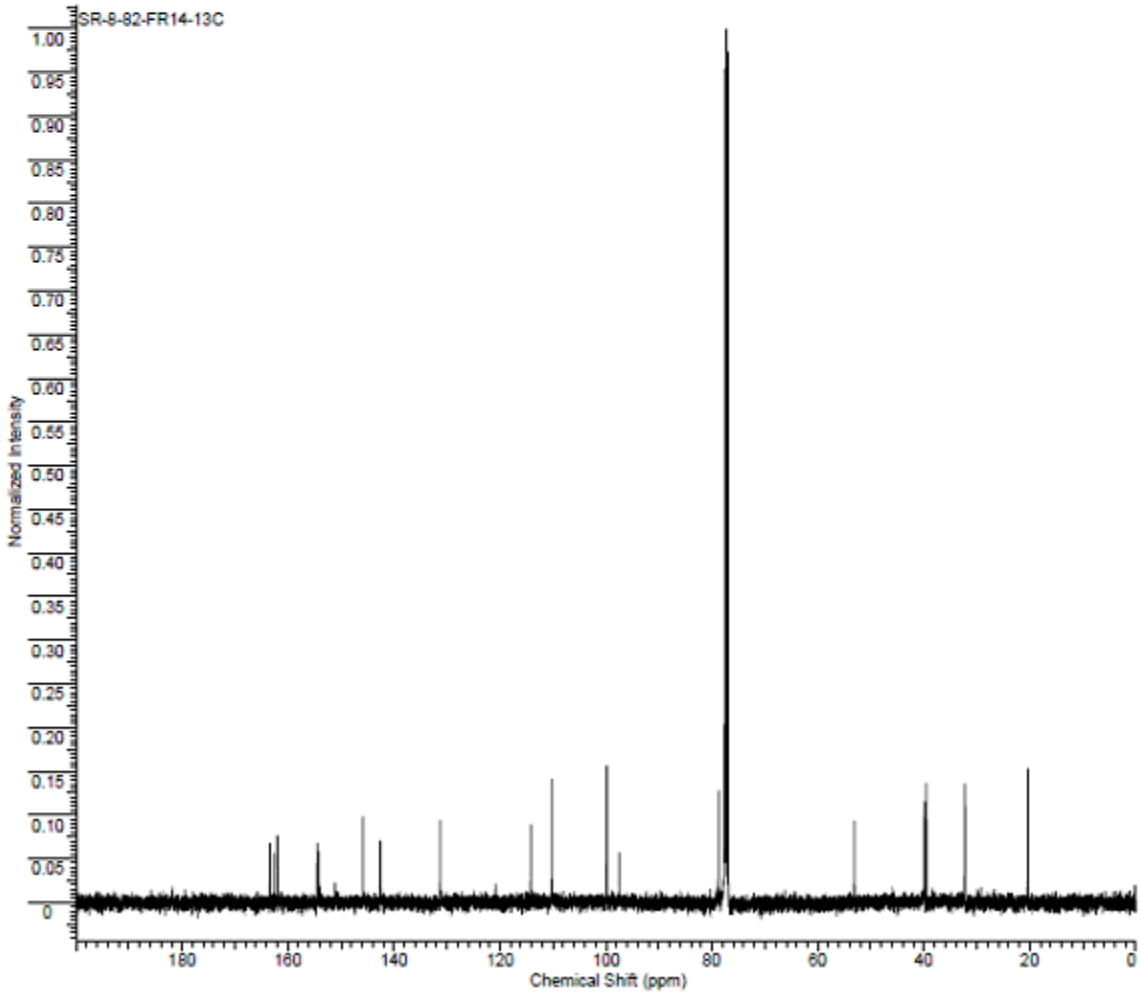

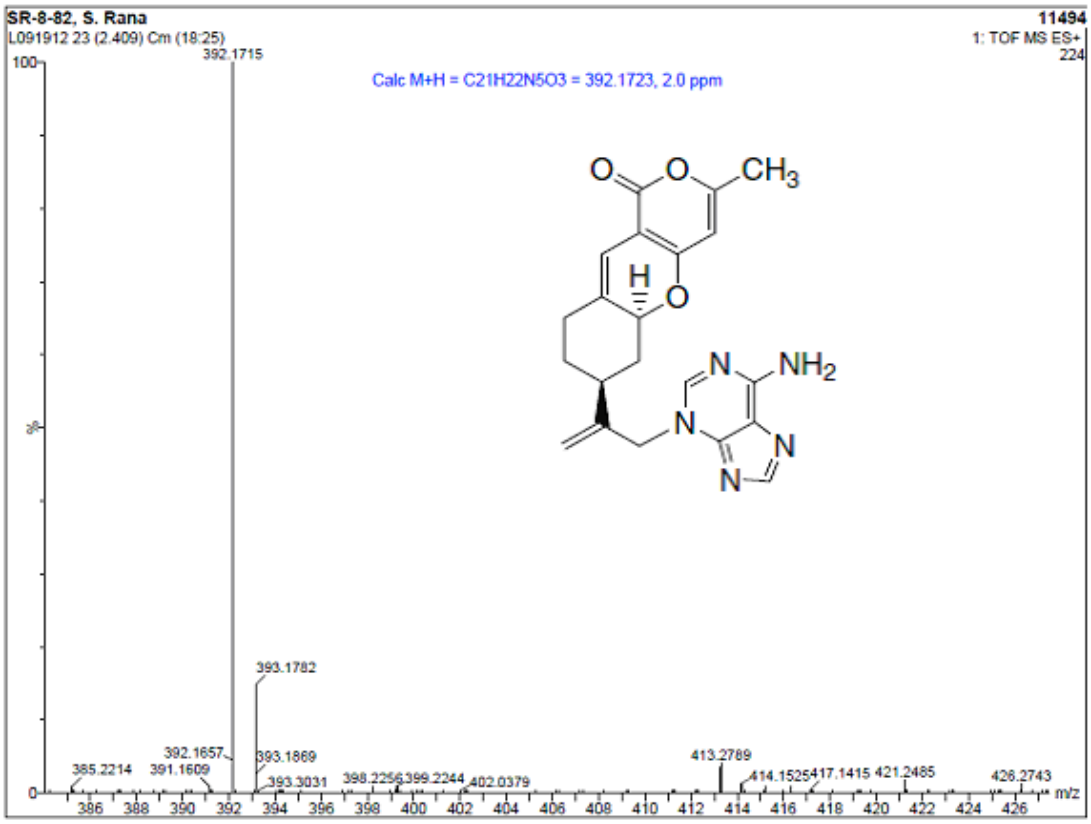
SR-8-82, S. Rana
11494
L091912 23 (2.409) Cm (18:25)
1: TOF MS ES+
224
392.1715
Calc M+H = C21H22N5O3 = 392.1723, 2.0 ppm
100
%
0
393.1782
392.1657
393.1869
385.2214
391.1609
393.3031
398.2256
399.2244
402.0379
413.2789
414.1525
417.1415
421.2485
426.2743
386 388 390 392 394 396 398 400 402 404 406 408 410 412 414 416 418 420 422 424 426
m/z

Formula $C_{15}H_{21}BrO_3$	FW	337.2514

Acquisition Time (sec)	2.0486	Comment	Std proton	Date	Jan 12 2008
Date Stamp	Jan 12 2008			File Name	C:\SANDEEP NMR\1 SR-TPBROMIDE
Frequency (MHz)	399.77	Nucleus	1H	Number of Transients	8
Original Points Count	13104	Points Count	16384	Pulse Sequence	s2pul
Receiver Gain	42.00	Solvent	CHLOROFORM-d		
Spectrum Offset (Hz)	2408.5327	Sweep Width (Hz)	6396.42	Temperature (degree C)	25.000

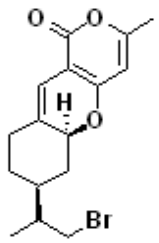

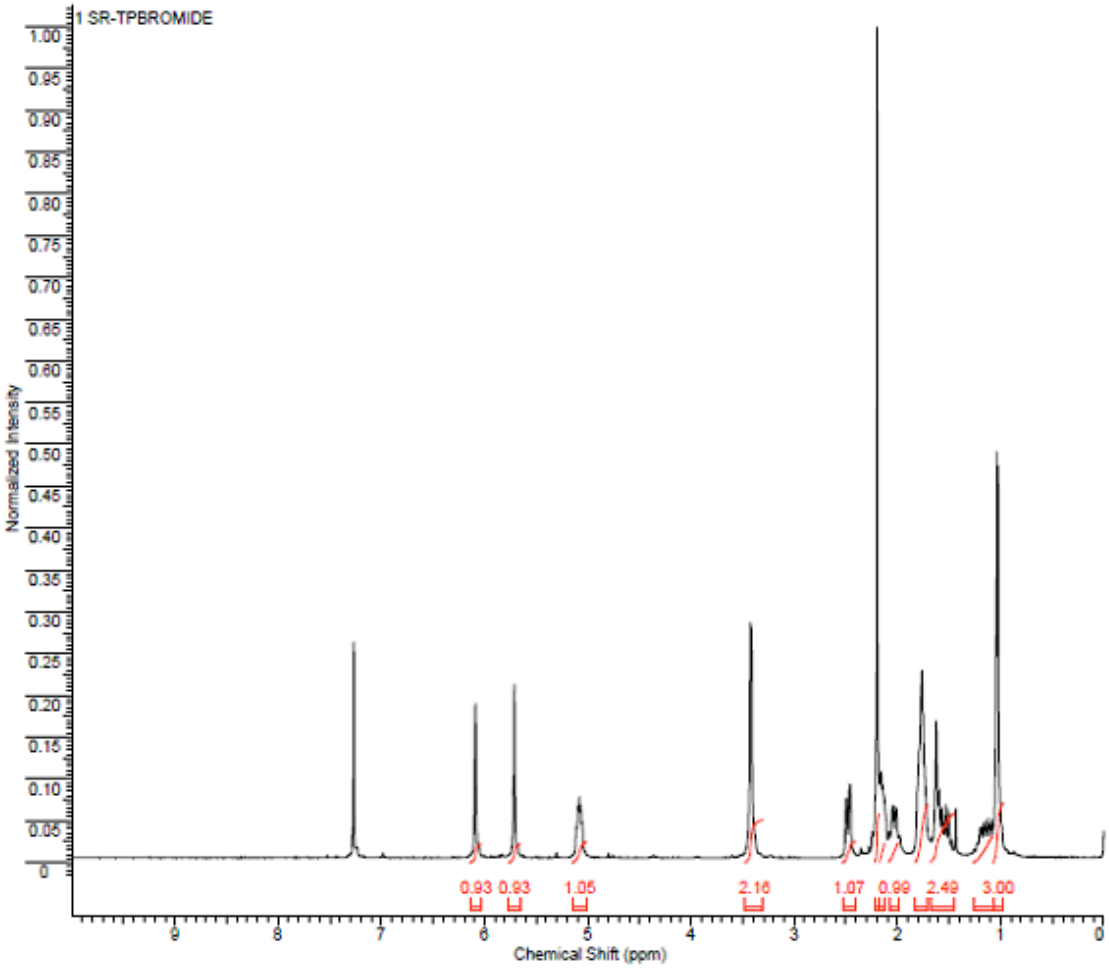

Formula $C_{17}H_{21}BrO_3$	FW	337.2514

Acquisition Time (sec)	1.3005	Comment	Std proton	Date	Jan 12 2008
Date Stamp	Jan 12 2008	File Name	C:\SANDEEP NMR\SR-TPBROMIDE-13C		
Frequency (MHz)	100.53	Nucleus	13C	Number of Transients	10000
Original Points Count	31375	Points Count	32768	Pulse Sequence	s2pul
Receiver Gain	30.00	Solvent	CHLOROFORM-d		
Spectrum Offset (Hz)	10552.7070	Sweep Width (Hz)	24125.45	Temperature (degree C)	25.000

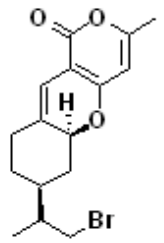

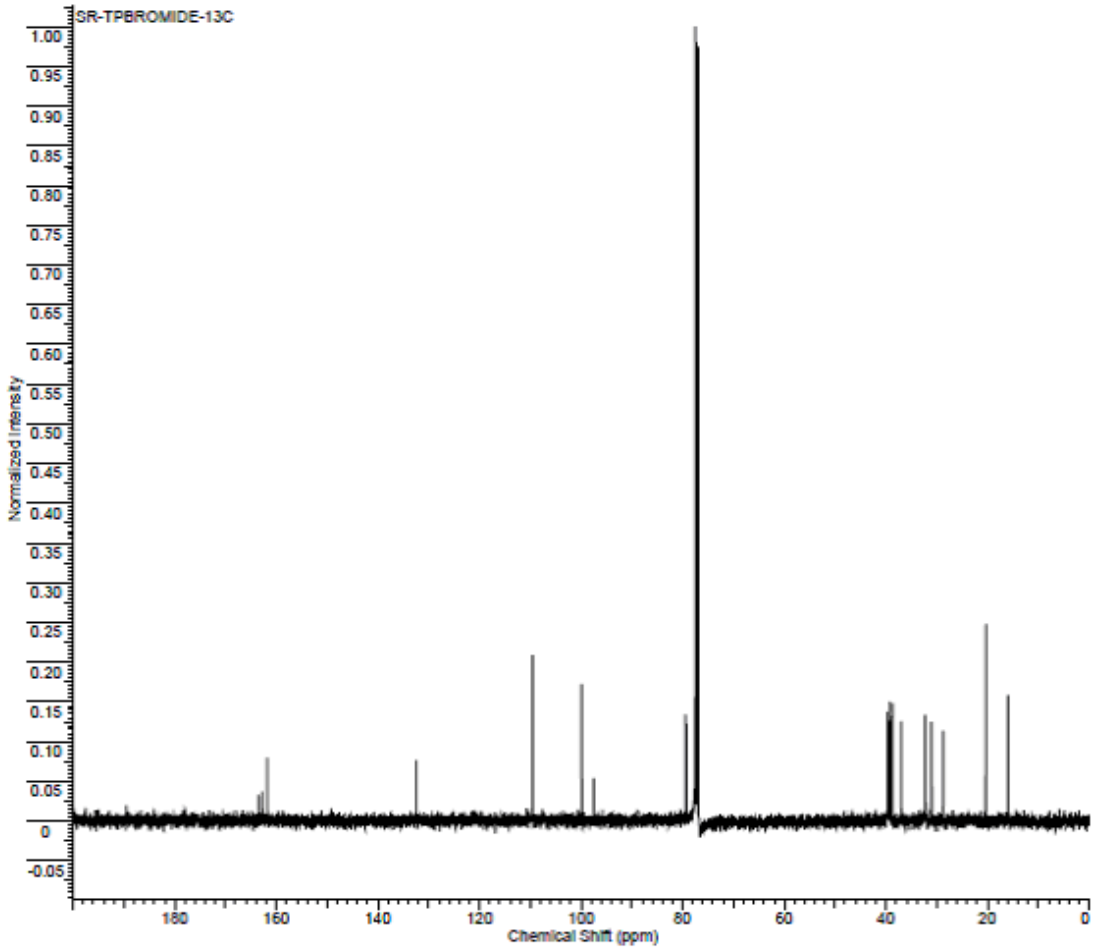

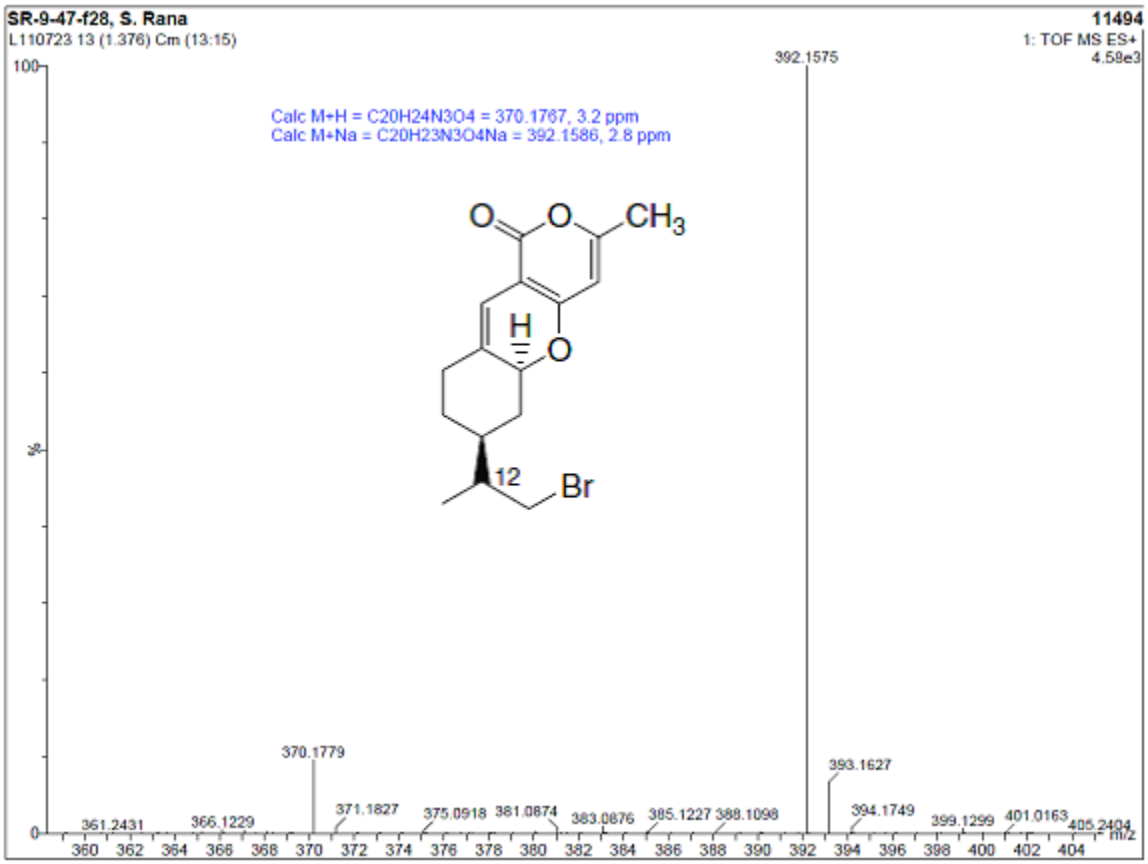
SR-9-47-f28, S. Rana
L110723 13 (1.376) Cm (13:15)
11494
1: TOF MS ES+
4.58e3
Calc M+H = C20H24N3O4 = 370.1767, 3.2 ppm
Calc M+Na = C20H23N3O4Na = 392.1586, 2.8 ppm
392.1575
370.1779
393.1627
361.2431
366.1229
371.1827
375.0918
381.0874
383.0876
385.1227
388.1098
394.1749
399.1299
401.0163
405.2404
m/z

Formula $C_{22}H_{20}ClN_5O_3$		FW	410.8966		
Acquisition Time (sec)	2.0486	Comment	Std proton	Date	Oct 2 2007
Date Stamp	Oct 2 2007			File Name	C:\SANDEEP NMR\SR-5-104-FR11
Frequency (MHz)	399.77	Nucleus	1H	Number of Transients	32
Original Points Count	9828	Points Count	16384	Pulse Sequence	s2pul
Receiver Gain	30.00	Solvent	CHLOROFORM-d		
Spectrum Offset (Hz)	2008.9603	Sweep Width (Hz)	4797.31	Temperature (degree C)	25.000

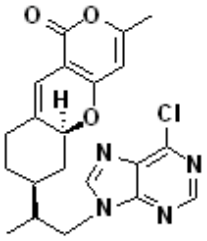

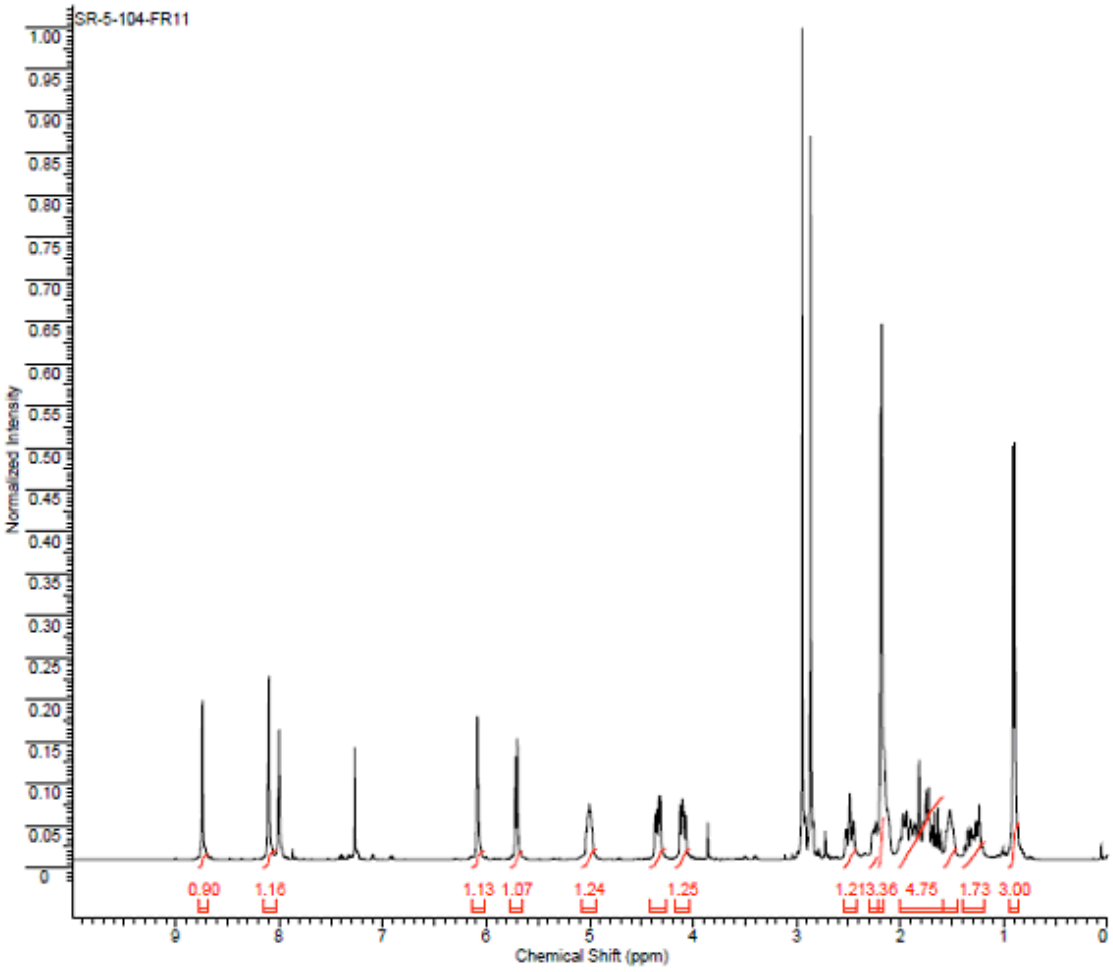

Formula $C_{20}H_{25}ClN_4O_5$		FW	412.9125		
Acquisition Time (sec)	1.3005	*Comment*	Std proton	*Date*	Oct 4 2007
Date Stamp	Oct 4 2007	*File Name*	C:\NMR 031009\400\SRANA\SR-5-104-FR11-TP7-13C		
Frequency (MHz)	100.53	*Nucleus*	13C	*Number of Transients*	10000
Original Points Count	31375	*Points Count*	32768	*Pulse Sequence*	s2pul
Receiver Gain	30.00	*Solvent*	CHLOROFORM-d		
Spectrum Offset (Hz)	10551.9717	*Sweep Width (Hz)*	24125.45	*Temperature (degree C)*	25.000

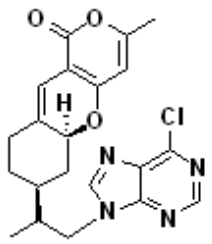

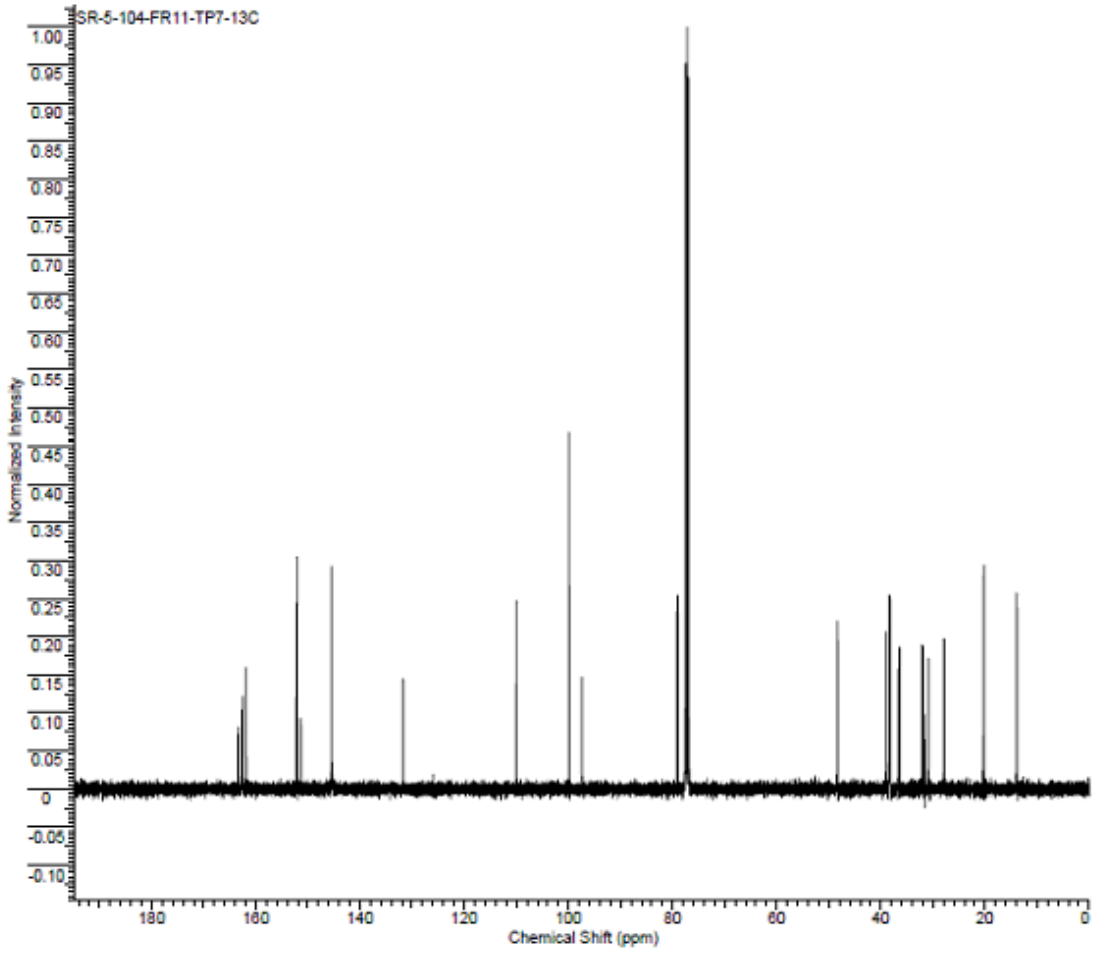

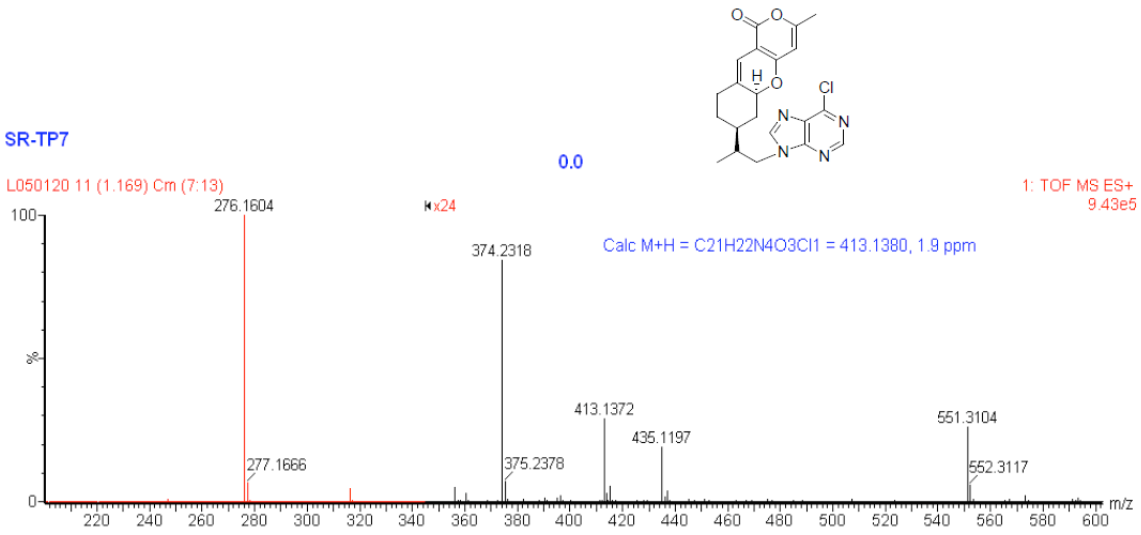
SR-TP7
0.0
L050120 11 (1.169) Cm (7:13)
1: TOF MS ES+
9.43e5
276.1604
x24
374.2318
Calc M+H = C21H22N4O3Cl1 = 413.1380, 1.9 ppm
413.1372
435.1197
551.3104
277.1666
375.2378
552.3117
100
%
0
220 240 260 280 300 320 340 360 380 400 420 440 460 480 500 520 540 560 580 600
m/z

Formula $C_{21}H_{25}N_3O_5$	FW	367.4415			
Acquisition Time (sec)	2.0487	Comment	Std proton	Date	Nov 5 2008
Date Stamp	Nov 5 2008				
File Name	C:\DOCUMENTS AND SETTINGS\DUY HUA\DESKTOP\SANDEEP\THESIS\NMR\NEW FOLDER\TP8AANDB\SR-9-47-FR28				
Frequency (MHz)	399.76	Nucleus	1H	Number of Transients	32
Original Points Count	13103	Points Count	16384	Pulse Sequence	s2pul
Receiver Gain	40.00	Solvent	CHLOROFORM-d	Spectrum Offset (Hz)	2416.1248
Sweep Width (Hz)	6395.91	Temperature (degree C)	25.000		

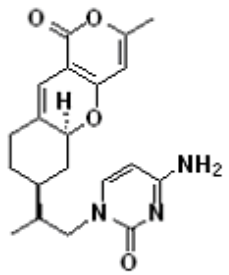

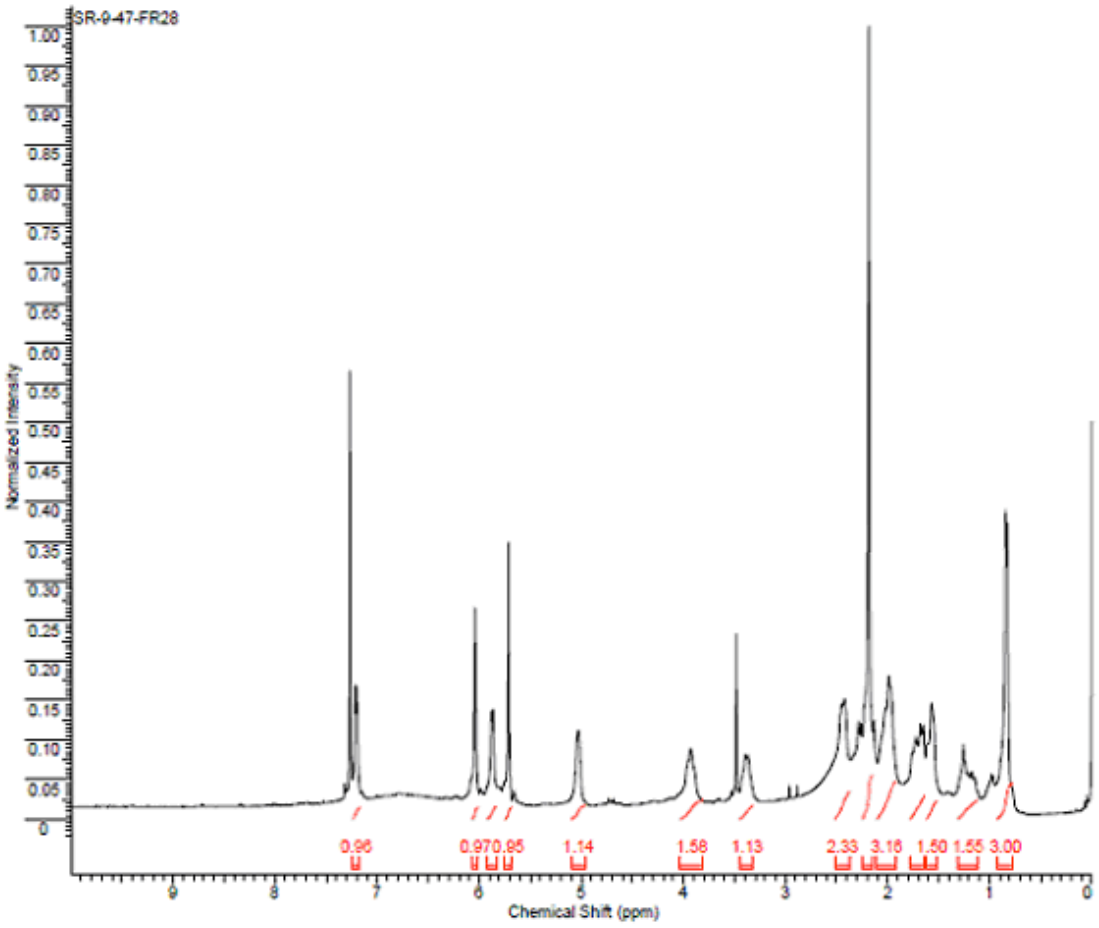

Formula $C_{20}H_{23}N_3O_5$	FW	369.4574

Acquisition Time (sec)	1.4976	Comment	13C OBSERVE	Date	Nov 5 2008
Date Stamp	Nov 5 2008				
File Name	C:\NMR BACKUP\010609NMR BACKUP\200\HUA-NEW\SANDEEP\BOOK 9\SR-9-47-FR28-13C				
Frequency (MHz)	50.29	Nucleus	13C	Number of Transients	100000000
Original Points Count	18720	Points Count	32768	Pulse Sequence	s2pul
Receiver Gain	40.00	Solvent	CHLOROFORM-d		
Spectrum Offset (Hz)	4878.9351	Sweep Width (Hz)	12500.00	Temperature (degree C)	29.000

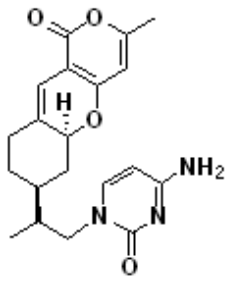

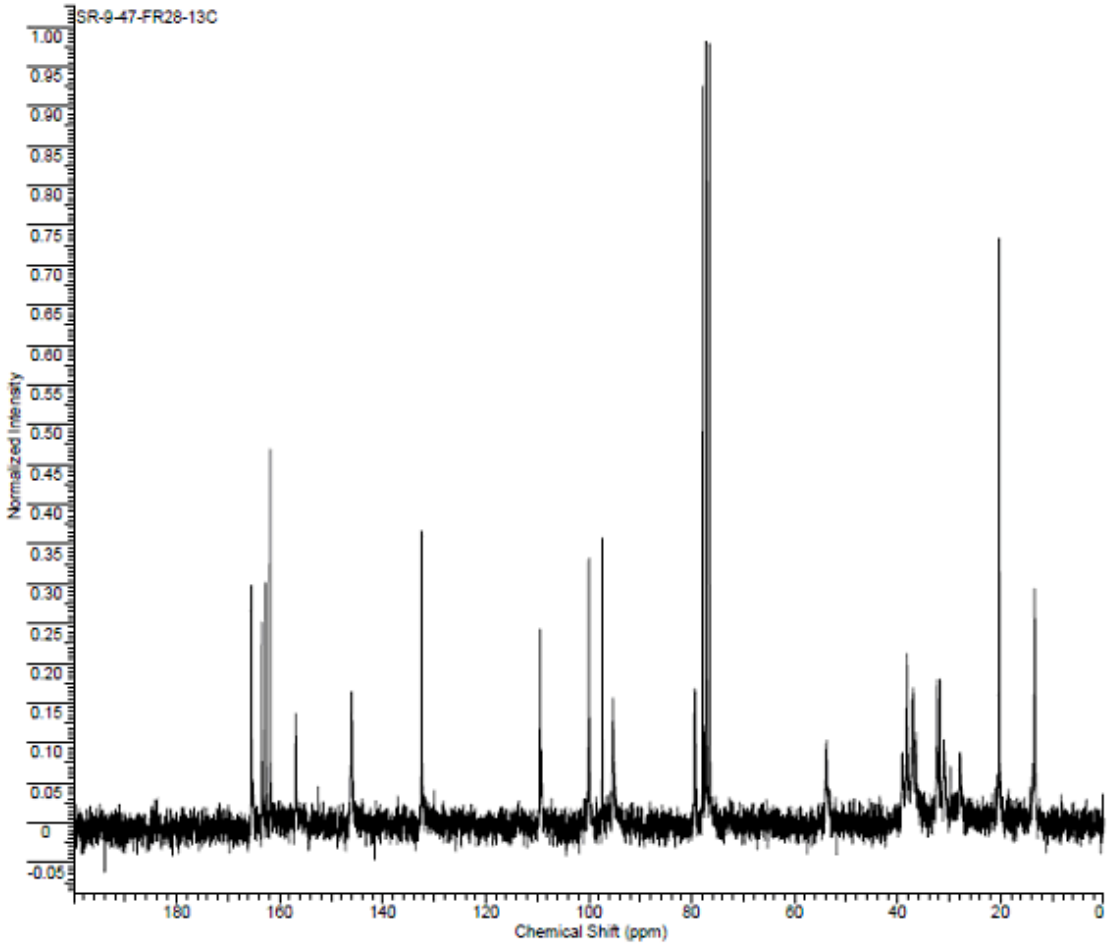

Formula $C_{21}H_{25}N_3O_5$	FW	367.4415		
Acquisition Time (sec)	2.0487	Comment	Std proton	Date Nov 5 2008
Date Stamp	Nov 5 2008			
File Name	C:\DOCUMENTS AND SETTINGS\DUY HUA\DESKTOP\SANDEEP\THESISNMR\NEW FOLDER\TP8AANDB\SR-9-47-FR11-17			
Frequency (MHz)	399.76	Nucleus	1H	Number of Transients 32
Original Points Count	13103	Points Count	16384	Pulse Sequence s2pul
Receiver Gain	44.00	Solvent	CHLOROFORM-d	Spectrum Offset (Hz) 2416.5151
Sweep Width (Hz)	6395.91	Temperature (degree C)	25.000	

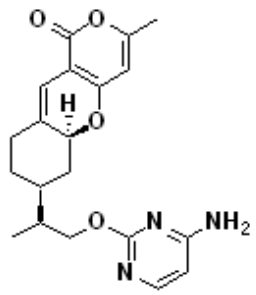

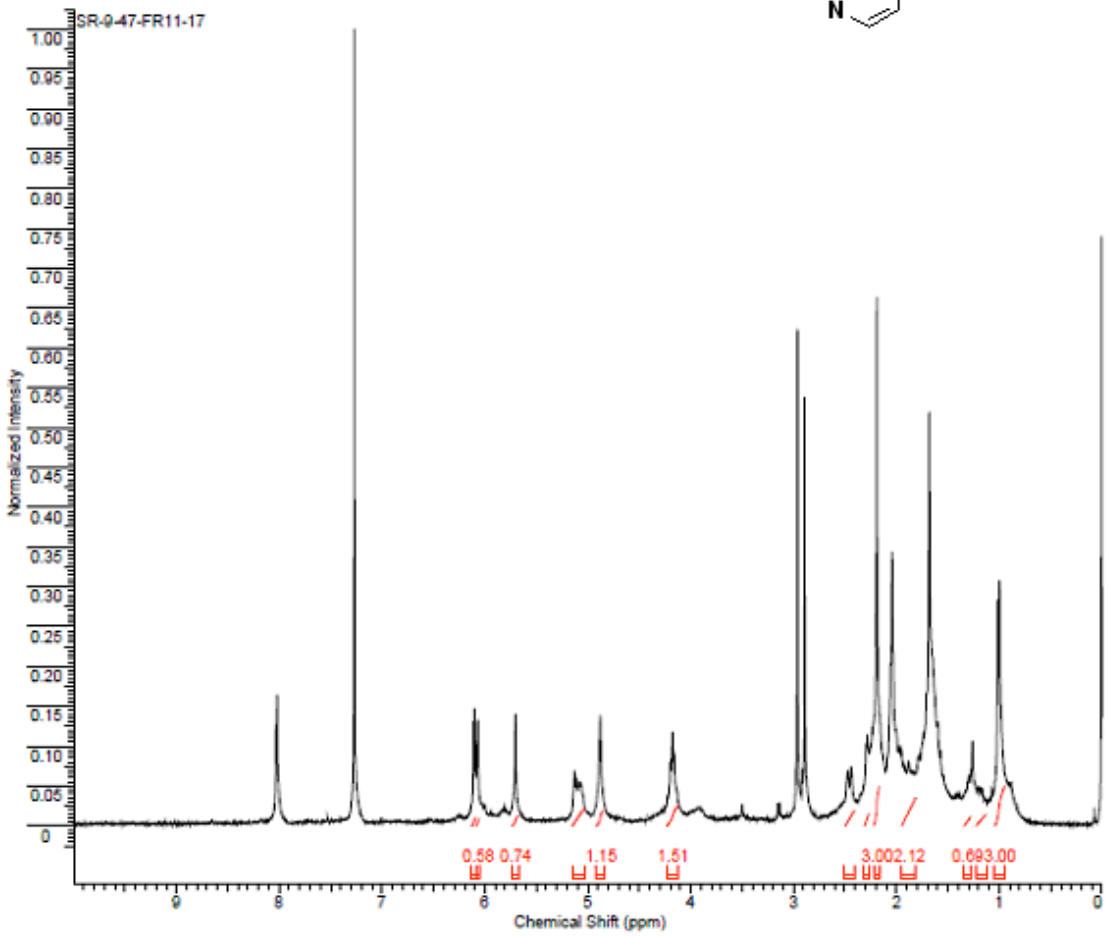

Formula $C_{21}H_{25}N_3O_5$	FW 367.4415

Acquisition Time (sec)	1.3005	*Comment*	Std proton	*Date*	Oct 27 2007
Date Stamp	Oct 27 2007	*File Name*	C:\SANDEEP NMR\SR-5-115-FR10-15-13C		
Frequency (MHz)	100.53	*Nucleus*	13C	*Number of Transients*	1000000
Original Points Count	31375	*Points Count*	32768	*Pulse Sequence*	s2pul
Receiver Gain	30.00	*Solvent*	CHLOROFORM-d		
Spectrum Offset (Hz)	10552.9121	*Sweep Width (Hz)*	24125.45	*Temperature (degree C)*	20.000

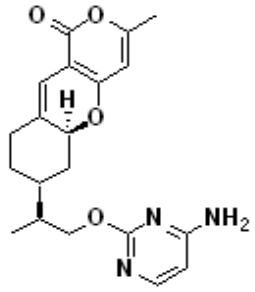

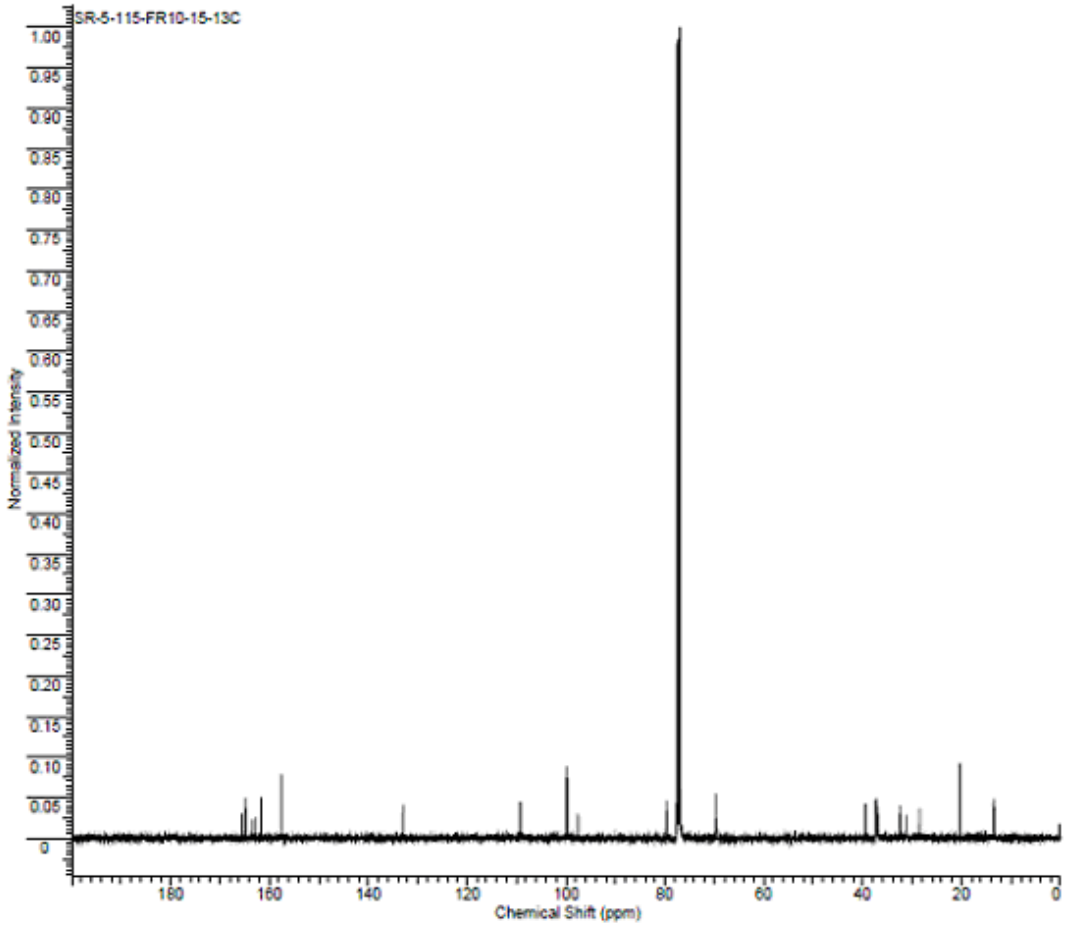

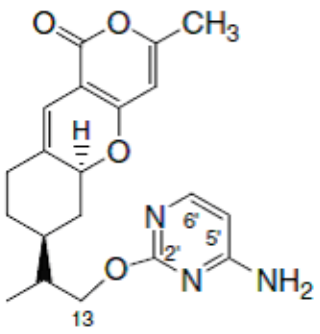
O
O
CH3
H
O
N
6'
5'
2'
O
N
NH2

13

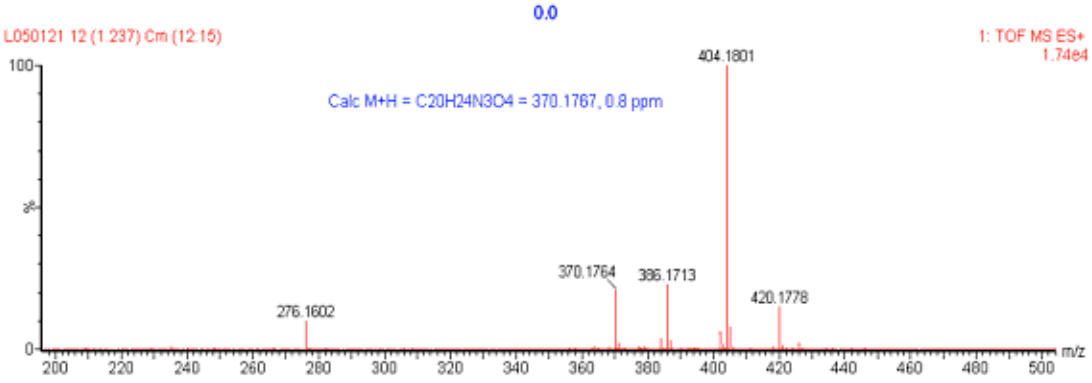
SR-TP8
0.0
L050121 12 (1.237) Cm (12:15)
1: TOF MS ES+
1.74e4
100
%
0
404.1801
Calc M+H = C20H24N3O4 = 370.1767, 0.8 ppm
370.1764
386.1713
420.1778
276.1602
200
220
240
260
280
300
320
340
360
380
400
420
440
460
480
500
m/z

Formula $C_{17}H_{23}NO_3$	FW	273.3700

Acquisition Time (sec)	2.0486	Comment	Std proton	Date	Nov 16 2007
Date Stamp	Nov 16 2007				
File Name	C:\SANDEEP NMR\SR-7-24-CRDUE-BASIC			Frequency (MHz)	399.77
Nucleus	1H	Number of Transients	32	Original Points Count	9828
Points Count	16384	Pulse Sequence	s2pul	Receiver Gain	36.00
Solvent	CHLOROFORM-d			Spectrum Offset (Hz)	2008.9603
Sweep Width (Hz)	4797.31	Temperature (degree C)	25.000		

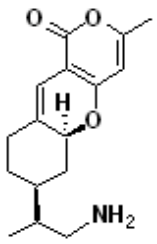

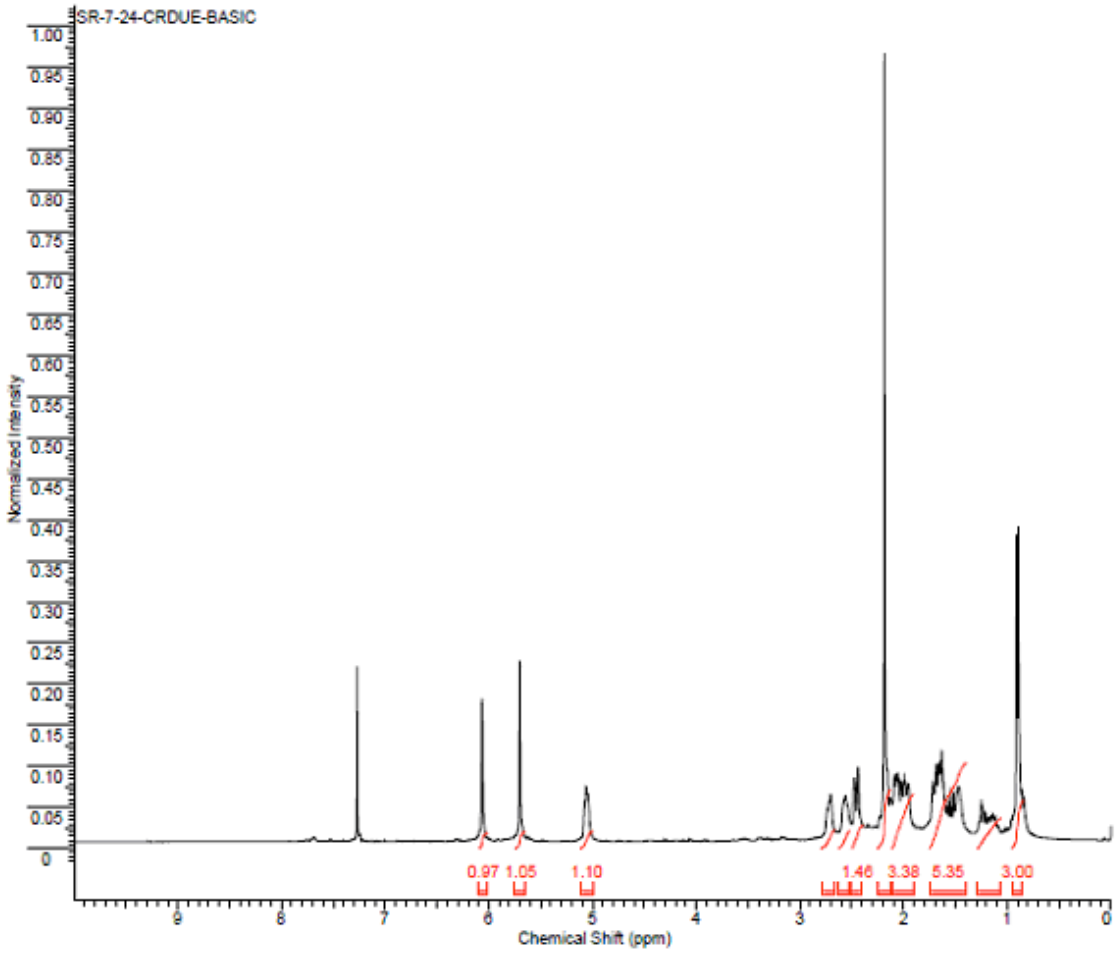

Formula $C_{11}H_{19}NO_3$	FW	273.3700

Acquisition Time (sec)	1.3005	Comment	Std proton	Date	Nov 25 2007
Date Stamp	Nov 25 2007			File Name	C:\SANDEEP NMR\SR-7-29-BASE-13C
Frequency (MHz)	100.53	Nucleus	13C	Number of Transients	5000
Original Points Count	31375	Points Count	32768	Pulse Sequence	s2pul
Receiver Gain	30.00	Solvent	CHLOROFORM-d		
Spectrum Offset (Hz)	10548.2900	Sweep Width (Hz)	24125.45	Temperature (degree C)	25.000

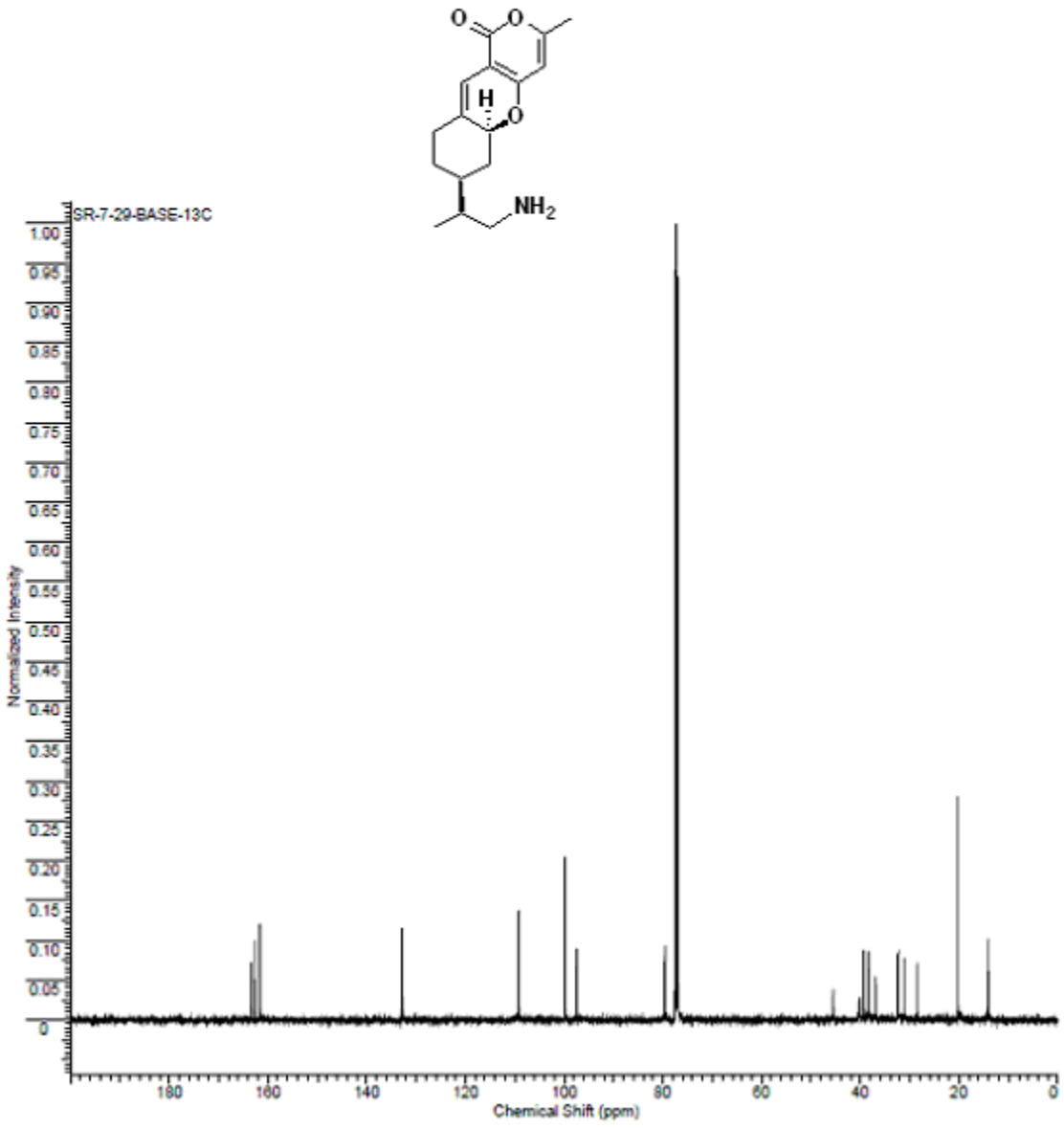

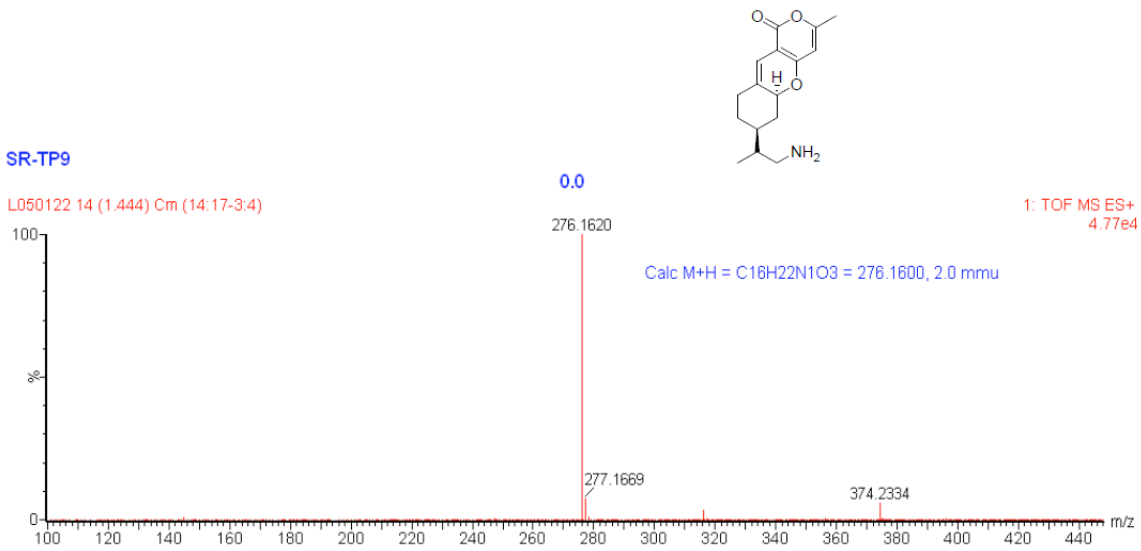
SR-TP9
0.0
L050122 14 (1.444) Cm (14:17-3:4)
1: TOF MS ES+
4.77e4
276.1620
Calc M+H = C16H22N1O3 = 276.1600, 2.0 mmu
277.1669
374.2334
100
%
0
m/z
100 120 140 160 180 200 220 240 260 280 300 320 340 360 380 400 420 440

Formula $C_{20}H_{22}N_4O_3$	FW	366.4137

Acquisition Time (sec)	2.0486	Comment	Std proton	Date	Jun 24 2008
Date Stamp	Jun 24 2008			File Name	C:\SANDEEP NMR\SR-8-64-FR32
Frequency (MHz)	399.76	Nucleus	1H	Number of Transients	32
Original Points Count	9827	Points Count	16384	Pulse Sequence	s2pul
Receiver Gain	48.00	Solvent	CHLOROFORM-d		
Spectrum Offset (Hz)	2018.3365	Sweep Width (Hz)	4797.03	Temperature (degree C)	25.000

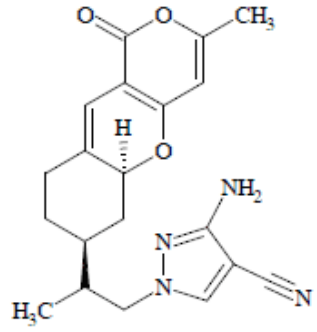

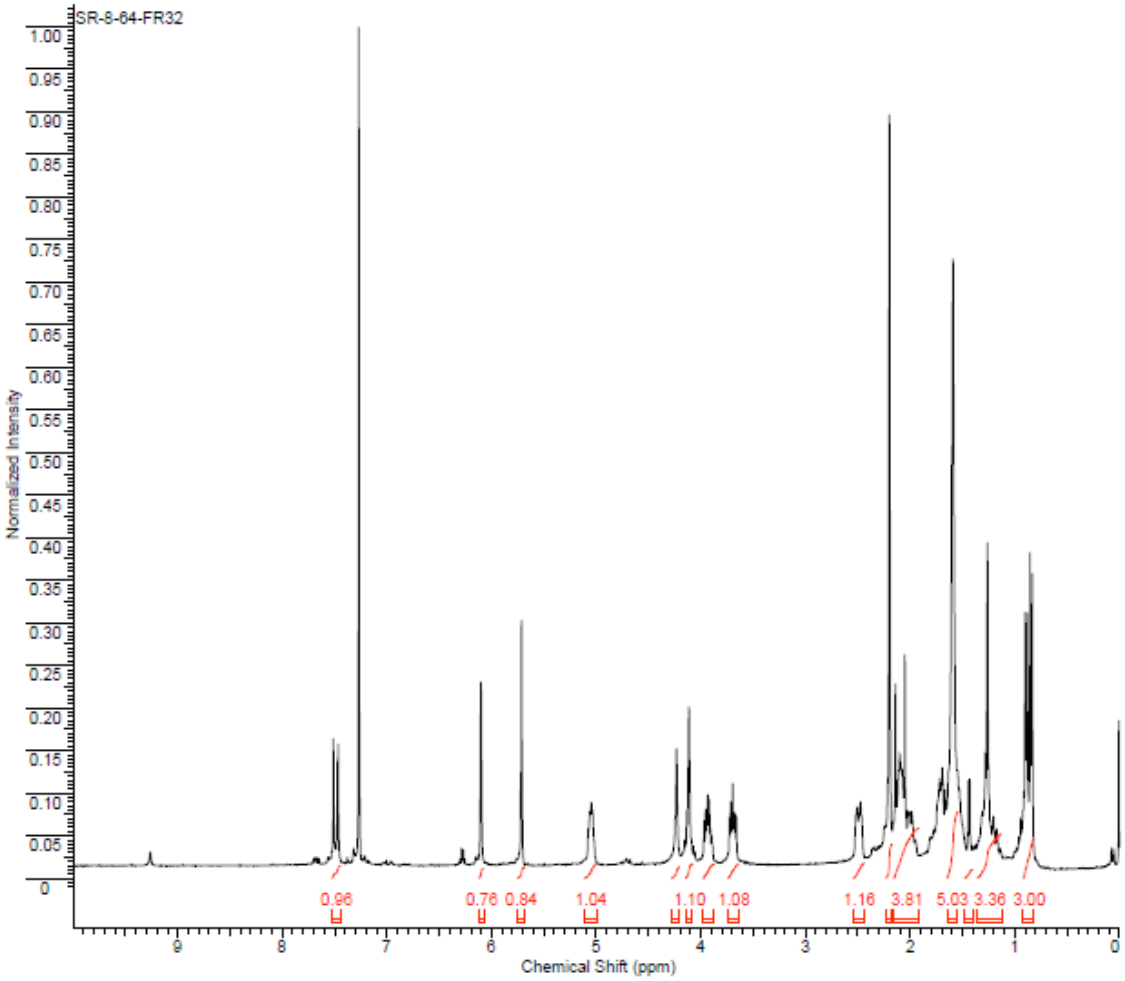

Formula $C_{20}H_{22}N_4O_3$	FW	366.4137

Acquisition Time (sec)	1.3005	Comment	Std proton	Date	Jun 24 2008
Date Stamp	Jun 24 2008	File Name	C:\SANDEEP NMR\SR-8-64-FR-30-37-13C		
Frequency (MHz)	100.53	Nucleus	13C	Number of Transients	25000
Original Points Count	31375	Points Count	32768	Pulse Sequence	s2pul
Receiver Gain	30.00	Solvent	CHLOROFORM-d		
Spectrum Offset (Hz)	10554.7900	Sweep Width (Hz)	24125.45	Temperature (degree C)	25.000

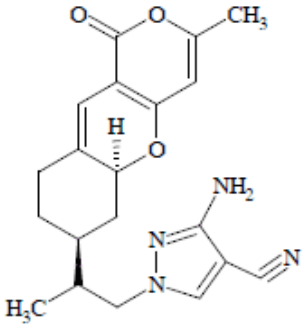

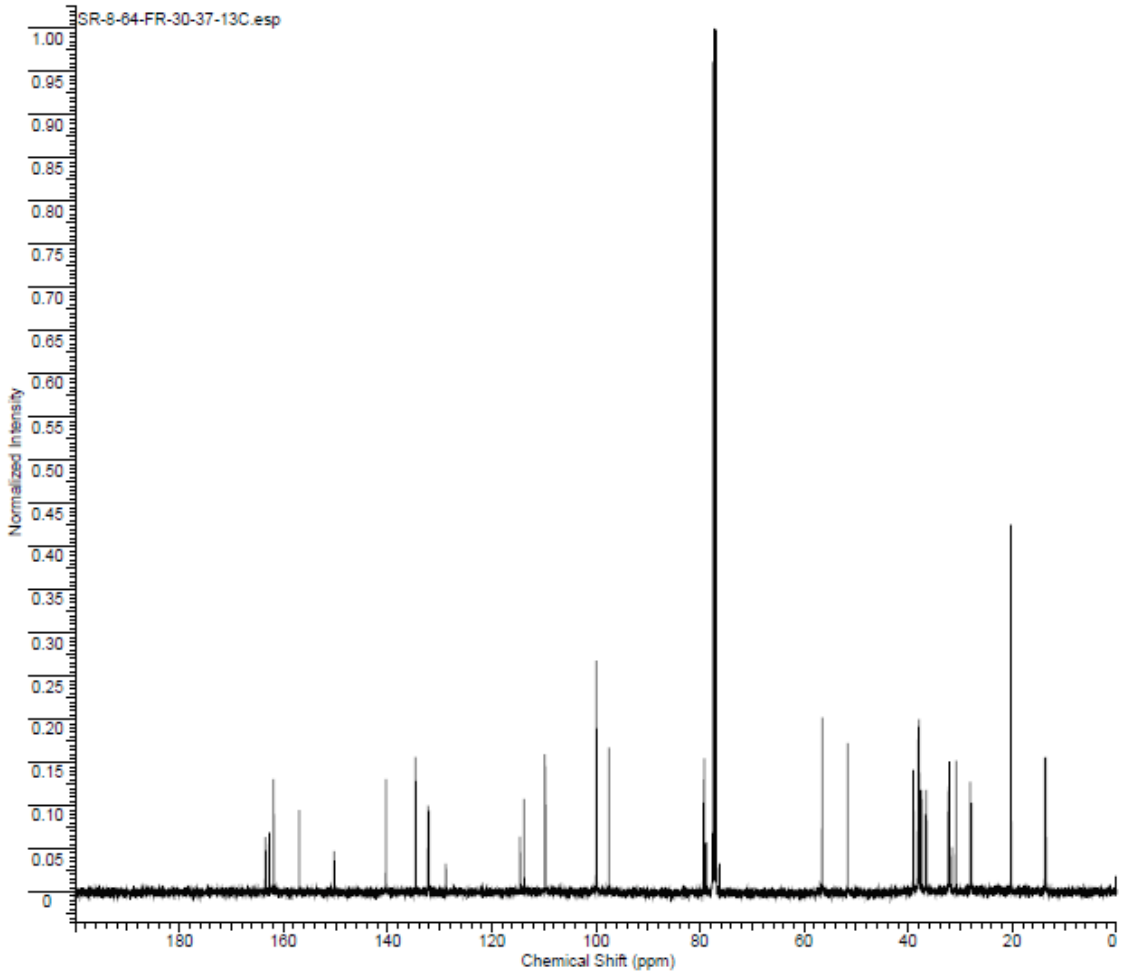

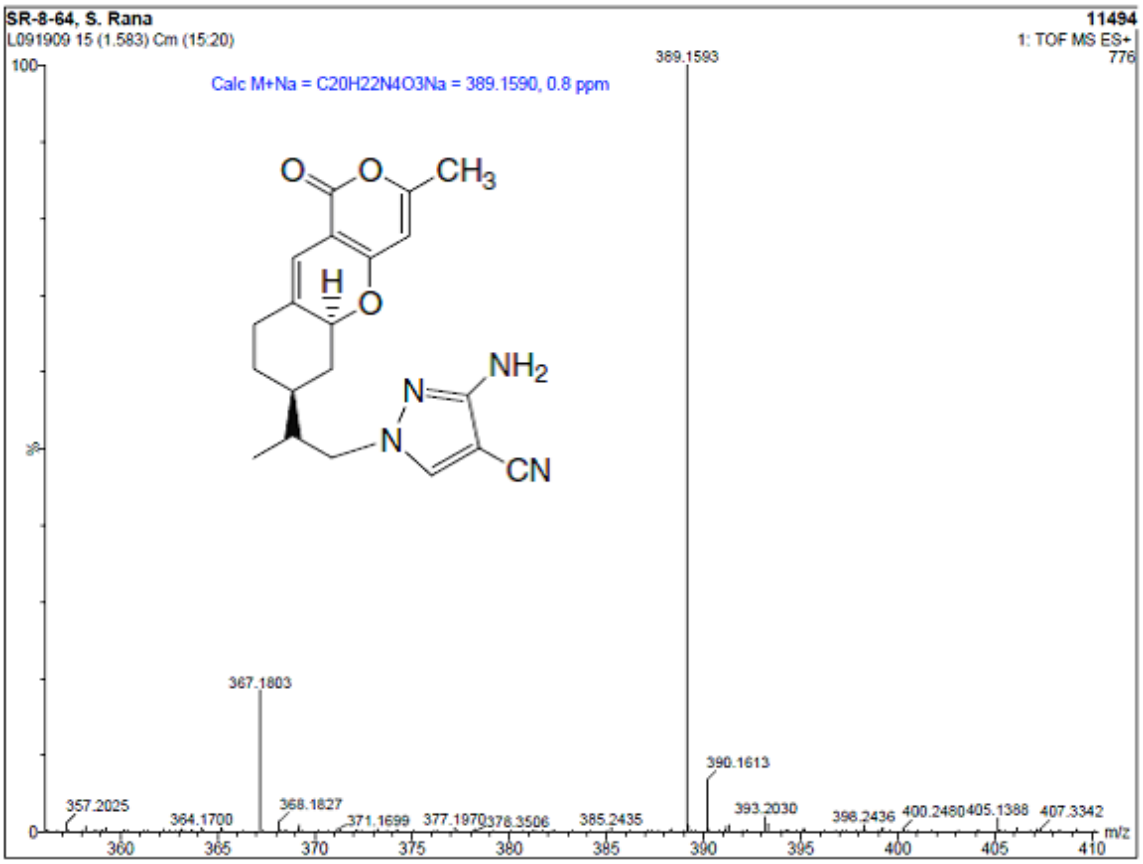
SR-8-64, S. Rana
L091909 15 (1.583) Cm (15:20)
11494
1: TOF MS ES+
776
389.1593
Calc M+Na = C20H22N4O3Na = 389.1590, 0.8 ppm
O
O
CH3
H
O
NH2
N
N
CN
%
100
0
367.1803
390.1613
357.2025
364.1700
368.1827
371.1699
377.1970
378.3506
385.2435
393.2030
398.2436
400.2480
405.1388
407.3342
m/z
360
365
370
375
380
385
390
395
400
405
410

Formula $C_{20}H_{22}N_2O_3S$	FW	370.4653

Acquisition Time (sec)	2.0486	Comment	SR-8-68(2)-fr27-28		
Date	Jul 10 2008	Date Stamp	Jul 10 2008	File Name	C:\SANDEEP NMR\SR-8-68-FR27-28
Frequency (MHz)	399.76	Nucleus	1H	Number of Transients	32
Original Points Count	9827	Points Count	16384	Pulse Sequence	s2pul
Receiver Gain	48.00	Solvent	CHLOROFORM-d		
Spectrum Offset (Hz)	2016.5797	Sweep Width (Hz)	4797.03	Temperature (degree C)	25.000

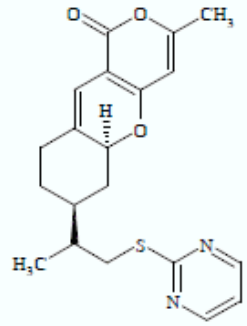

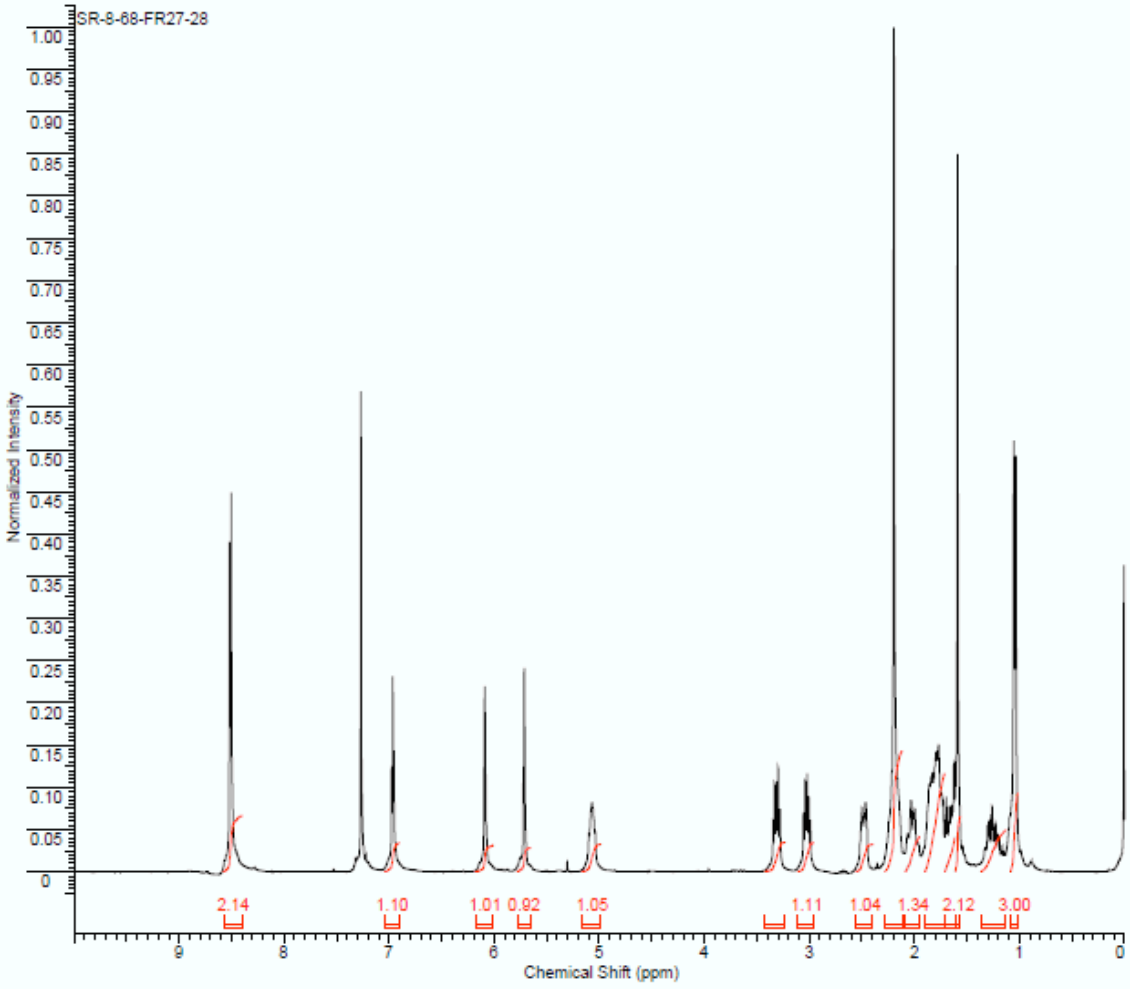

Formula $C_{20}H_{22}N_2O_3S$	FW	370.4653		
Acquisition Time (sec)	1.3005	Comment	SR-8-68-fr29-13C	
Date	Jul 10 2008	Date Stamp	Jul 10 2008	File Name C:\SANDEEP NMR\SR-8-68-FR29-13C
Frequency (MHz)	100.53	Nucleus	13C	Number of Transients 2000
Original Points Count	31375	Points Count	32768	Pulse Sequence s2pul
Receiver Gain	30.00	Solvent	CHLOROFORM-d	
Spectrum Offset (Hz)	10551.1094	Sweep Width (Hz)	24125.45	Temperature (degree C) 25.000

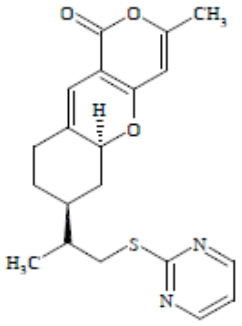

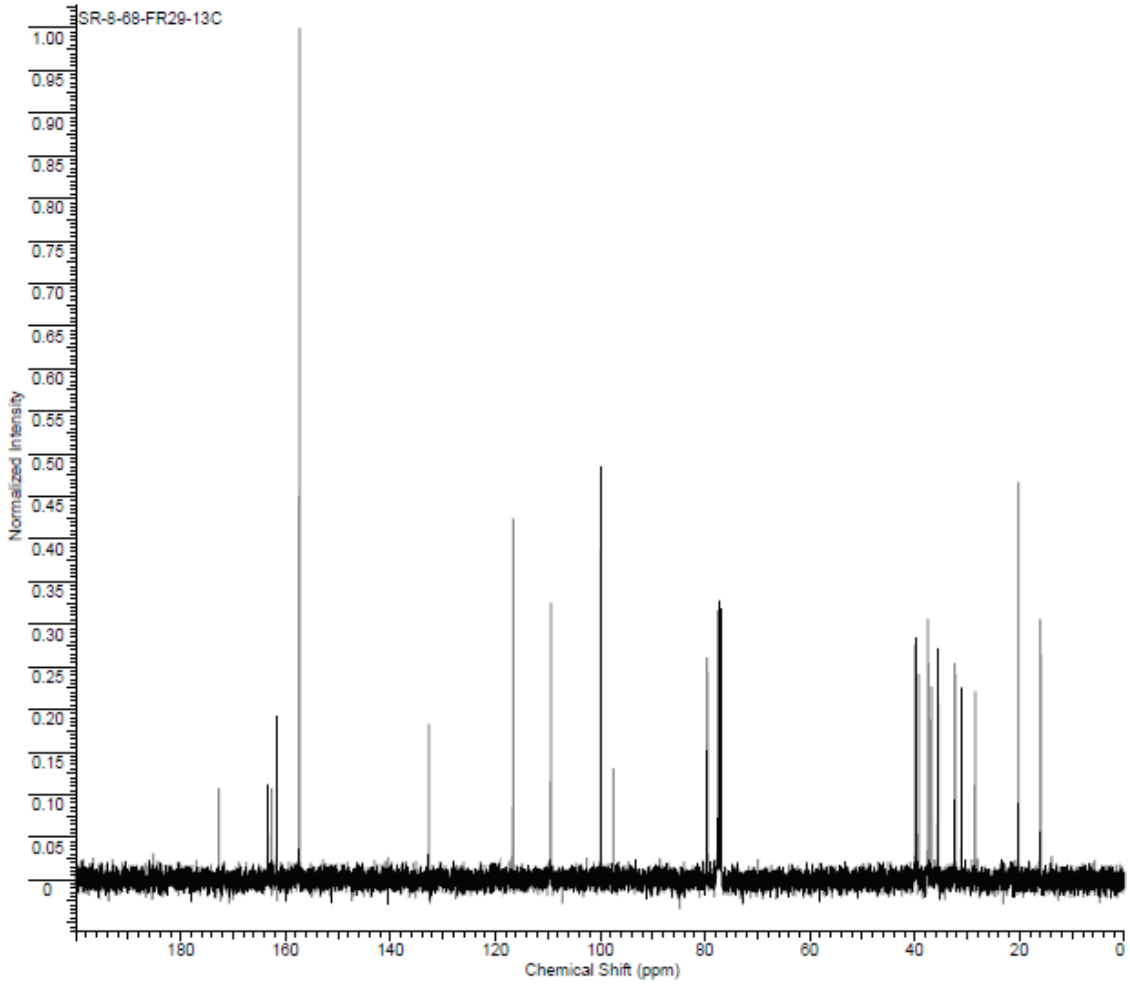

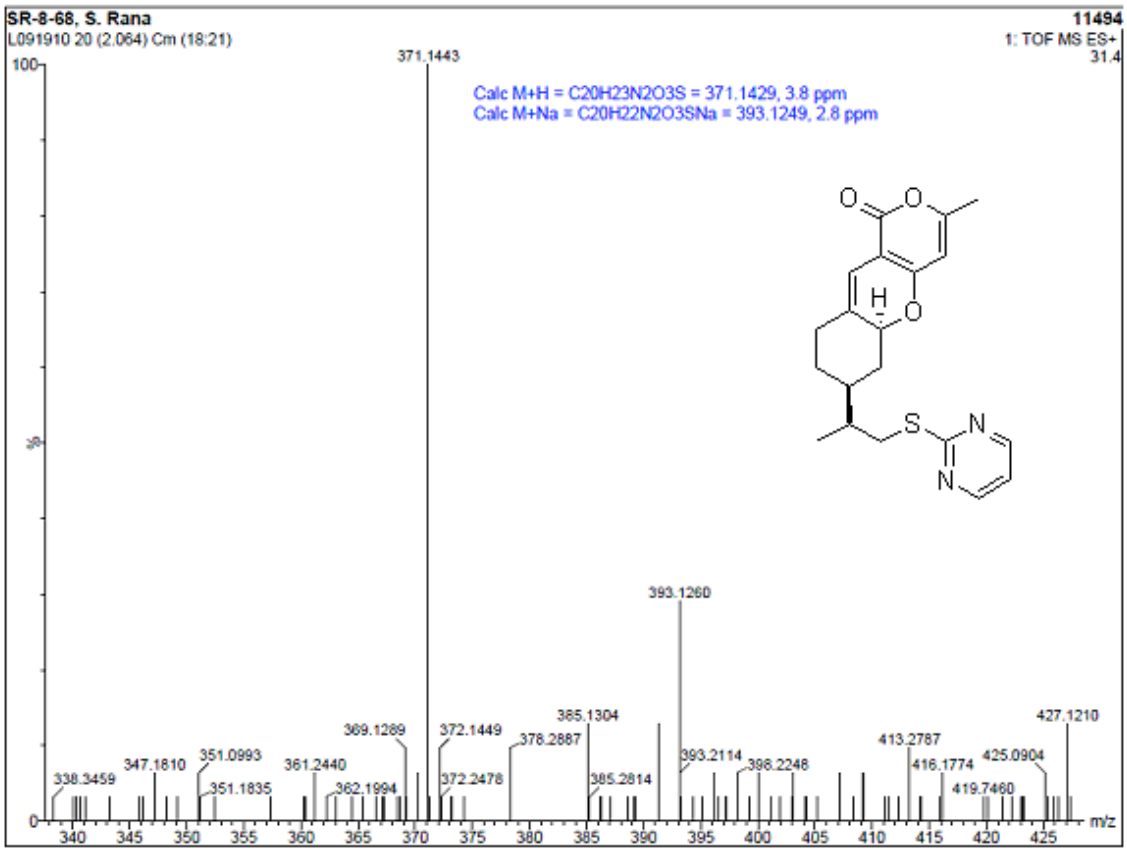
SR-8-68, S. Rana
11494
L091910 20 (2.064) Cm (18:21)
1: TOF MS ES+
31.4
100
%
0
371.1443
Calc M+H = C20H23N2O3S = 371.1429, 3.8 ppm
Calc M+Na = C20H22N2O3SNa = 393.1249, 2.8 ppm
O
O
O
H
S
N
N
393.1260
385.1304
427.1210
369.1289
372.1449
378.2887
413.2787
347.1810
351.0993
361.2440
393.2114
398.2248
416.1774
425.0904
338.3459
351.1835
362.1994
372.2478
385.2814
419.7460
340
345
350
355
360
365
370
375
380
385
390
395
400
405
410
415
420
425
m/z

Formula $C_{26}H_{28}N_4O_4$	FW	448.5142

Acquisition Time (sec)	2.0486	Comment	Std proton	Date	Jan 30 2008
Date Stamp	Jan 30 2008	File Name	C:\SANDEEP NMR\SR-5-115-FR10-15-13C.FID\SR-7-68-FR12-DP		
Frequency (MHz)	399.77	Nucleus	1H	Number of Transients	32
Original Points Count	13104	Points Count	16384	Pulse Sequence	s2pul
Receiver Gain	52.00	Solvent	CHLOROFORM-d		
Spectrum Offset (Hz)	2409.1055	Sweep Width (Hz)	6396.42	Temperature (degree C)	25.000

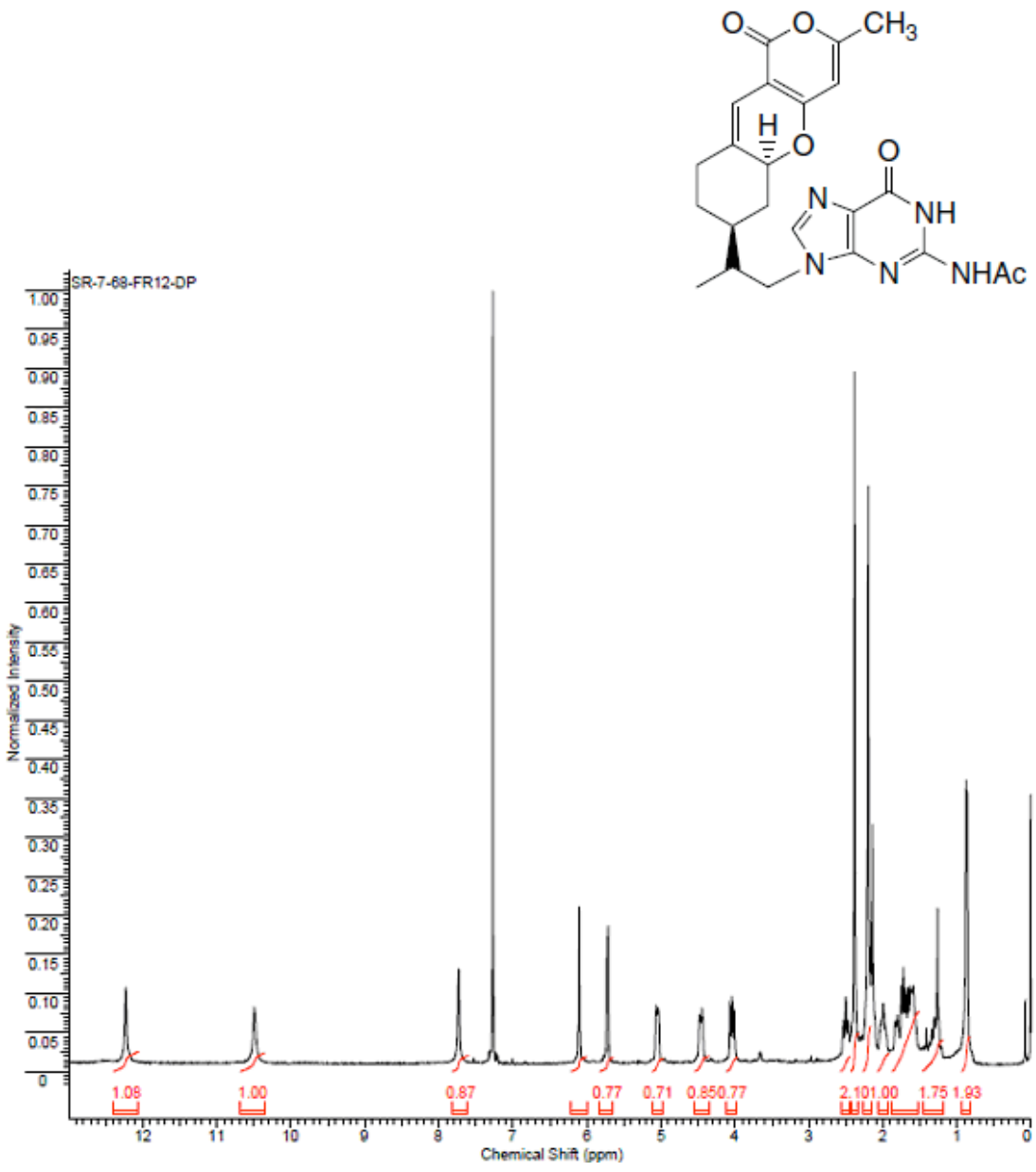

Formula $C_{24}H_{27}N_5O_6$	FW 449.5023

Acquisition Time (sec)	1.3005	Comment	Std proton	Date	Feb 2 2008
Date Stamp	Feb 2 2008	File Name	C:\SANDEEP NMR\SR-7-68-FR11-12-13C-DP		
Frequency (MHz)	100.53	Nucleus	13C	Number of Transients	64000000
Original Points Count	31375	Points Count	32768	Pulse Sequence	s2pul
Receiver Gain	30.00	Solvent	CHLOROFORM-d		
Spectrum Offset (Hz)	10554.7441	Sweep Width (Hz)	24125.45	Temperature (degree C)	25.000

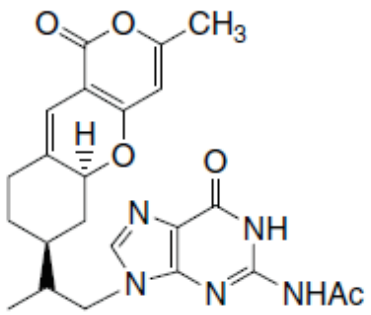

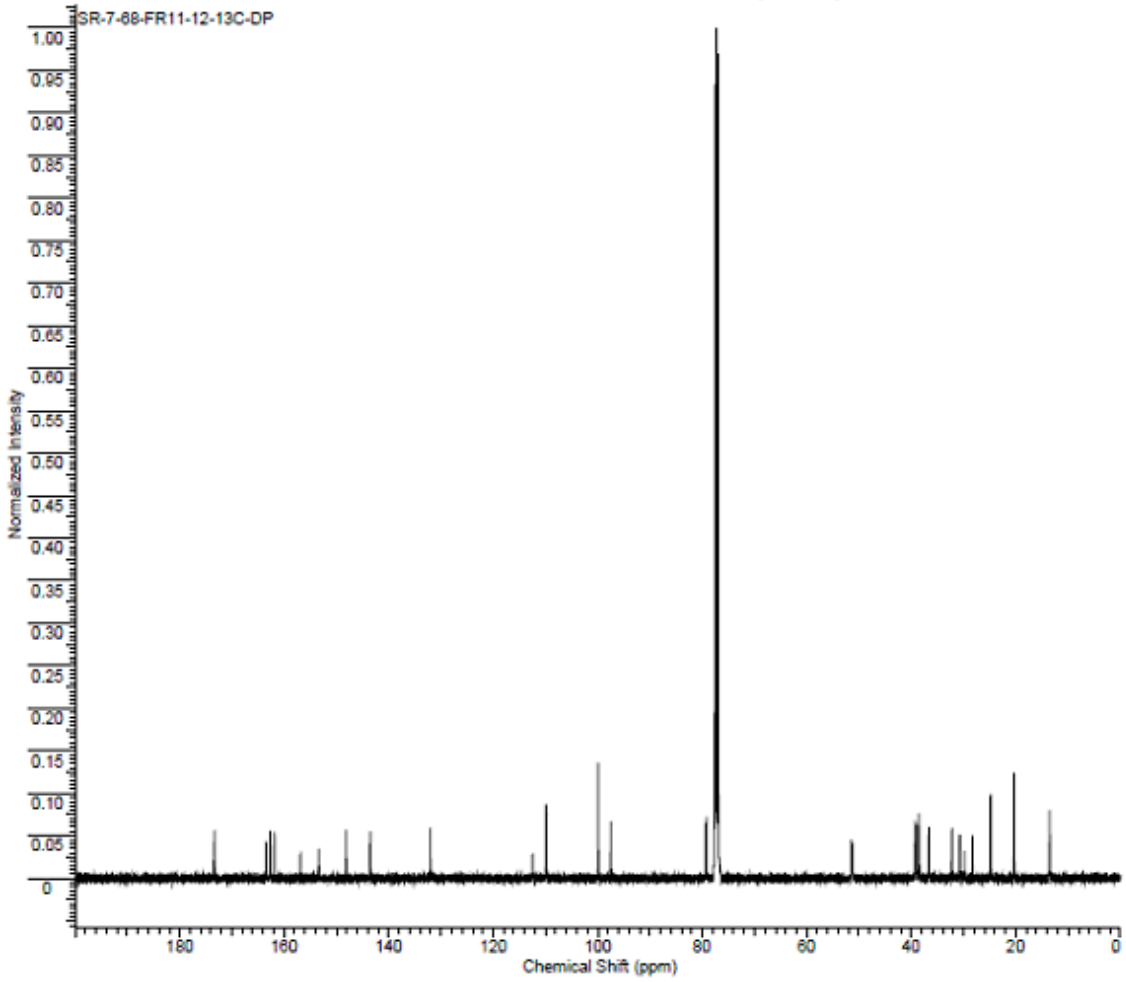

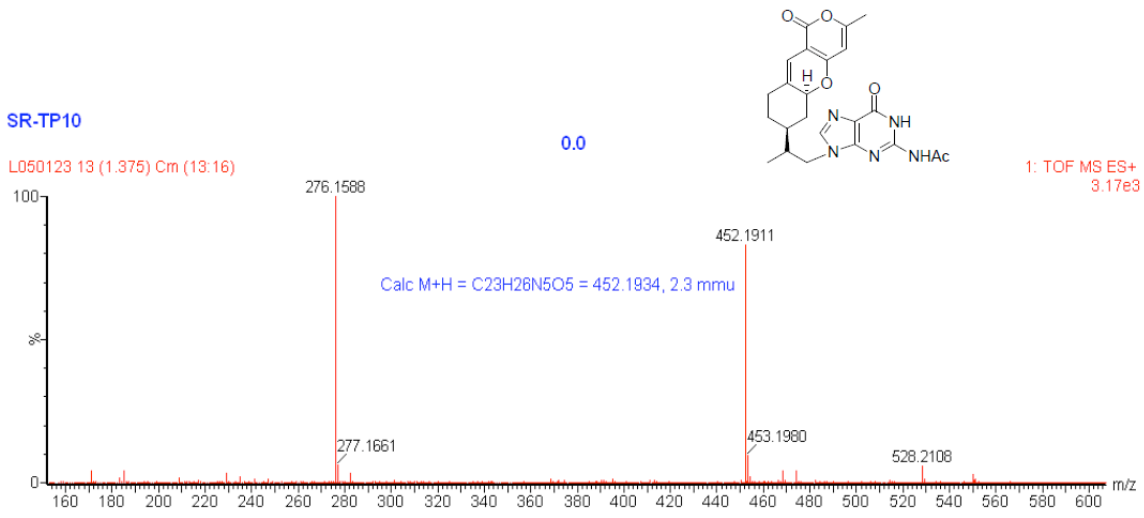
SR-TP10
0.0
L050123 13 (1.375) Cm (13:16)
1: TOF MS ES+
3.17e3
276.1588
452.1911
Calc M+H = C23H26N5O5 = 452.1934, 2.3 mmu
277.1661
453.1980
528.2108
100
%
0
160 180 200 220 240 260 280 300 320 340 360 380 400 420 440 460 480 500 520 540 560 580 600
m/z
O
O
H
O
N
N
O
NH
N
NHAc

Formula $C_{20}H_{26}N_2O_4$	FW	382.4528

Acquisition Time (sec)	2.0486	Comment	Std proton	Date	Oct 9 2007
Date Stamp	Oct 9 2007	File Name	C:\SANDEEP NMR\SR-5-109-FR7-10-AFTERWORKUP		
Frequency (MHz)	399.77	Nucleus	1H	Number of Transients	32
Original Points Count	9828	Points Count	16384	Pulse Sequence	s2pul
Receiver Gain	30.00	Solvent	CHLOROFORM-d		
Spectrum Offset (Hz)	2008.3746	Sweep Width (Hz)	4797.31	Temperature (degree C)	25.000

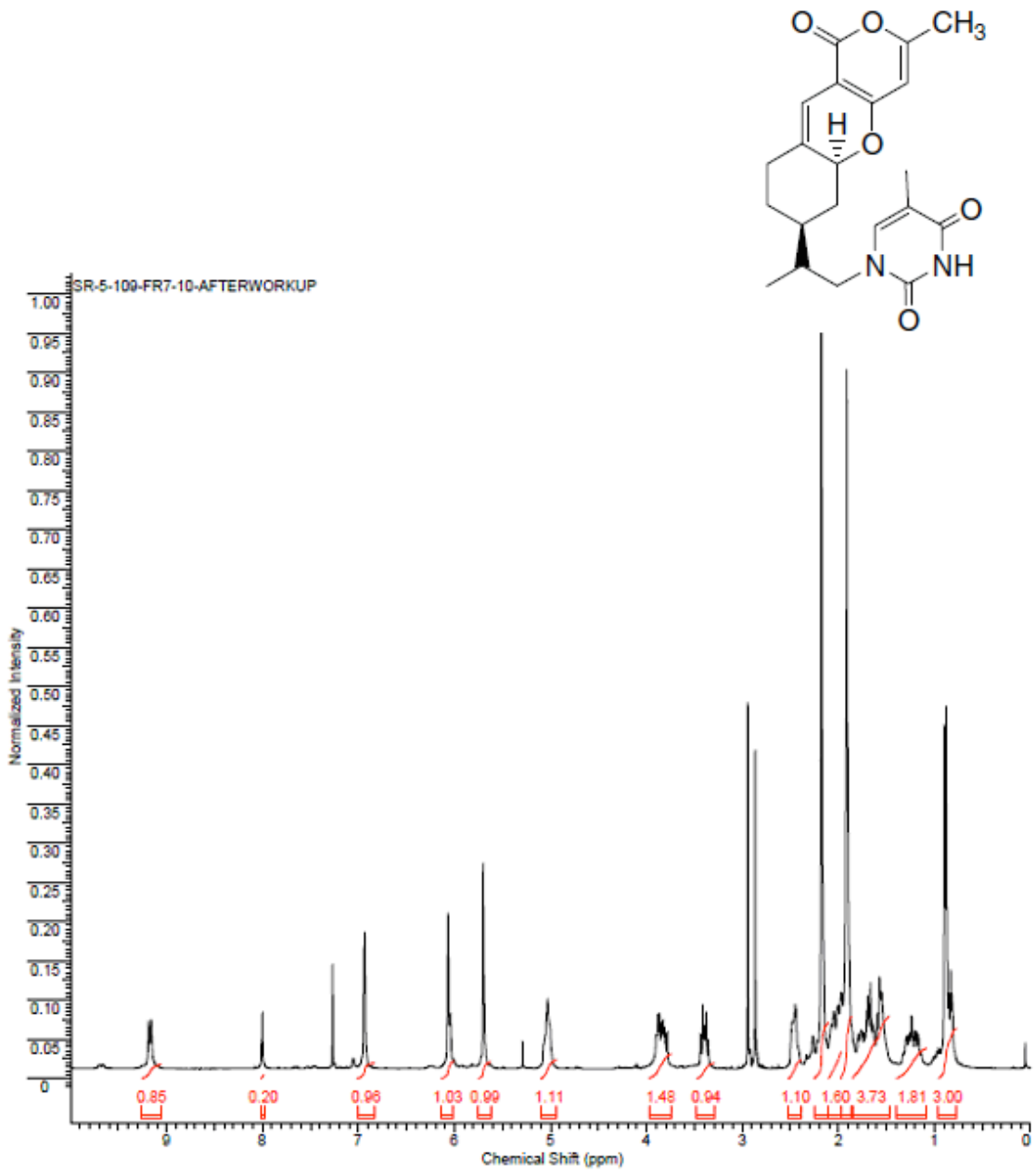

Formula $C_{20}H_{26}N_2O_4$	FW	382.4528

Acquisition Time (sec)	1.3005	Comment	Std proton	Date	Oct 9 2007
Date Stamp	Oct 9 2007	File Name	C:\SANDEEP NMR\SR-5-109-FR8-13C		
Frequency (MHz)	100.53	Nucleus	13C	Number of Transients	20000
Original Points Count	31375	Points Count	32768	Pulse Sequence	s2pul
Receiver Gain	30.00	Solvent	CHLOROFORM-d		
Spectrum Offset (Hz)	10548.2900	Sweep Width (Hz)	24125.45	Temperature (degree C)	20.000

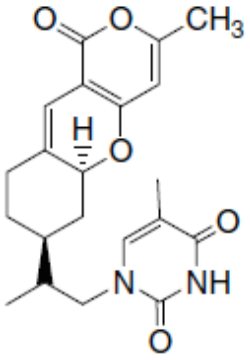

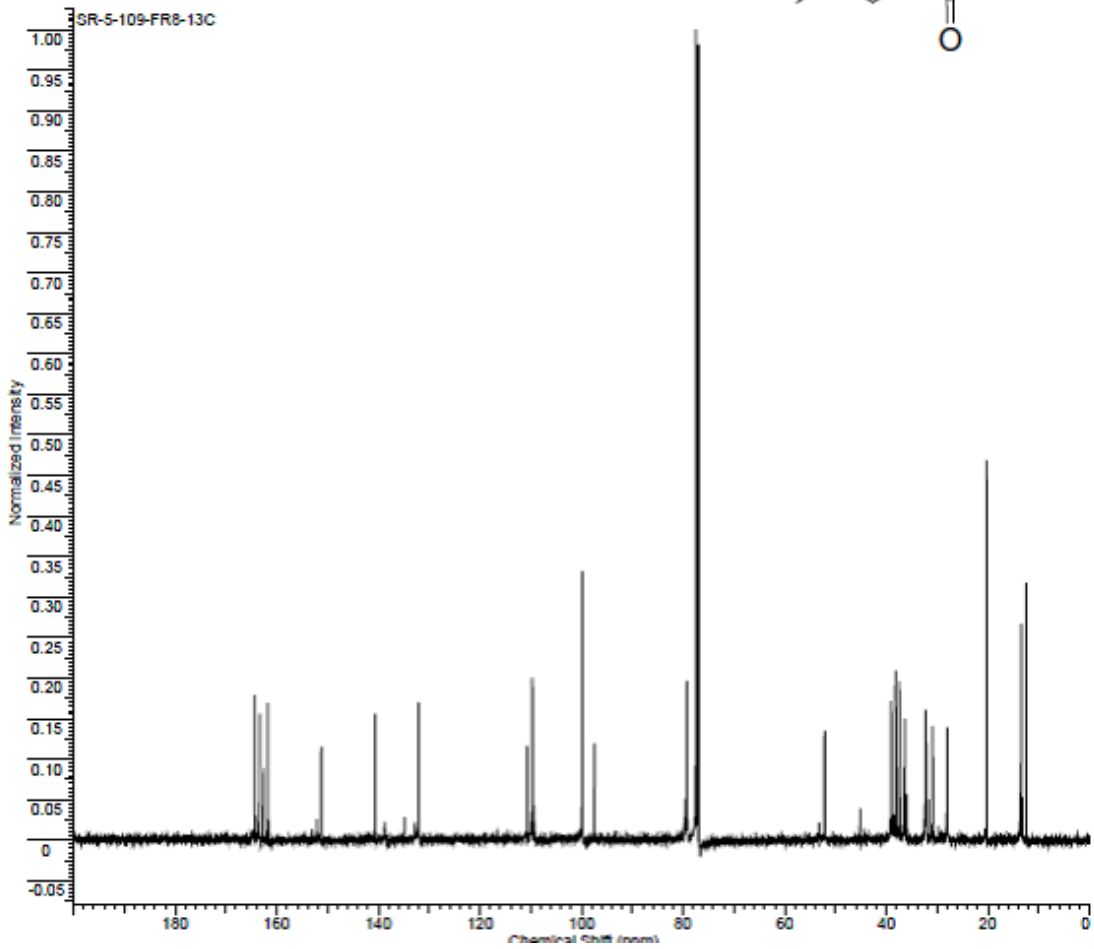

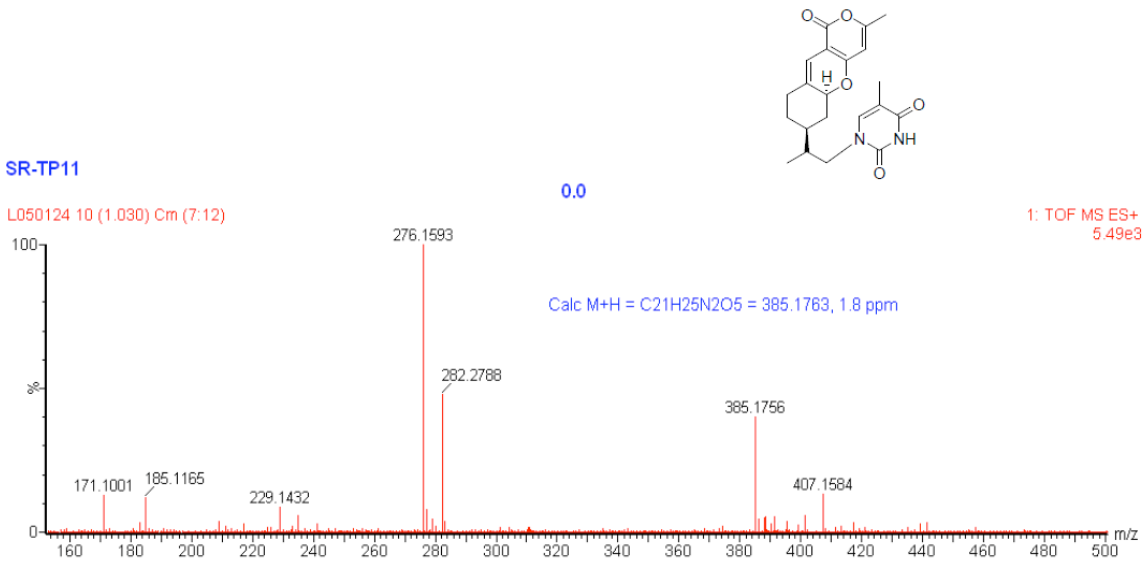
SR-TP11
0.0
L050124 10 (1.030) Cm (7:12)
1: TOF MS ES+
5.49e3
100
%
0
276.1593
282.2788
385.1756
171.1001
185.1165
229.1432
407.1584
Calc M+H = C21H25N2O5 = 385.1763, 1.8 ppm
160
180
200
220
240
260
280
300
320
340
360
380
400
420
440
460
480
500
m/z

Formula $C_{22}H_{29}N_5O_3$	FW	391.4662

Acquisition Time (sec)	2.0486	Comment	Std proton	Date	Jan 17 2008
Date Stamp	Jan 17 2008			File Name	C:\SANDEEP NMR\SR-7-58-FR12
Frequency (MHz)	399.77	Nucleus	1H	Number of Transients	16
Original Points Count	13104	Points Count	16384	Pulse Sequence	s2pul
Receiver Gain	30.00	Solvent	CHLOROFORM-d		
Spectrum Offset (Hz)	2409.1052	Sweep Width (Hz)	6396.42	Temperature (degree C)	25.000

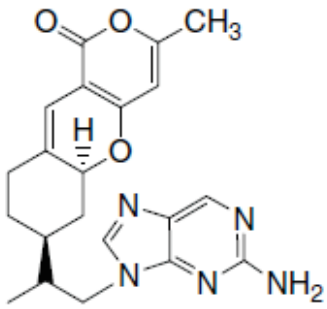

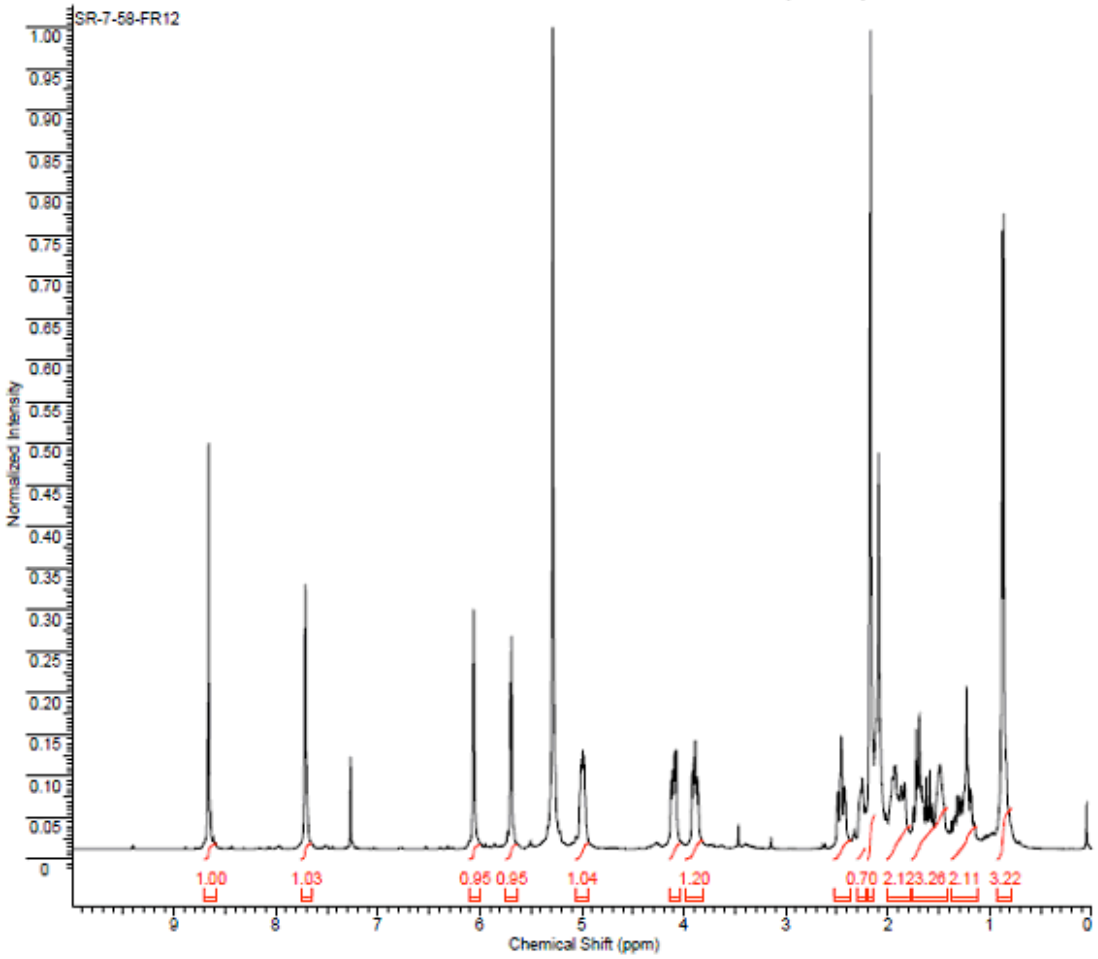

Formula $C_{20}H_{26}N_6O_3$	FW	391.4662

Acquisition Time (sec)	1.3005	Comment	Std proton	Date	Jan 27 2008
Date Stamp	Jan 27 2008	File Name	C:\SANDEEP NMR\SR-7-58-FR12-13C		
Frequency (MHz)	100.53	Nucleus	13C	Number of Transients	10000
Original Points Count	31375	Points Count	32768	Pulse Sequence	s2pul
Receiver Gain	30.00	Solvent	CHLOROFORM-d		
Spectrum Offset (Hz)	10546.0811	Sweep Width (Hz)	24125.45	Temperature (degree C)	25.000

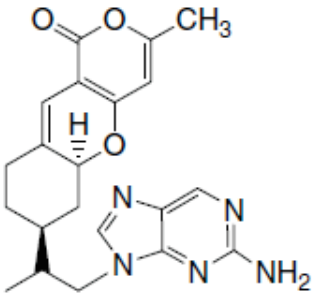

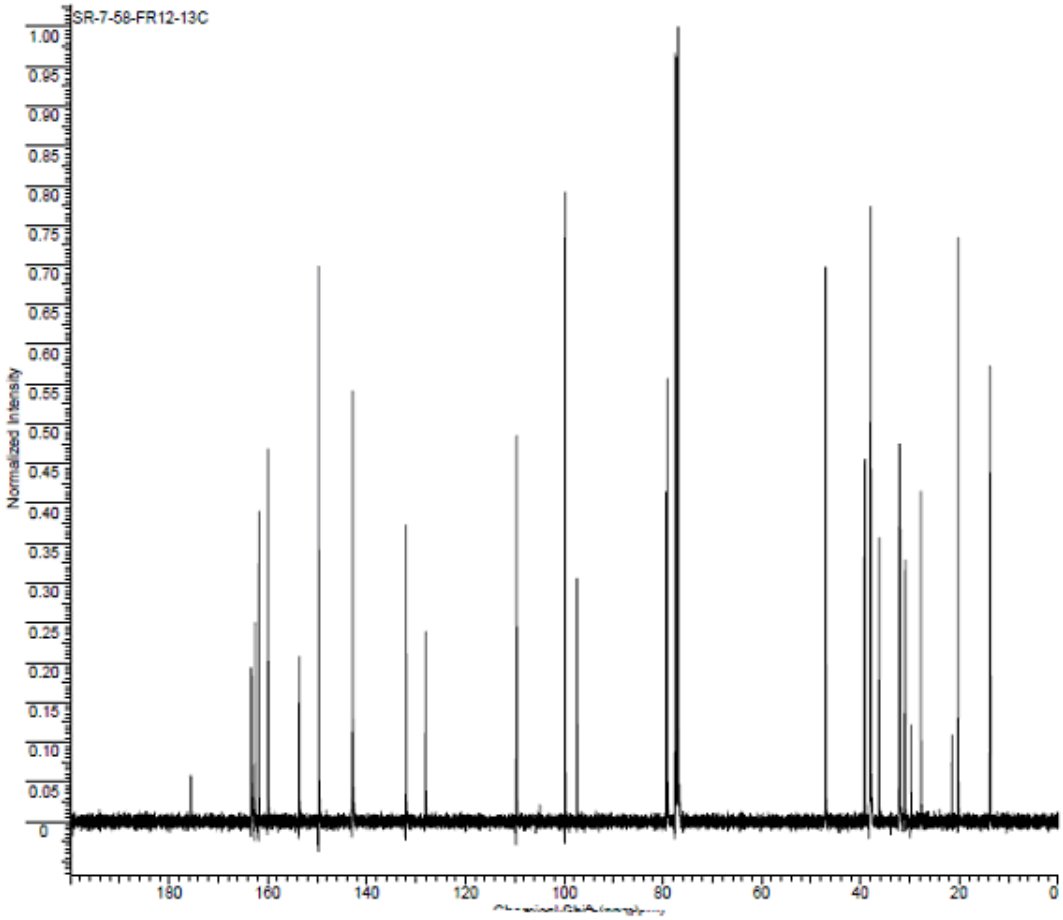

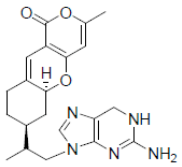

SR-TP13

0.0

L050125 10 (1.031) Cm (7:10)

1: TOF MS ES+
5.49e3

Calc M+H = C21H24N5O3 = 394.1879, 0.3 ppm

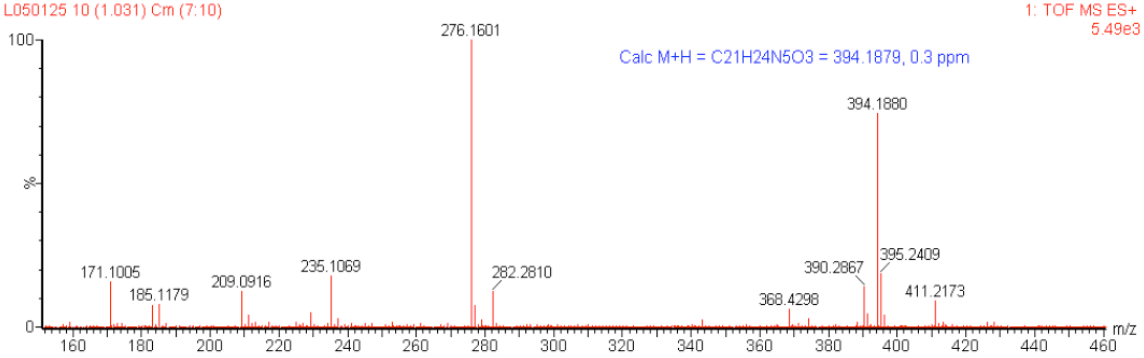

Formula $C_6H_5BrO_2$	FW	189.0067

Acquisition Time (sec)	1.9945	Comment	STANDARD 1H OBSERVE		
Date	Aug 28 2008	Date Stamp	Aug 28 2008		
File Name	C:\NMR 031009\200\BOOK 9\SR-9-011-DP			Frequency (MHz)	199.98
Nucleus	1H	Number of Transients	64	Original Points Count	5984
Points Count	8192	Pulse Sequence	s2pul	Receiver Gain	40.00
Solvent	CHLOROFORM-d			Spectrum Offset (Hz)	1002.0226
Sweep Width (Hz)	3000.30	Temperature (degree C)	29.000		

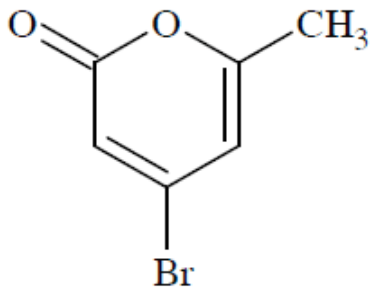

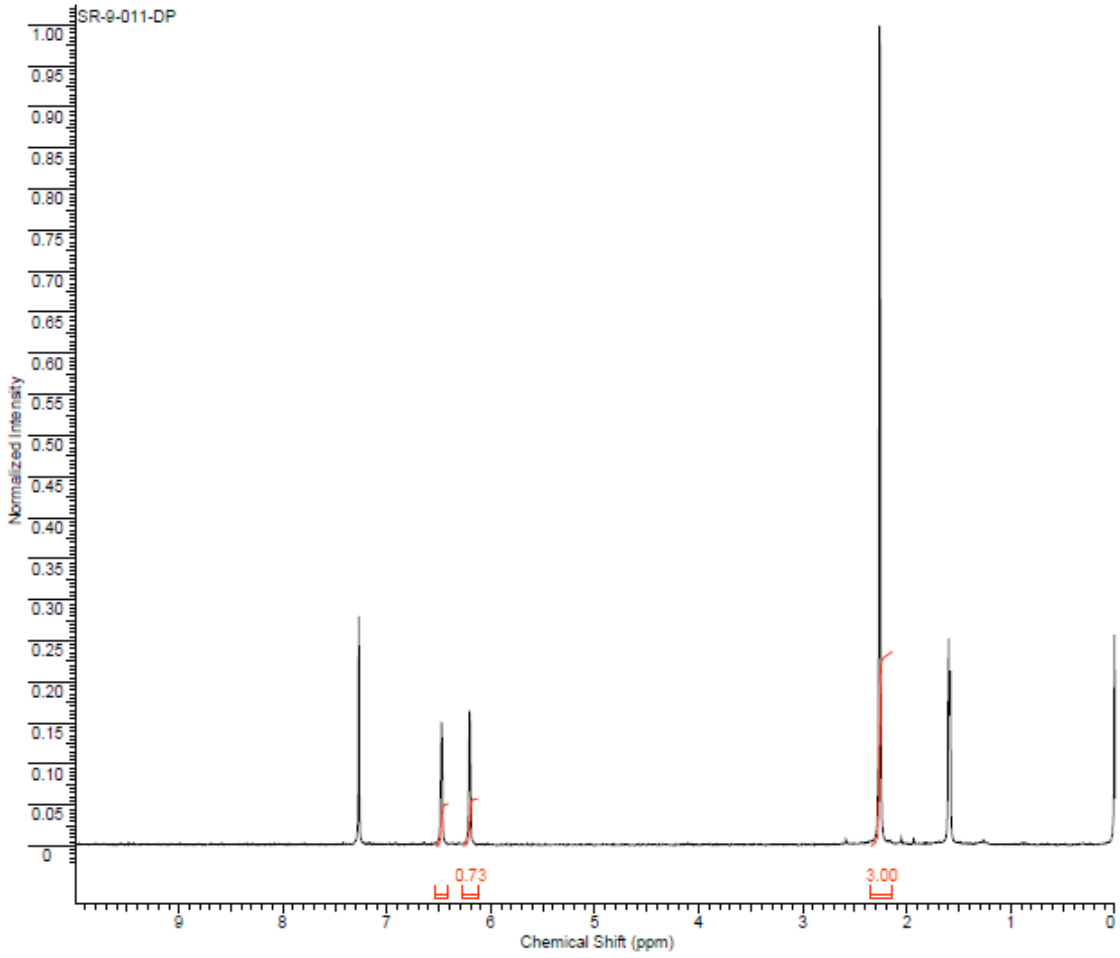

Formula $C_6H_5N_3O_2$	FW	151.1228

Acquisition Time (sec)	1.9945	*Comment*	STANDARD 1H OBSERVE		
Date	Aug 29 2008	*Date Stamp*	Aug 29 2008	*File Name*	C:\NMR 031009\200\BOOK 9\SR-9-12-DP
Frequency (MHz)	199.98	*Nucleus*	1H	*Number of Transients*	32
Original Points Count	5984	*Points Count*	8192	*Pulse Sequence*	s2pul
Receiver Gain	40.00	*Solvent*	CHLOROFORM-d		
Spectrum Offset (Hz)	1002.0226	*Sweep Width (Hz)*	3000.30	*Temperature (degree C)*	29.000

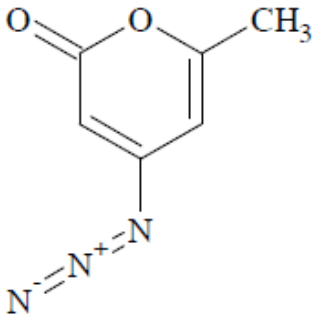

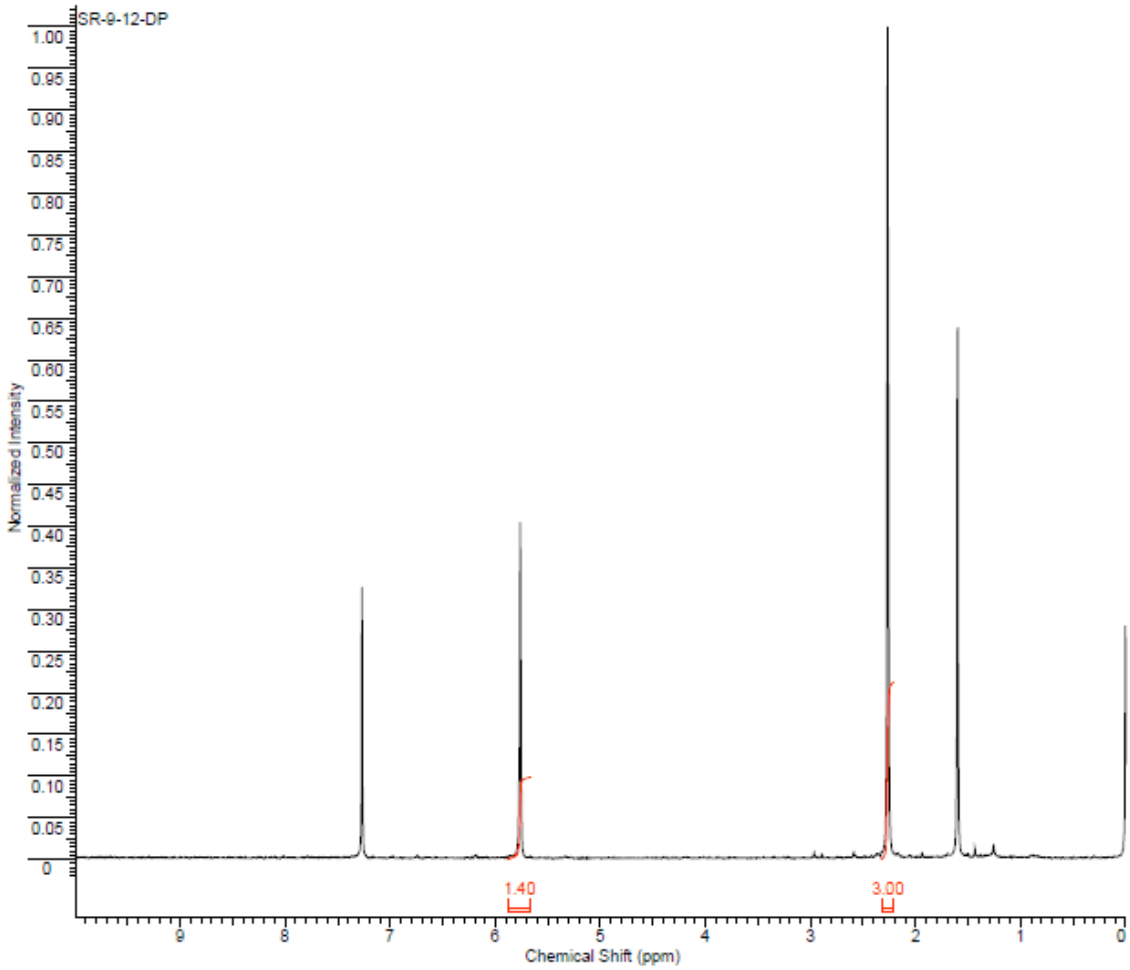

Formula $C_7H_7N_3O$	FW	149.1500

Acquisition Time (sec)	1.4976	Comment	13C OBSERVE	Date	Apr 25 2008
Date Stamp	Apr 25 2008				
File Name	C:\NMR BACKUP\010609NMR BACKUP\200\HUA-NEW\SANDEEP\BOOK8\SR-8-16-13C				
Frequency (MHz)	50.29	Nucleus	13C	Number of Transients	2000
Original Points Count	18720	Points Count	32768	Pulse Sequence	s2pul
Receiver Gain	40.00	Solvent	CHLOROFORM-d		
Spectrum Offset (Hz)	4869.7793	Sweep Width (Hz)	12500.00	Temperature (degree C)	29.000

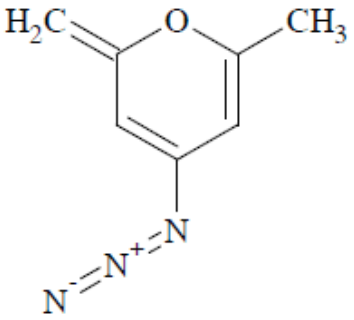

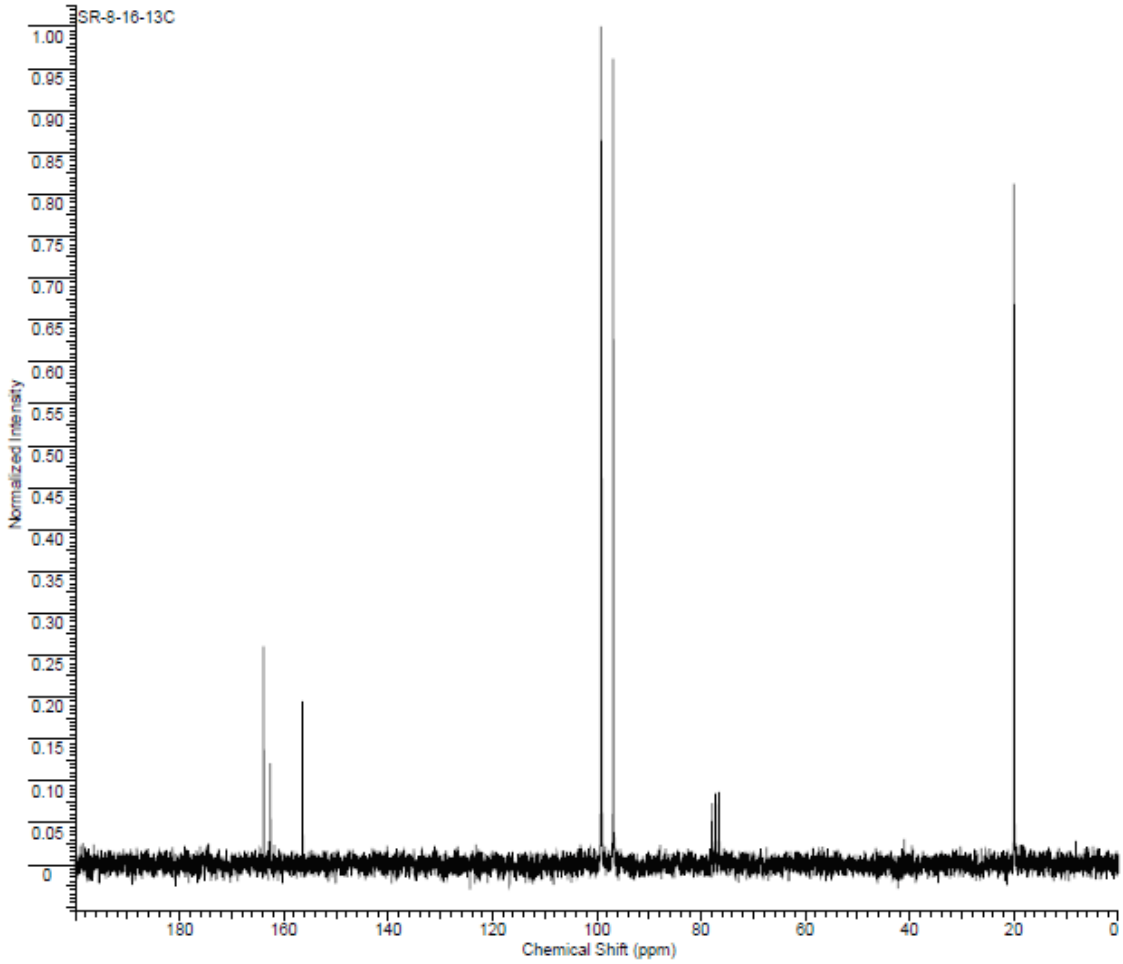

Formula $C_6H_7NO_2$	FW	125.1253			
Acquisition Time (sec)	1.9945	Comment	STANDARD 1H OBSERVE		
Date	Aug 21 2008	Date Stamp	Aug 21 2008		
File Name	C:\NMR BACKUP\010609NMR BACKUP\200\HUA-NEW\SANDEEP\BOOK8\SR-8-110-DP				
Frequency (MHz)	199.98	Nucleus	1H	Number of Transients	64
Original Points Count	5984	Points Count	8192	Pulse Sequence	s2pul
Receiver Gain	40.00	Solvent	CHLOROFORM-d		
Spectrum Offset (Hz)	1002.0226	Sweep Width (Hz)	3000.30	Temperature (degree C)	29.000

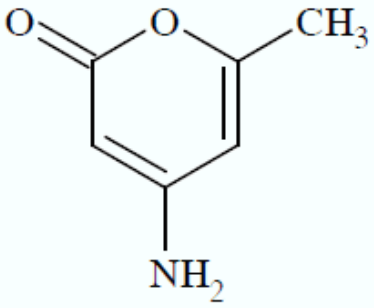

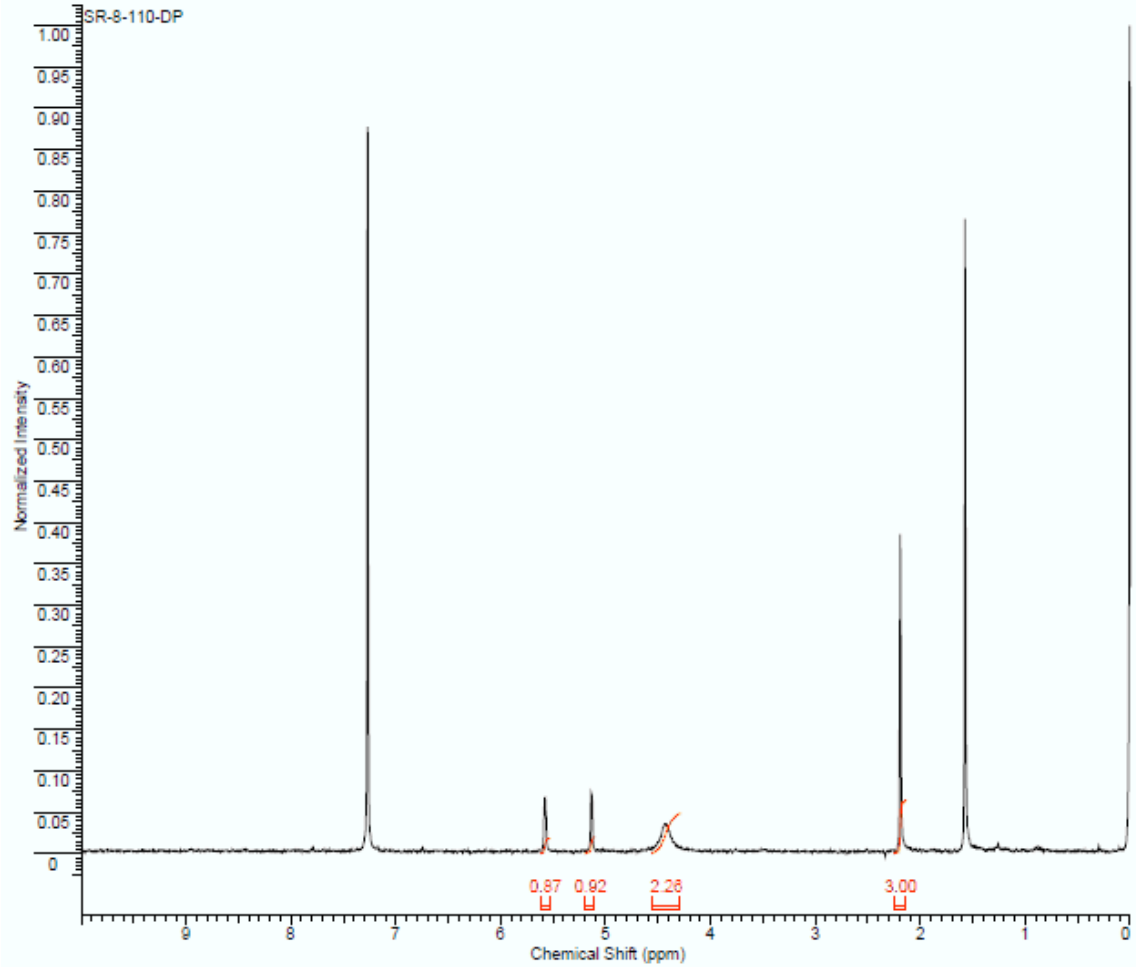

Formula $C_{16}H_{17}NO_2$	FW	255.3117		

Acquisition Time (sec)	1.9945	*Comment*	STANDARD 1H OBSERVE		
Date	May 10 2008	*Date Stamp*	May 10 2008	*File Name*	C:\SANDEEP NMR\SR-8-34-FR20
Frequency (MHz)	199.98	*Nucleus*	1H	*Number of Transients*	32
Original Points Count	5984	*Points Count*	8192	*Pulse Sequence*	s2pul
Receiver Gain	28.00	*Solvent*	CHLOROFORM-d		
Spectrum Offset (Hz)	1002.0226	*Sweep Width (Hz)*	3000.30	*Temperature (degree C)*	29.000

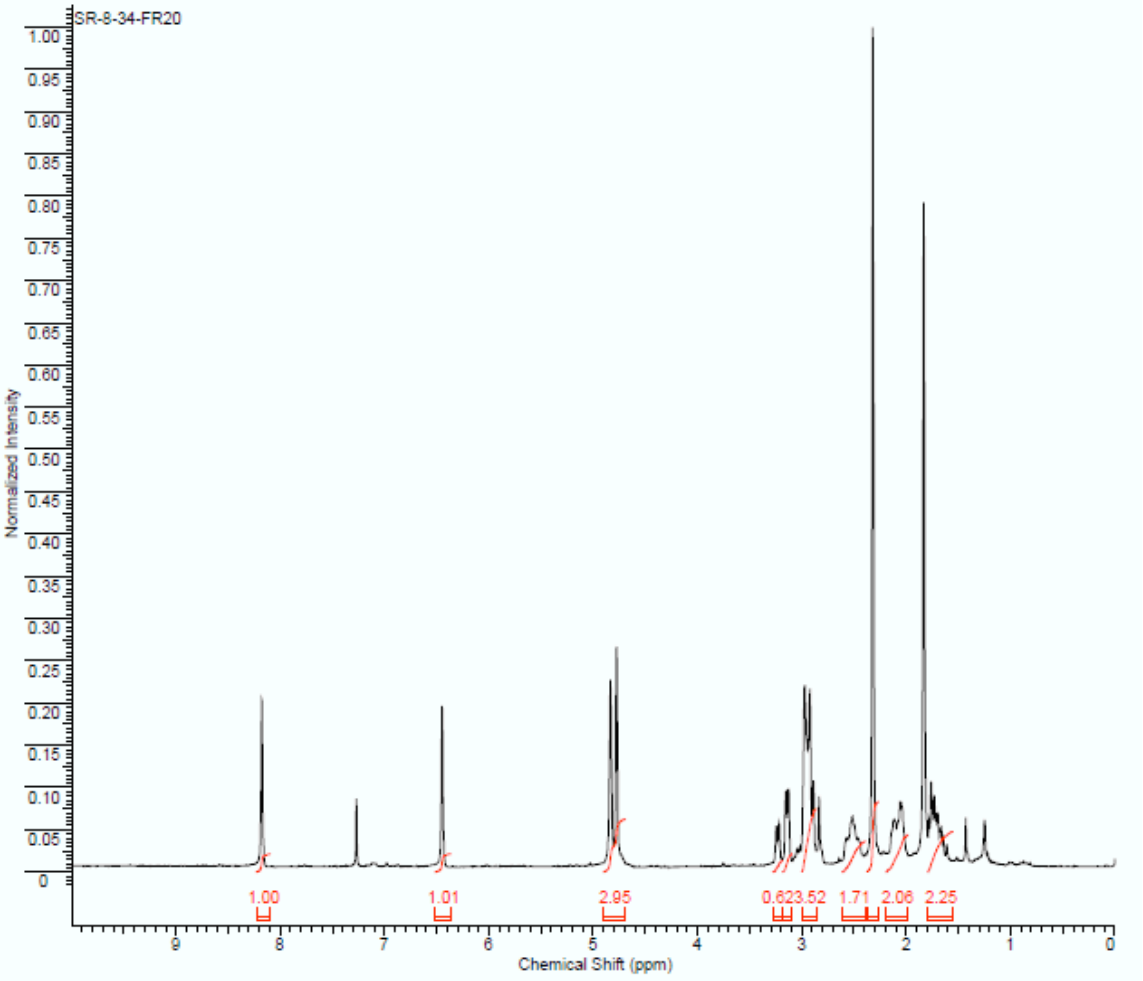

Formula $C_{16}H_{17}NO_2$	FW	255.3117

Acquisition Time (sec)	1.4976	Comment	13C OBSERVE		
Date	May 10 2008	Date Stamp	May 10 2008	File Name	C:\SANDEEP NMR\SR-8-34-FR20-13C
Frequency (MHz)	50.29	Nucleus	13C	Number of Transients	20000
Original Points Count	18720	Points Count	32768	Pulse Sequence	s2pul
Receiver Gain	40.00	Solvent	CHLOROFORM-d		
Spectrum Offset (Hz)	4880.0796	Sweep Width (Hz)	12500.00	Temperature (degree C)	29.000

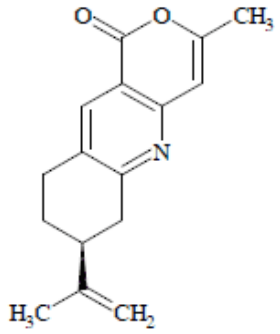

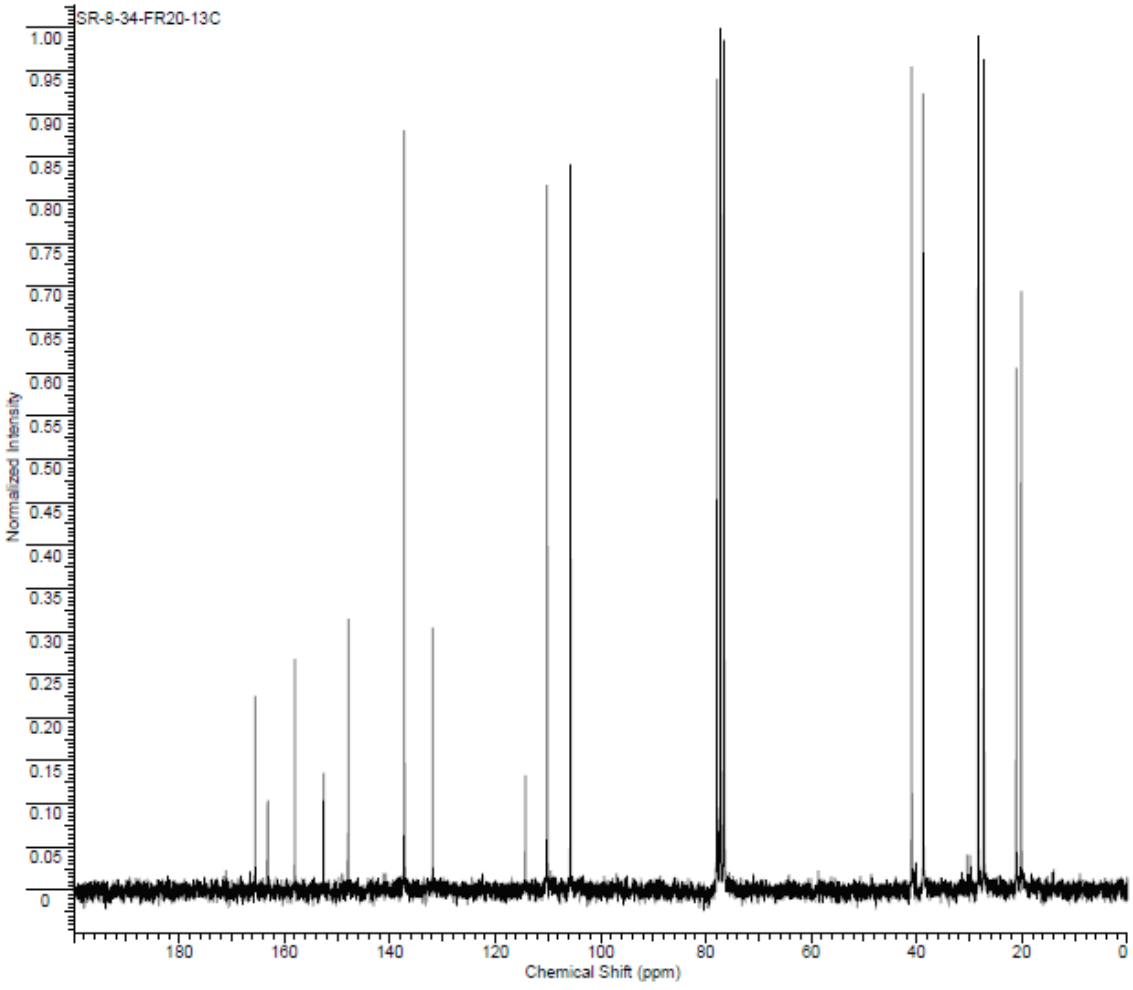

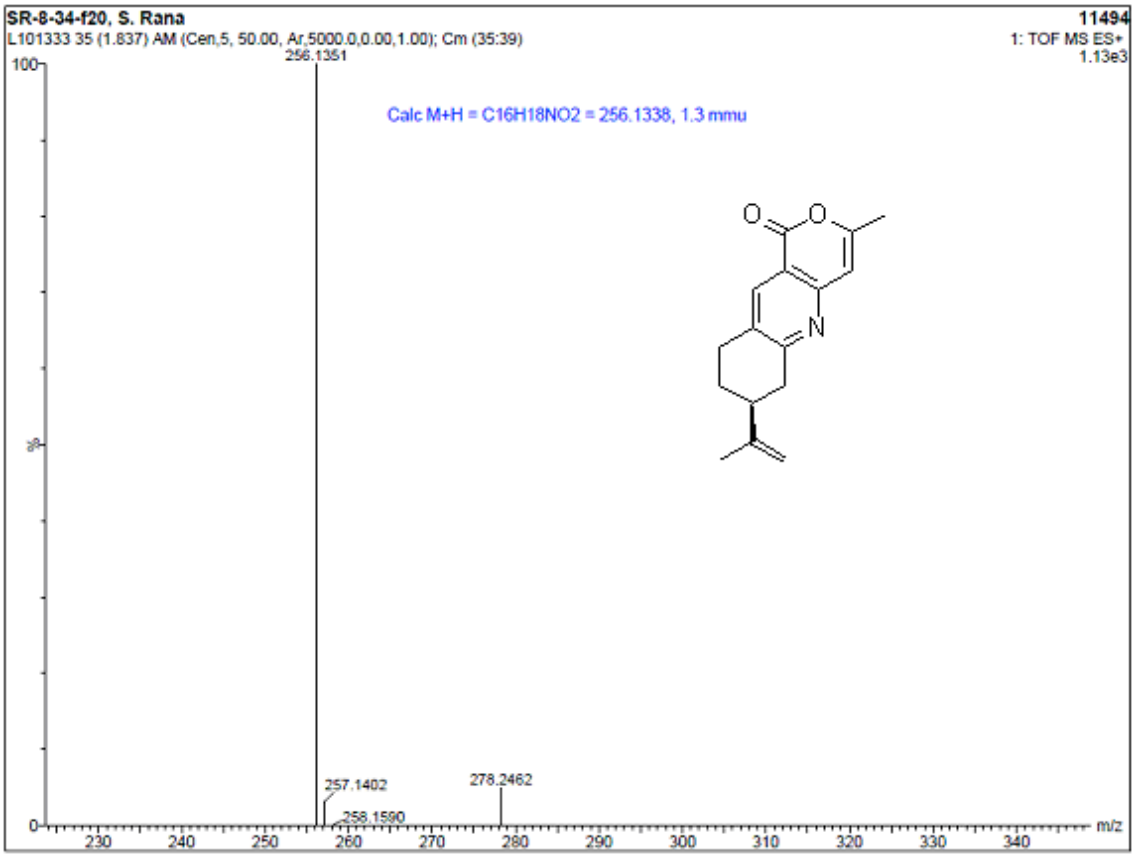
SR-8-34-f20, S. Rana
11494
L101333 35 (1.837) AM (Cen,5, 50.00, Ar,5000.0,0.00,1.00); Cm (35:39)
1: TOF MS ES+
1.13e3
256.1351
Calc M+H = C16H18NO2 = 256.1338, 1.3 mmu
257.1402
278.2462
258.1590
%
m/z

Formula $C_{15}H_{17}NO_2$	FW	255.3117		
Acquisition Time (sec)	1.9945	Comment	STANDARD 1H OBSERVE	
Date	Aug 19 2008	Date Stamp	Aug 19 2008	
File Name	C:\NMR BACKUP\010609NMR BACKUP\200\HUA-NEW\SANDEEP\BOOK8\SR-L-SHAPE-PYRONE-TFA			
Frequency (MHz)	199.98	Nucleus	1H	Number of Transients 64
Original Points Count	5984	Points Count	8192	Pulse Sequence s2pul
Receiver Gain	40.00	Solvent	CHLOROFORM-d	
Spectrum Offset (Hz)	1002.0226	Sweep Width (Hz)	3000.30	Temperature (degree C) 29.000

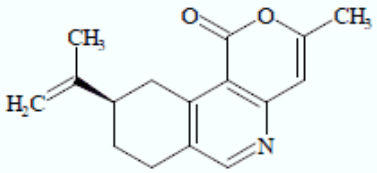

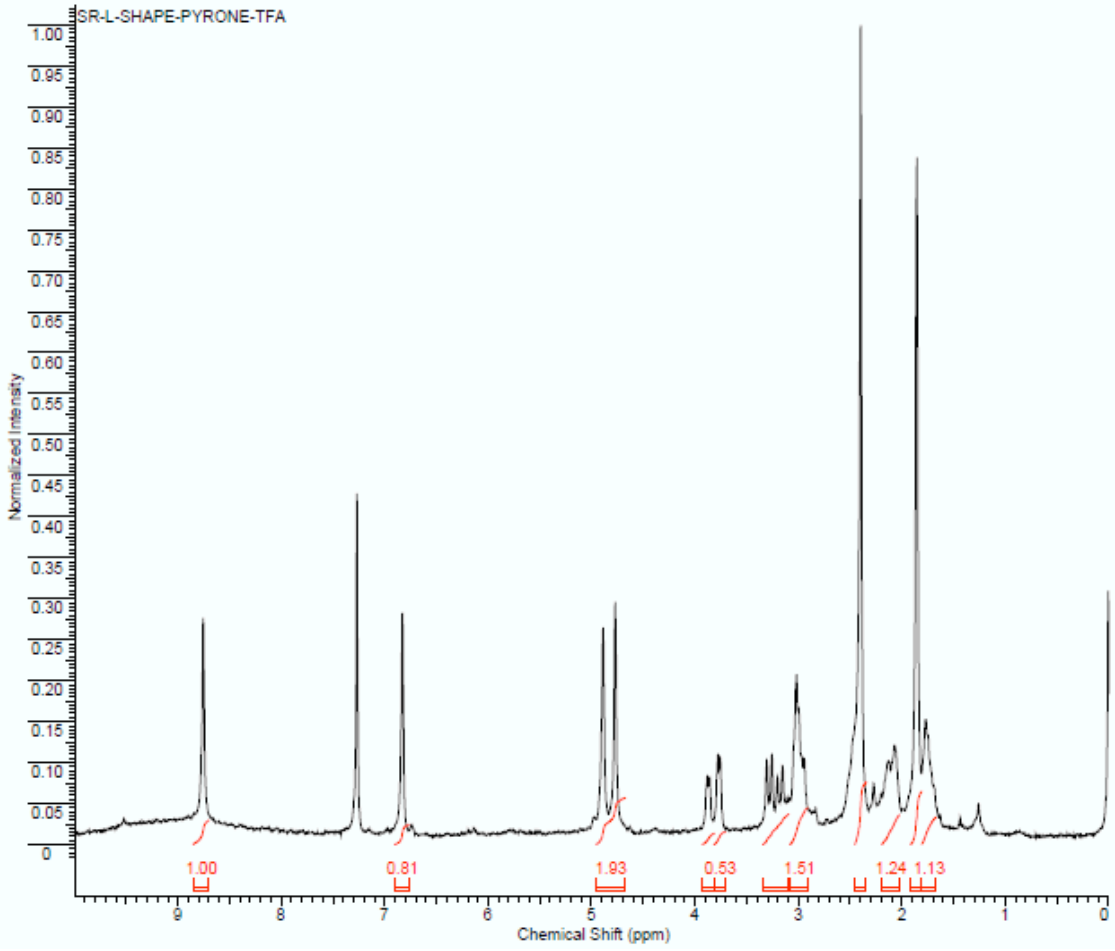

Formula $C_{16}H_{17}NO_3$	FW	255.3117

Acquisition Time (sec)	1.3005	Comment	Std proton	Date	May 11 2008
Date Stamp	May 11 2008			File Name	C:\SANDEEP NMR\SR-8-34-FR29-13C
Frequency (MHz)	100.53	Nucleus	13C	Number of Transients	5000
Original Points Count	31375	Points Count	32768	Pulse Sequence	s2pul
Receiver Gain	30.00	Solvent	CHLOROFORM-d		
Spectrum Offset (Hz)	10556.2627	Sweep Width (Hz)	24125.45	Temperature (degree C)	25.000

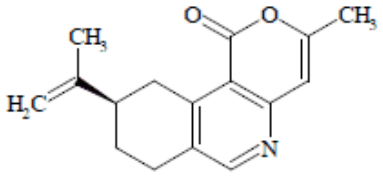

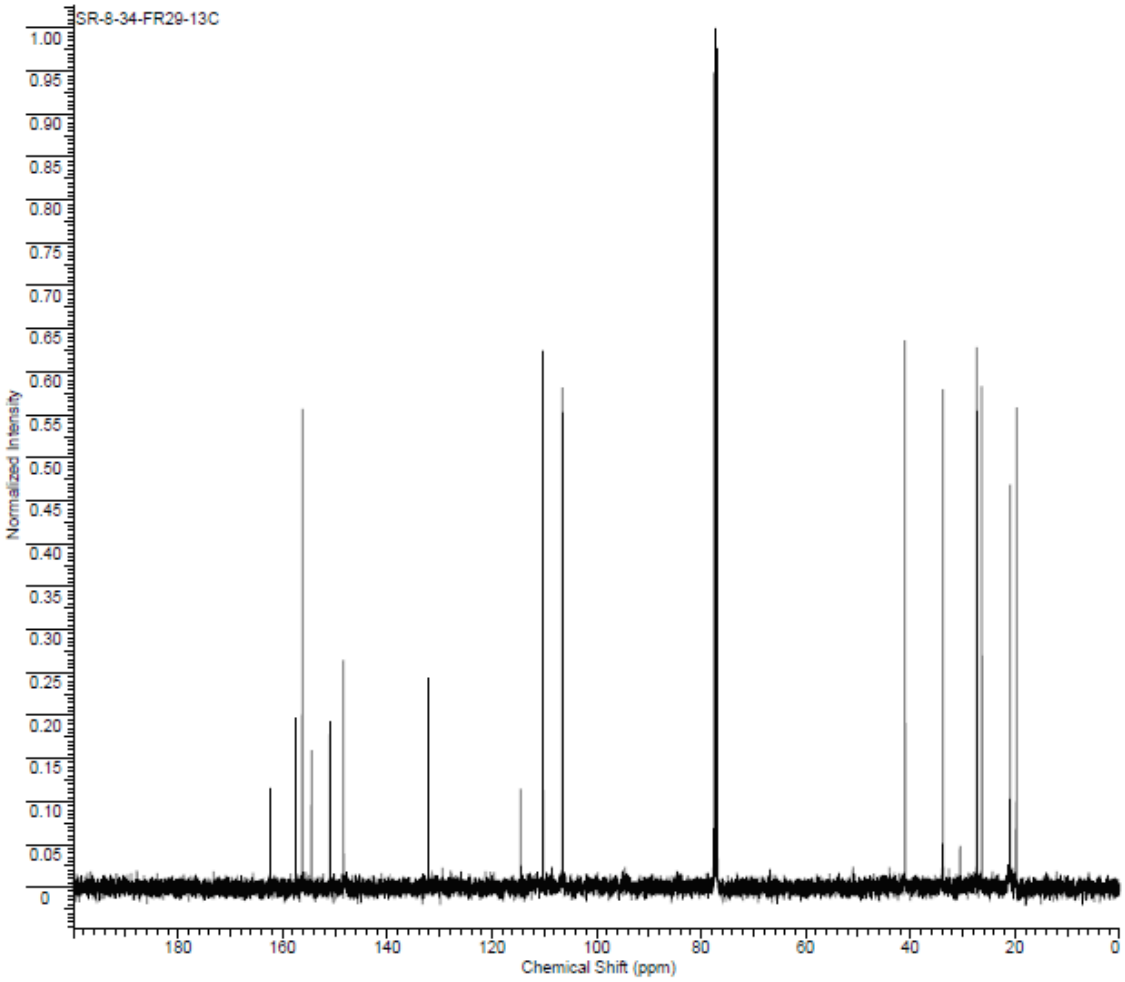

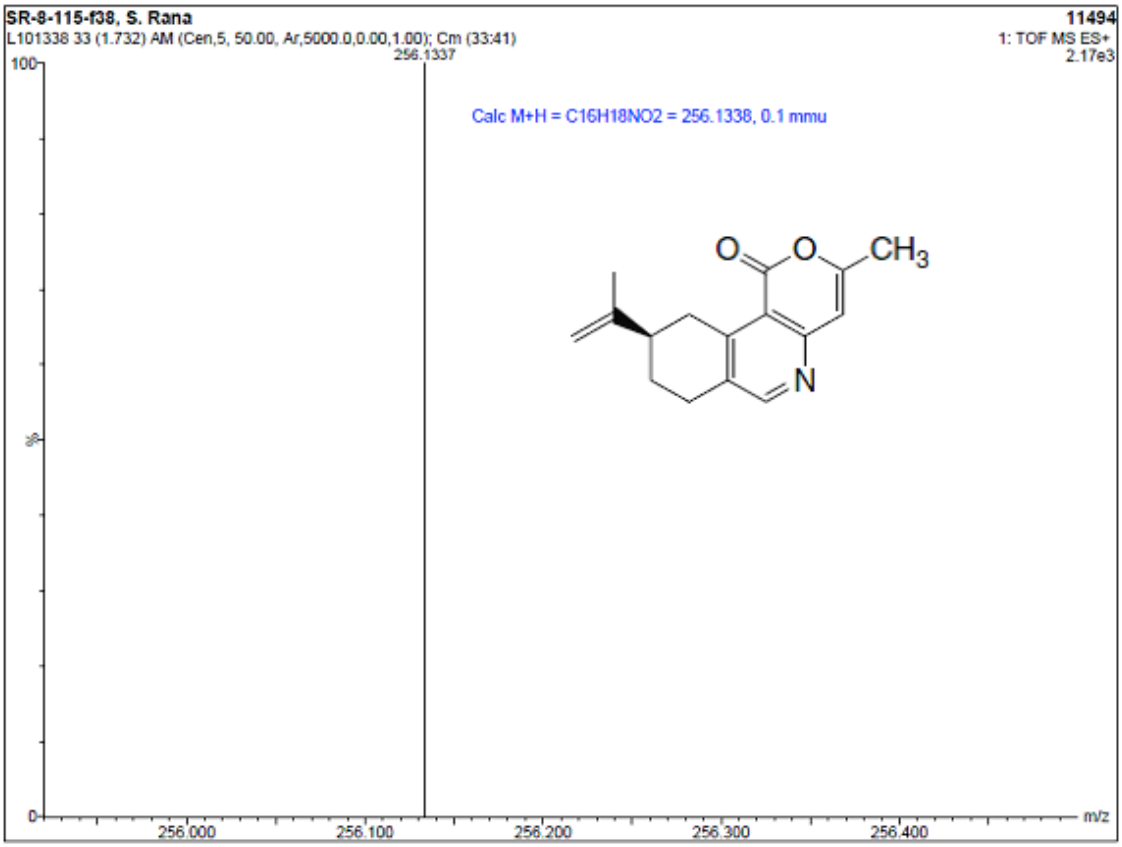
SR-8-115-f38, S. Rana
L101338 33 (1.732) AM (Cen,5, 50.00, Ar,5000.0,0.00,1.00); Cm (33:41)
11494
1: TOF MS ES+
2.17e3
256.1337
100
%
0
Calc M+H = C16H18NO2 = 256.1338, 0.1 mmu
O
O
CH3
N
256.000
256.100
256.200
256.300
256.400
m/z

Formula $C_{16}H_{17}NO_2$	FW	243.3010

Acquisition Time (sec)	2.0487	Comment	Std proton	Date	Nov 3 2008
Date Stamp	Nov 3 2008			File Name	C:\SANDEEP NMR\SR-9-44-DMSO
Frequency (MHz)	399.76	Nucleus	1H	Number of Transients	16
Original Points Count	13103	Points Count	16384	Pulse Sequence	s2pul
Receiver Gain	20.00	Solvent	DMSO-d6	Spectrum Offset (Hz)	2418.7058
Sweep Width (Hz)	6395.91	Temperature (degree C)	25.000		

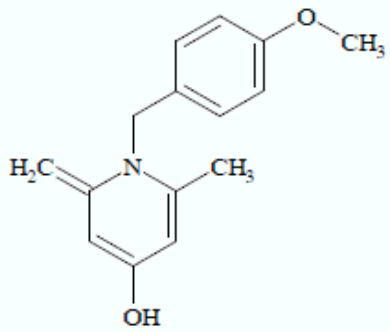

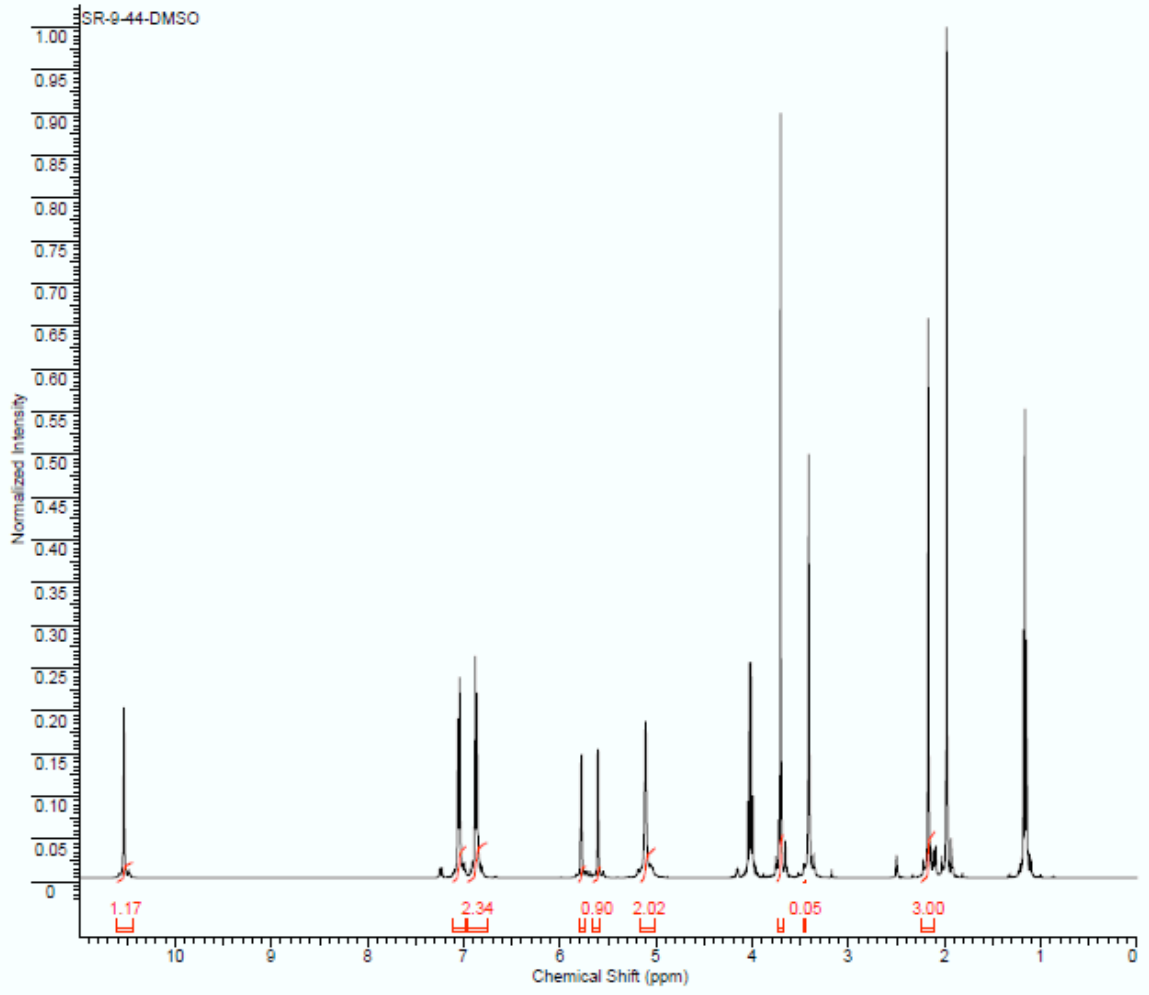

Formula $C_{15}H_{17}NO_2$	FW 243.3010

Acquisition Time (sec)	1.3005	Comment	Std proton	Date	Nov 2 2008
Date Stamp	Nov 2 2008	File Name	C:\SANDEEP NMR\SR-9-44-13C-DMSO		
Frequency (MHz)	100.53	Nucleus	13C	Number of Transients	20000
Original Points Count	31375	Points Count	32768	Pulse Sequence	s2pul
Receiver Gain	30.00	Solvent	DMSO-d6	Spectrum Offset (Hz)	10493.5039
Sweep Width (Hz)	24125.45	Temperature (degree C)	25.000		

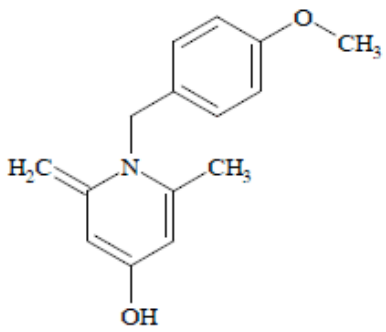

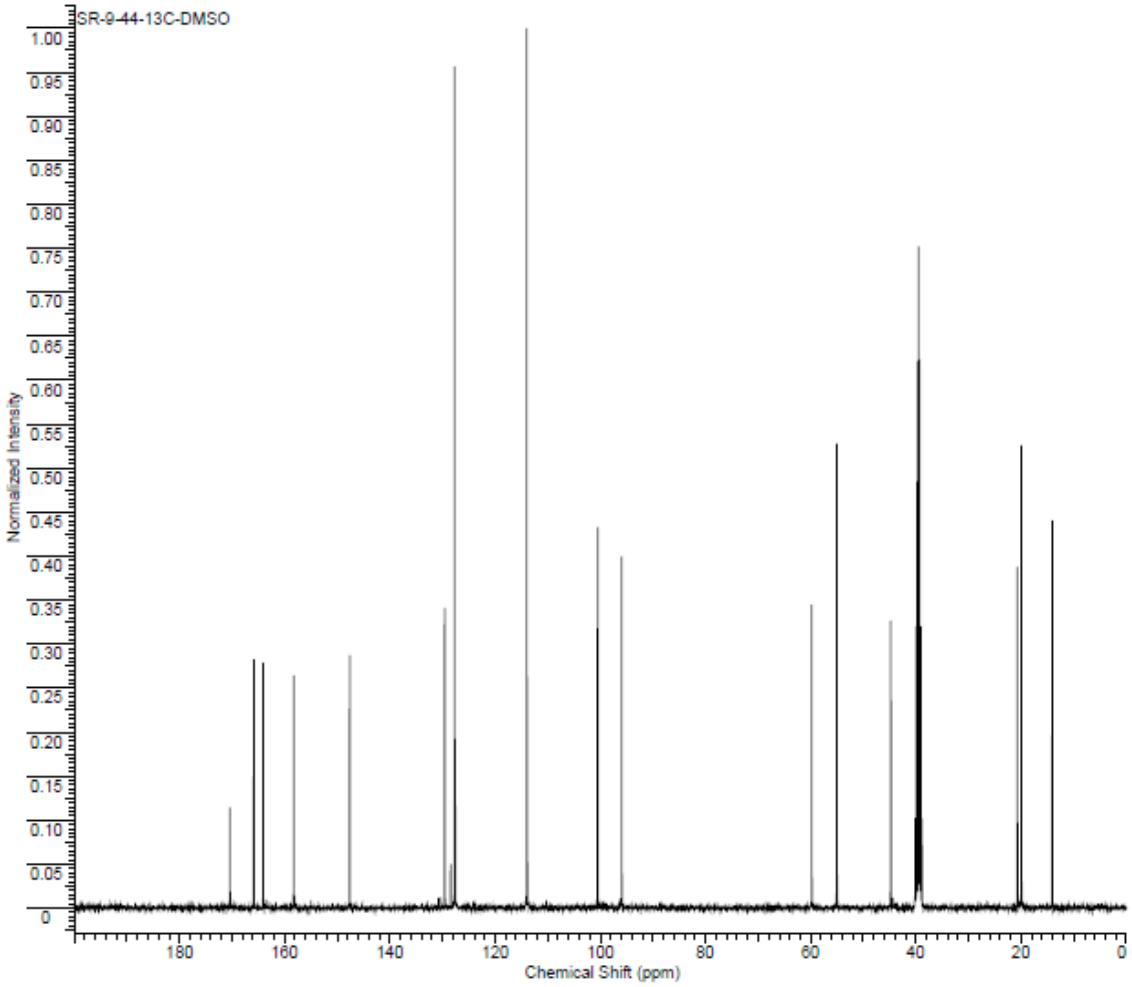

Formula $C_{24}H_{27}NO_3$	FW	377.4761		

Acquisition Time (sec)	1.9945	Comment	STANDARD 1H OBSERVE		
Date	Jun 18 2008	Date Stamp	Jun 18 2008	File Name	C:\SANDEEP NMR\SR-8-60-FR11
Frequency (MHz)	199.98	Nucleus	1H	Number of Transients	32
Original Points Count	5984	Points Count	8192	Pulse Sequence	s2pul
Receiver Gain	28.00	Solvent	CHLOROFORM-d		
Spectrum Offset (Hz)	1001.6563	Sweep Width (Hz)	3000.30	Temperature (degree C)	29.000

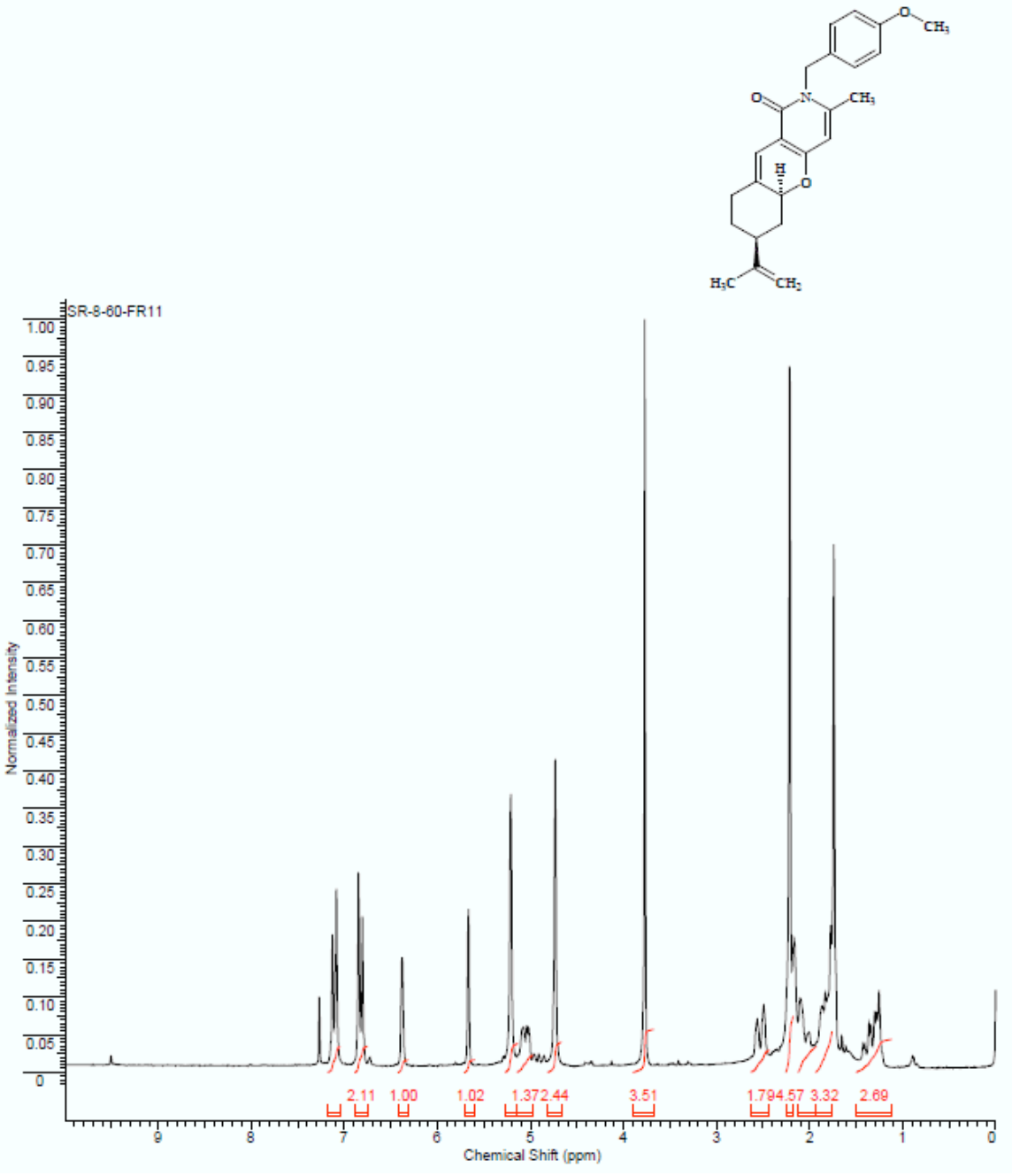

Formula $C_{24}H_{27}NO_3$	FW 377.4761

Acquisition Time (sec)	1.4976	Comment	13C OBSERVE		
Date	Jun 20 2008	Date Stamp	Jun 20 2008	File Name	C:\SANDEEP NMR\SR-8-61-FR6-10-13C
Frequency (MHz)	50.29	Nucleus	13C	Number of Transients	20000
Original Points Count	16720	Points Count	32768	Pulse Sequence	s2pul
Receiver Gain	40.00	Solvent	CHLOROFORM-d		
Spectrum Offset (Hz)	4872.8311	Sweep Width (Hz)	12500.00	Temperature (degree C)	29.000

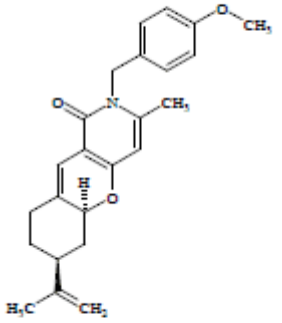

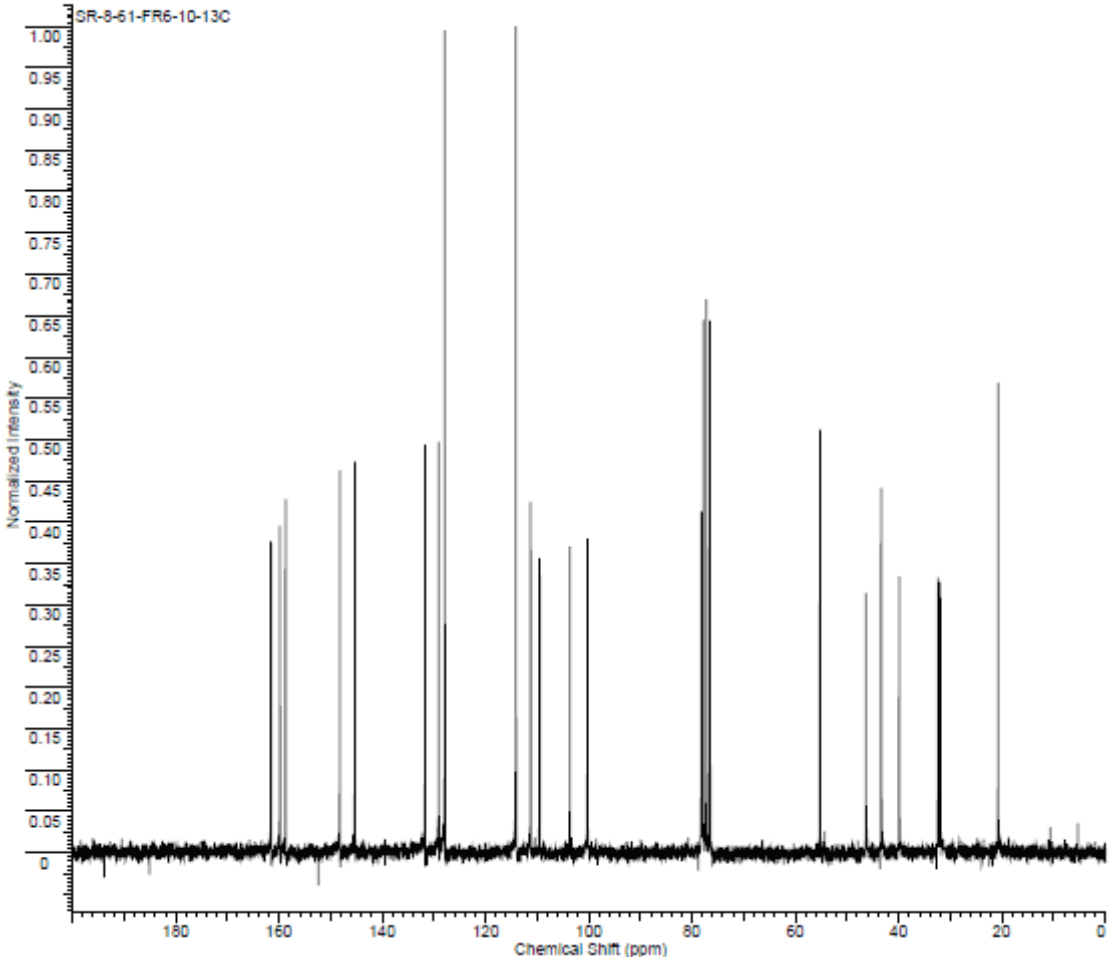

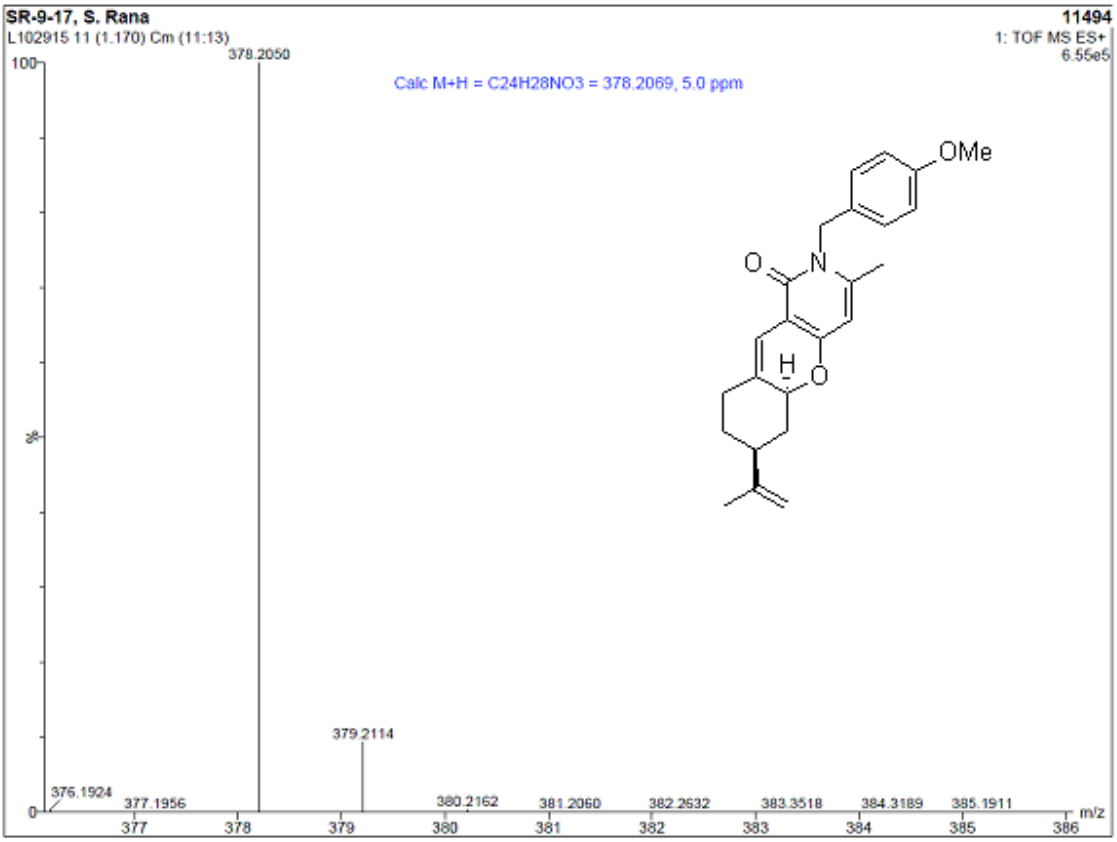
SR-9-17, S. Rana
11494
L102915 11 (1.170) Cm (11:13)
1: TOF MS ES+
6.55e5
100
%
0
378.2050
Calc M+H = C24H28NO3 = 378.2069, 5.0 ppm
OMe
O
N
H
O
379.2114
376.1924
377.1956
380.2162
381.2060
382.2632
383.3518
384.3189
385.1911
m/z
377
378
379
380
381
382
383
384
385
386

Formula $C_{24}H_{28}NO_4$	FW	395.4914

Acquisition Time (sec)	2.0486	Comment	SR-8-71-fr20		
Date	Jun 30 2008			Date Stamp	Jun 30 2008
File Name	C:\SANDEEP NMR\SR-8-71-FR20			Frequency (MHz)	399.76
Nucleus	1H	Number of Transients	32	Original Points Count	9827
Points Count	16384	Pulse Sequence	s2pul	Receiver Gain	26.00
Solvent	CHLOROFORM-d			Spectrum Offset (Hz)	2017.4581
Sweep Width (Hz)	4797.03	Temperature (degree C)	25.000		

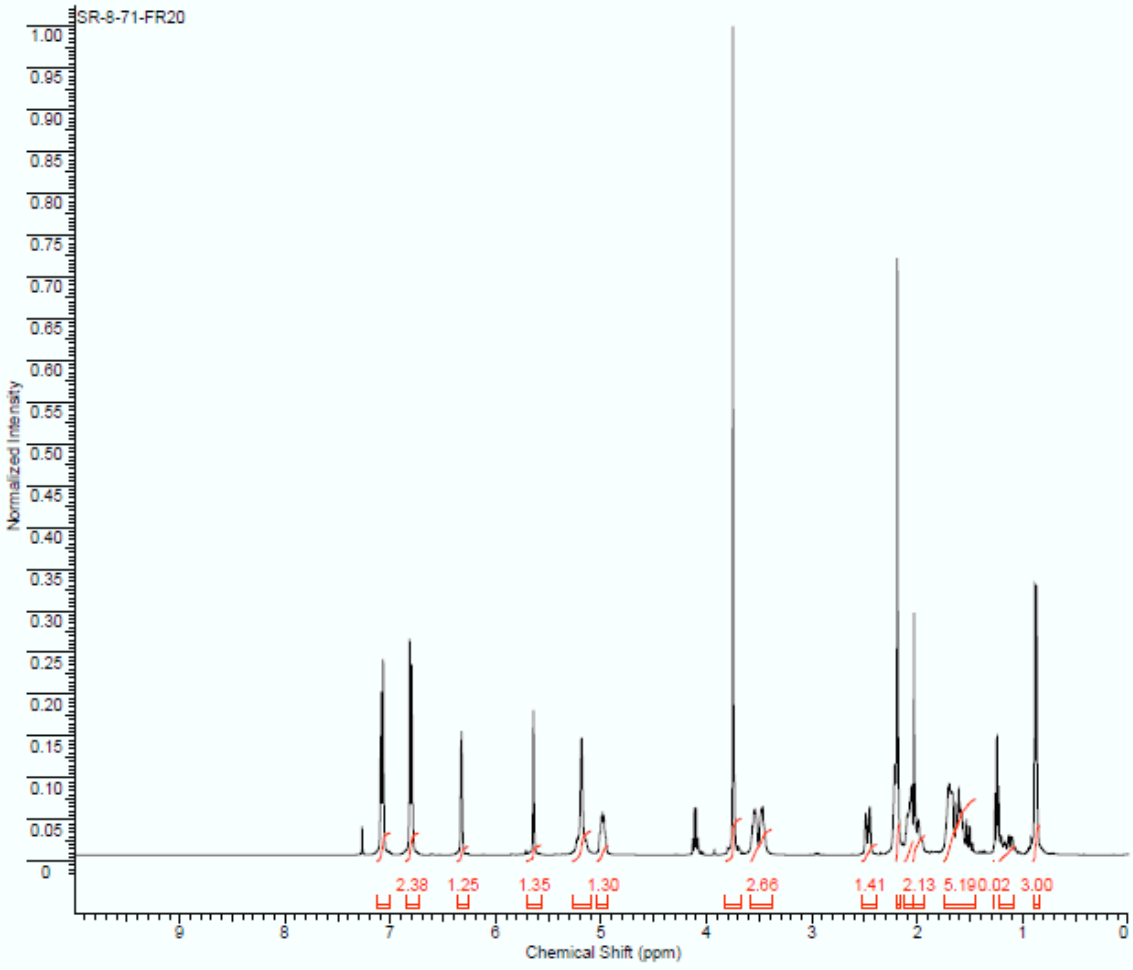

Formula $C_{24}H_{28}NO_4$	FW	395.4914

Acquisition Time (sec)	1.3005	Comment	SR-8-71-fr20		
Date	Jul 2 2008	Date Stamp	Jul 2 2008	File Name	C:\SANDEEP NMR\SR-8-71-FR20-13C
Frequency (MHz)	100.53	Nucleus	13C	Number of Transients	2000
Original Points Count	31375	Points Count	32768	Pulse Sequence	s2pul
Receiver Gain	30.00	Solvent	CHLOROFORM-d		
Spectrum Offset (Hz)	10554.7900	Sweep Width (Hz)	24125.45	Temperature (degree C)	25.000

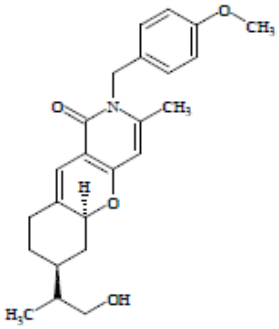

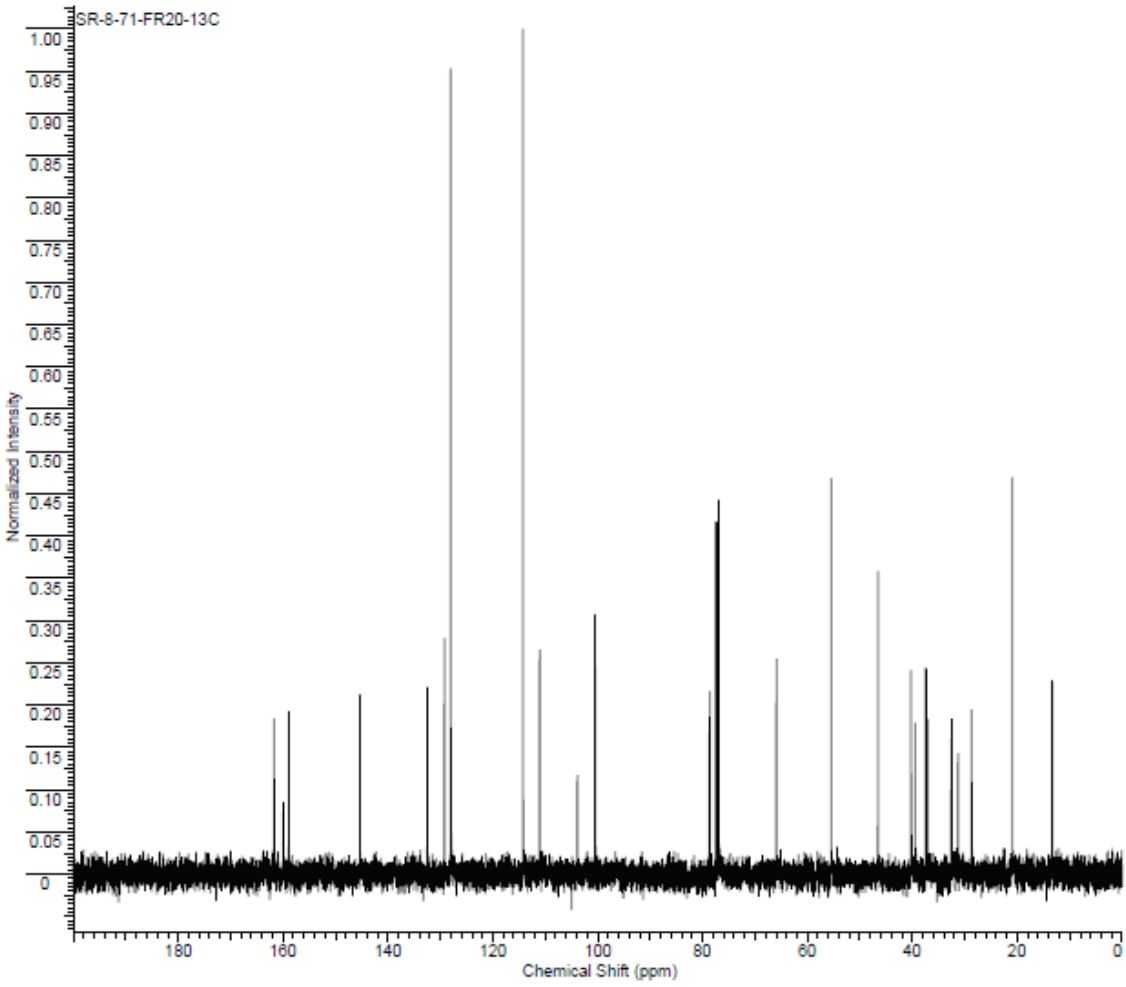

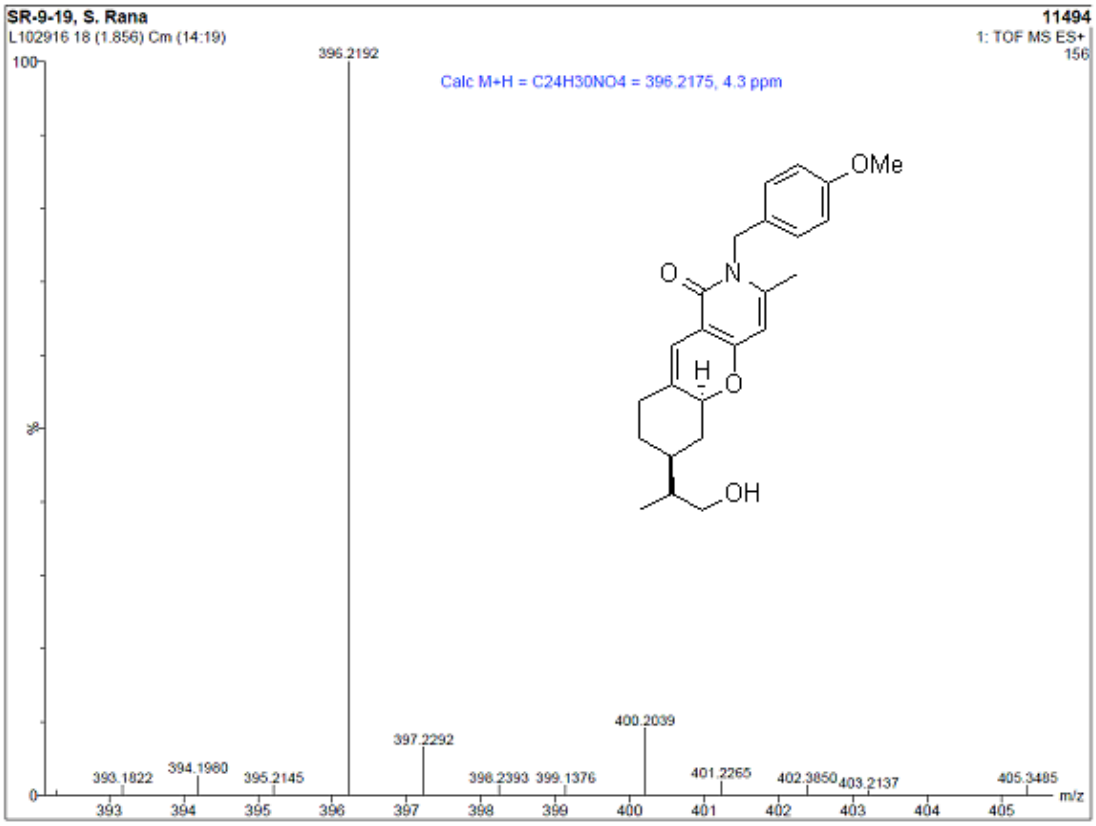
SR-9-19, S. Rana
11494
L102916 18 (1.856) Cm (14:19)
1: TOF MS ES+
156
396.2192
Calc M+H = C24H30NO4 = 396.2175, 4.3 ppm
OMe
O
N
H
O
OH
100
%
0
393.1822
394.1980
395.2145
397.2292
398.2393
399.1376
400.2039
401.2265
402.3850
403.2137
405.3485
393
394
395
396
397
398
399
400
401
402
403
404
405
m/z

Formula $C_{24}H_{28}NO_3^+$	FW	378.4840+?

Acquisition Time (sec)	2.0487	Comment	SR-8-74-fr14		
Date	Jul 2 2008	Date Stamp	Jul 2 2008	File Name	C:\SANDEEP NMR\SR-8-74-FR14
Frequency (MHz)	399.76	Nucleus	1H	Number of Transients	32
Original Points Count	13103	Points Count	16384	Pulse Sequence	s2pul
Receiver Gain	44.00	Solvent	CHLOROFORM-d		
Spectrum Offset (Hz)	2417.2959	Sweep Width (Hz)	6395.91	Temperature (degree C)	25.000

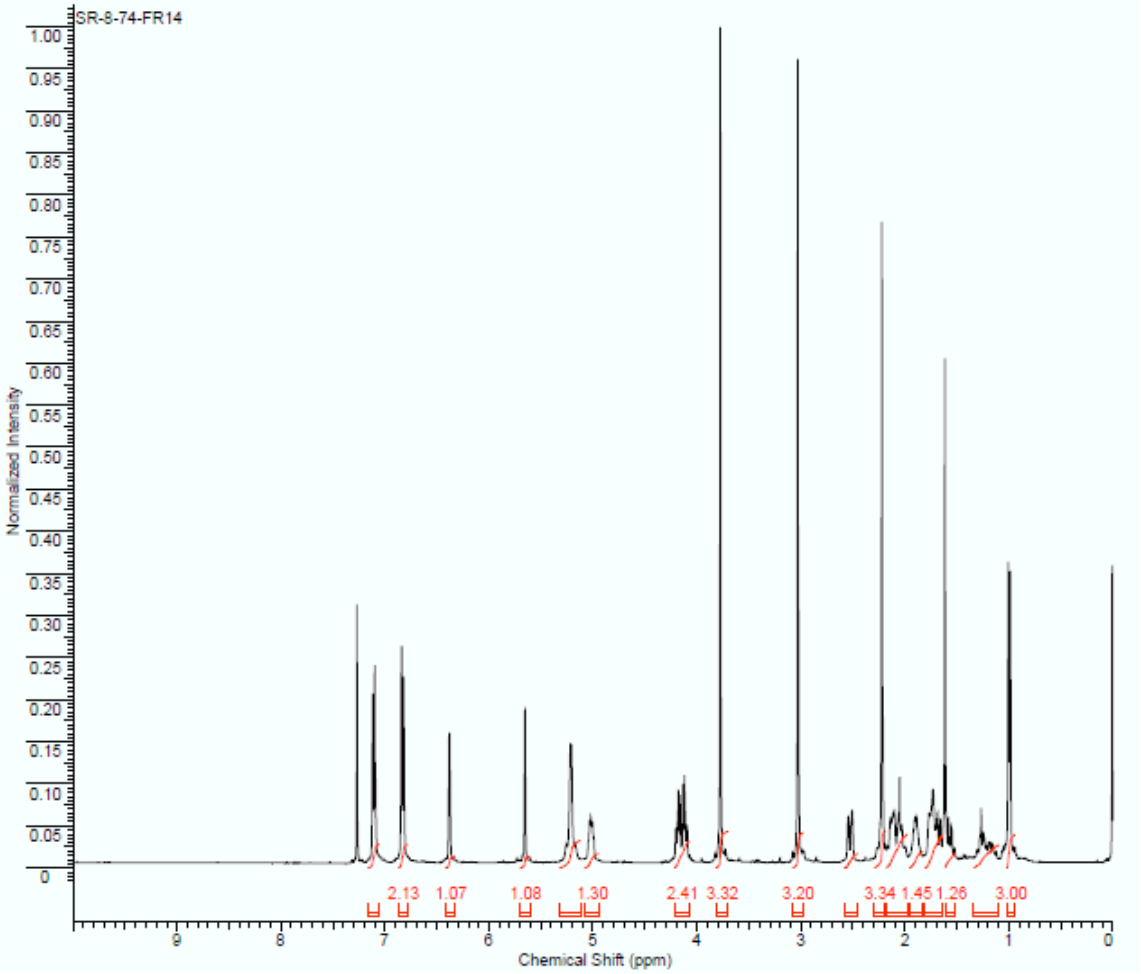

Formula $C_{24}H_{29}NO_3$?	FW	378.4840+?

Acquisition Time (sec)	1.3004	Comment	SR-8-74-13Cwft aph		
Date	Jul 2 2008	Date Stamp	Jul 2 2008	File Name	C:\SANDEEP NMR\SR-8-74-13C
Frequency (MHz)	100.53	Nucleus	13C	Number of Transients	2000
Original Points Count	31373	Points Count	32768	Pulse Sequence	s2pul
Receiver Gain	30.00	Solvent	CHLOROFORM-d		
Spectrum Offset (Hz)	10546.6904	Sweep Width (Hz)	24125.45	Temperature (degree C)	25.000

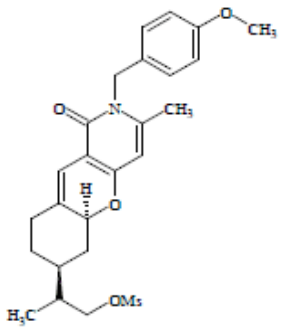

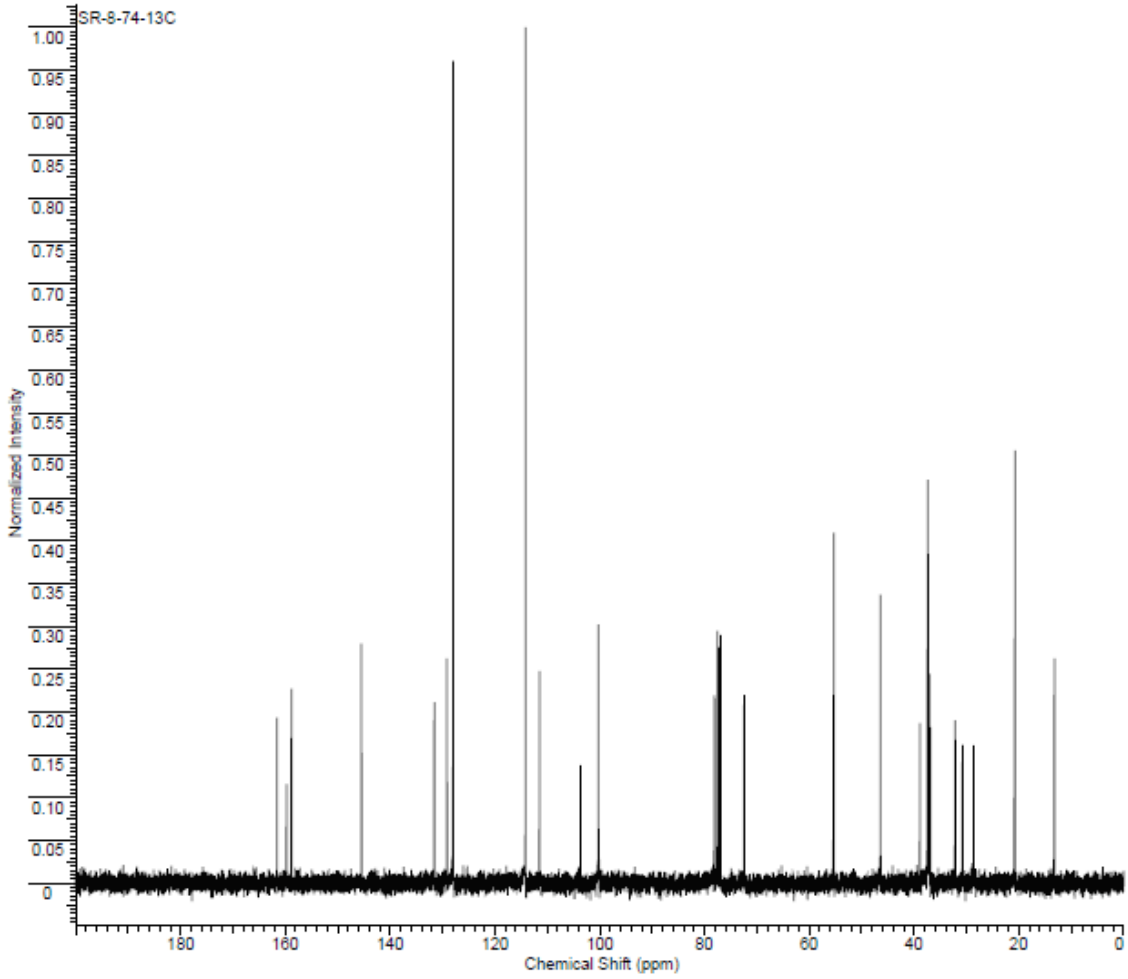

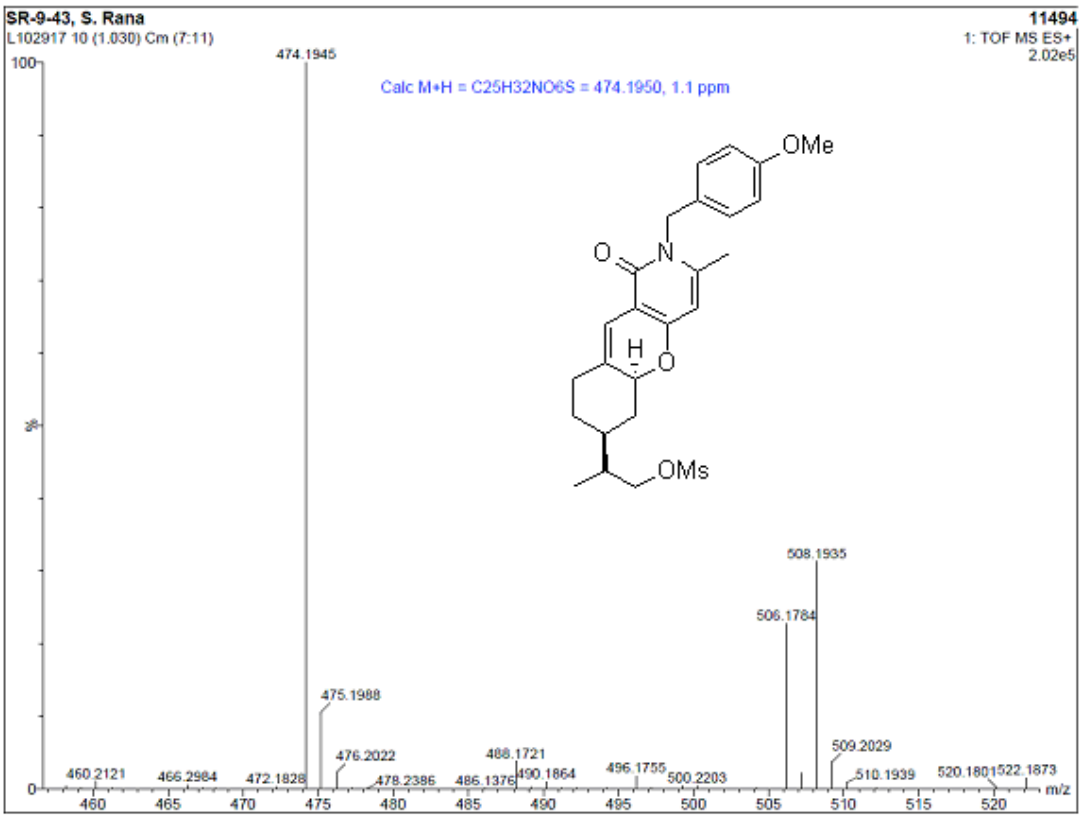
SR-9-43, S. Rana
L102917 10 (1.030) Cm (7:11)
11494
1: TOF MS ES+
2.02e5
Calc M+H = C25H32NO6S = 474.1950, 1.1 ppm
OMe
O
N
H
O
OMs
%
m/z
474.1945
475.1988
476.2022
460.2121
466.2984
472.1828
478.2386
488.1721
486.1376
490.1864
496.1755
500.2203
508.1935
506.1784
509.2029
510.1939
520.1801
522.1873

Formula $C_{29}H_{32}N_6O_3$	FW	512.6028

Acquisition Time (sec)	1.9945	Comment	STANDARD 1H OBSERVE		
Date	Jul 7 2008	Date Stamp	Jul 7 2008	File Name	C:\SANDEEP NMR\SR-8-78-FR27
Frequency (MHz)	199.98	Nucleus	1H	Number of Transients	64
Original Points Count	5984	Points Count	8192	Pulse Sequence	s2pul
Receiver Gain	40.00	Solvent	CHLOROFORM-d		
Spectrum Offset (Hz)	1002.0226	Sweep Width (Hz)	3000.30	Temperature (degree C)	29.000

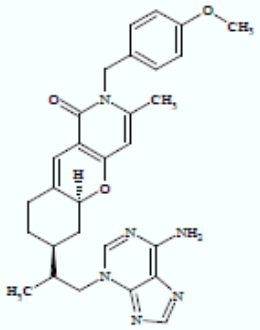

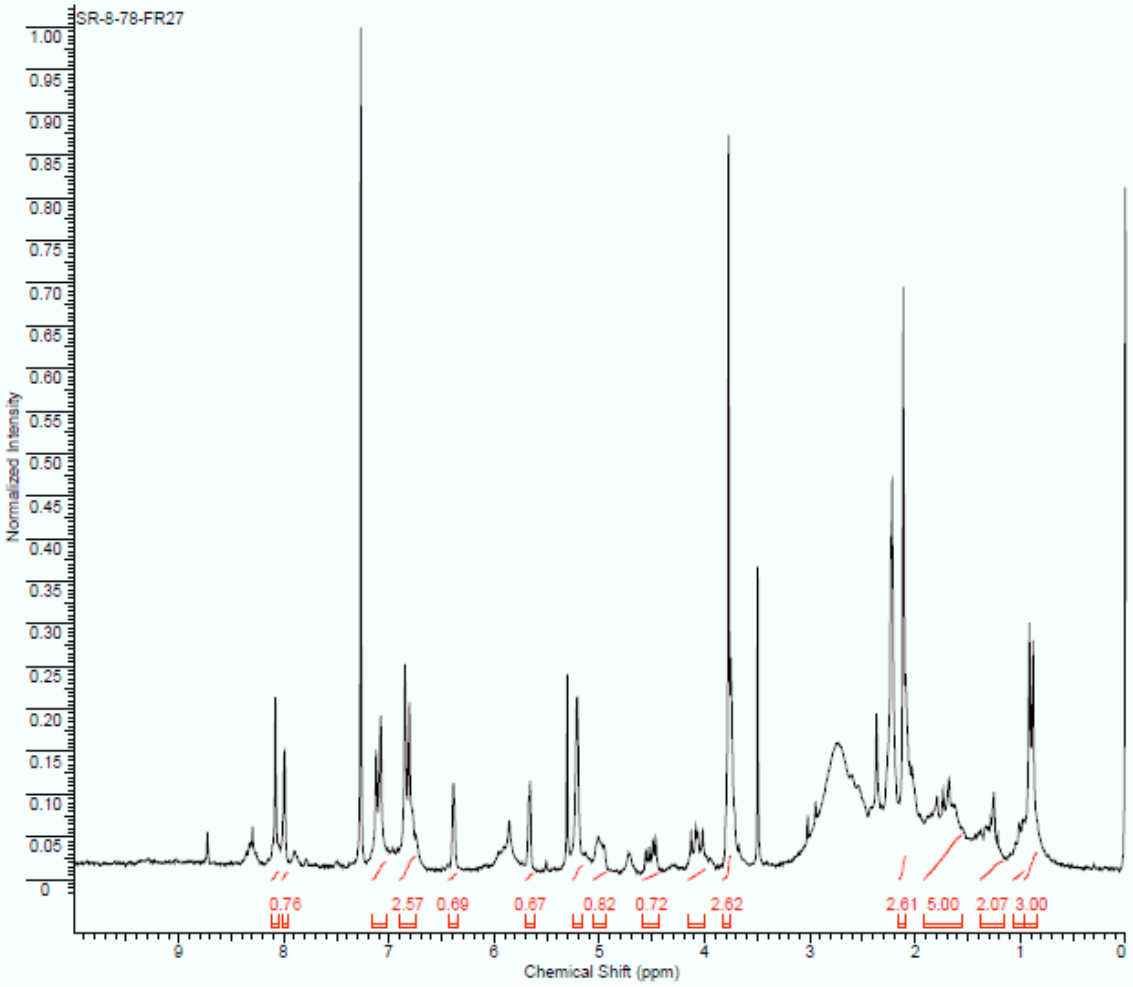

Formula $C_{20}H_{32}N_6O_3$	FW	512.6028

Acquisition Time (sec)	1.3005	Comment	Std proton	Date	Jul 8 2008
Date Stamp	Jul 8 2008	File Name	C:\SANDEEP NMR\SR-8-79-FR27-13C		
Frequency (MHz)	100.53	Nucleus	13C	Number of Transients	2000
Original Points Count	31375	Points Count	32768	Pulse Sequence	s2pul
Receiver Gain	30.00	Solvent	CHLOROFORM-d		
Spectrum Offset (Hz)	10552.5811	Sweep Width (Hz)	24125.45	Temperature (degree C)	25.000

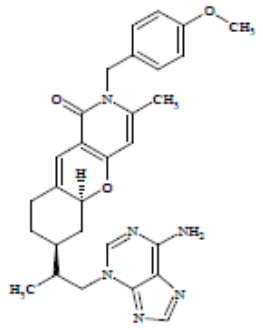

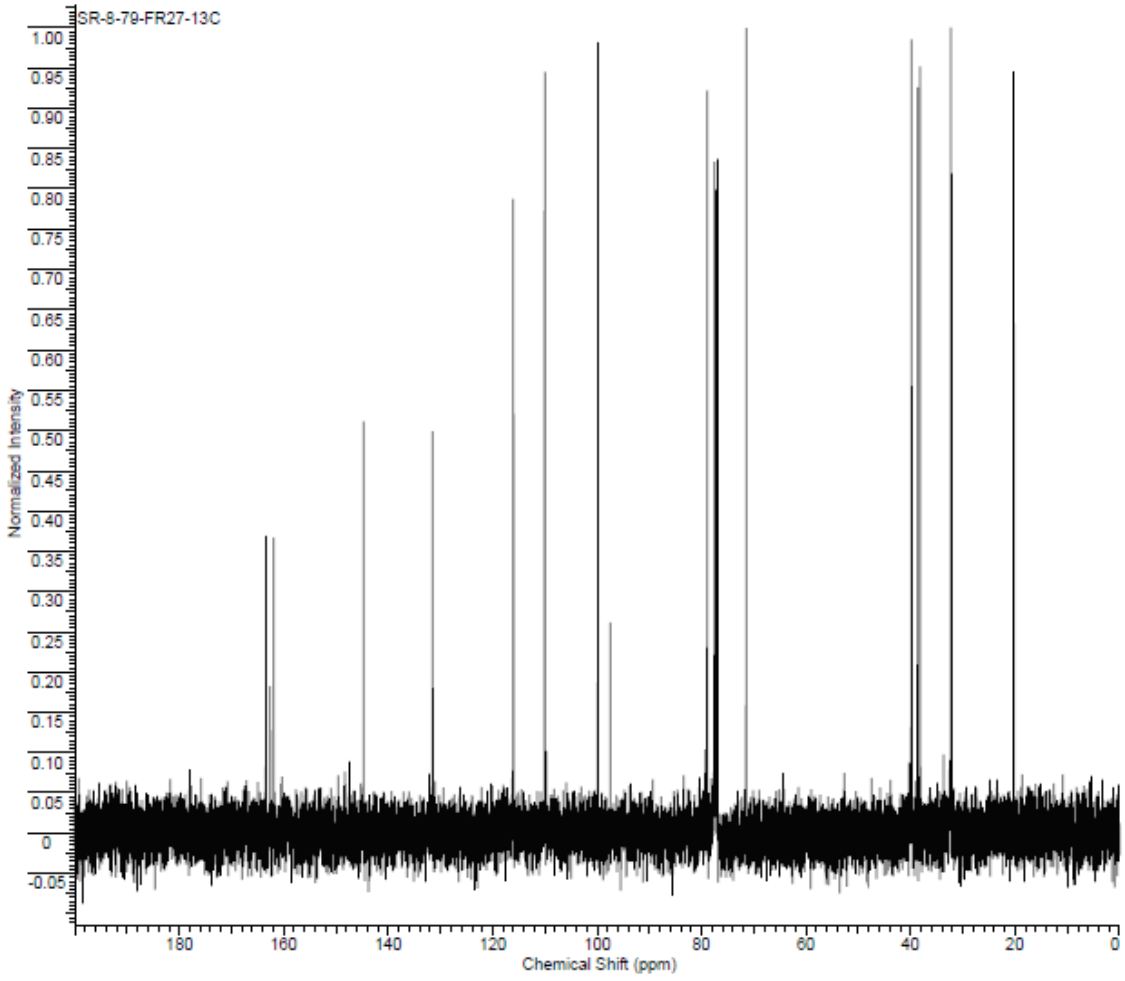

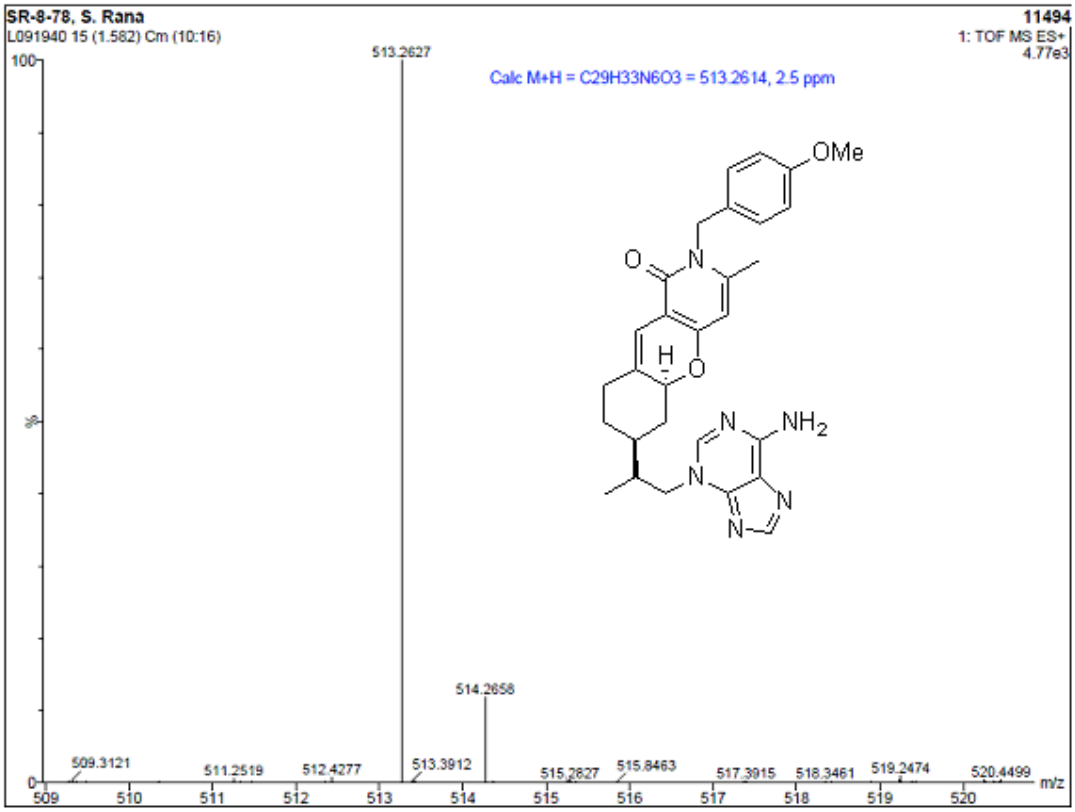
SR-8-78, S. Rana
L091940 15 (1.582) Cm (10:16)
11494
1: TOF MS ES+
4.77e3
513.2627
Calc M+H = C29H33N6O3 = 513.2614, 2.5 ppm
OMe
O
N
H
O
N
NH2
N
N
N
514.2658
509.3121
511.2519
512.4277
513.3912
515.2627
515.8463
517.3915
518.3461
519.2474
520.4499
100
%
0
509
510
511
512
513
514
515
516
517
518
519
520
m/z

Formula $C_{31}H_{34}N_6O_3$	FW	514.6187	
Acquisition Time (sec)	1.0945	Comment	STANDARD 1H OBSERVE
Date	Jul 22 2008	Date Stamp	Jul 22 2008
File Name	C:\NMR BACKUP\010609NMR BACKUP\200\HUA-NEW\SANDEEP\BOOK8\SR-8-78-FR23		
Frequency (MHz)	199.98	Nucleus	1H
Original Points Count	5994	Points Count	8192
Receiver Gain	40.00	Solvent	CHLOROFORM-d
Spectrum Offset (Hz)	1002.0226	Sweep Width (Hz)	3000.30

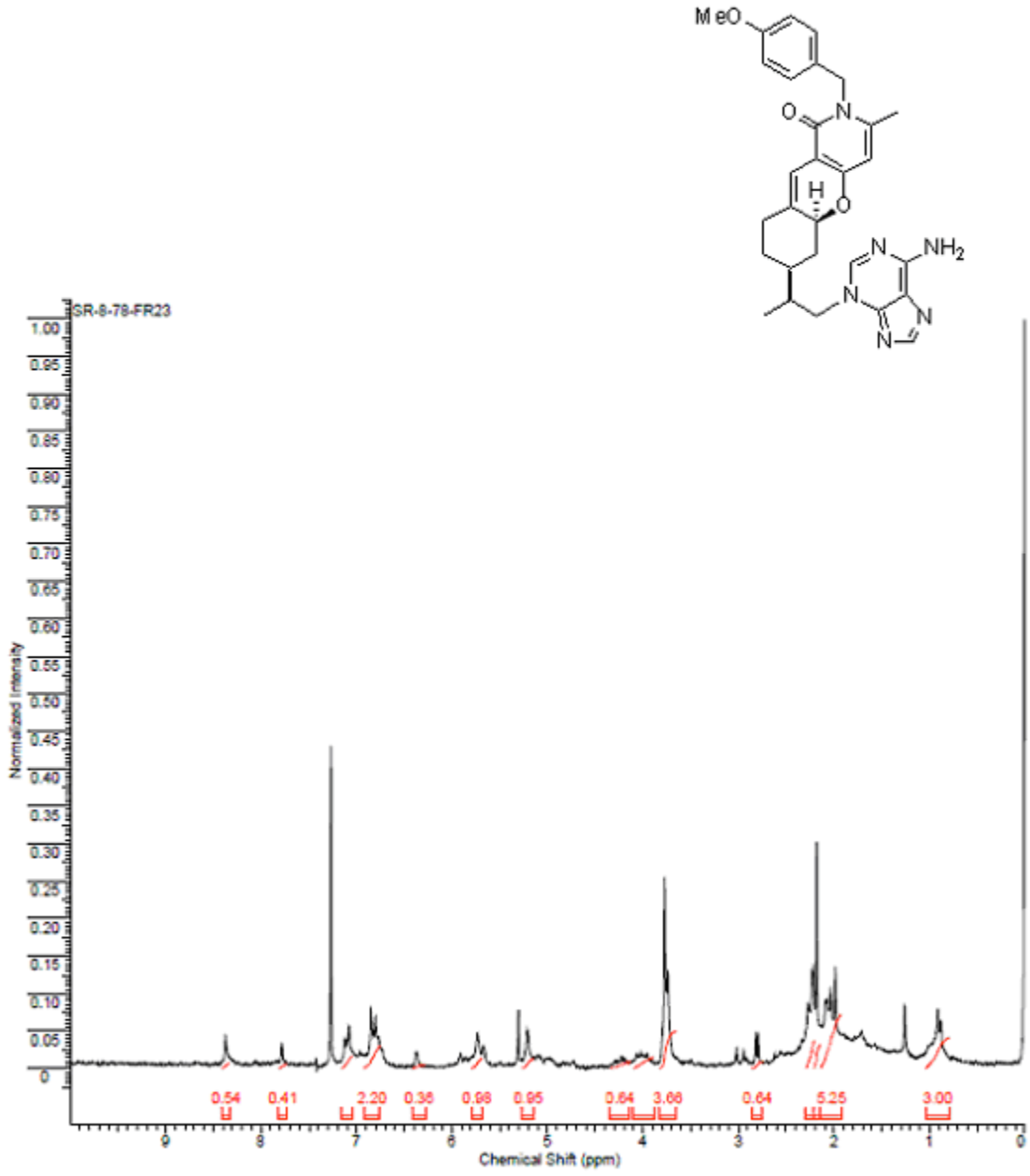

Formula $C_5H_7NO_2$	FW	125.1253

Acquisition Time (sec)	2.0487	Comment	Std proton	Date	Mar 10 2009
Date Stamp	Mar 10 2009	File Name	C:\NMR 031009\400\SRANA\SR-9-119-FIRSTBATCH		
Frequency (MHz)	399.75	Nucleus	1H	Number of Transients	32
Original Points Count	13103	Points Count	16384	Pulse Sequence	s2pul
Receiver Gain	46.00	Solvent	DMSO-d6	Spectrum Offset (Hz)	2406.1804
Sweep Width (Hz)	6395.91	Temperature (degree C)	25.000		

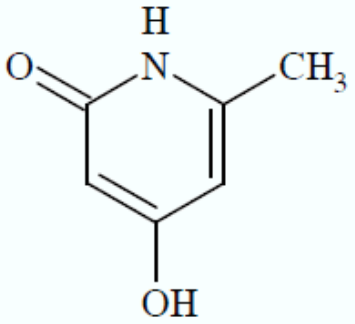

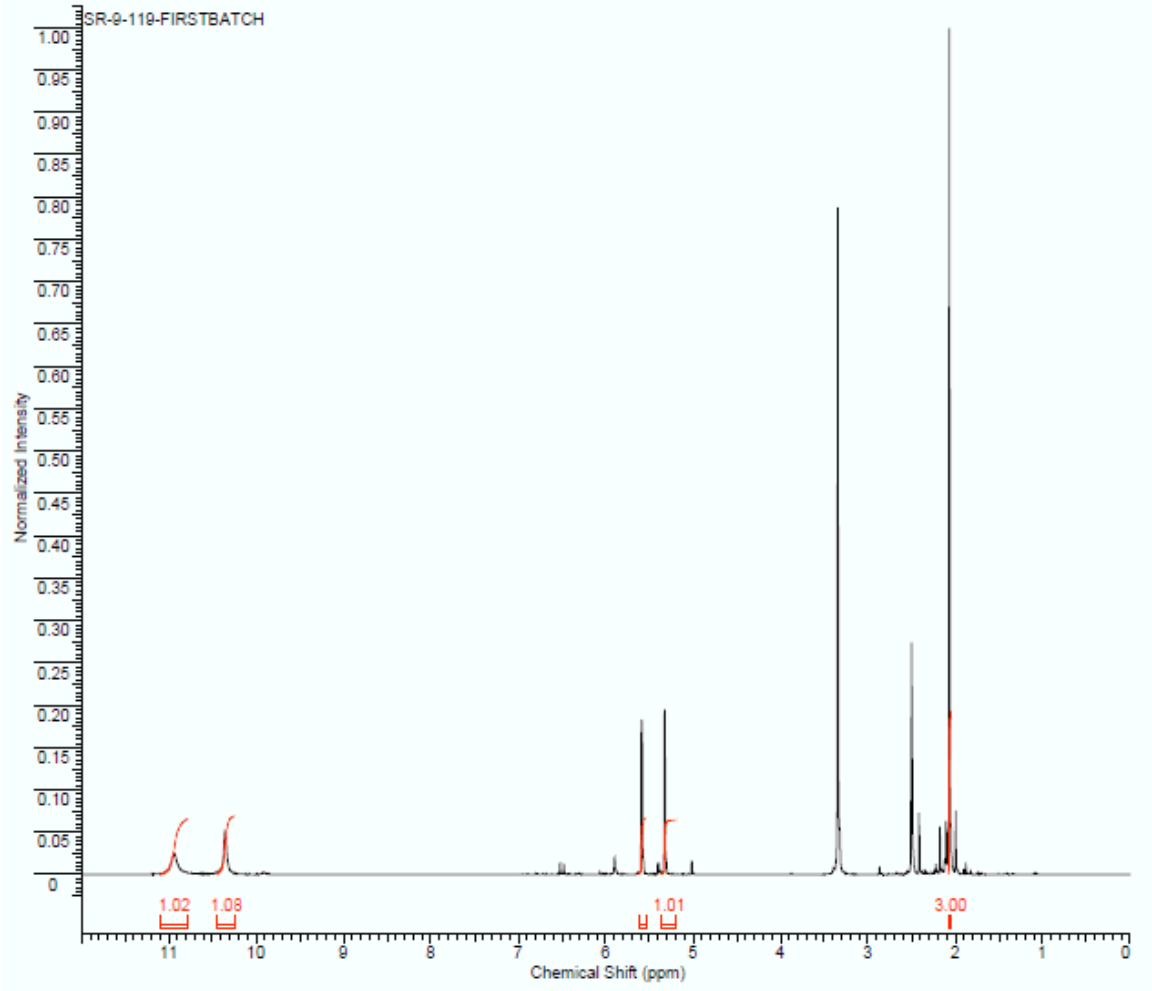

Formula C_7H_9NO	FW	123.1525

Acquisition Time (sec)	1.4976	*Comment*	13C OBSERVE	*Date*	Nov 20 2008
Date Stamp	Nov 20 2008				
File Name	C:\NMR BACKUP\010609NMR BACKUP\200\HUA-NEW\SANDEEP\BOOK 9\SR-9-58-13C				
Frequency (MHz)	50.29	*Nucleus*	13C	*Number of Transients*	20000
Original Points Count	18720	*Points Count*	32768	*Pulse Sequence*	s2pul
Receiver Gain	40.00	*Solvent*	DMSO-d6	*Spectrum Offset (Hz)*	4916.1436
Sweep Width (Hz)	12500.00	*Temperature (degree C)*	29.000		

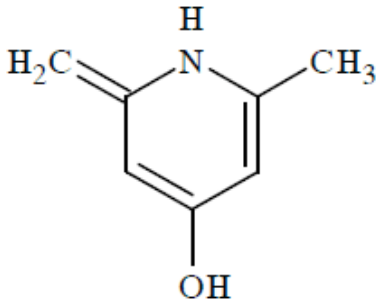

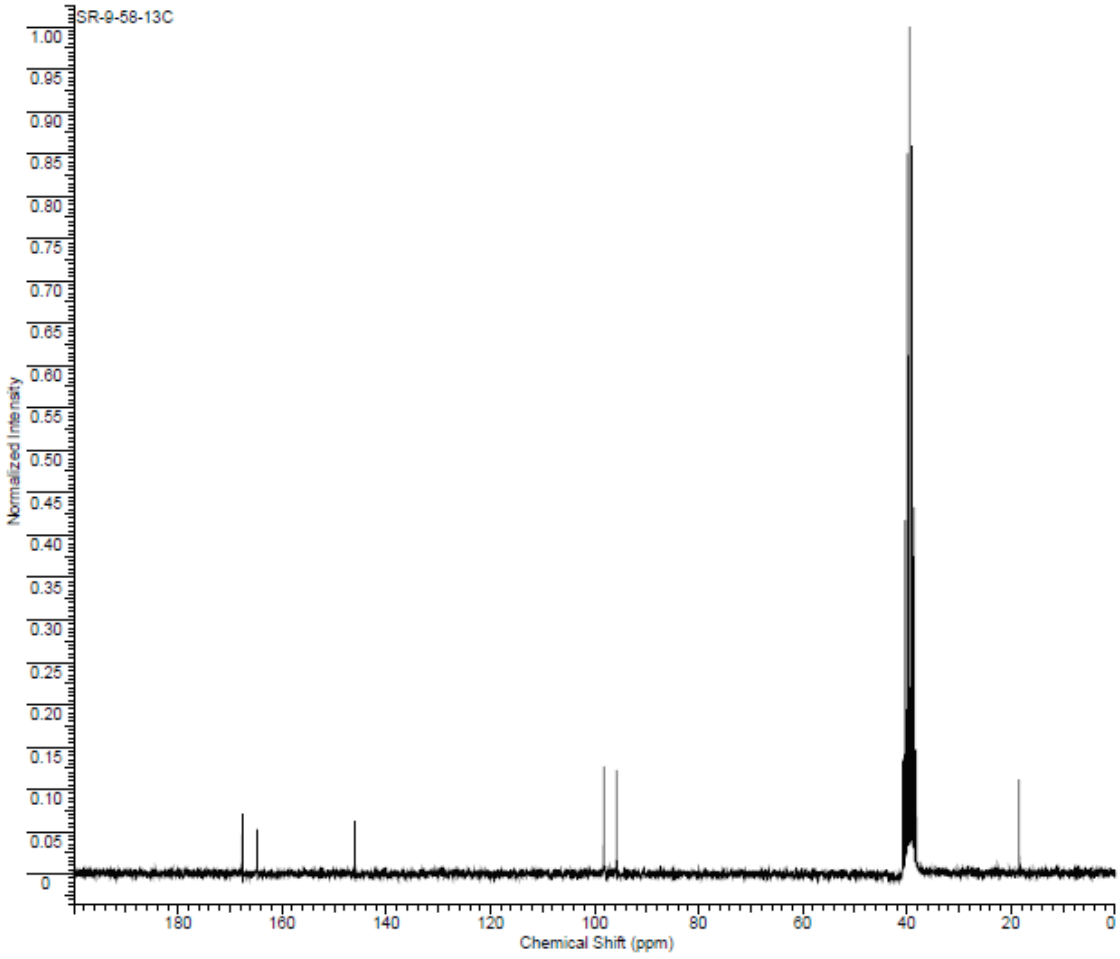

Formula $C_{15}H_{17}NO_2$	FW	259.3434

Acquisition Time (sec)	2.0487	Comment	Std proton	Date	Nov 17 2008
Date Stamp	Nov 17 2008			File Name	C:\NMR 031009\400\SRANA\SR-9-61-DP
Frequency (MHz)	399.78	Nucleus	1H	Number of Transients	32
Original Points Count	13103	Points Count	16384	Pulse Sequence	s2pul
Receiver Gain	30.00	Solvent	CHLOROFORM-d		
Spectrum Offset (Hz)	2416.5151	Sweep Width (Hz)	6395.91	Temperature (degree C)	25.000

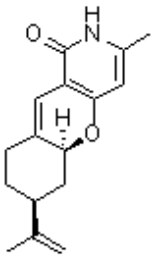

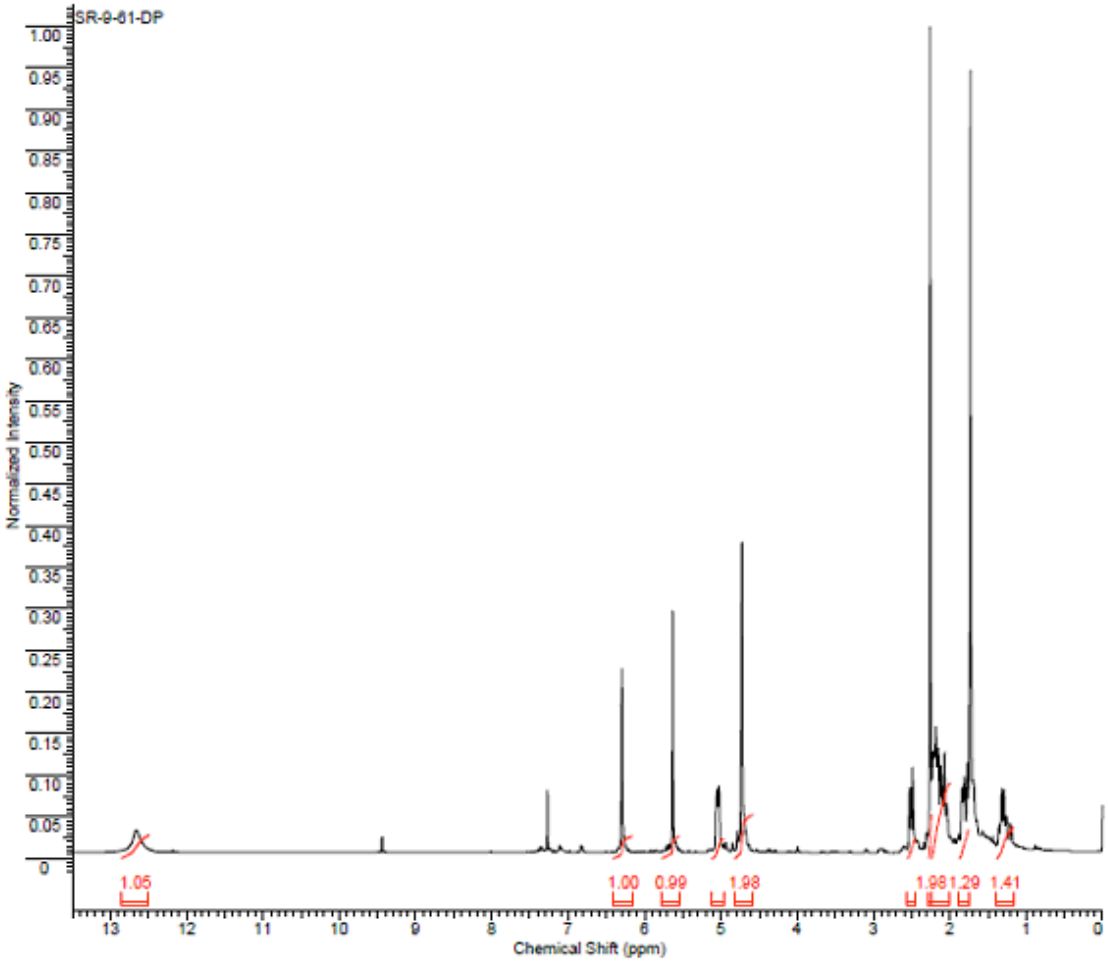

Formula $C_{14}H_{21}NO_2$	FW	259.3434

Acquisition Time (sec)	1.3005	Comment	Std proton	Date	Nov 17 2008
Date Stamp	Nov 17 2008	File Name	C:\NMR 031009\400\SRANA\SR-9-61-13C		
Frequency (MHz)	100.53	Nucleus	13C	Number of Transients	500
Original Points Count	31375	Points Count	32768	Pulse Sequence	s2pul
Receiver Gain	30.00	Solvent	CHLOROFORM-d		
Spectrum Offset (Hz)	10554.7910	Sweep Width (Hz)	24125.45	Temperature (degree C)	25.000

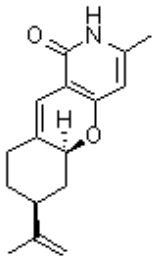

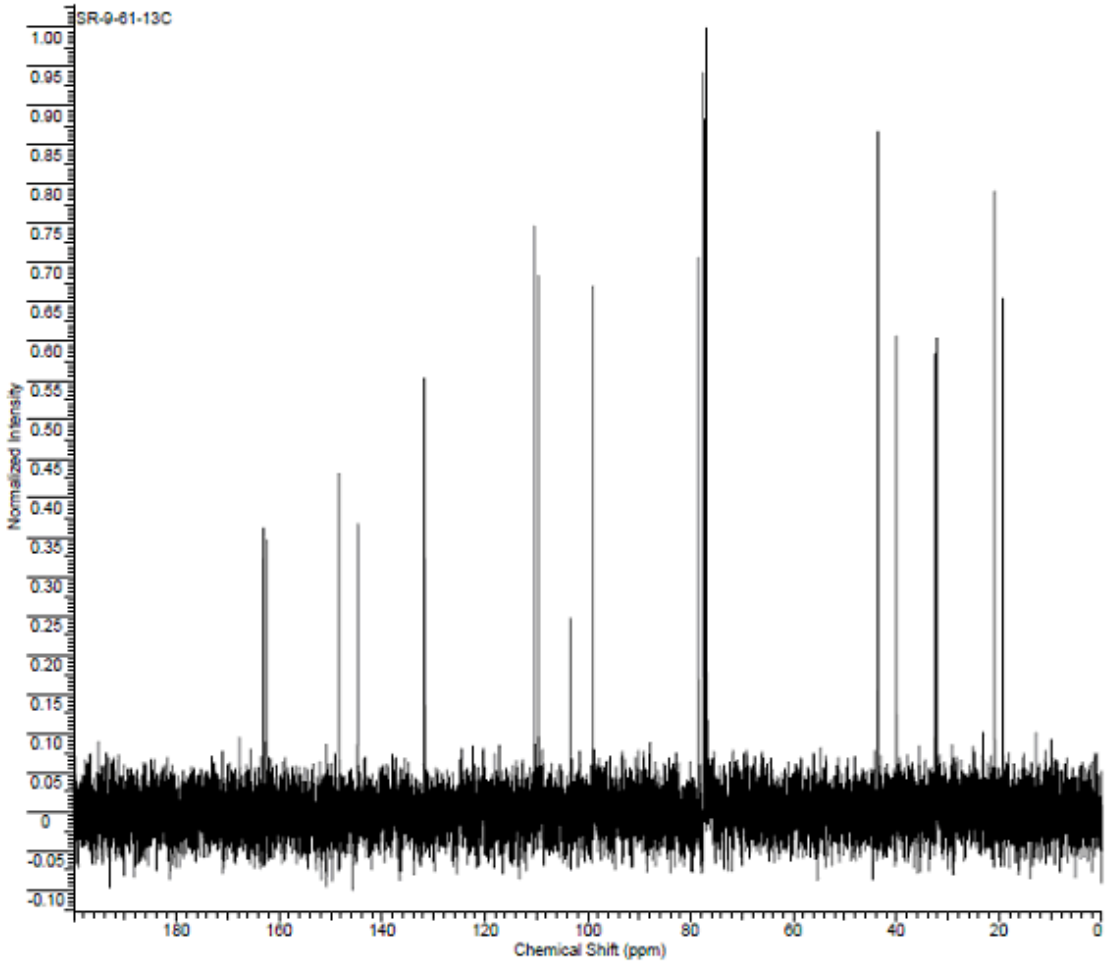

Formula $C_{21}H_{26}NO_4$	FW	359.4593

Acquisition Time (sec)	2.0487	Comment	Std proton	Date	Nov 17 2008
Date Stamp	Nov 17 2008			File Name	C:\NMR 031009\400\SRANA\SR-9-60-DP
Frequency (MHz)	399.76	Nucleus	1H	Number of Transients	32
Original Points Count	13103	Points Count	16384	Pulse Sequence	s2pul
Receiver Gain	12.00	Solvent	CHLOROFORM-d		
Spectrum Offset (Hz)	2415.3440	Sweep Width (Hz)	6395.91	Temperature (degree C)	25.000

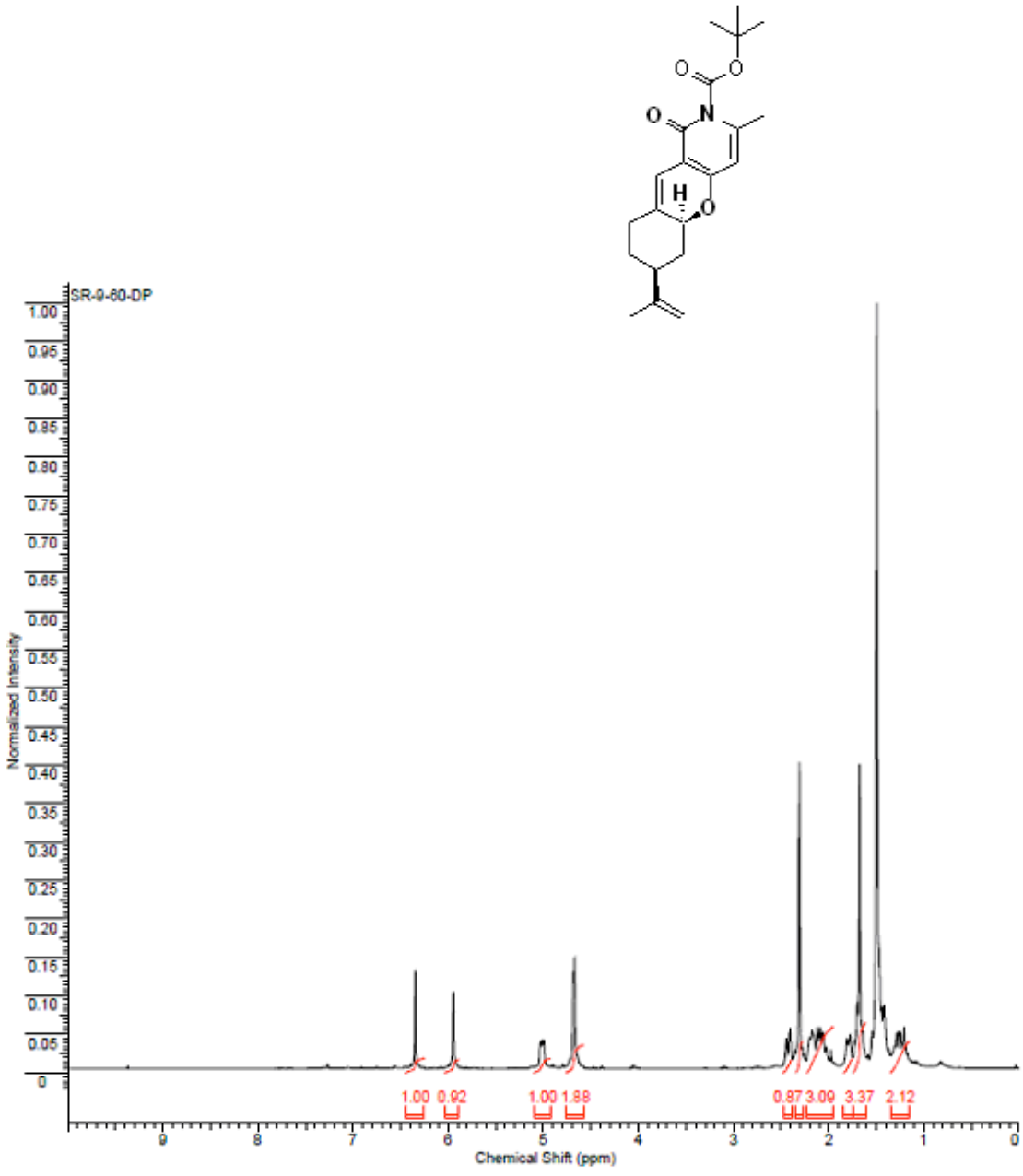

Formula $C_{21}H_{29}NO_4$	FW	359.4593

Acquisition Time (sec)	1.3005	Comment	Std proton	Date	Nov 17 2008
Date Stamp	Nov 17 2008	File Name	C:\NMR 031009\400\SRANA\SR-9-60-13C		
Frequency (MHz)	100.53	Nucleus	13C	Number of Transients	2000
Original Points Count	31375	Points Count	32768	Pulse Sequence	s2pul
Receiver Gain	30.00	Solvent	CHLOROFORM-d		
Spectrum Offset (Hz)	10540.8008	Sweep Width (Hz)	24125.45	Temperature (degree C)	25.000

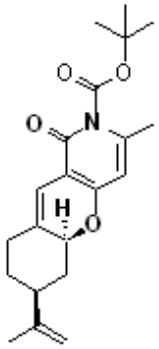

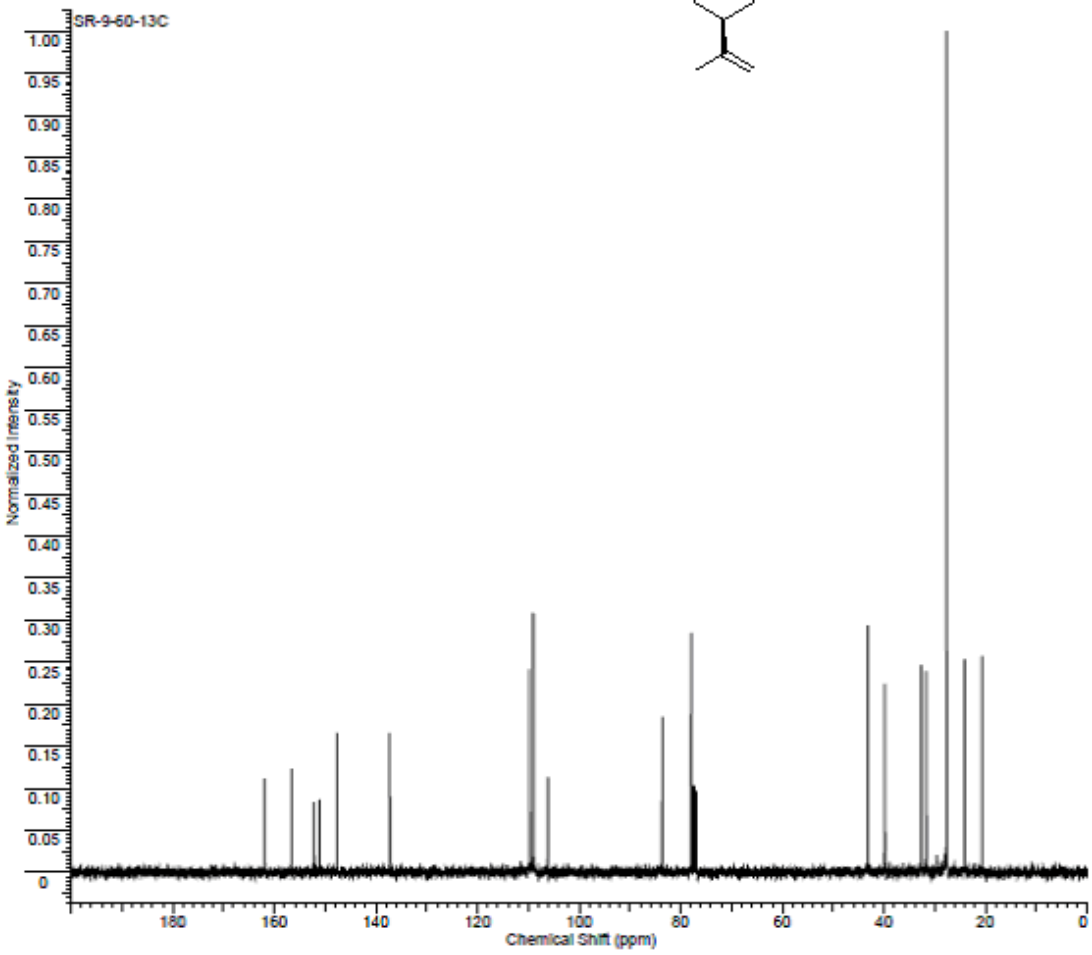

Formula $C_{21}H_{25}NO_4$	FW	375.4587

Acquisition Time (sec)	2.0487	Comment	Std proton	Date	Dec 2 2008
Date Stamp	Dec 2 2008	File Name	C:\NMR 031009\400\SRANA\SR-9-67-DP		
Frequency (MHz)	399.75	Nucleus	1H	Number of Transients	32
Original Points Count	13103	Points Count	16384	Pulse Sequence	s2pul
Receiver Gain	54.00	Solvent	CHLOROFORM-d		
Spectrum Offset (Hz)	2403.5376	Sweep Width (Hz)	6395.91	Temperature (degree C)	25.000

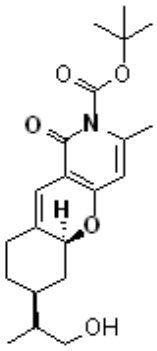

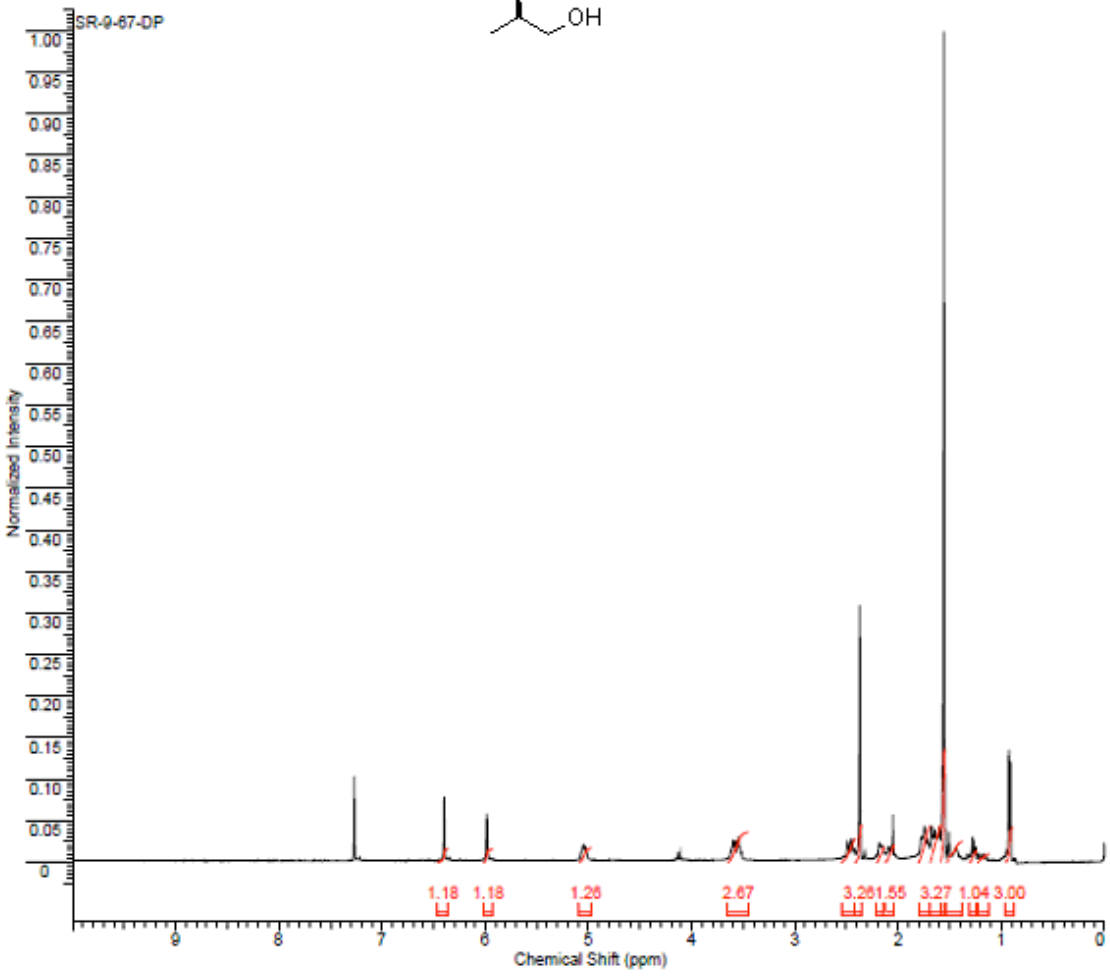

Formula $C_{20}H_{29}NO_4$	FW	375.5017		
Acquisition Time (sec)	1.3005	Comment	Std proton	Date Nov 20 2008
Date Stamp	Nov 20 2008			
File Name	C:\NMR BACKUP\010609NMR BACKUP\400\SRANA\SRANA\SR-9-63-FR11-13-13C			
Frequency (MHz)	100.53	Nucleus	13C	Number of Transients 300
Original Points Count	31375	Points Count	32768	Pulse Sequence s2pul
Receiver Gain	30.00	Solvent	CHLOROFORM-d	
Spectrum Offset (Hz)	10551.8457	Sweep Width (Hz)	24125.45	Temperature (degree C) 25.000

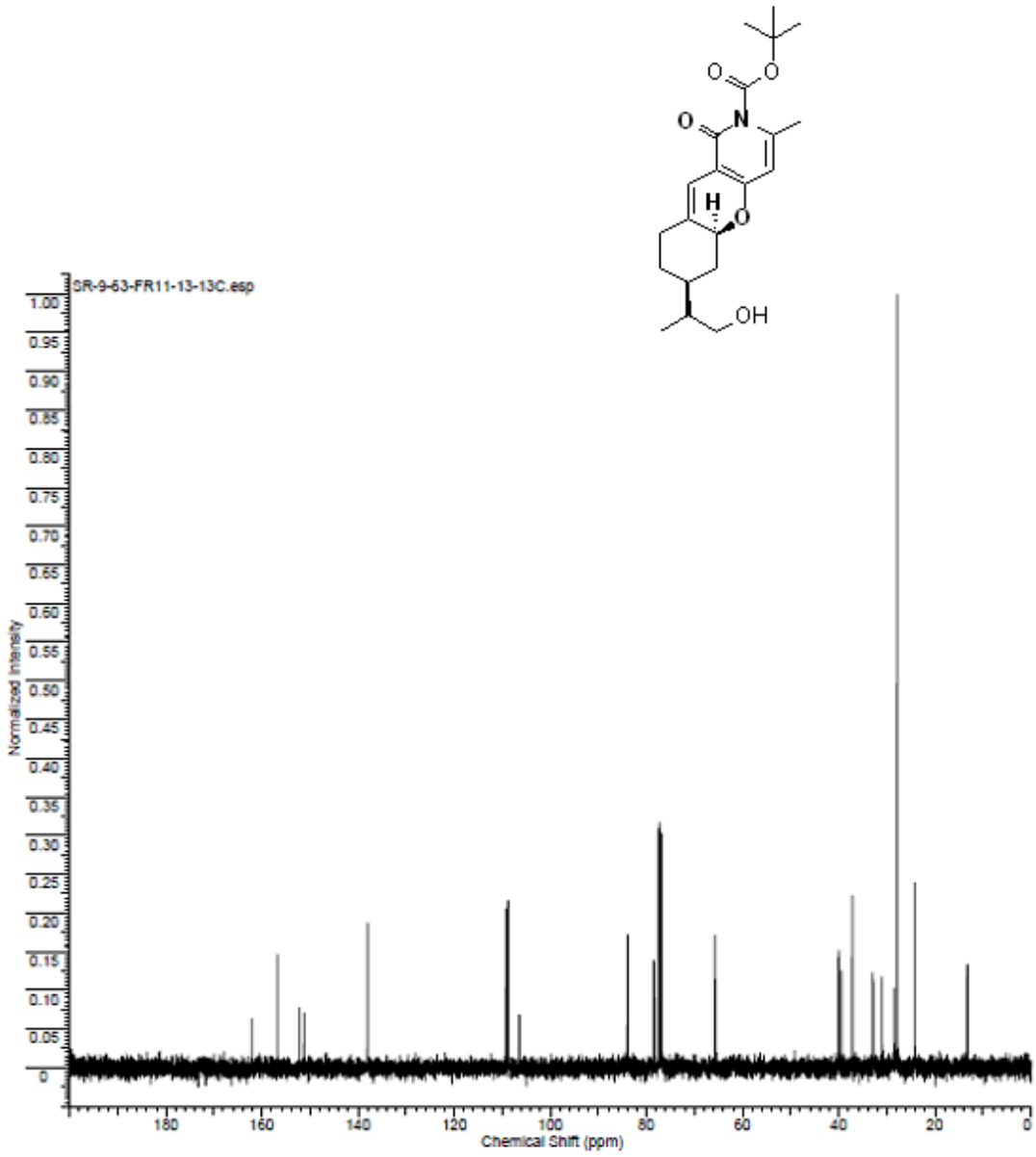

Formula $C_{21}H_{26}NO_5$?	FW	358.4513+?

Acquisition Time (sec)	1.9945	*Comment*	STANDARD 1H OBSERVE		
Date	Dec 3 2008	*Date Stamp*	Dec 3 2008	*File Name*	C:\NMR 031009\200\BOOK 9\SR-9-73-DP
Frequency (MHz)	199.98	*Nucleus*	1H	*Number of Transients*	32
Original Points Count	5984	*Points Count*	8192	*Pulse Sequence*	s2pul
Receiver Gain	4.00	*Solvent*	CHLOROFORM-d		
Spectrum Offset (Hz)	1006.6158	*Sweep Width (Hz)*	3000.30	*Temperature (degree C)*	29.000

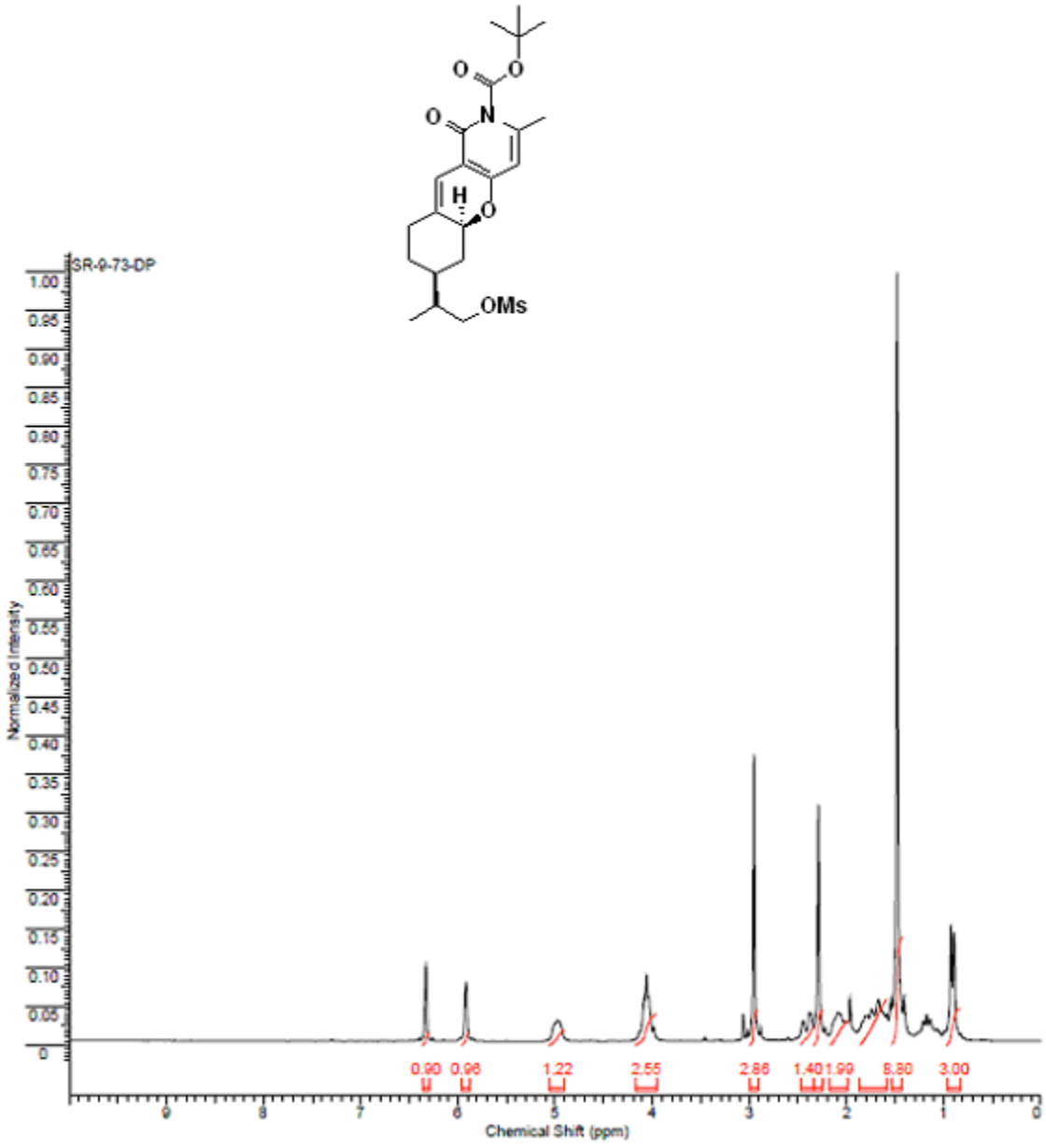

Formula C[illegible]H[illegible]NO[illegible]?	FW 358.4944+?

Acquisition Time (sec)	1.4976	Comment	13C OBSERVE	Date	Dec 3 2008
Date Stamp	Dec 3 2008				
File Name	C:\NMR BACKUP\010609NMR BACKUP\200\HUA-NEW\SANDEEP\BOOK 9\SR-9-73-13C				
Frequency (MHz)	50.29	Nucleus	13C	Number of Transients	400
Original Points Count	18720	Points Count	32768	Pulse Sequence	s2pul
Receiver Gain	40.00	Solvent	CHLOROFORM-d		
Spectrum Offset (Hz)	4867.1089	Sweep Width (Hz)	12500.00	Temperature (degree C)	29.000

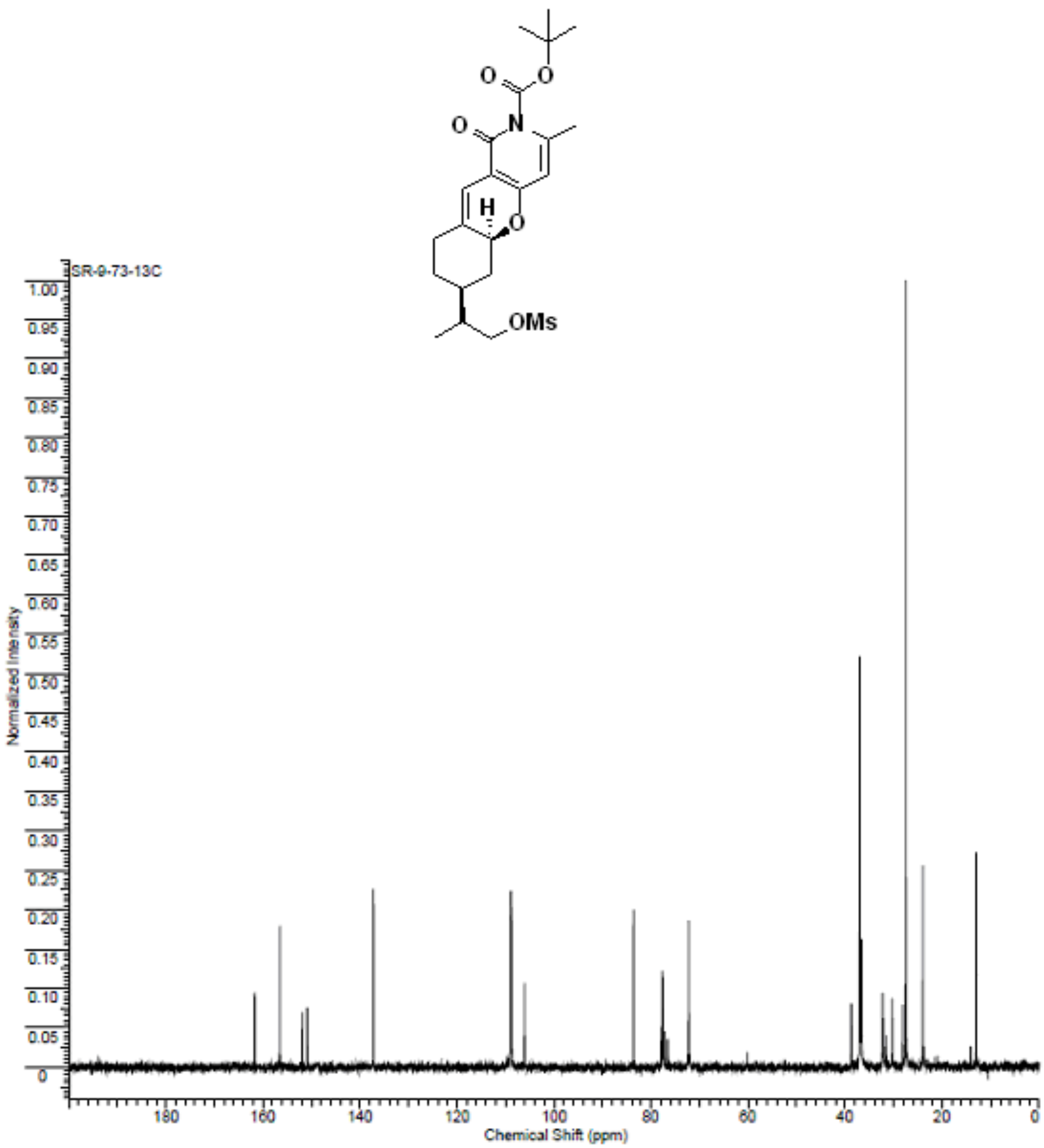

Formula $C_{21}H_{24}N_6O_2$	FW	392.4543

Acquisition Time (sec)	2.0486	Comment	Std proton	Date	Jan 12 2009
Date Stamp	Jan 12 2009	File Name	C:\NMR 031009\400\SRANA\SR-AP-1-11-FR24-25		
Frequency (MHz)	399.75	Nucleus	1H	Number of Transients	32
Original Points Count	9827	Points Count	16384	Pulse Sequence	s2pul
Receiver Gain	60.00	Solvent	CHLOROFORM-d		
Spectrum Offset (Hz)	2003.8943	Sweep Width (Hz)	4797.03	Temperature (degree C)	25.000

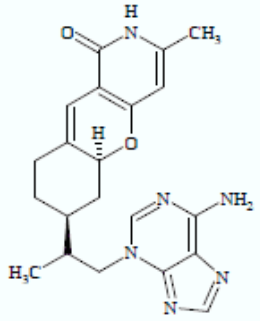

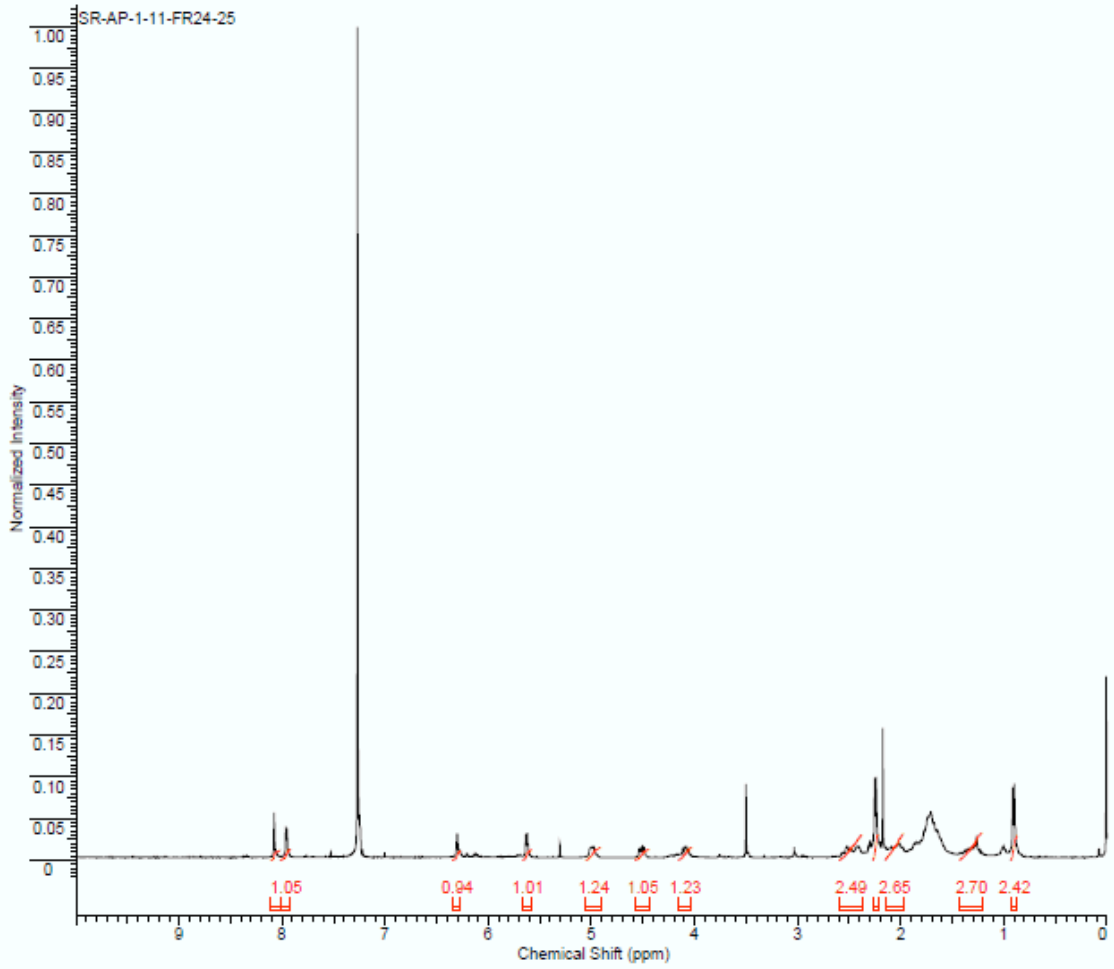

Formula $C_{21}H_{24}N_6O_2$	FW 392.4543

Acquisition Time (sec)	1.3005	*Comment*	Std proton	*Date*	Feb 26 2009
Date Stamp	Feb 26 2009	*File Name*	C:\NMR 031009\400\SRANA\SR-AP-1-42-13C		
Frequency (MHz)	100.53	*Nucleus*	13C	*Number of Transients*	2000
Original Points Count	31375	*Points Count*	32768	*Pulse Sequence*	s2pul
Receiver Gain	30.00	*Solvent*	CHLOROFORM-d		
Spectrum Offset (Hz)	10553.0635	*Sweep Width (Hz)*	24125.45	*Temperature (degree C)*	25.000

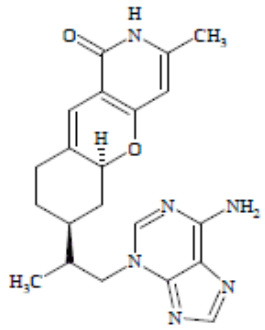

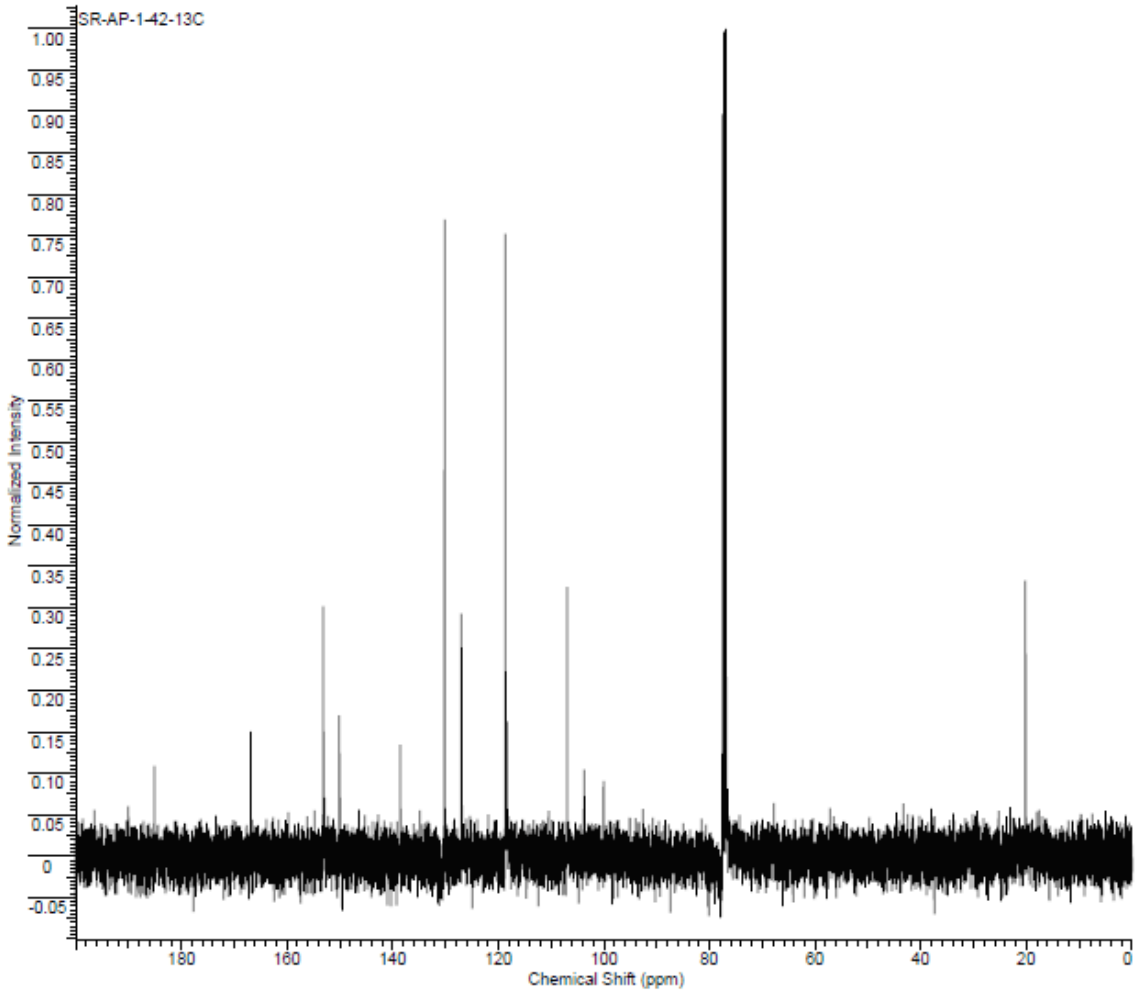

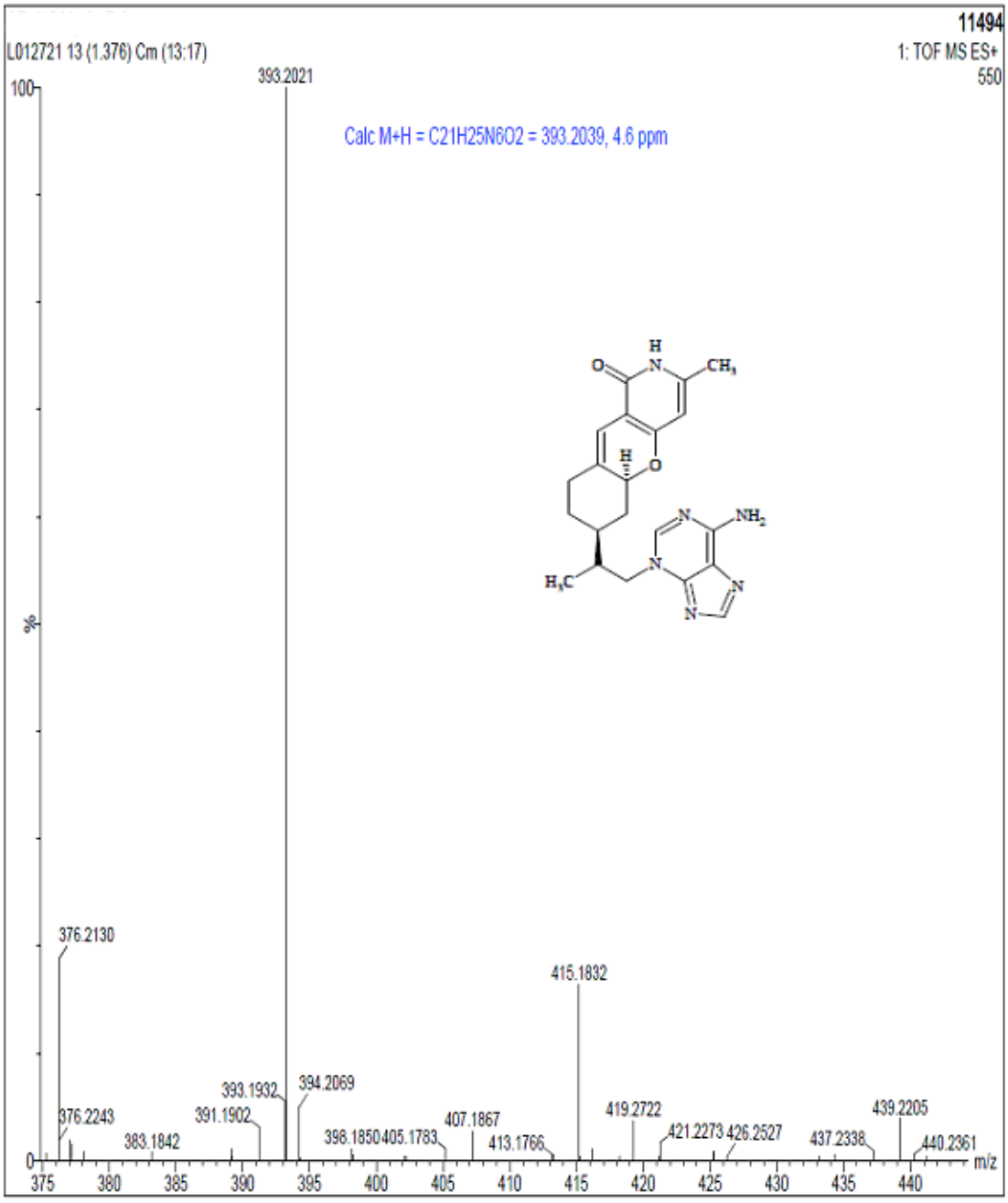
11494
L012721 13 (1.376) Cm (13:17)
1: TOF MS ES+
550
393.2021
100
Calc M+H = C21H25N6O2 = 393.2039, 4.6 ppm
%
376.2130
415.1832
393.1932
394.2069
376.2243
391.1902
407.1867
419.2722
439.2205
383.1842
398.1850
405.1783
413.1766
421.2273
426.2527
437.2338
440.2361
0
m/z
375
380
385
390
395
400
405
410
415
420
425
430
435
440

Formula $C_{14}H_{14}N_2O$	FW	226.2738

Acquisition Time (sec)	2.0485	Comment	Std proton	Date	Feb 26 2009
Date Stamp	Feb 26 2009			File Name	C:\NMR 031009\400\SRANA\SR-AP-1-42
Frequency (MHz)	399.75	Nucleus	1H	Number of Transients	16
Original Points Count	13102	Points Count	16384	Pulse Sequence	s2pul
Receiver Gain	40.00	Solvent	CHLOROFORM-d		
Spectrum Offset (Hz)	2402.3203	Sweep Width (Hz)	6395.91	Temperature (degree C)	25.000

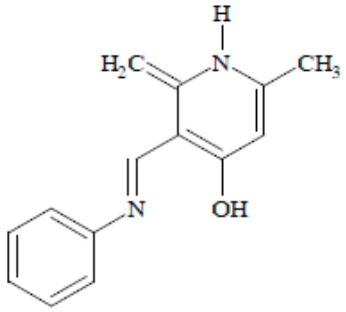

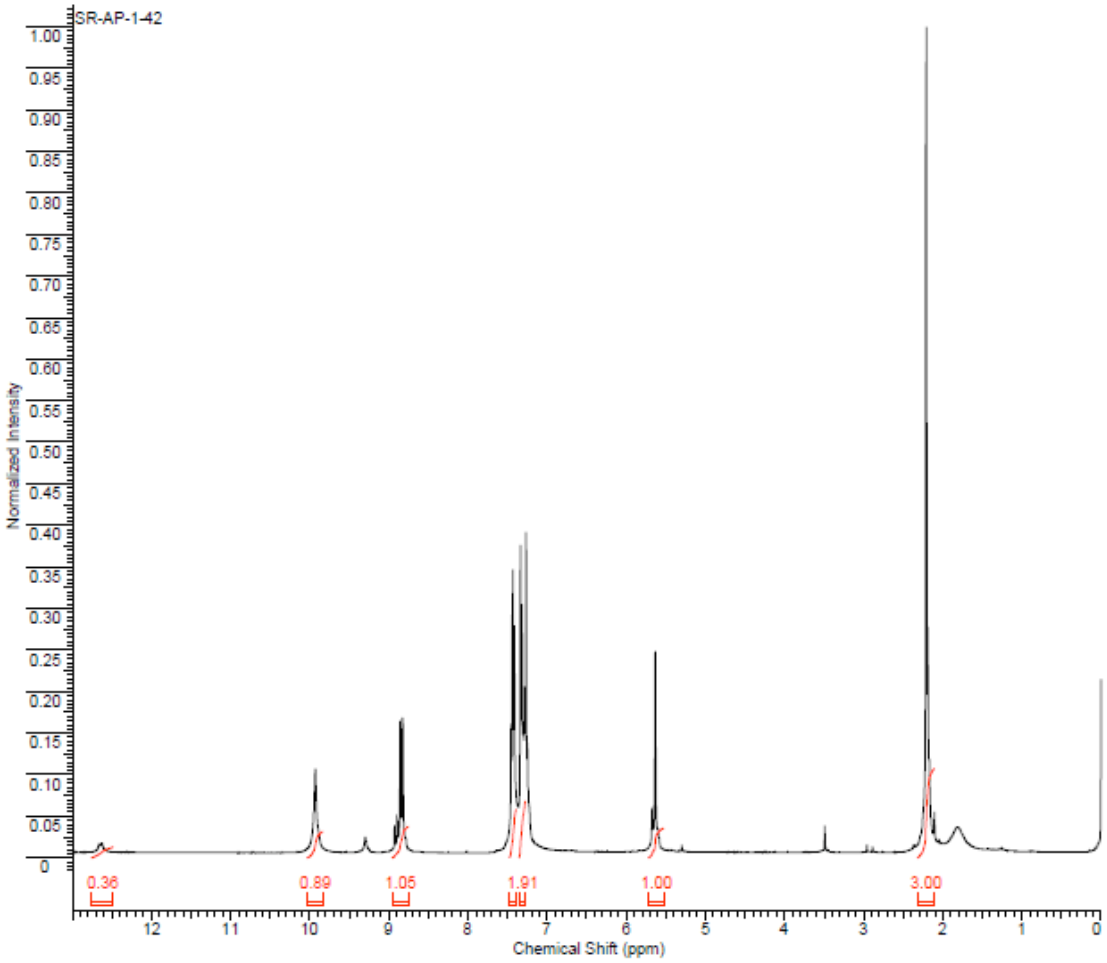

Formula $C_{14}H_{14}N_2O$	FW	226.2738

Acquisition Time (sec)	1.3005	*Comment*	Std proton	*Date*	Feb 26 2009
Date Stamp	Feb 26 2009	*File Name*	C:\NMR 031009\400\SRANA\SR-AP-1-42-13C		
Frequency (MHz)	100.53	*Nucleus*	13C	*Number of Transients*	2000
Original Points Count	31375	*Points Count*	32768	*Pulse Sequence*	s2pul
Receiver Gain	30.00	*Solvent*	CHLOROFORM-d		
Spectrum Offset (Hz)	10553.0635	*Sweep Width (Hz)*	24125.45	*Temperature (degree C)*	25.000

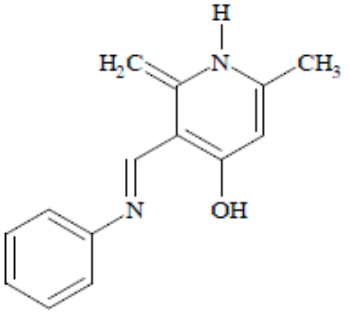

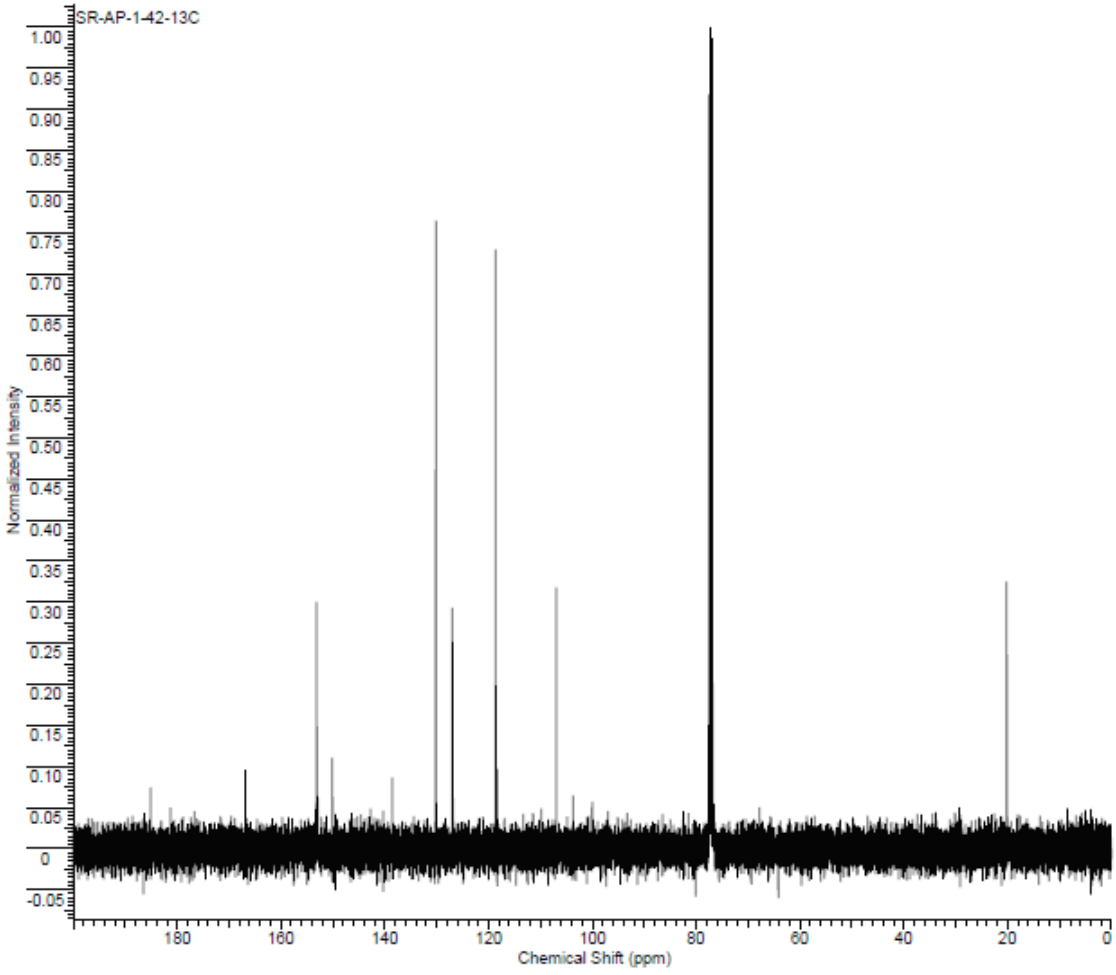

Formula $C_7H_7NO_3$	FW	153.1354

Acquisition Time (sec)	2.0485	Comment	Std proton	Date	Mar 2 2009
Date Stamp	Mar 2 2009	File Name	C:\NMR 031009\400\SRANA\SR-9-114-SM		
Frequency (MHz)	399.75	Nucleus	1H	Number of Transients	32
Original Points Count	13102	Points Count	16384	Pulse Sequence	s2pul
Receiver Gain	50.00	Solvent	CHLOROFORM-d		
Spectrum Offset (Hz)	2403.9280	Sweep Width (Hz)	6395.91	Temperature (degree C)	25.000

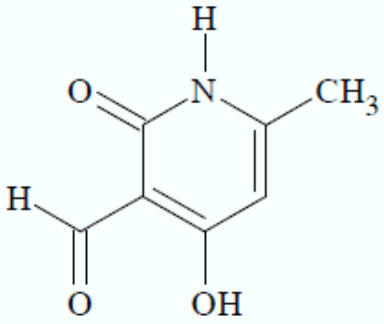

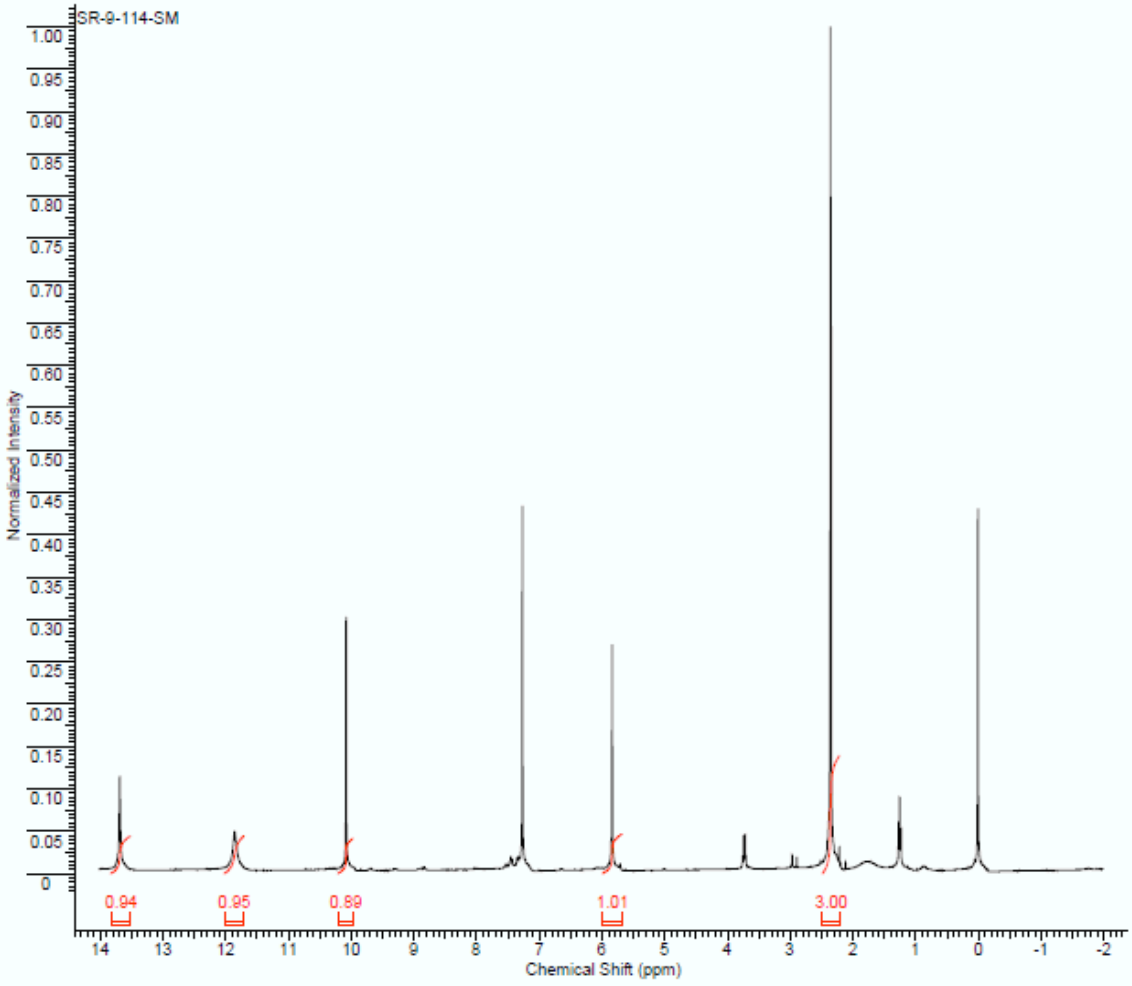

Formula $C_7H_7NO_3$	FW	153.1354

Acquisition Time (sec)	1.3005	Comment	Std proton	Date	Mar 2 2009
Date Stamp	Mar 2 2009	File Name	C:\NMR 031009\400\SRANA\SR-9-114-SM-DMSO-13C		
Frequency (MHz)	100.53	Nucleus	13C	Number of Transients	2000
Original Points Count	31375	Points Count	32768	Pulse Sequence	s2pul
Receiver Gain	30.00	Solvent	DMSO-d6	Spectrum Offset (Hz)	10486.0117
Sweep Width (Hz)	24125.45	Temperature (degree C)	25.000		

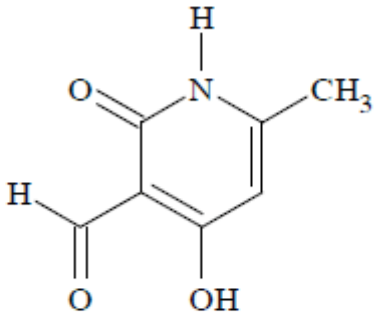

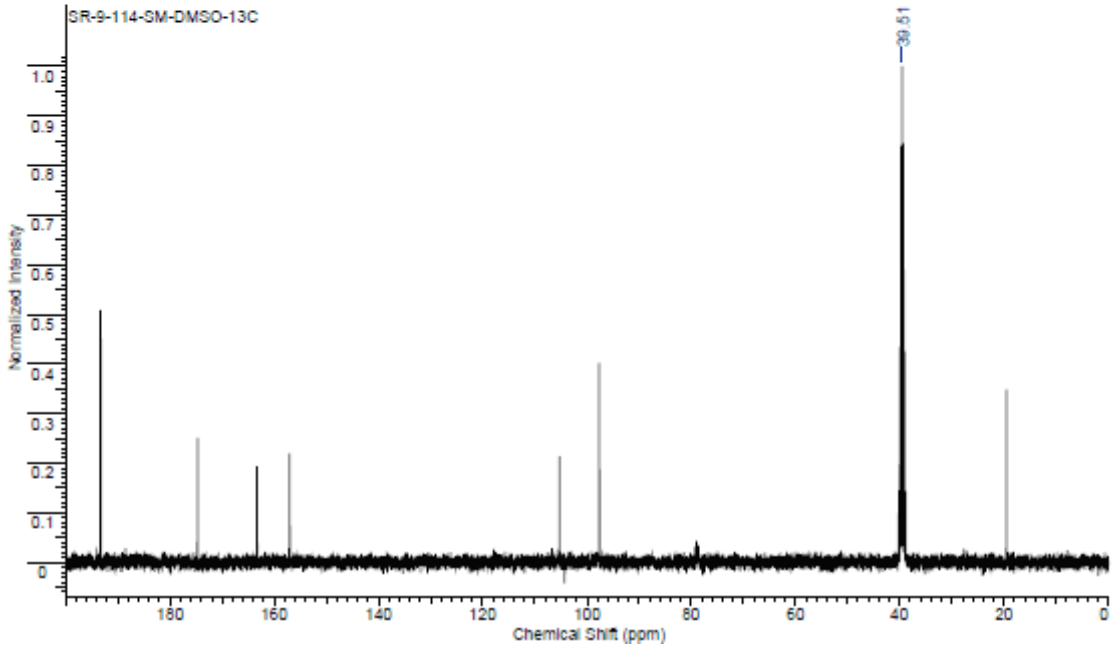

Formula $C_9H_7NO_3$	FW	177.1568

Acquisition Time (sec)	2.0487	Comment	Std proton	Date	Mar 6 2009
Date Stamp	Mar 6 2009			File Name	C:\NMR 031009\400\SRANA\SR-9-114-DP
Frequency (MHz)	399.75	Nucleus	1H	Number of Transients	64
Original Points Count	13103	Points Count	16384	Pulse Sequence	s2pul
Receiver Gain	46.00	Solvent	DMSO-d6	Spectrum Offset (Hz)	2406.1804
Sweep Width (Hz)	6395.91	Temperature (degree C)	25.000		

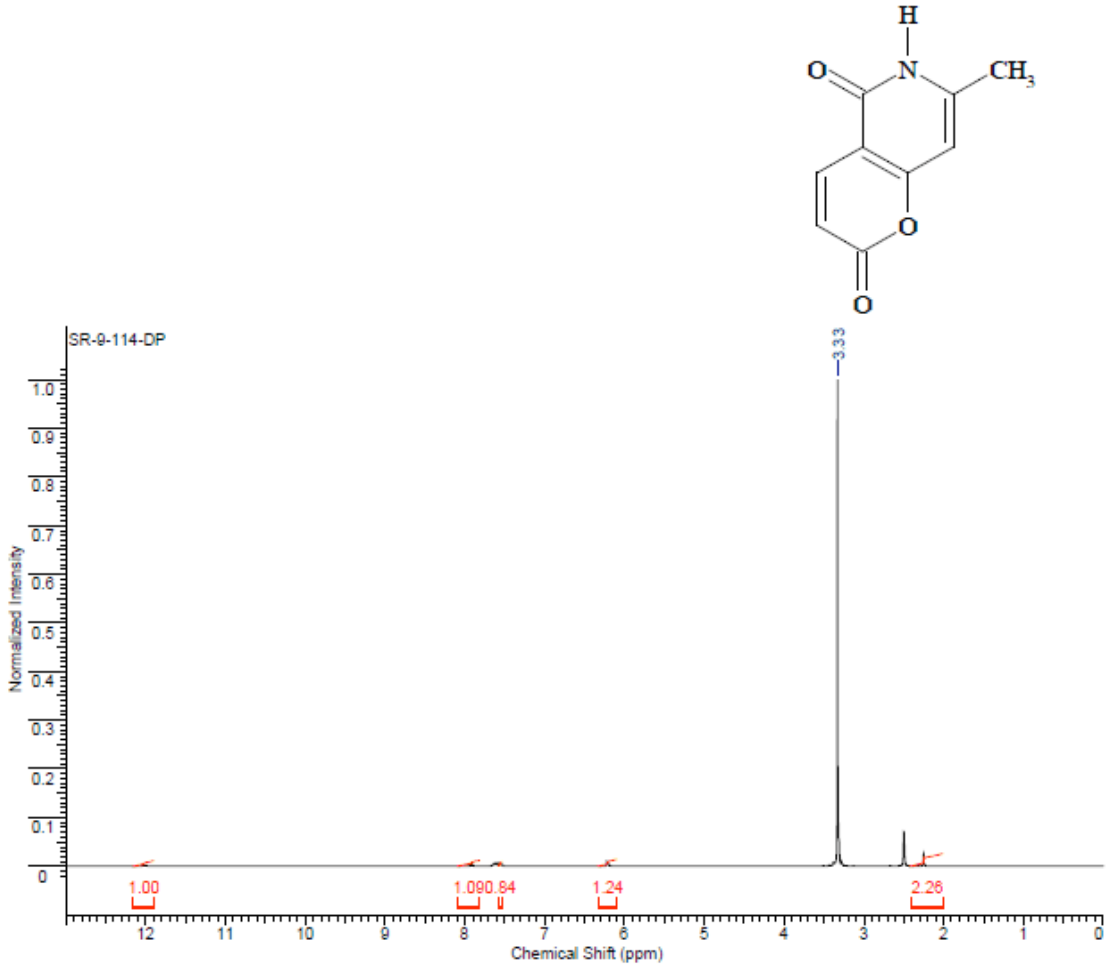

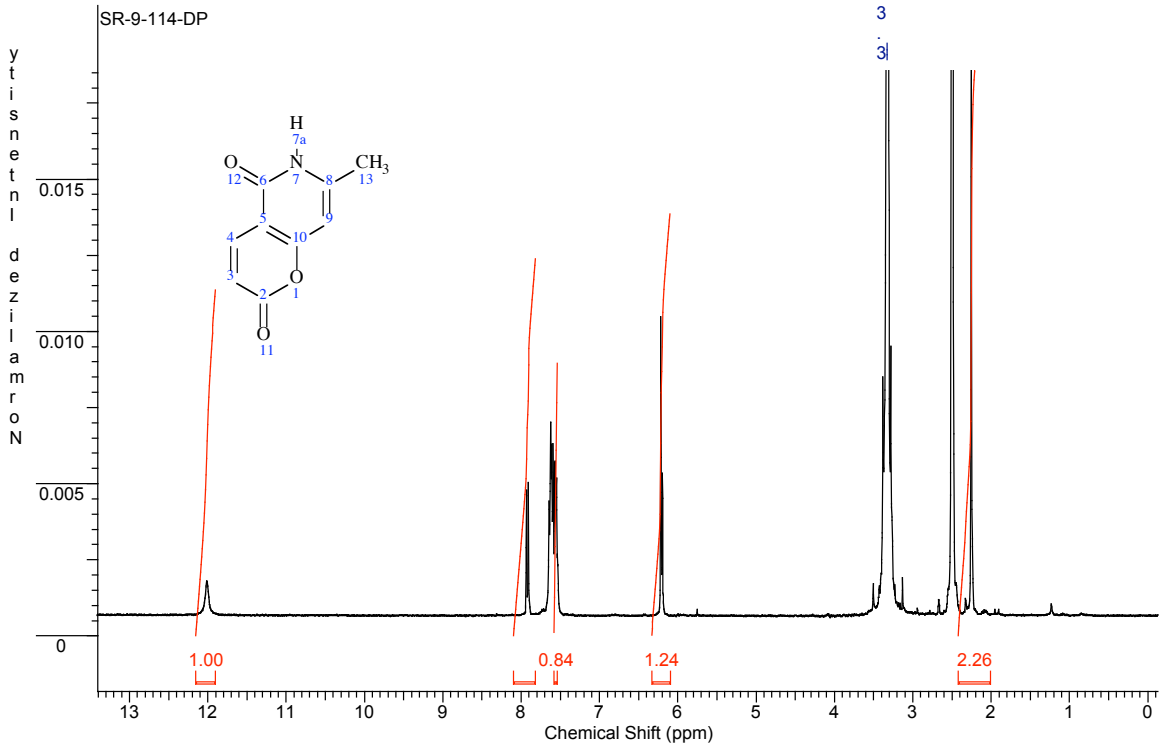
SR-9-114-DP
Intensity
0.015
0.010
0.005
0
1.00
0.84
1.24
2.26
13
12
11
10
9
8
7
6
5
4
3
2
1
0
Chemical Shift (ppm)